Single Site Addressing

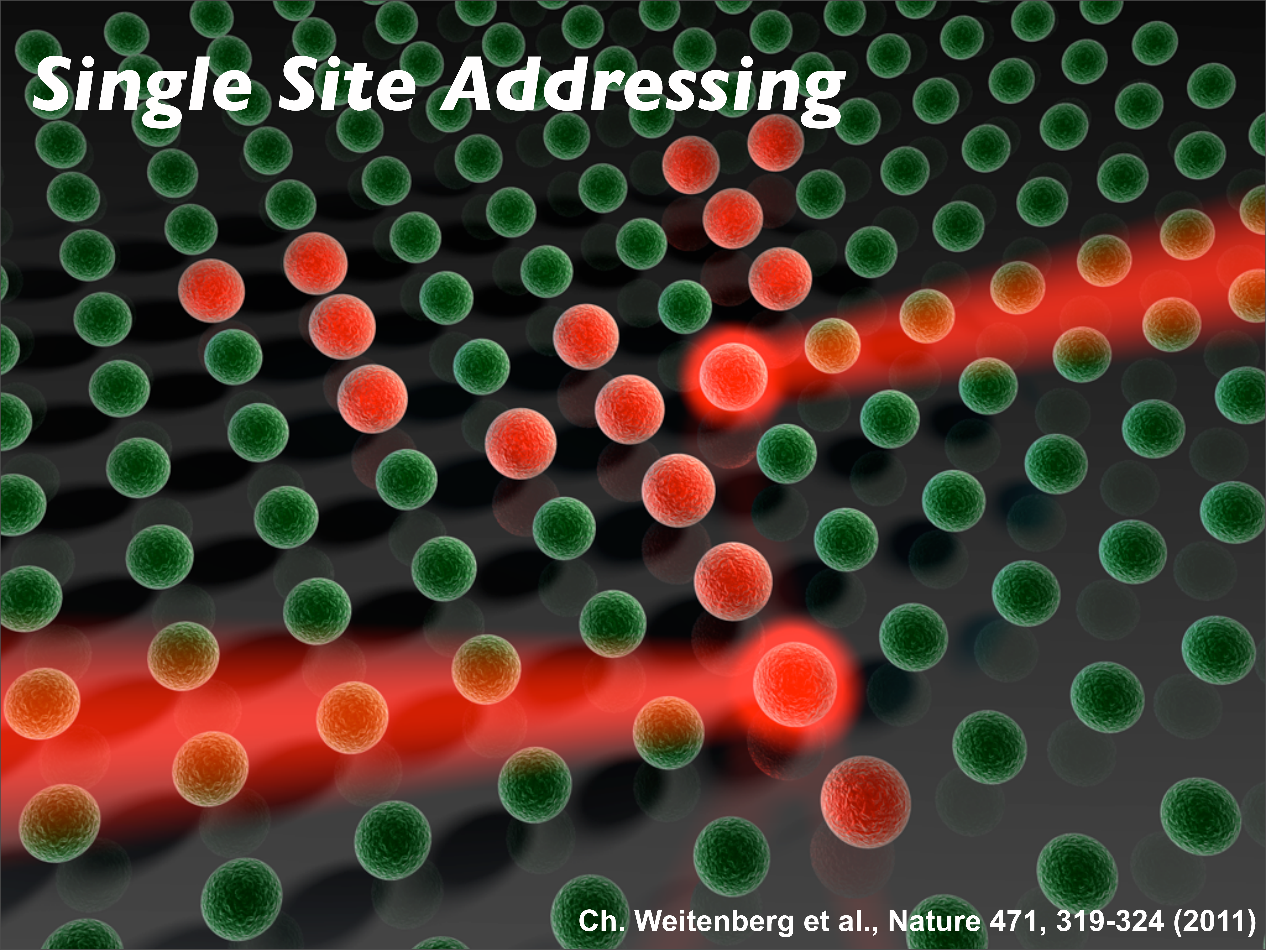

Ch. Weitenberg et al., Nature 471, 319-324 (2011)

Coherent Addressing of Atoms

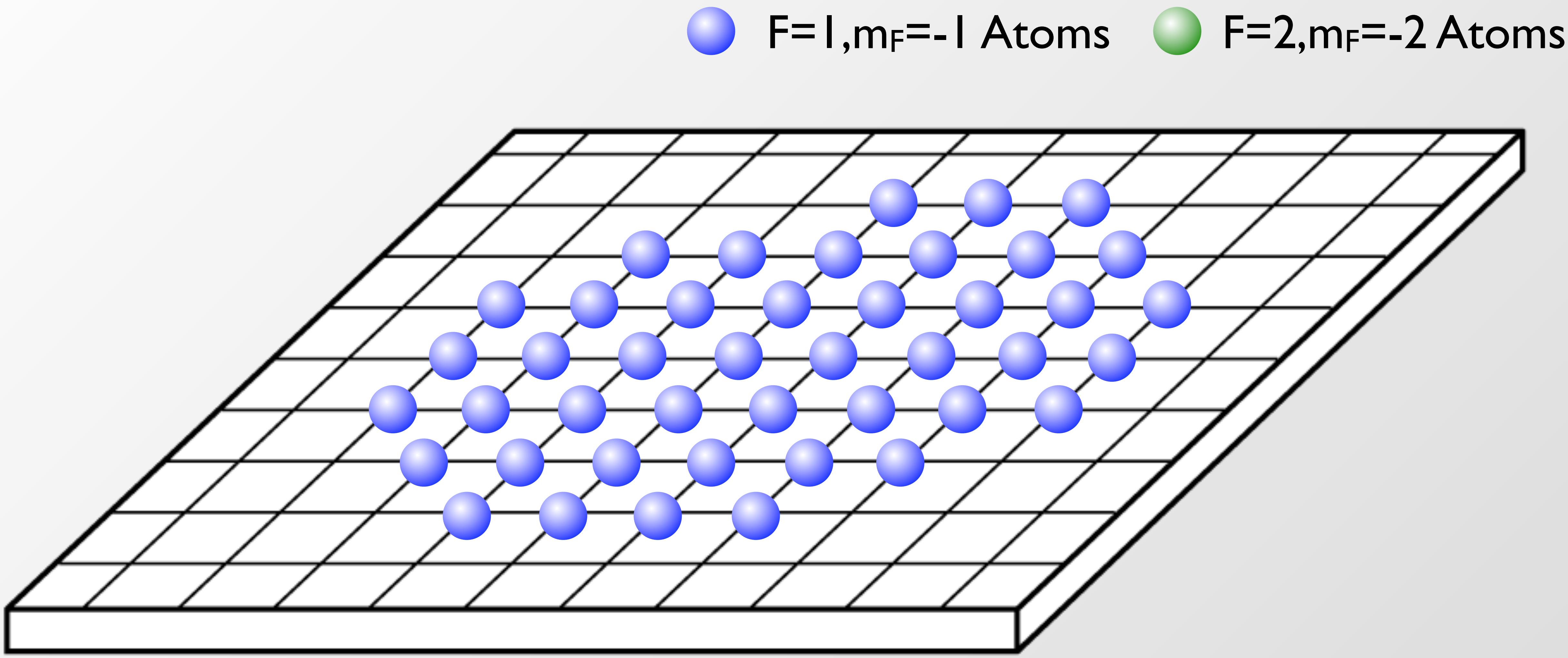

Differential light shift allows to coherently address single atoms!

Landau-Zener Microwave sweep to coherently convert atoms between spin-states.

D.S. Weiss et al., PRA (2004),
Zhang *et al.*, PRA (2006)

Coherent Addressing of Atoms

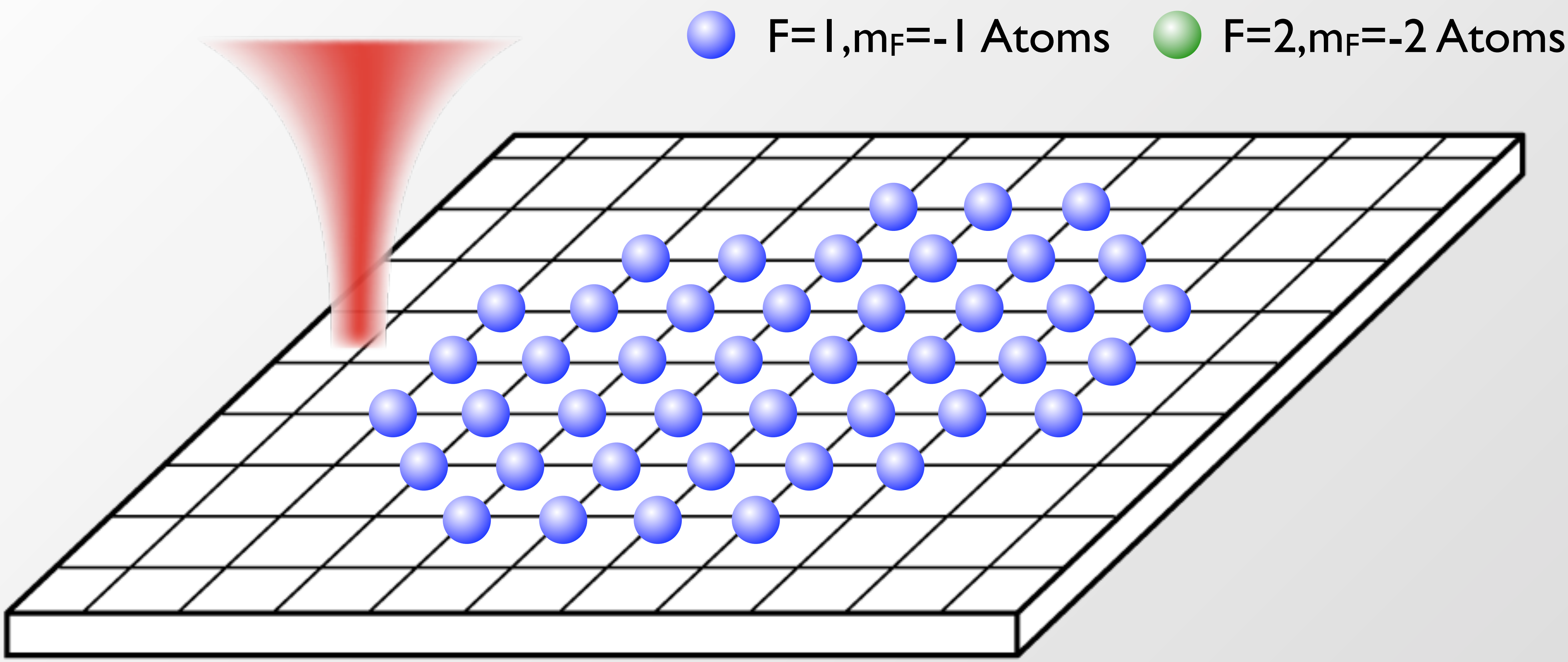

Differential light shift allows to coherently address single atoms!
Landau-Zener Microwave sweep to coherently convert atoms between spin-states.

D.S. Weiss et al., PRA (2004),
Zhang *et al.*, PRA (2006)

Coherent Addressing of Atoms

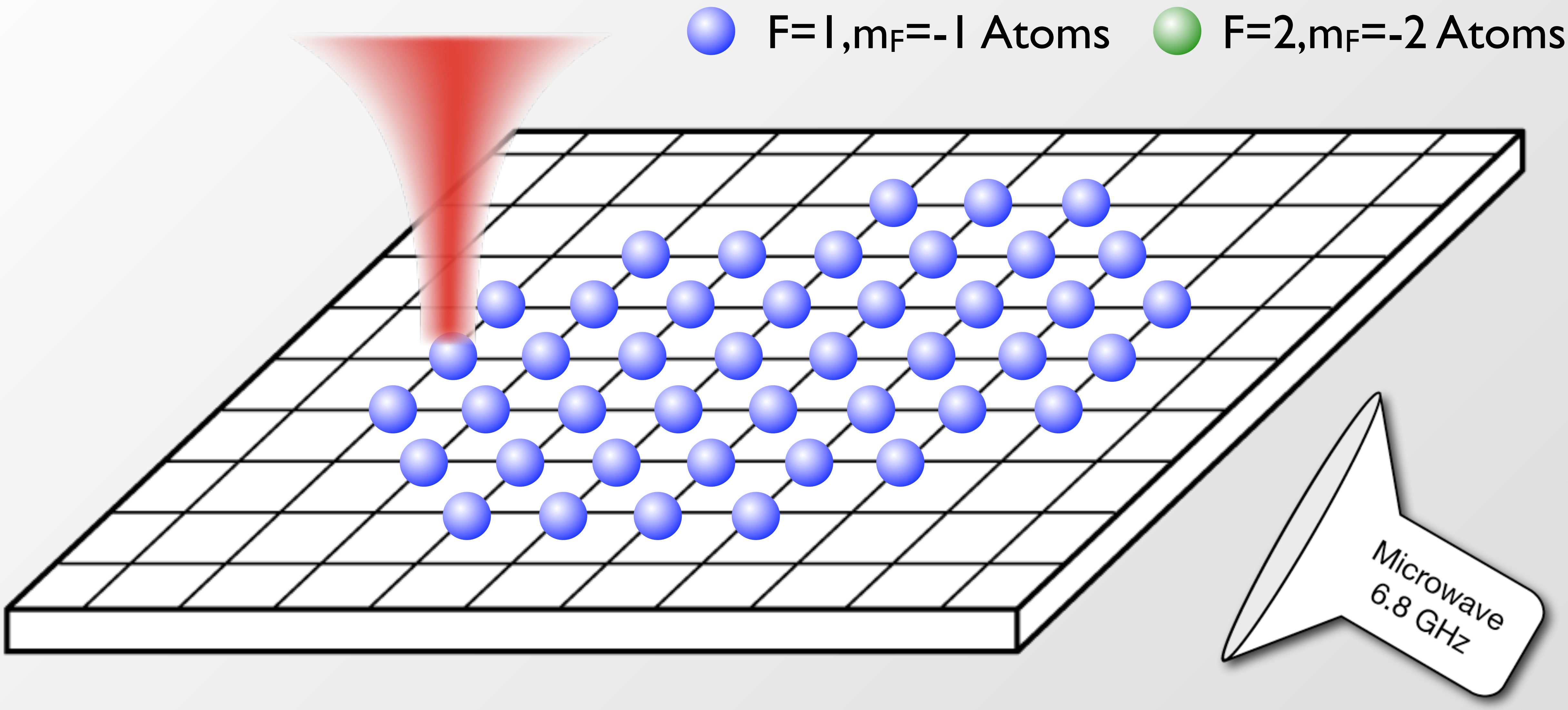

Differential light shift allows to coherently address single atoms!

Landau-Zener Microwave sweep to coherently convert atoms between spin-states.

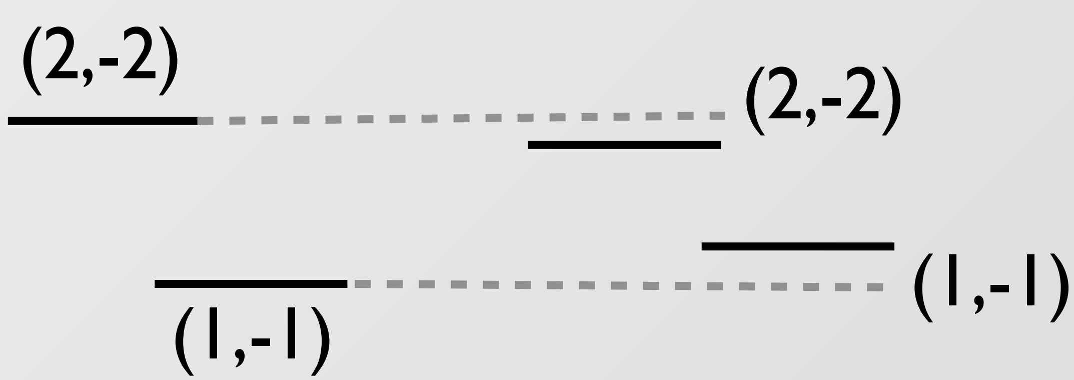

D.S. Weiss et al., PRA (2004),
Zhang *et al.*, PRA (2006)

Coherent Addressing of Atoms

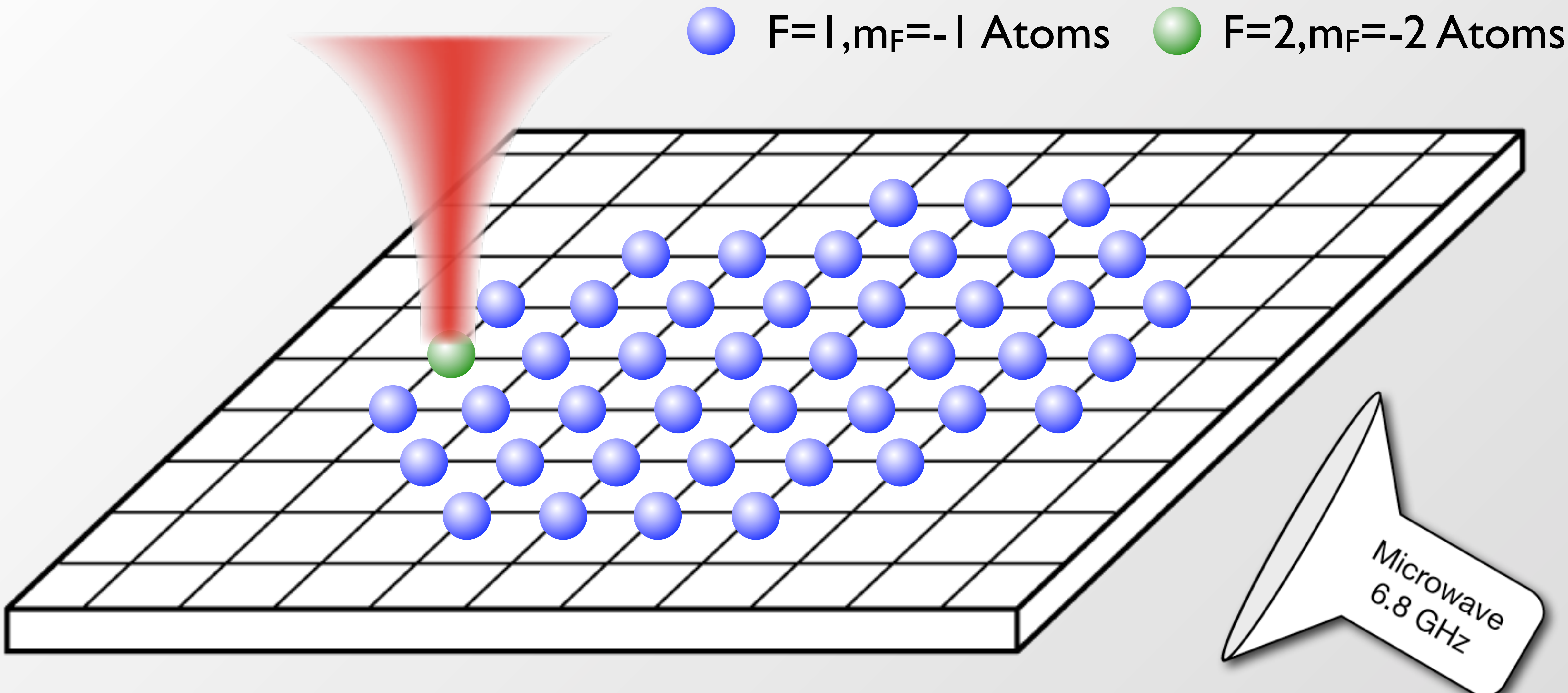

Differential light shift allows to coherently address single atoms!

Landau-Zener Microwave sweep to coherently convert atoms between spin-states.

D.S. Weiss et al., PRA (2004),
Zhang *et al.*, PRA (2006)

Coherent Addressing of Atoms

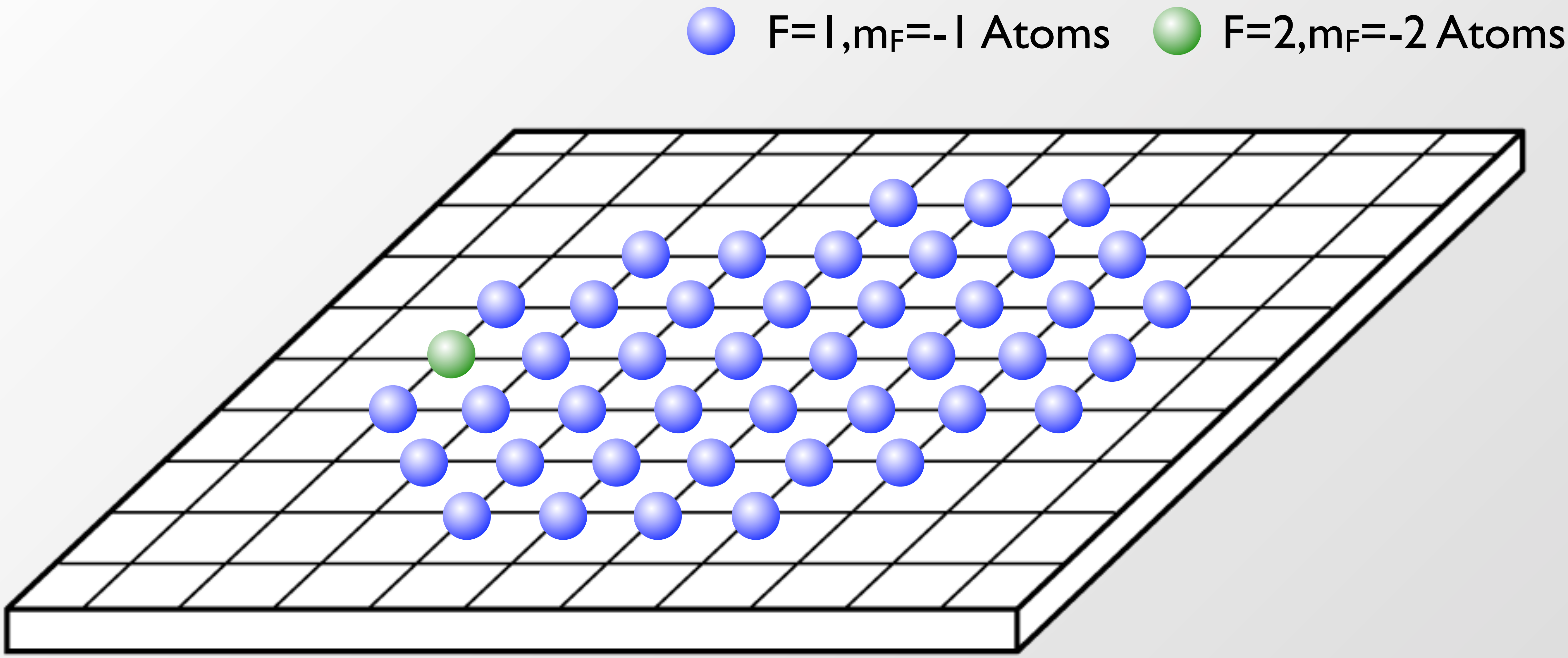

Differential light shift allows to coherently address single atoms!

Landau-Zener Microwave sweep to coherently convert atoms between spin-states.

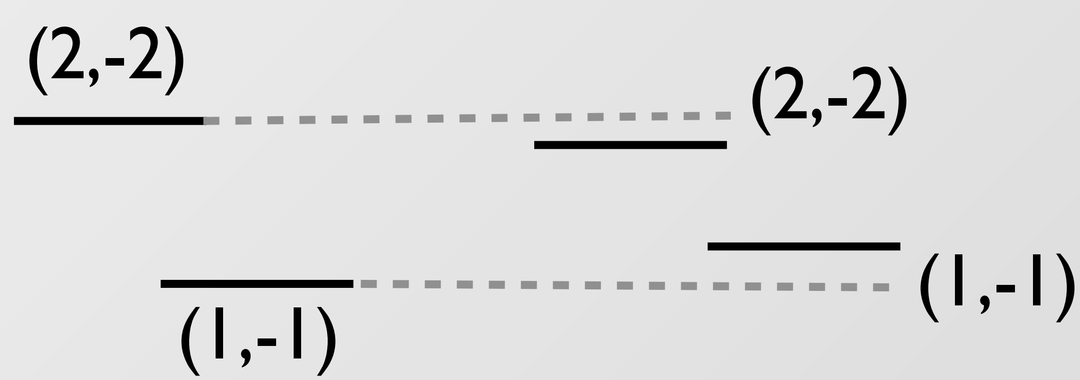

D.S. Weiss et al., PRA (2004),
Zhang *et al.*, PRA (2006)

Coherent Addressing of Atoms

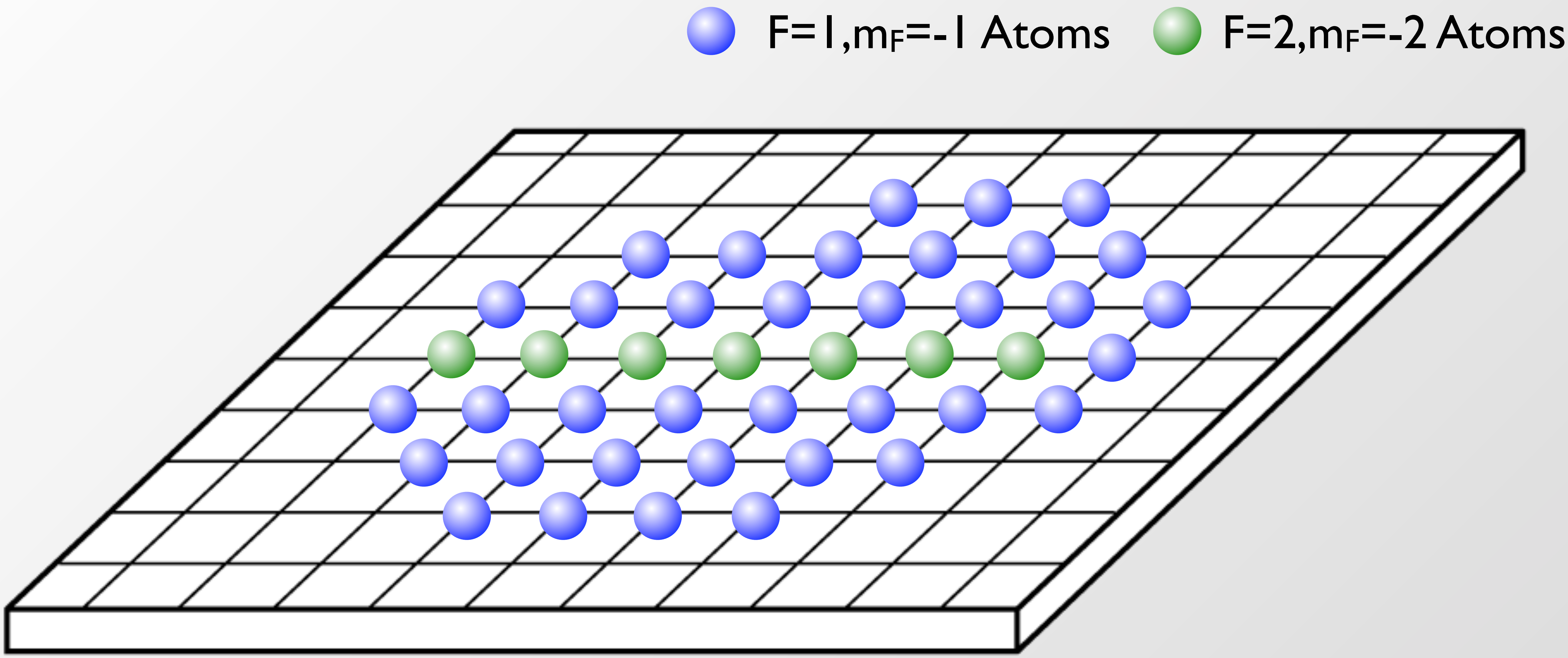

Differential light shift allows to coherently address single atoms!

Landau-Zener Microwave sweep to coherently convert atoms between spin-states.

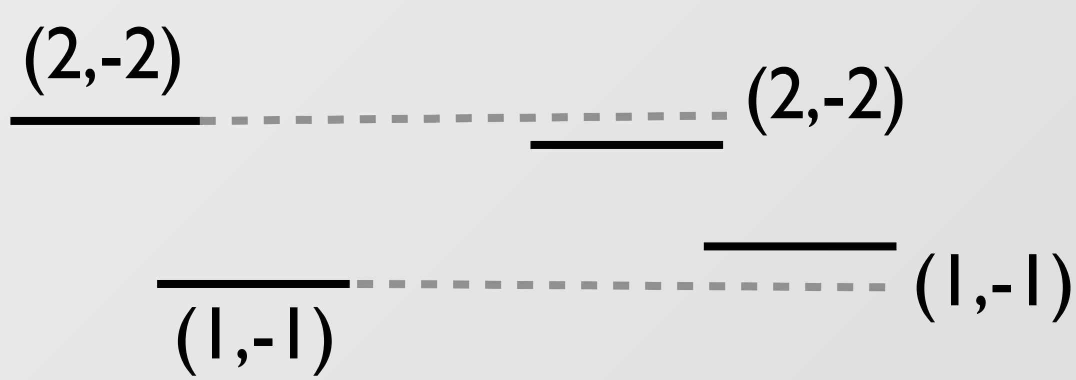

D.S. Weiss et al., PRA (2004),
Zhang *et al.*, PRA (2006)

Coherent Addressing of Atoms

F=1,m_F=-1 Atoms   F=2,m_F=-2 Atoms

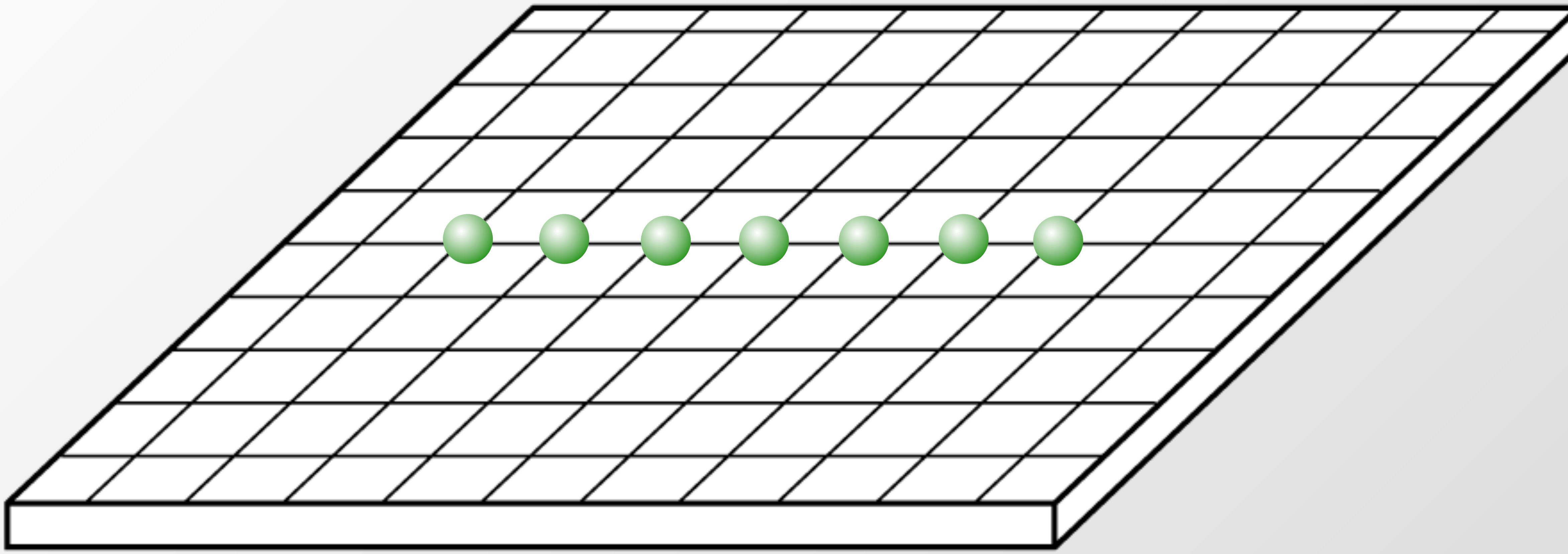

Differential light shift allows to coherently address single atoms!

Landau-Zener Microwave sweep to coherently convert atoms between spin-states.

D.S. Weiss et al., PRA (2004),
Zhang *et al.*, PRA (2006)

Coherent Spin Flips - Positive Imaging

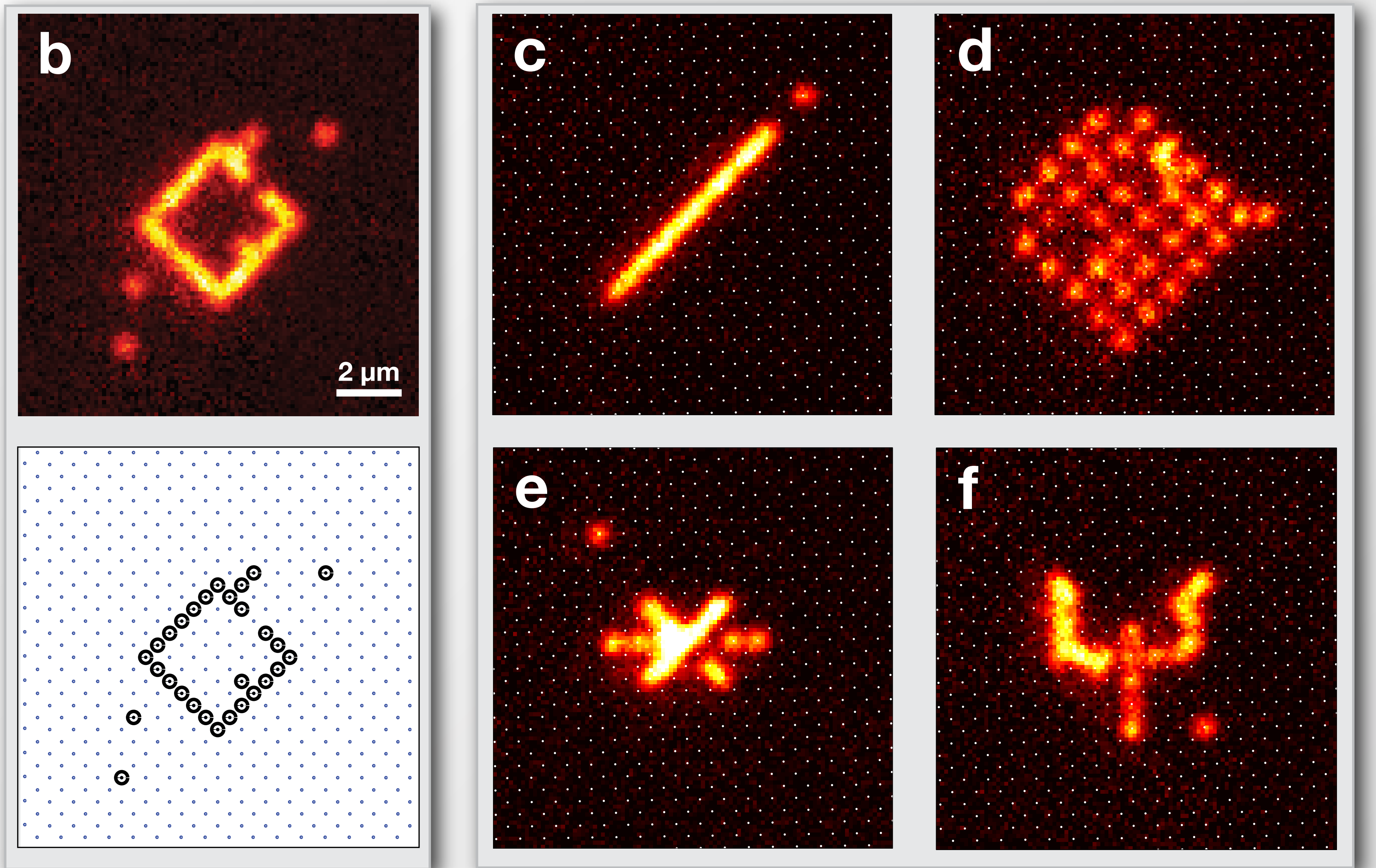

Subwavelength spatial resolution: 50 nm

Ch. Weitenberg et al., Nature **471**, 319-324 (2011)

Arbitrary Light Patterns

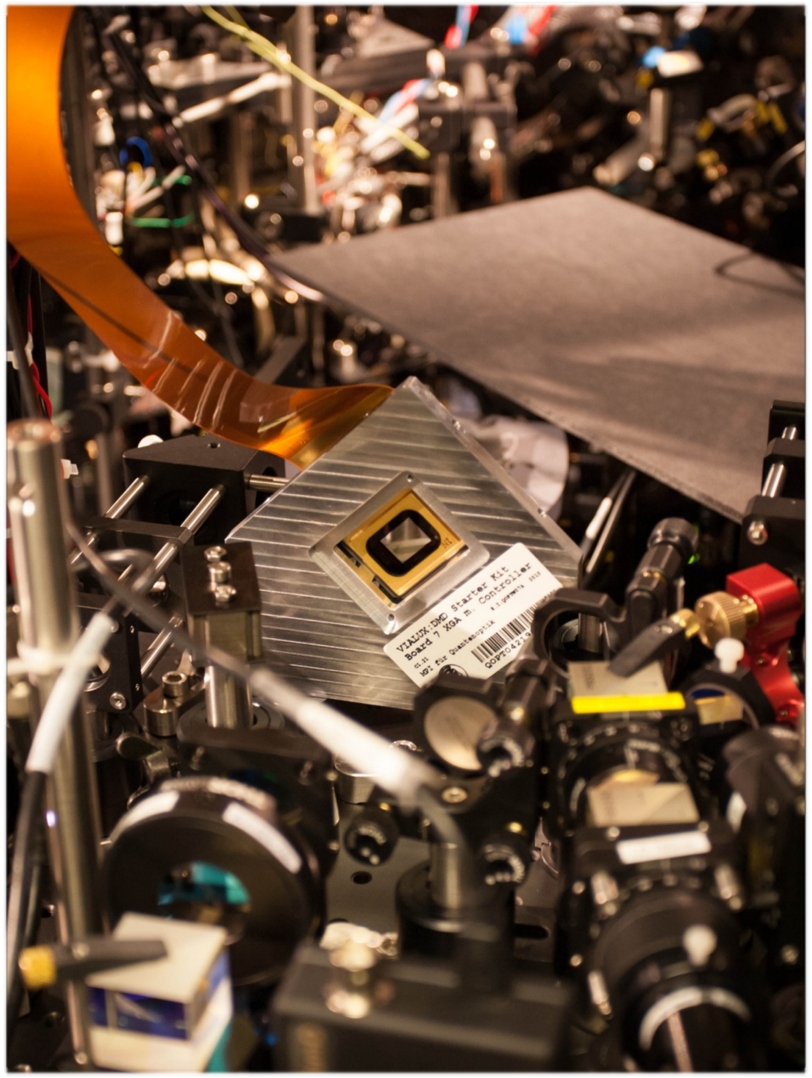

Digital Mirror Device
(DMD)

Arbitrary Light Patterns

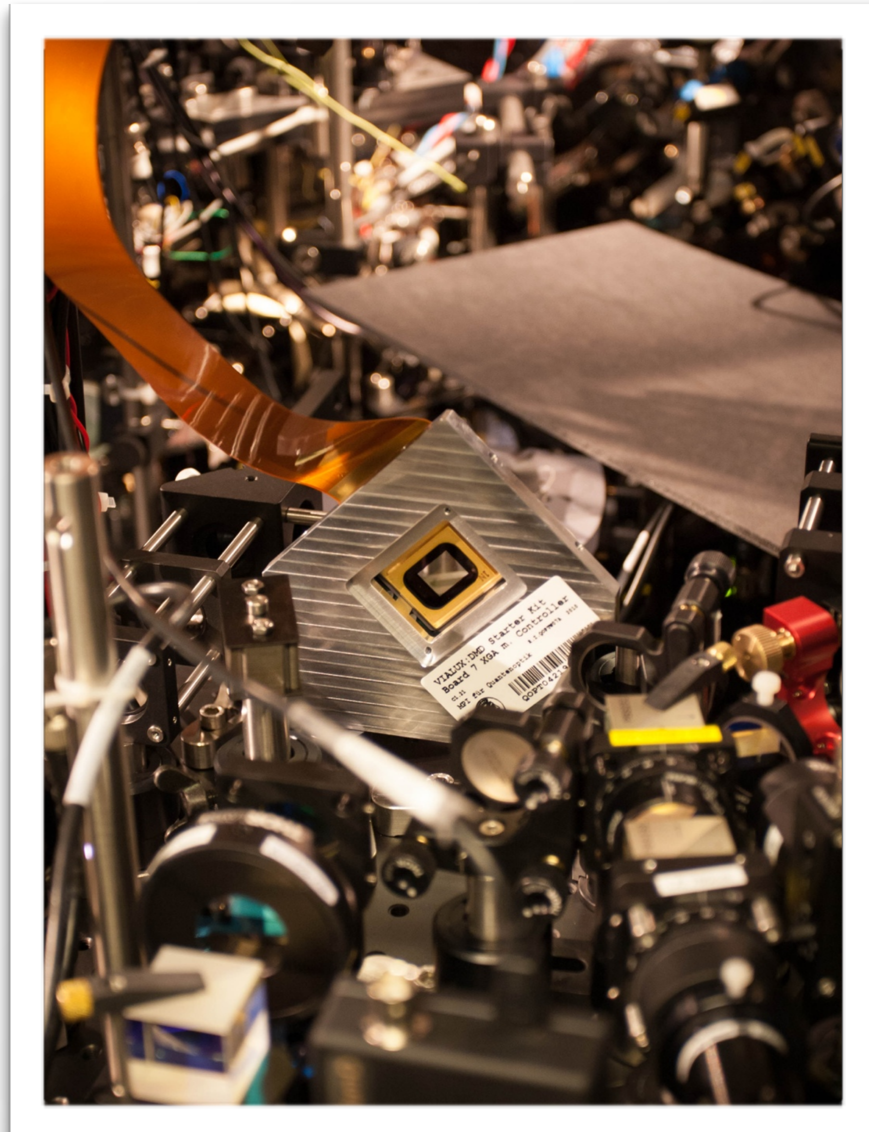

Digital Mirror Device
(DMD)

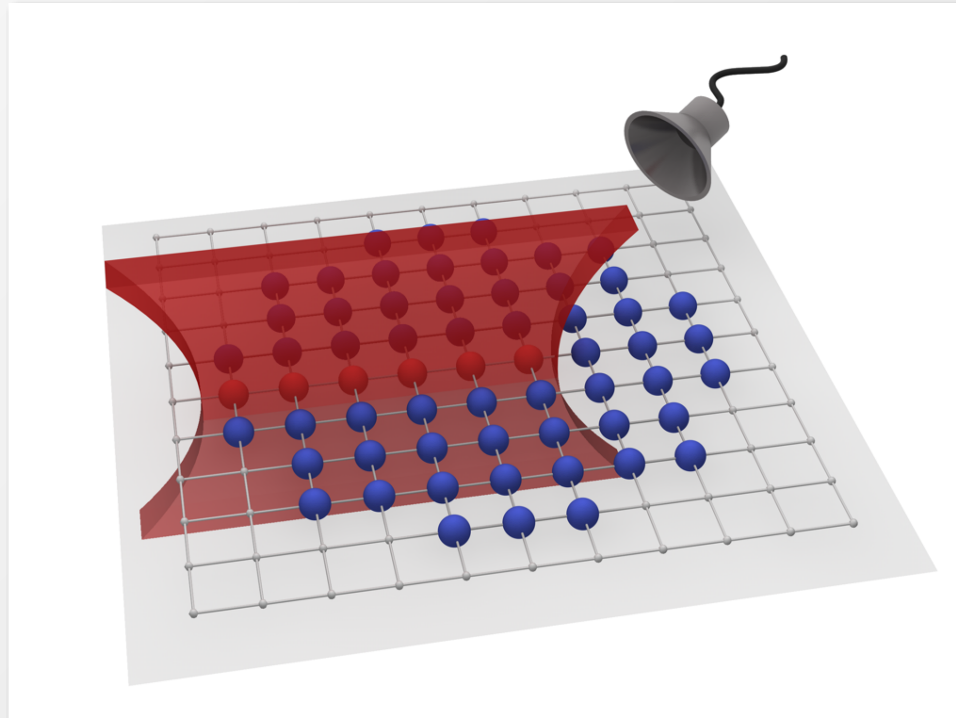

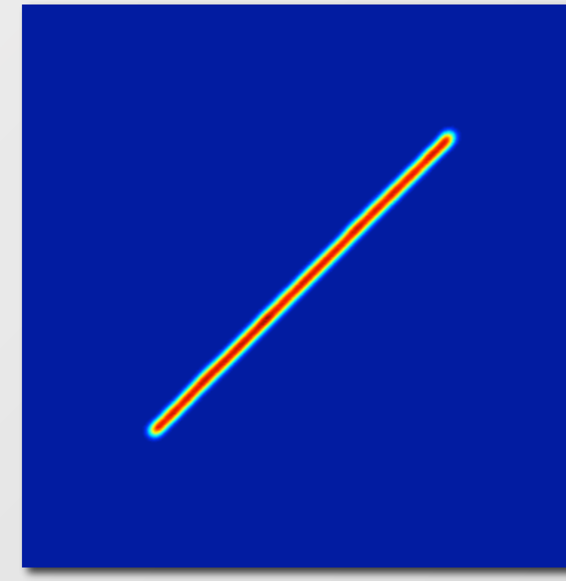

Measured Light Pattern

Arbitrary Light Patterns

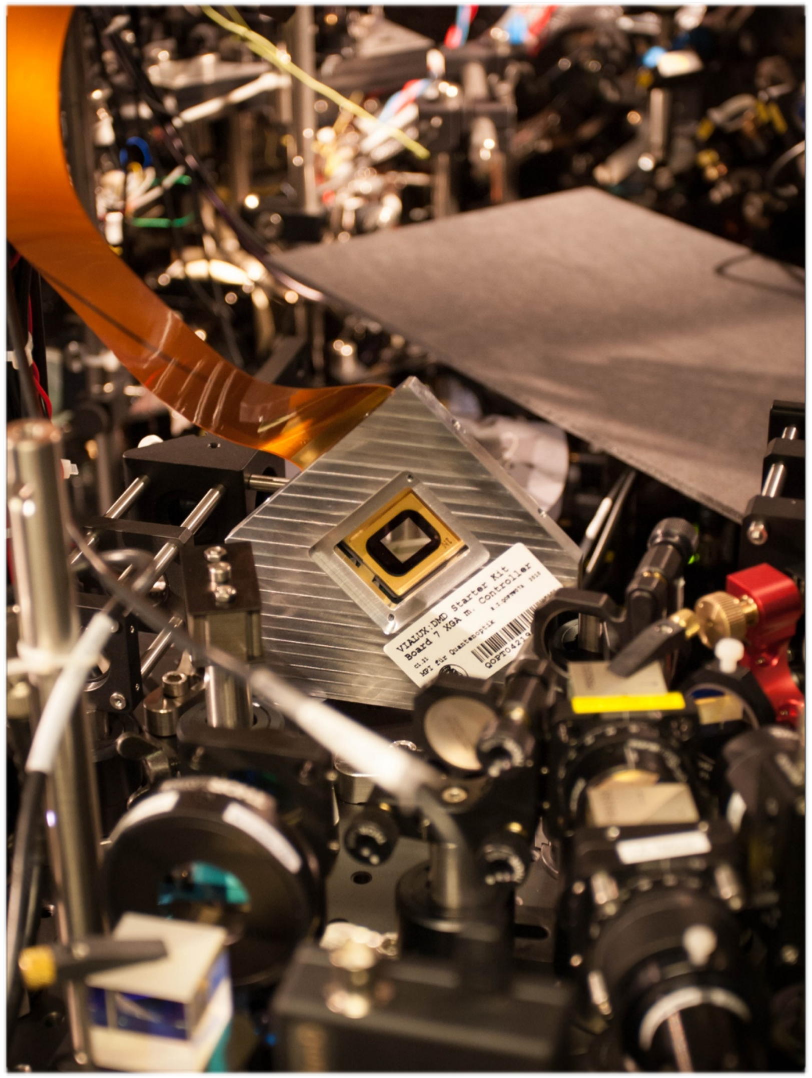

Digital Mirror Device (DMD)

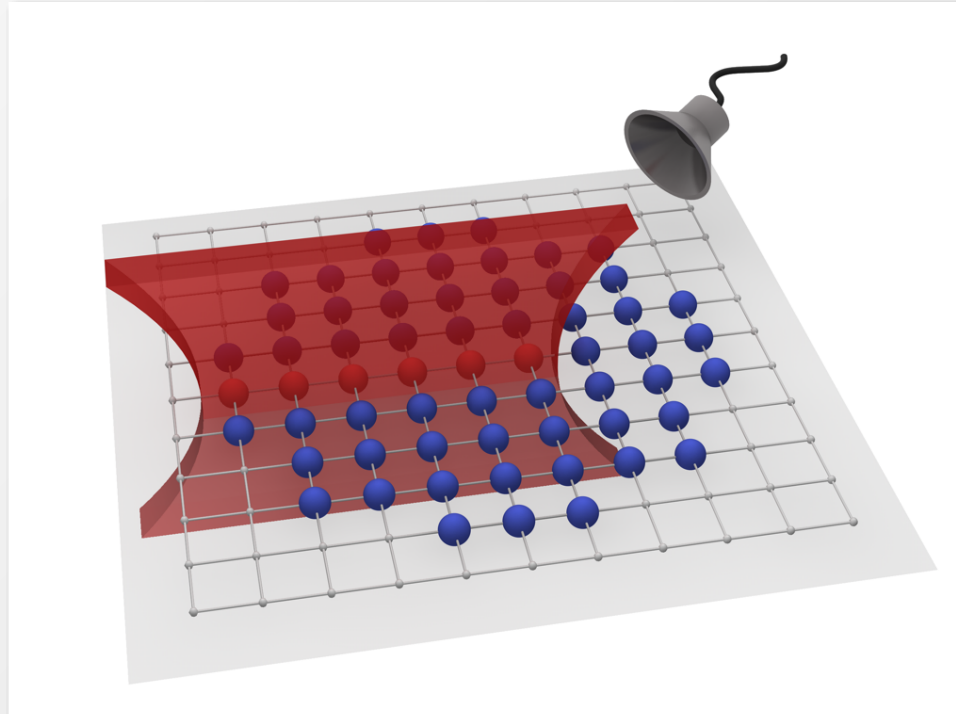

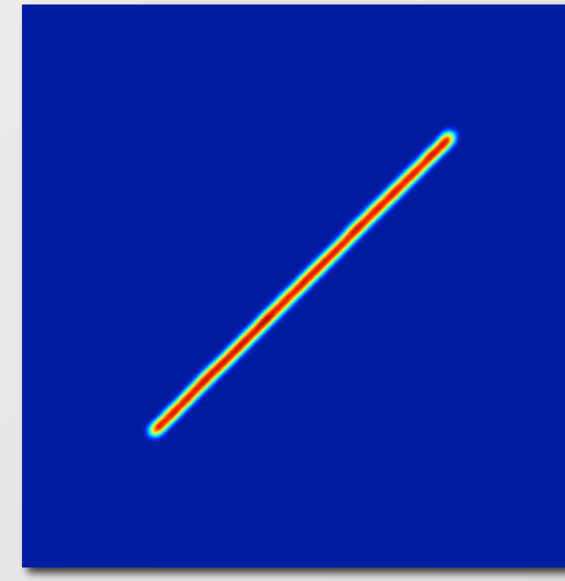

Measured Light Pattern

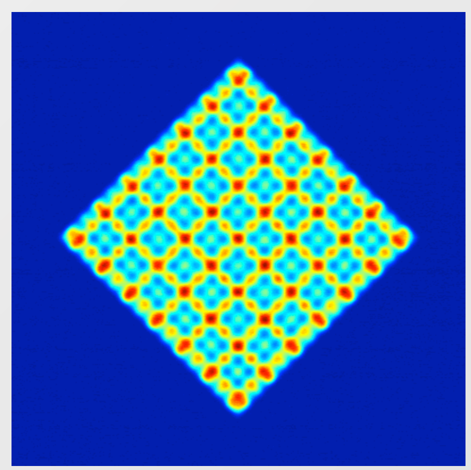

Exotic Lattices

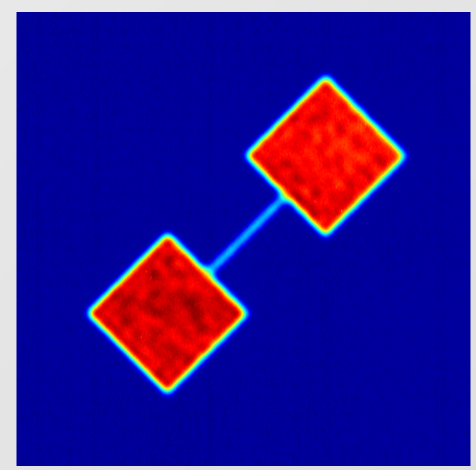

Quantum Wires

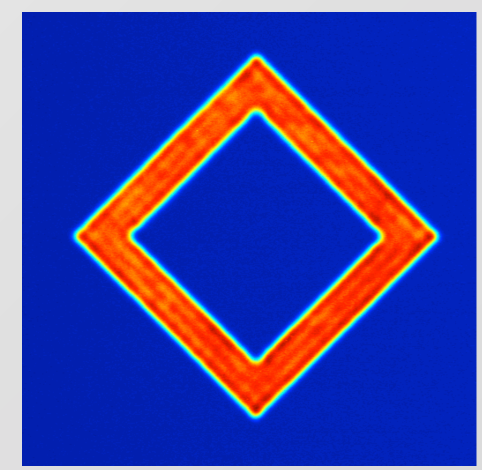

Box Potentials

Almost Arbitrary Light Patterns Possible!

Single Spin Impurity Dynamics, Domain Walls, Quantum Wires, Novel Exotic Lattice Geometries, ...

Spin impurity dynamics

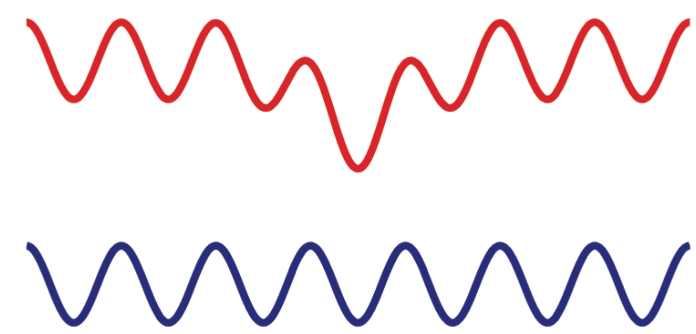

$|2\rangle = |F=2, m_F=-2\rangle$

$|1\rangle = |F=1, m_F=-1\rangle$

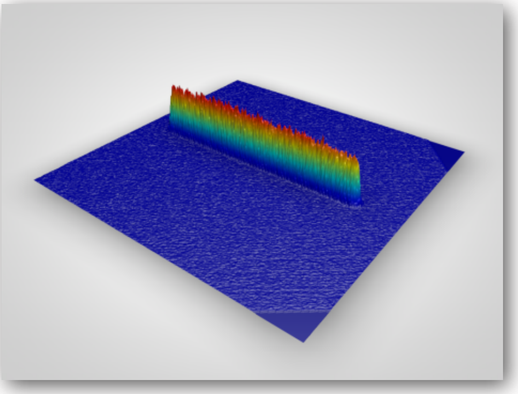

Line-shaped light field created with DMD SLM

T. Fukuhara et al., Nature Physics **9**, 235 (2013)

Spin impurity dynamics

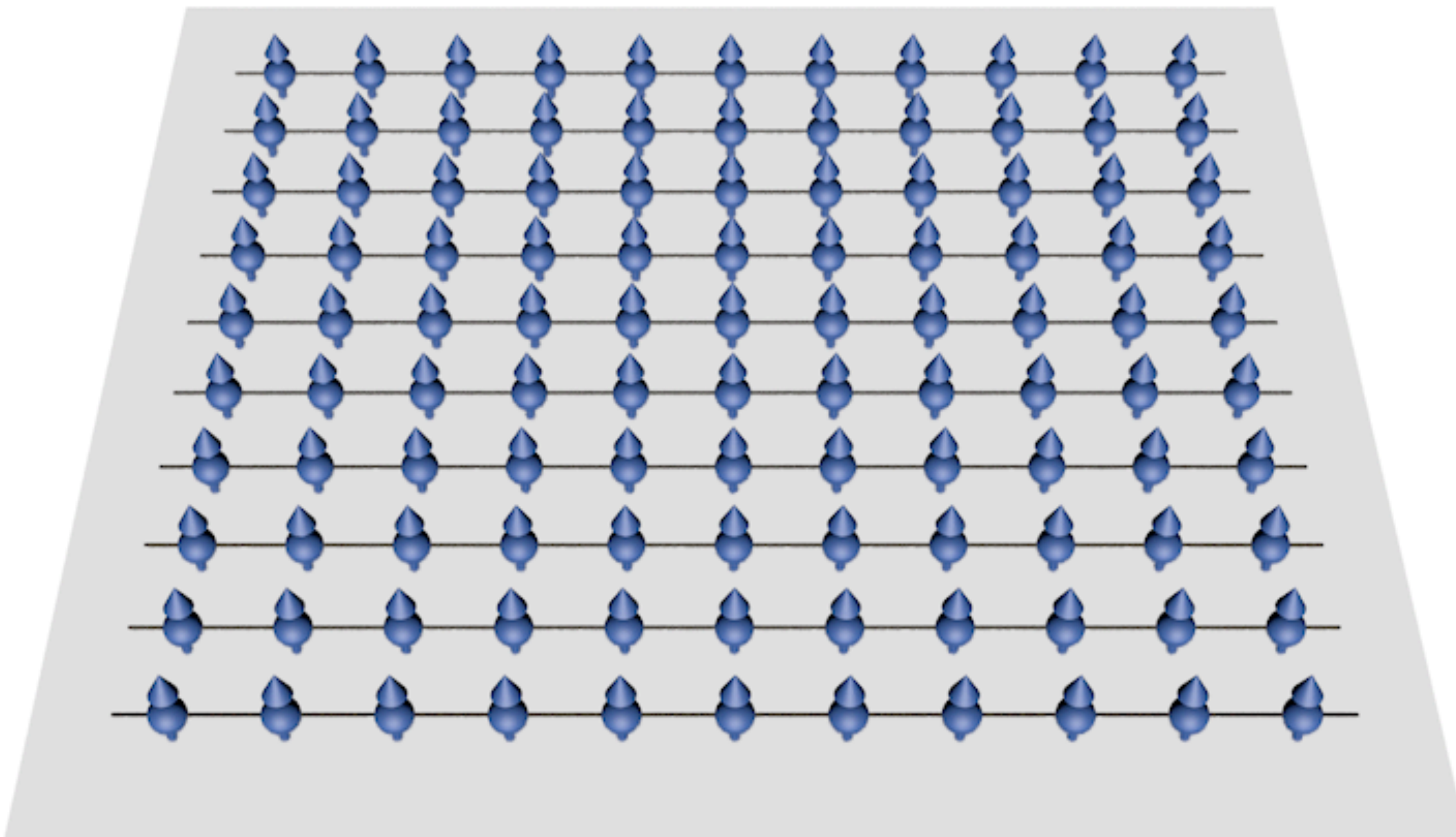

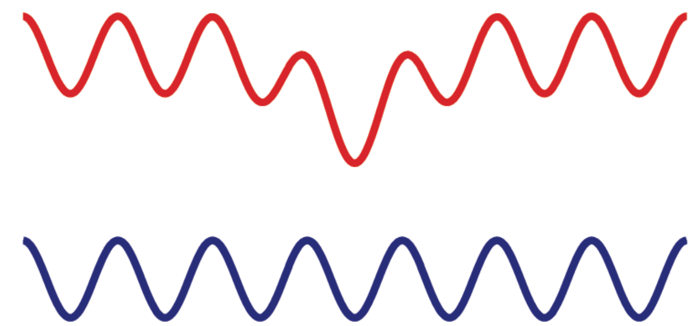

$|2\rangle = |F=2, m_F=-2\rangle$

$|1\rangle = |F=1, m_F=-1\rangle$

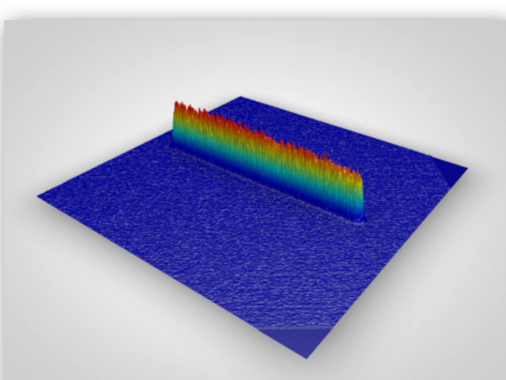

Line-shaped light field created with DMD SLM

T. Fukuhara et al., Nature Physics **9**, 235 (2013)

Ultimate Size Control in 2D

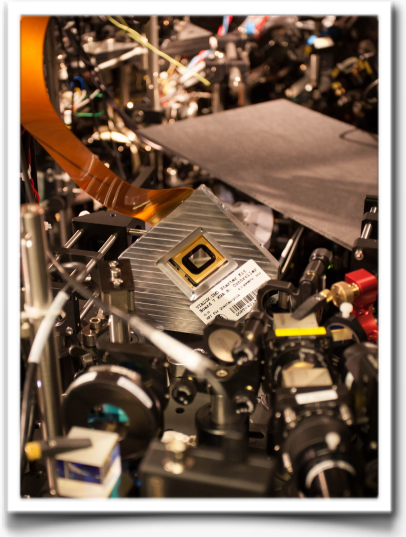

Digital Mirror Device (Size Control)

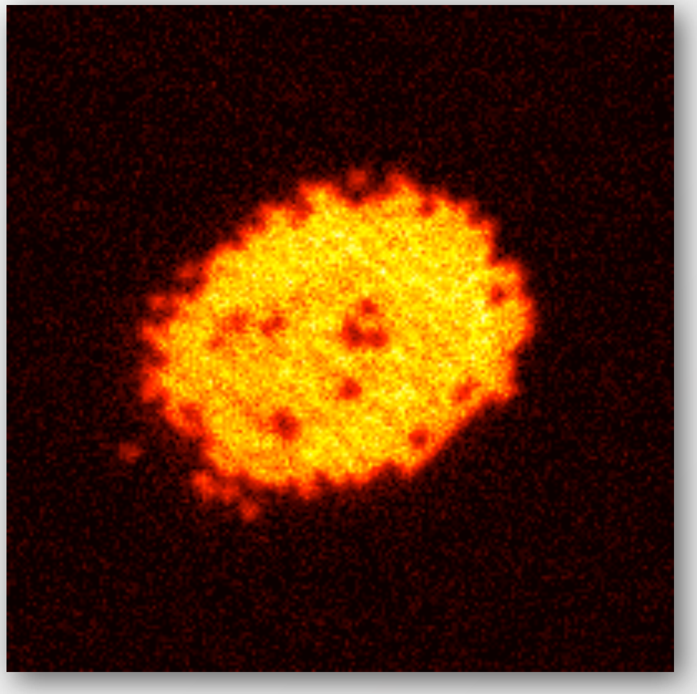

Fluctuating Size and non-perfect shape

Ultimate Size Control in 2D

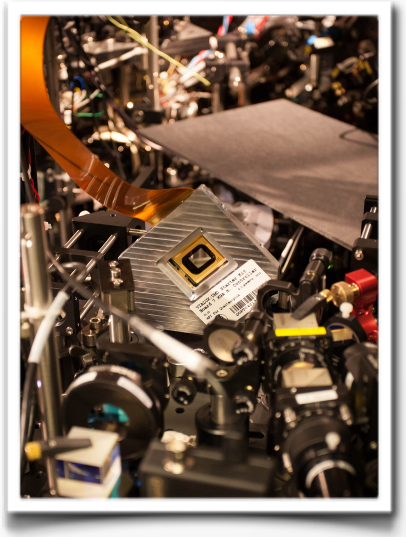

Digital Mirror Device (Size Control)

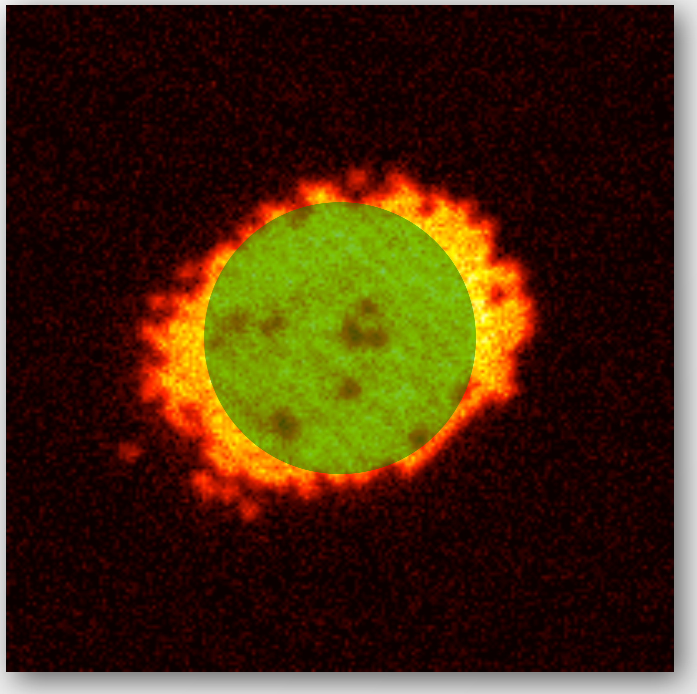

Fluctuating Size and non-perfect shape

Ultimate Size Control in 2D

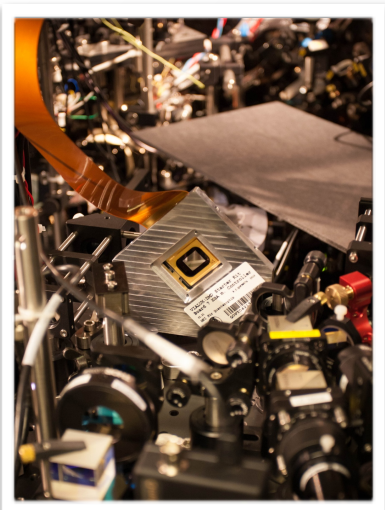

Digital Mirror
Device (Size Control)

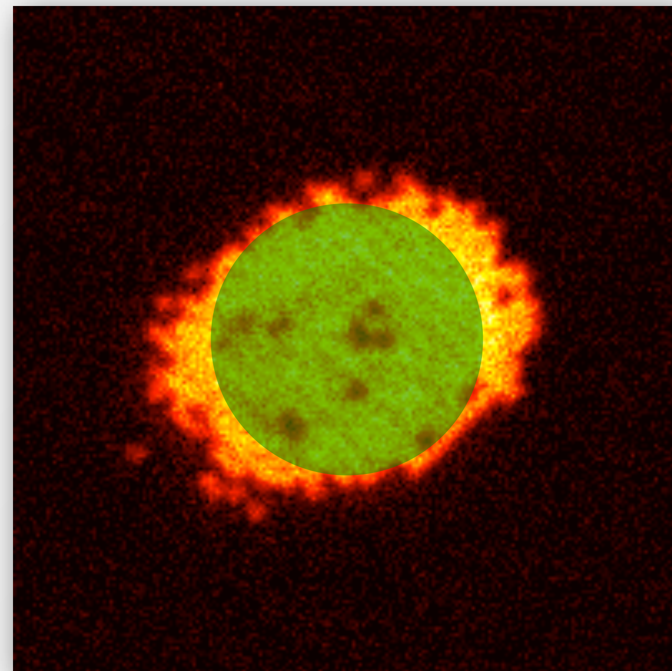

Fluctuating Size and
non-perfect shape

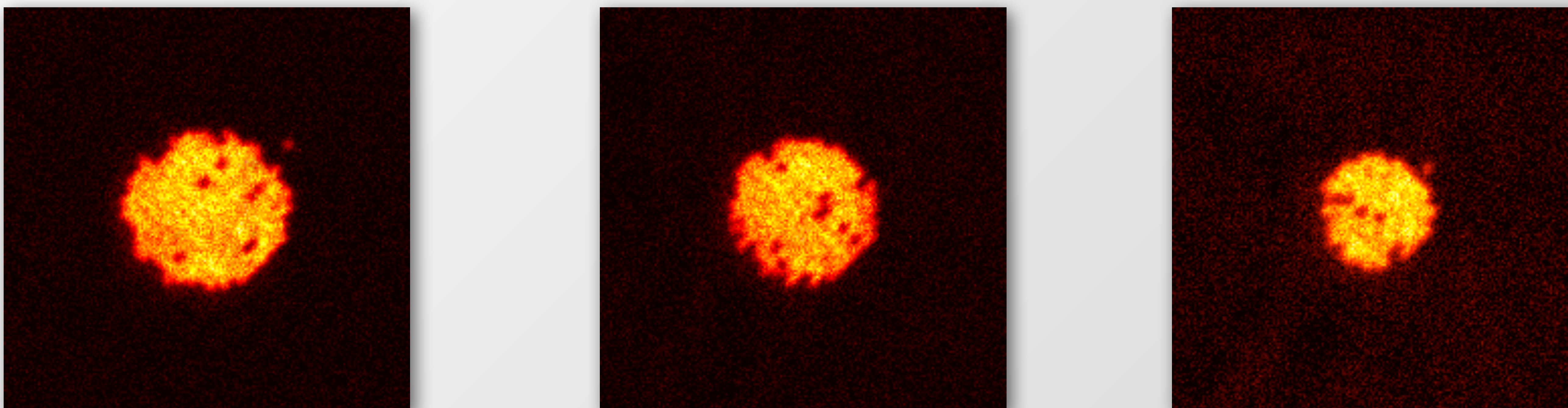

Size & atom number perfectly controlled

Ultimate Size Control in 2D

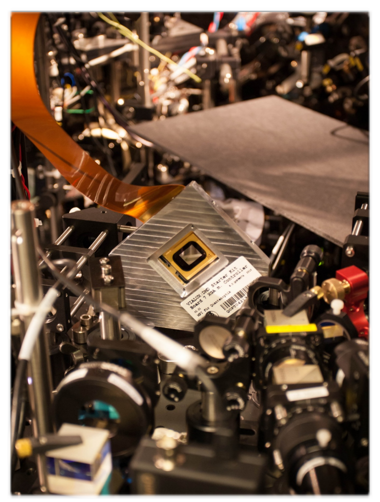

Digital Mirror Device (Size Control)

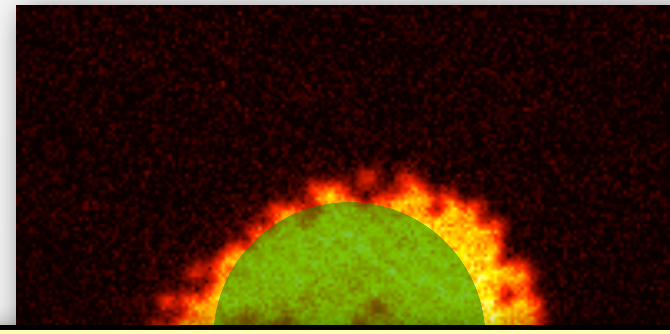

Fluctuating Size and

- **Sub Shot Noise Atom Number Preparation**
- **Geometric & atom number control**
(crucial e.g. for quantum criticality)
- **Hard wall potentials realized**
(crucial for edge states)

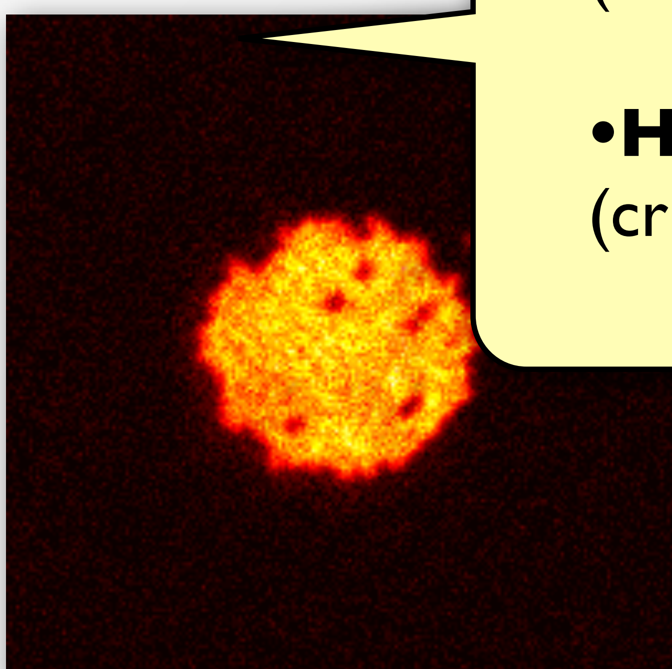

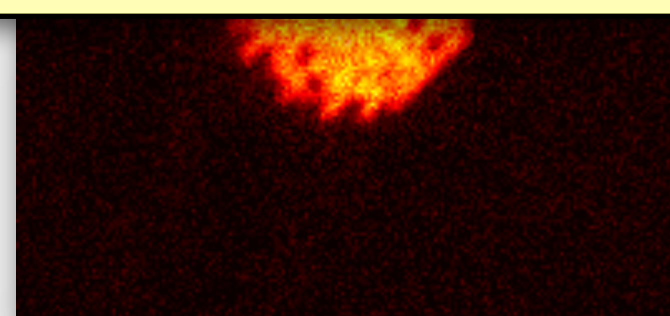

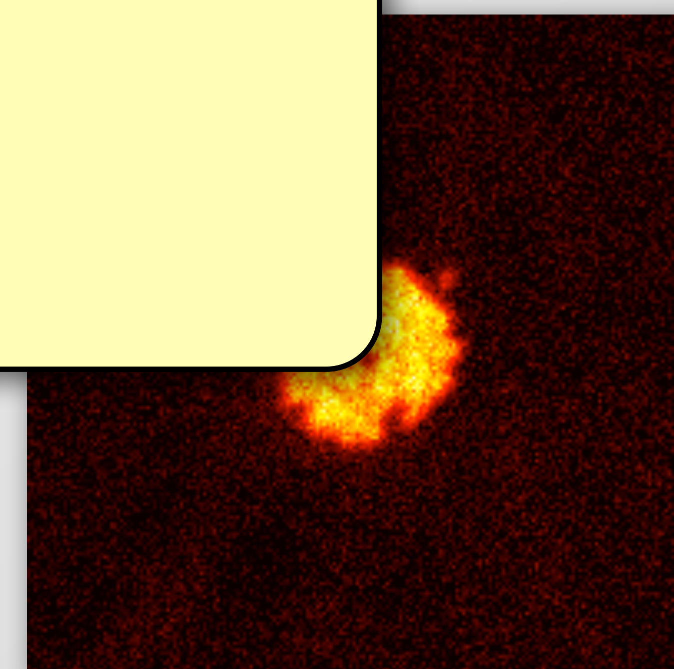

Size & atom number perfectly controlled

Ultimate Size Control in 2D

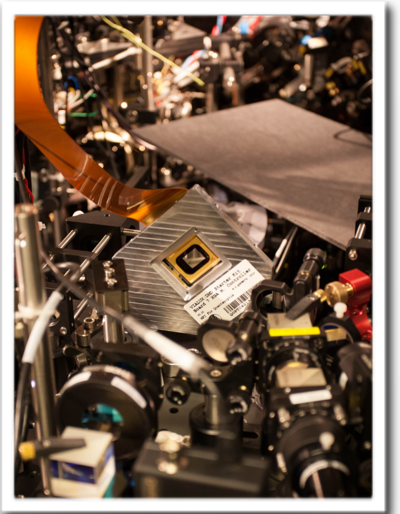

Digital Mirror Device (Size Control)

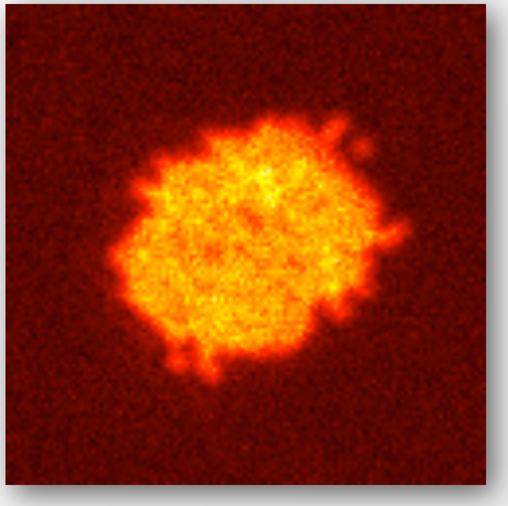

Initial MI

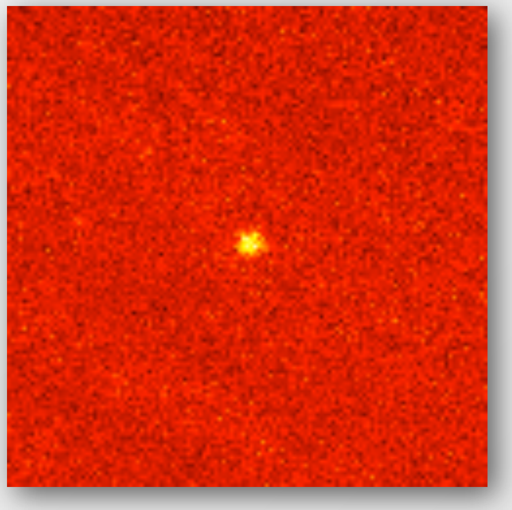

Single Atom

Ultimate Size Control in 2D

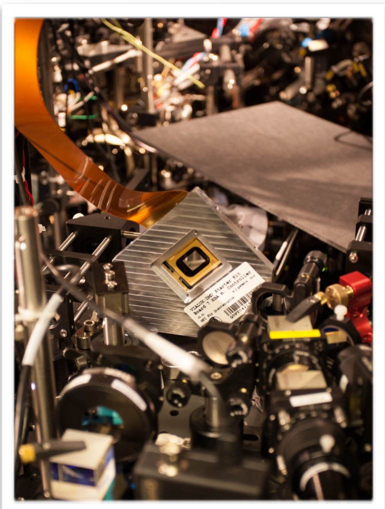

Digital Mirror Device (Size Control)

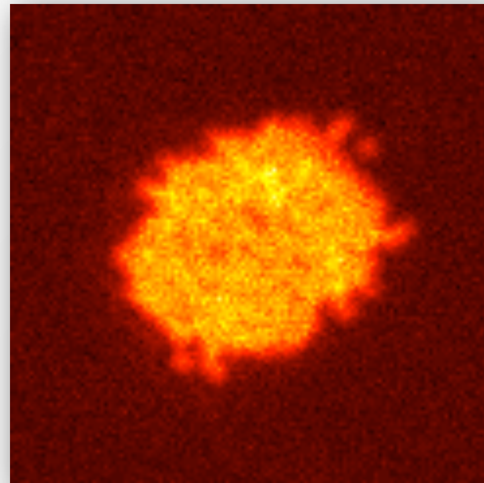

Initial MI

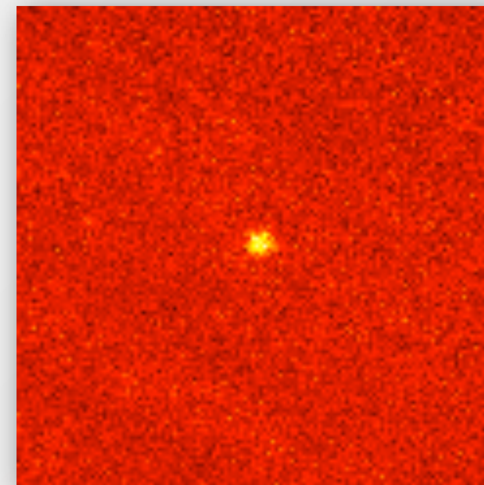

Single Atom

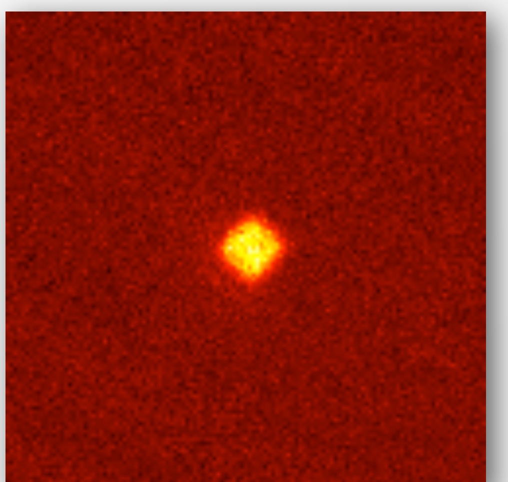

3x3

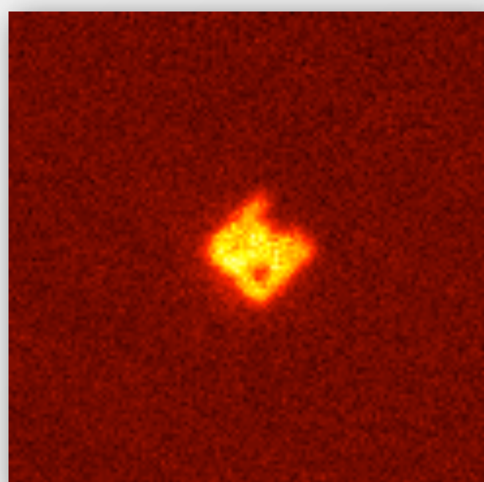

5x5

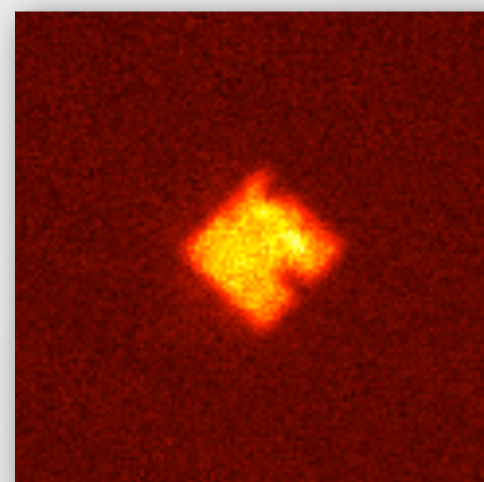

7x7

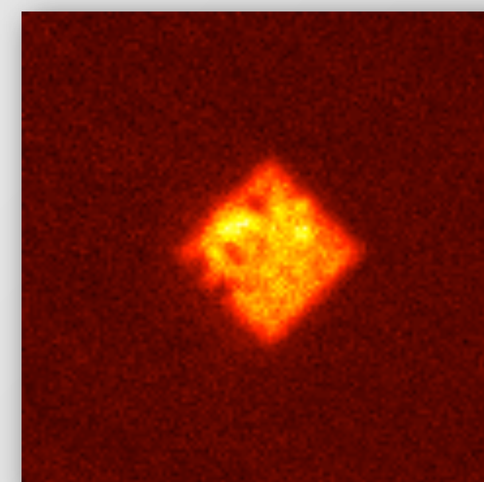

8x8

atoms

Tunneling of a Single Atom

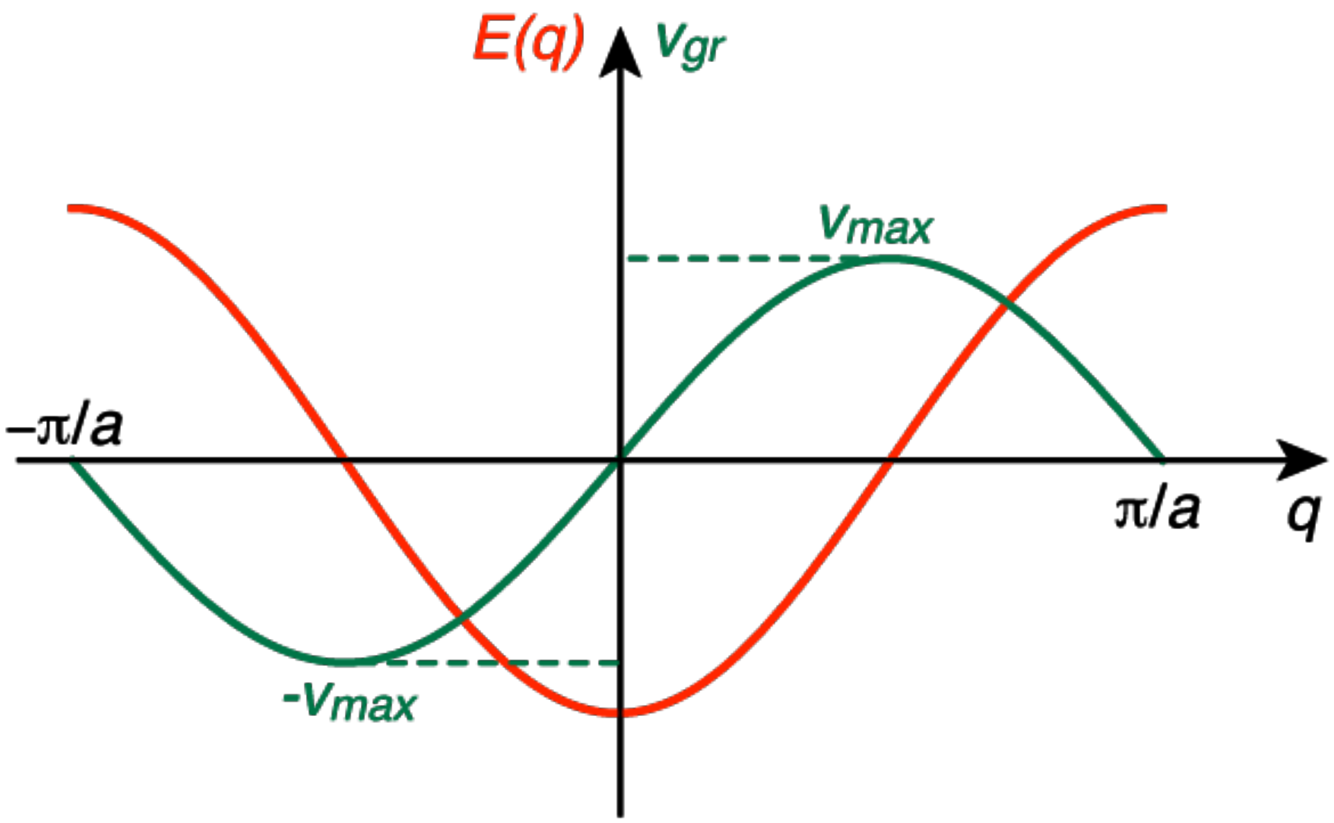

Probability

Position (lattice site)

$$H = -J^{(0)} \sum_{\langle i,j \rangle} \hat{a}_i^\dagger \hat{a}_j + \sum_i \frac{1}{2} m\omega^2 a_{\text{lat}}^2 i^2 \hat{n}_i$$

Tunneling of a Single Atom

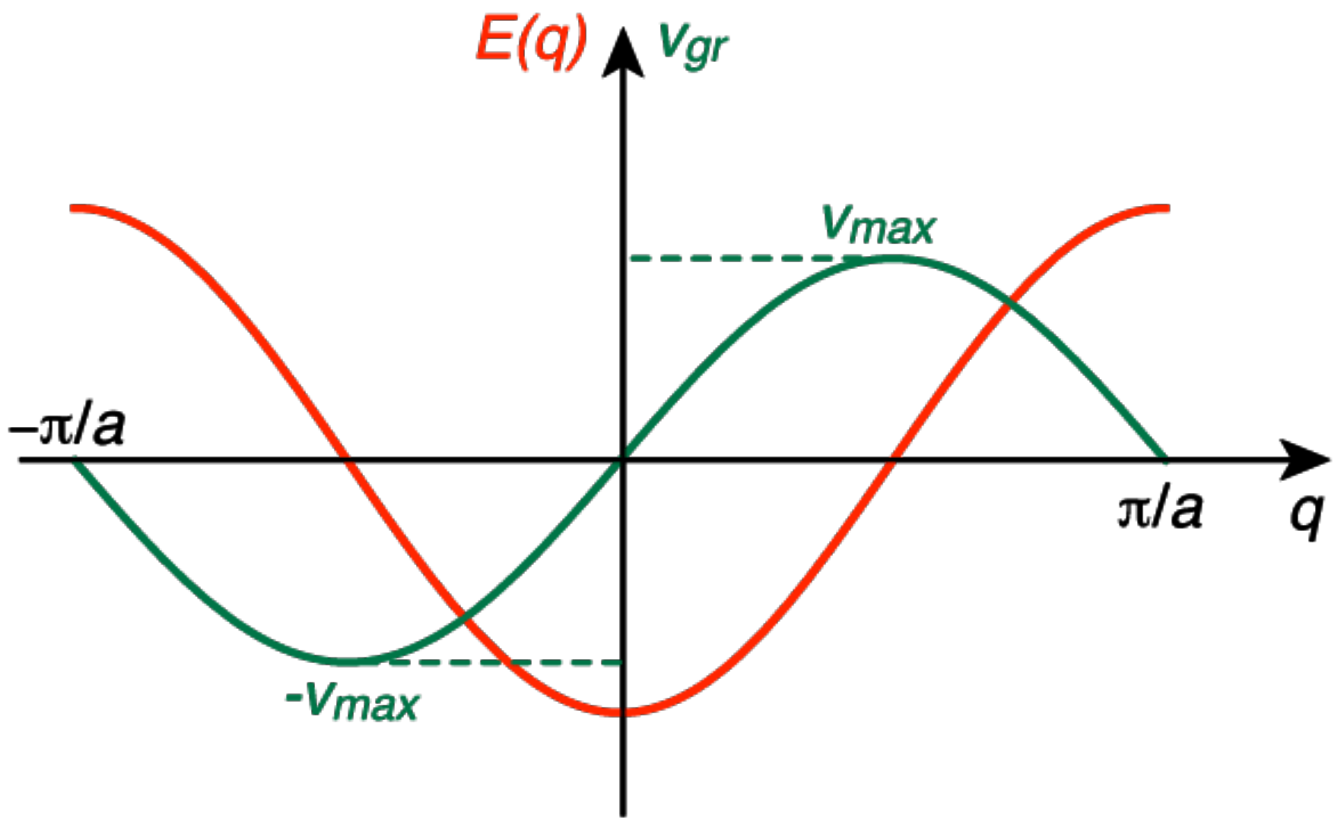

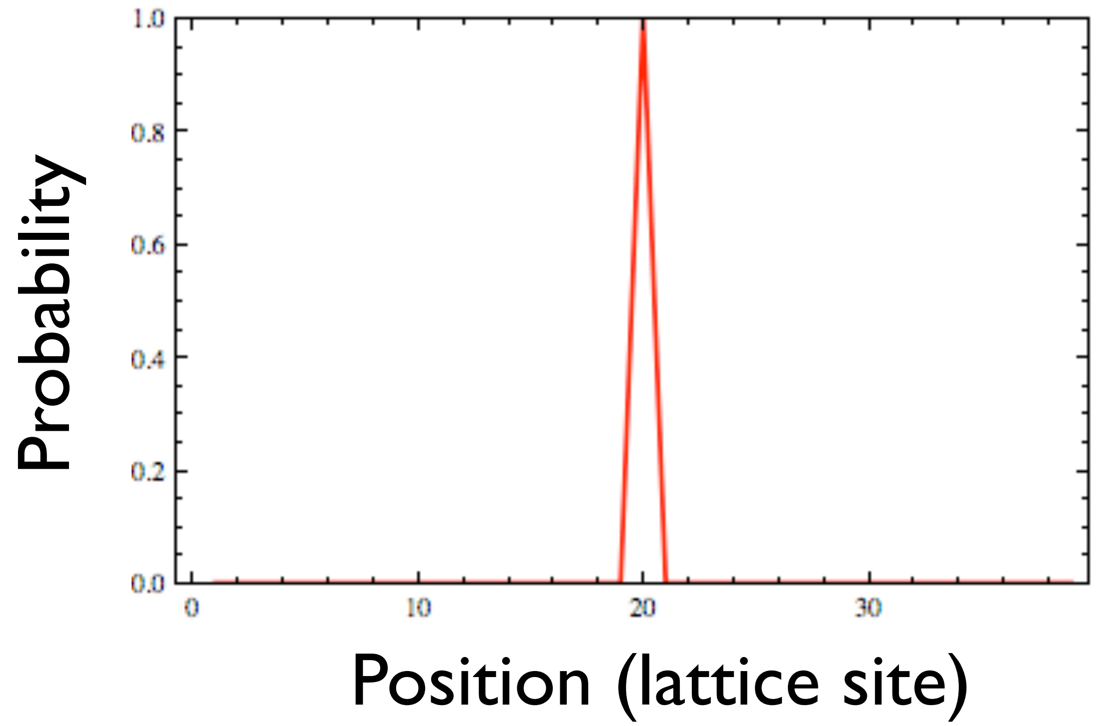

$$H = -J^{(0)} \sum_{\langle i,j \rangle} \hat{a}_i^\dagger \hat{a}_j + \sum_i \frac{1}{2} m\omega^2 a_{\mathrm{lat}}^2 i^2 \hat{n}_i$$

Tunneling of a Single Atom

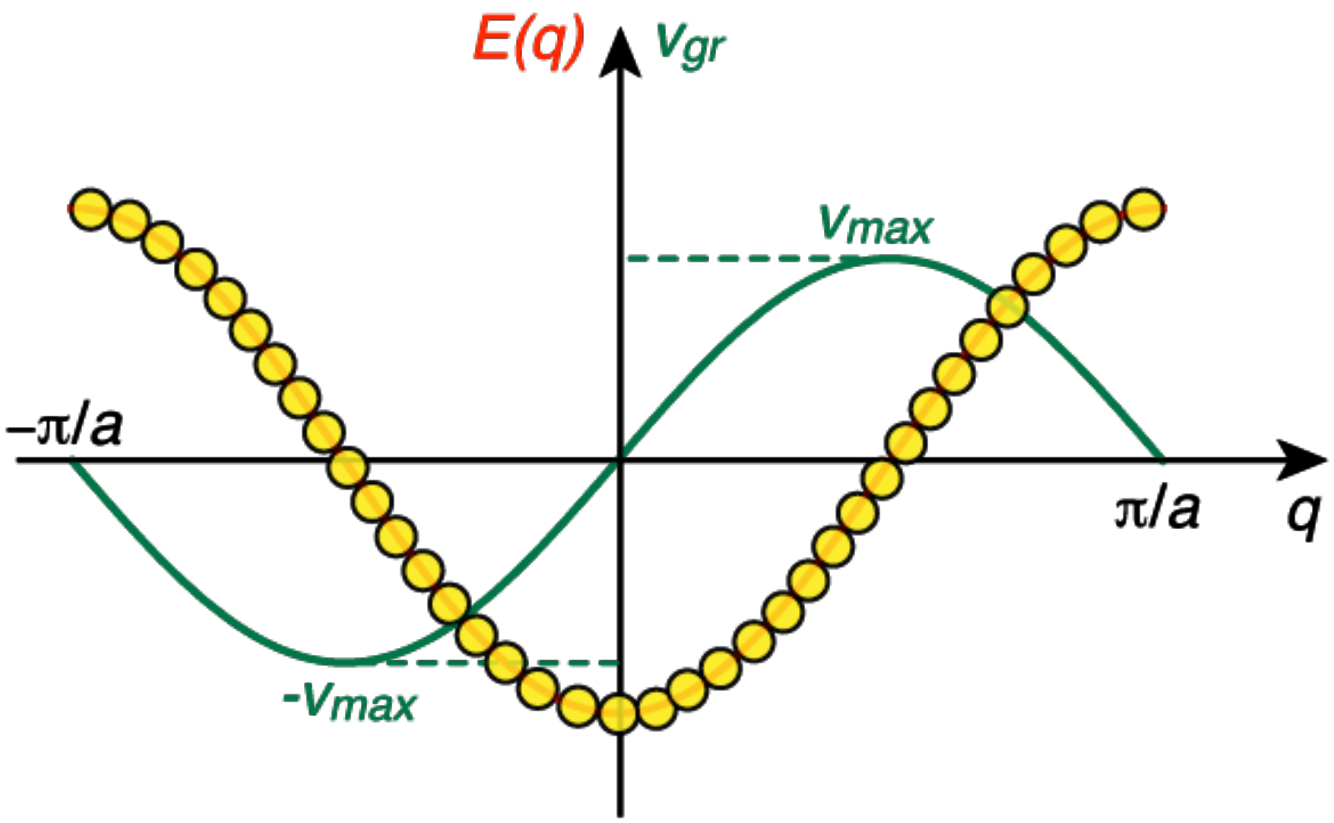

$$v_{max} = \frac{2Ja}{\hbar}$$

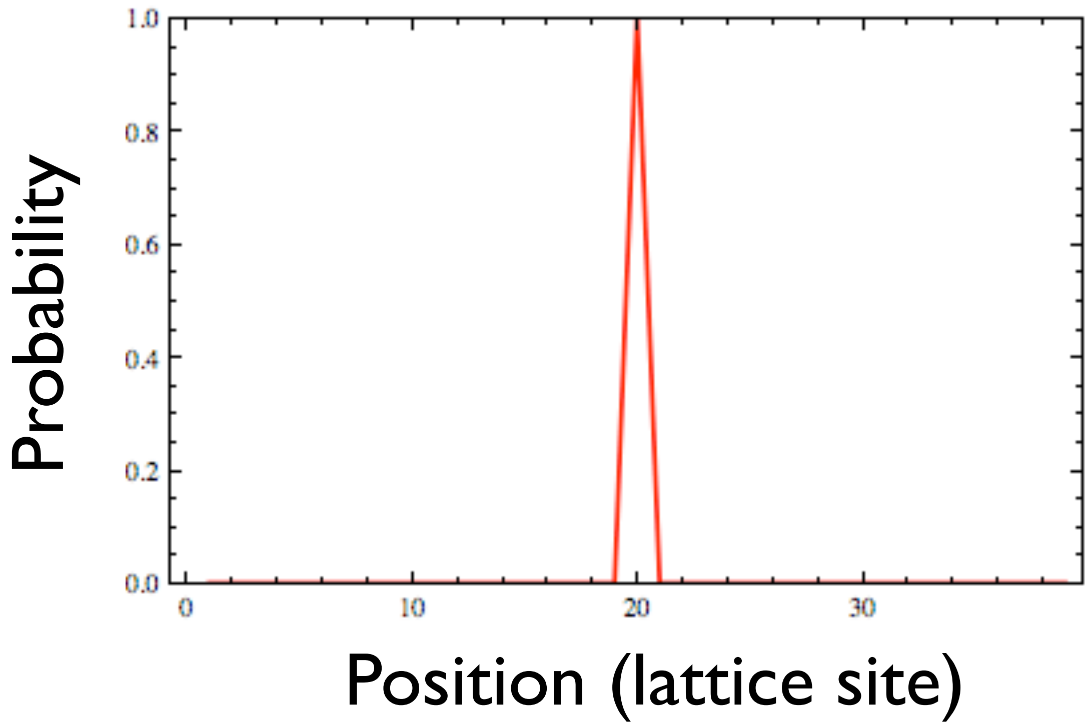

$$H = -J^{(0)} \sum_{\langle i,j \rangle} \hat{a}_i^{\dagger} \hat{a}_j + \sum_i \frac{1}{2} m \omega^2 a_{\mathrm{lat}}^2 i^2 \hat{n}_i$$

Single Atom Tunnelling

Single Atom Tunnelling

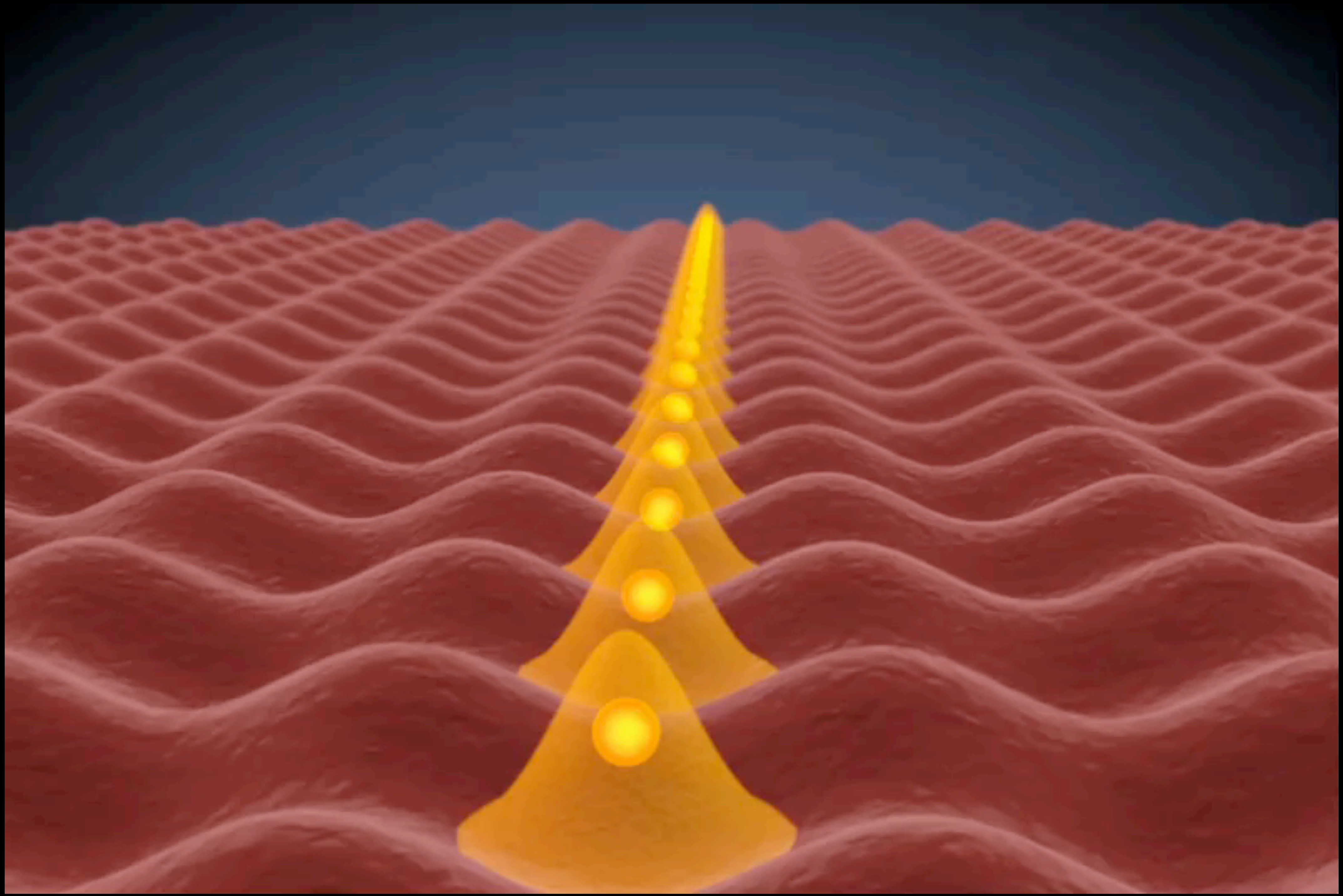

Motional State Affected?

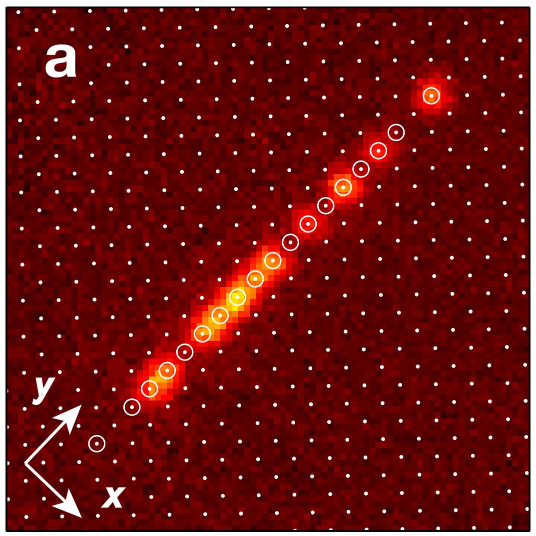

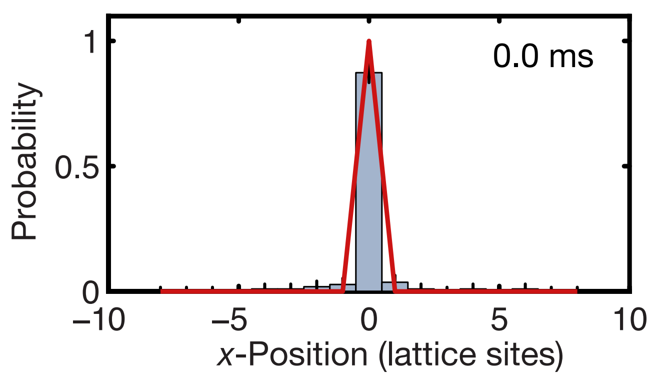

see exp: Y. Silberberg (photonic waveguides), D. Meschede & R. Blatt (quantum walks)...

Motional State Affected?

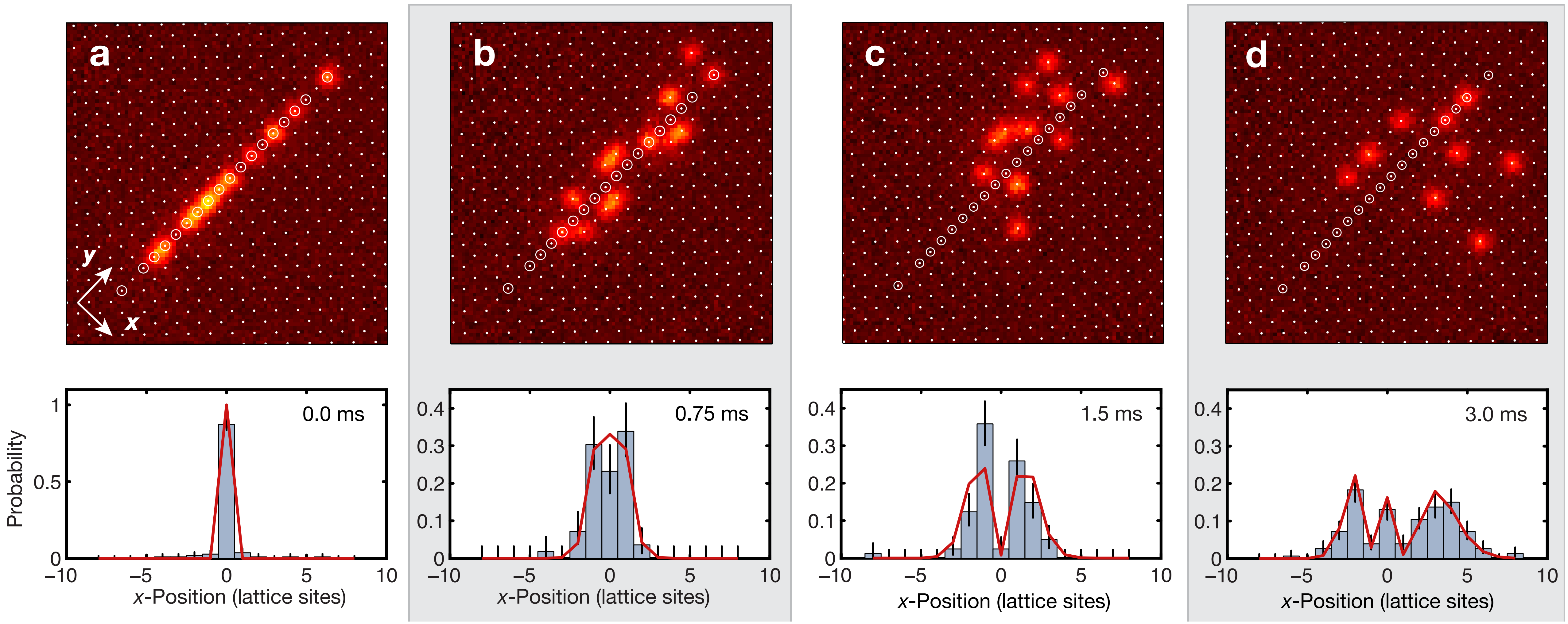

see exp: Y. Silberberg (photonic waveguides), D. Meschede & R. Blatt (quantum walks)...

Higher Band Tunneling

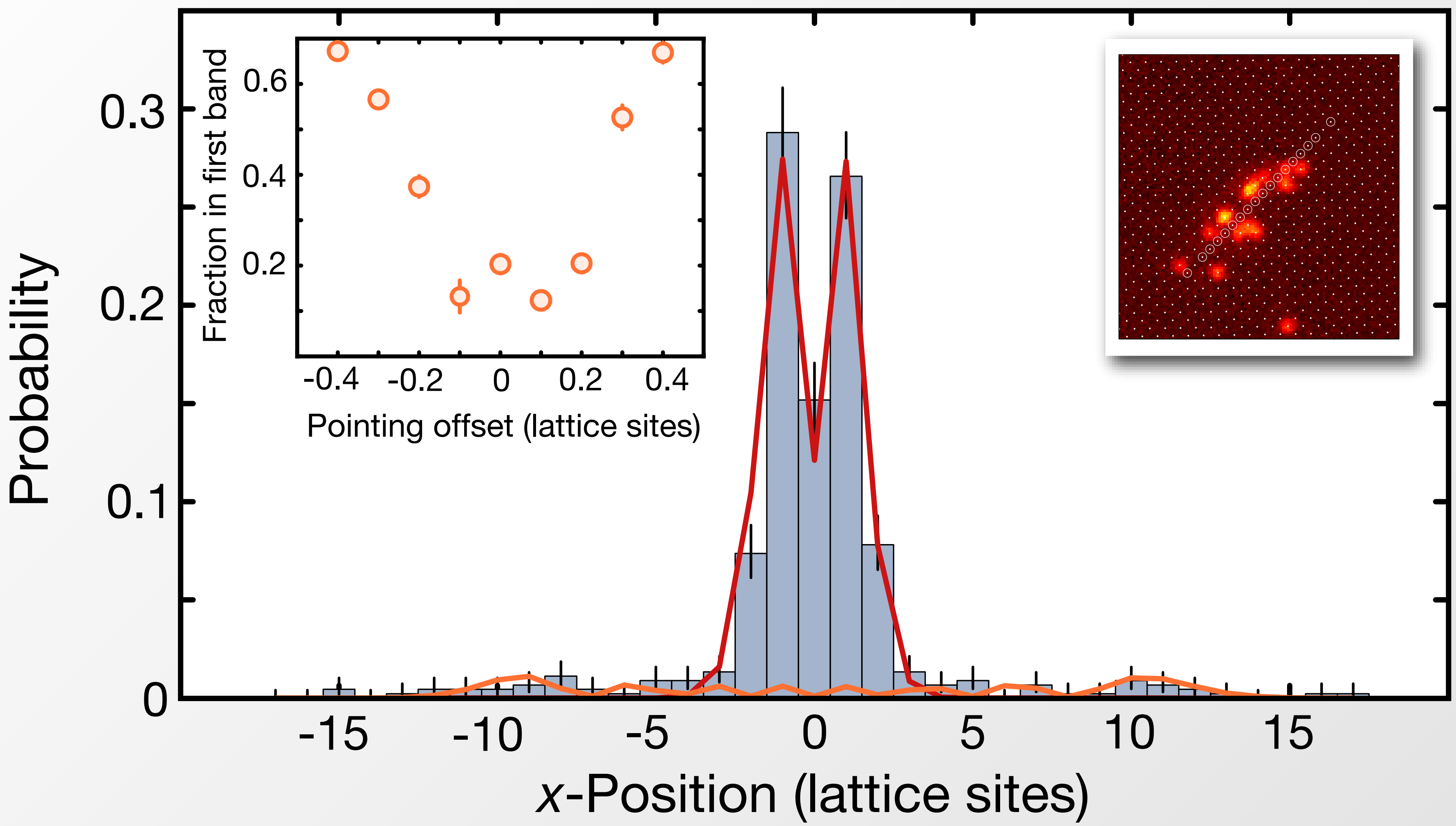

Higher Band Tunneling

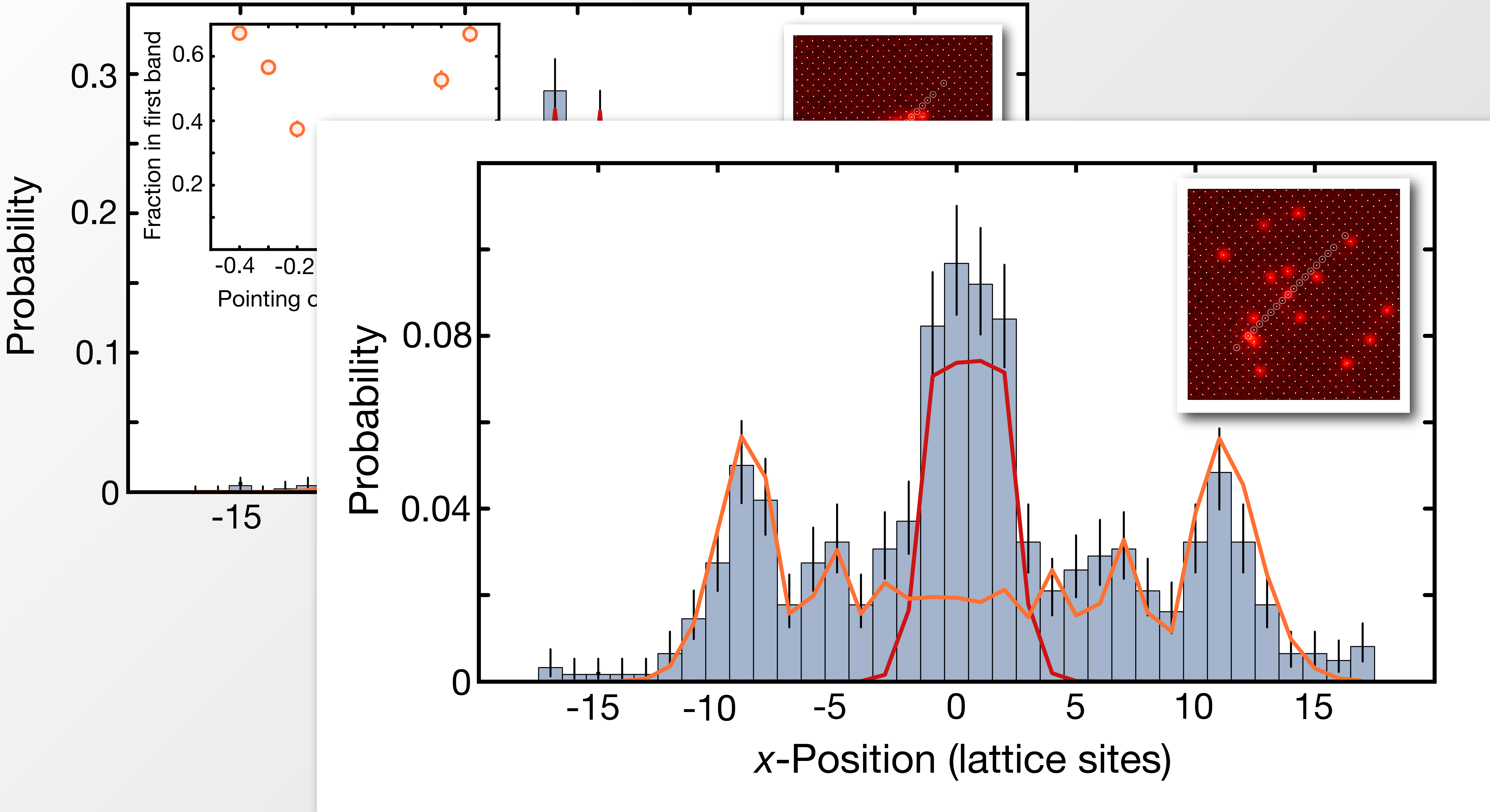

Excellent agreement with simulation.

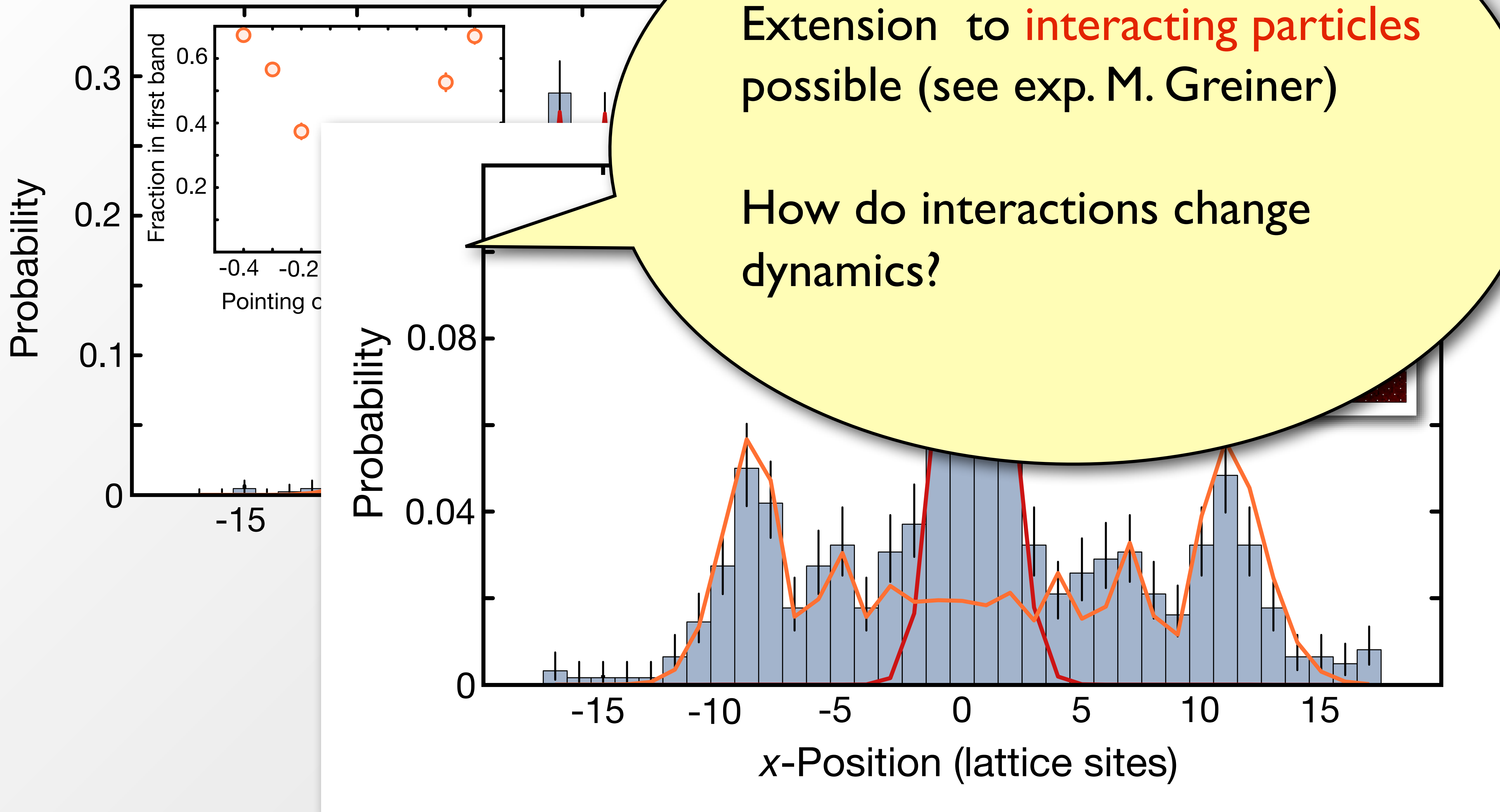

Extension to interacting particles possible (see exp. M. Greiner)

How do interactions change dynamics?

Excellent agreement with simulation.

Controlling Superexchange Interactions

Origin of Spin-Spin Interactions – Exchange Interactions

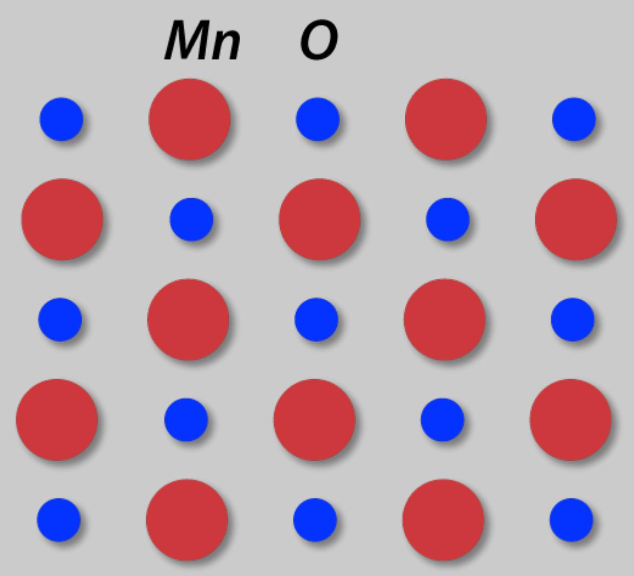

?

Important ionic solids with no direct exchange between magnetic ions show magnetic ordering (MnO, CuO)!

„Super"-exchange interactions must be at work!

P.W. Anderson, Phys. Rev. **79**, 350 (1950)

Deriving the Effective Spin Hamiltonian (1)

How do we get from $-J\sum_{\langle i,j\rangle}\hat{a}_i^\dagger\hat{a}_j+\frac{1}{2}U\sum_i\hat{n}_i(\hat{n}_i-1)$ to $H=-J_{ex}\sum_{\langle i,j\rangle}\mathbf{S}_i\cdot\mathbf{S}_j$?

U

Deriving the Effective Spin Hamiltonian (1)

How do we get from $-J\sum_{\langle i,j\rangle}\hat{a}_i^\dagger\hat{a}_j+\frac{1}{2}U\sum_i\hat{n}_i(\hat{n}_i-1)$ to $H=-J_{ex}\sum_{\langle i,j\rangle}\mathbf{S}_i\cdot\mathbf{S}_j$?

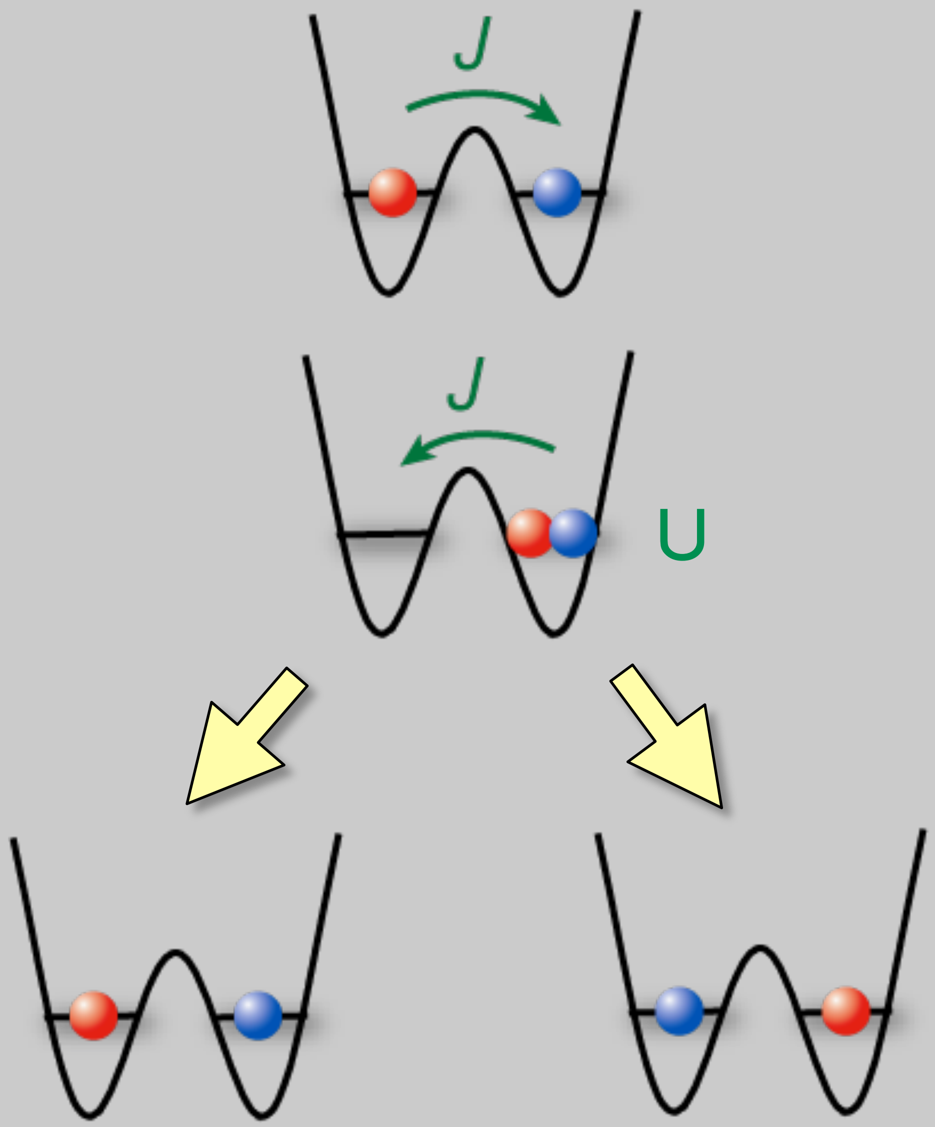

Deriving the Effective Spin Hamiltonian (1)

How do we get from $-J\sum_{\langle i,j\rangle}\hat{a}_i^{\dagger}\hat{a}_j+\frac{1}{2}U\sum_i\hat{n}_i(\hat{n}_i-1)$ to $H=-J_{ex}\sum_{\langle i,j\rangle}\mathbf{S}_i\cdot\mathbf{S}_j$?

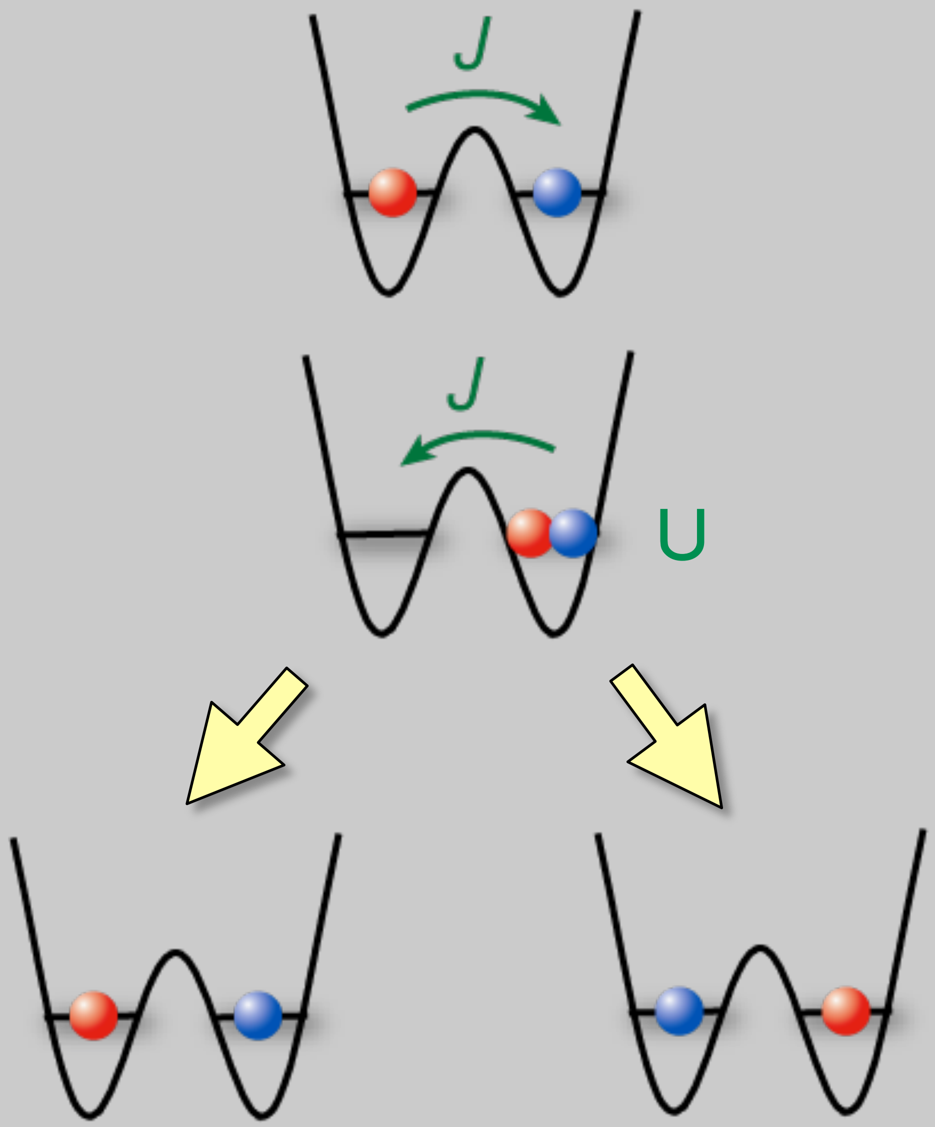

$$\hat{1} \qquad + \qquad \hat{X}_{LR}$$

Deriving the Effective Spin Hamiltonian (2)

Second order hopping can be written as $$H = -2\frac{J^2}{U}\left(1+\hat{X}_{LR}\right)$$

Deriving the Effective Spin Hamiltonian (2)

Second order hopping can be written as

$$H = -2\frac{J^2}{U}\left(1 + \hat{X}_{LR}\right)$$

$$\hat{X}_{LR}\left[\frac{|\uparrow\downarrow\rangle - |\downarrow\uparrow\rangle}{\sqrt{2}}\right] = -\left[\frac{|\uparrow\downarrow\rangle - |\downarrow\uparrow\rangle}{\sqrt{2}}\right]$$

$$\hat{X}_{LR}\left[\frac{|\uparrow\downarrow\rangle + |\downarrow\uparrow\rangle}{\sqrt{2}}\right] = +\left[\frac{|\uparrow\downarrow\rangle + |\downarrow\uparrow\rangle}{\sqrt{2}}\right]$$

Deriving the Effective Spin Hamiltonian (2)

Second order hopping can be written as

$$H = -2\frac{J^2}{U}\left(1+\hat{X}_{LR}\right)$$

$$\hat{X}_{LR}\left[\frac{|\uparrow\downarrow\rangle - |\downarrow\uparrow\rangle}{\sqrt{2}}\right] = -\left[\frac{|\uparrow\downarrow\rangle - |\downarrow\uparrow\rangle}{\sqrt{2}}\right]$$

$$\hat{X}_{LR}\left[\frac{|\uparrow\downarrow\rangle + |\downarrow\uparrow\rangle}{\sqrt{2}}\right] = +\left[\frac{|\uparrow\downarrow\rangle + |\downarrow\uparrow\rangle}{\sqrt{2}}\right]$$

$$H = -J_{ex}\,\hat{P}_{\mathrm{triplet}}$$

Deriving the Effective Spin Hamiltonian (3)

$$\hat{P}_{\text{triplet}} = \hat{P}_{S=1}$$

$$\begin{aligned}
\mathbf{S}_L \cdot \mathbf{S}_R &= \frac{(\mathbf{S}_L + \mathbf{S}_R)^2}{2} - \frac{3}{4} \\
&= \frac{S(S+1)}{2} - \frac{3}{4} \\
&= \hat{P}_{S=1} - \frac{3}{4}
\end{aligned}$$

$$\boxed{H = -J_{ex}\left(\mathbf{S}_L \cdot \mathbf{S}_R + \frac{3}{4}\right)}$$

Direct Detection of Superexchange Interactions

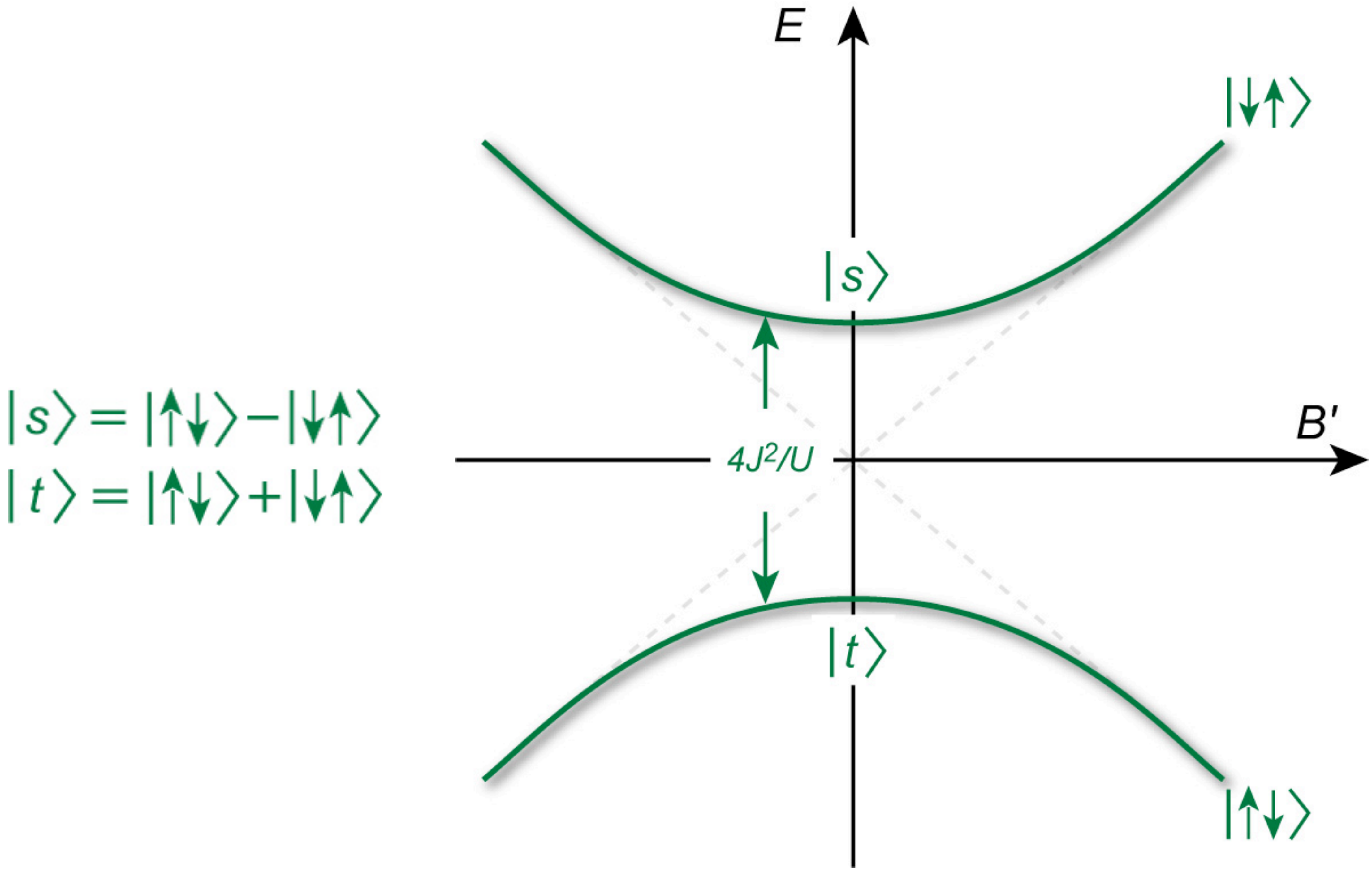

$$H_{eff} = -J_{ex}\,\vec{S}_L \cdot \vec{S}_R - \mu_B B'\left(S_{z,L} - S_{z,R}\right)$$

Direct Detection of Superexchange Interactions (2)

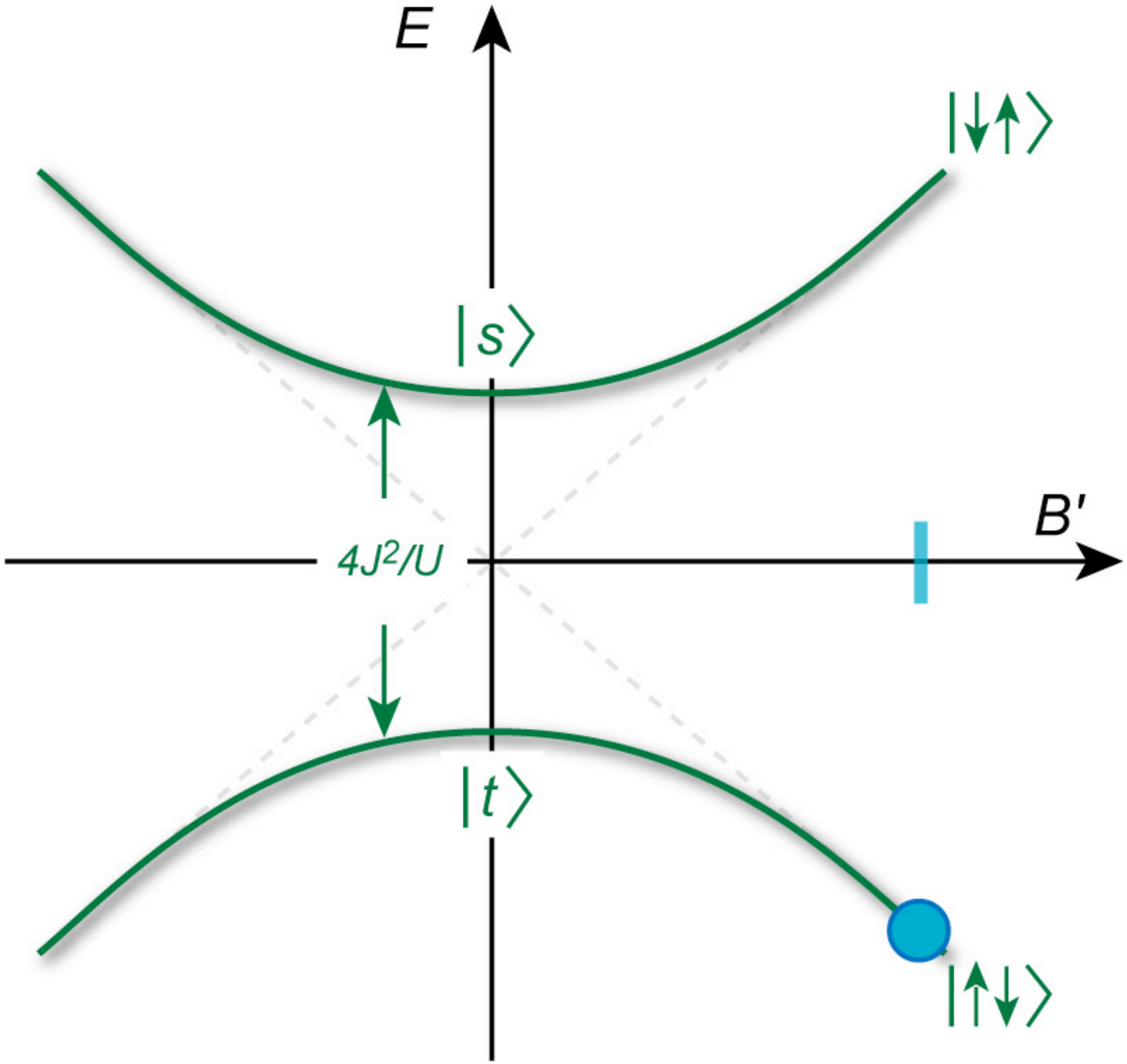

Direct Detection of Superexchange Interactions (2)

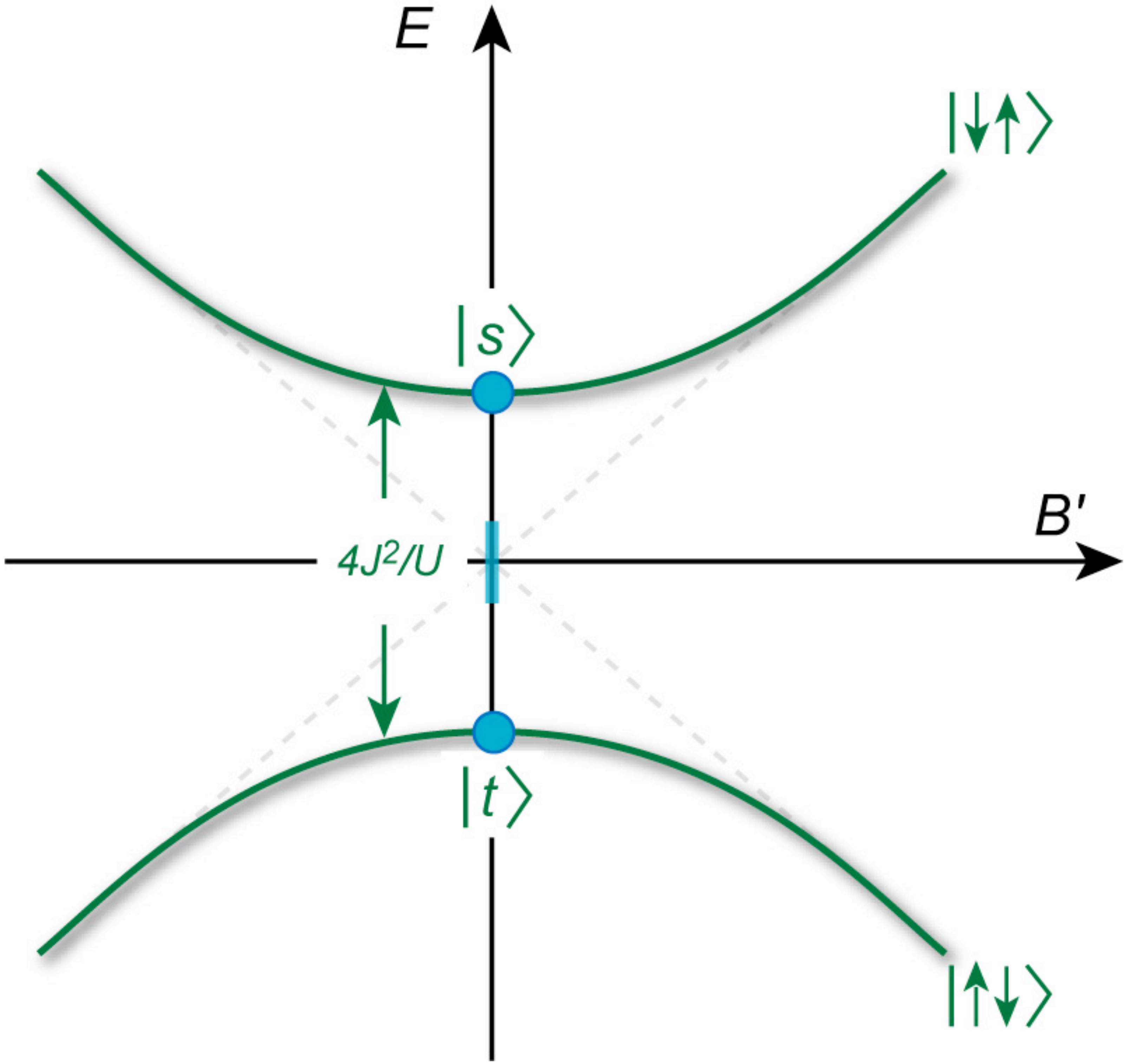

Superexchange Coupling in Quantum Dots

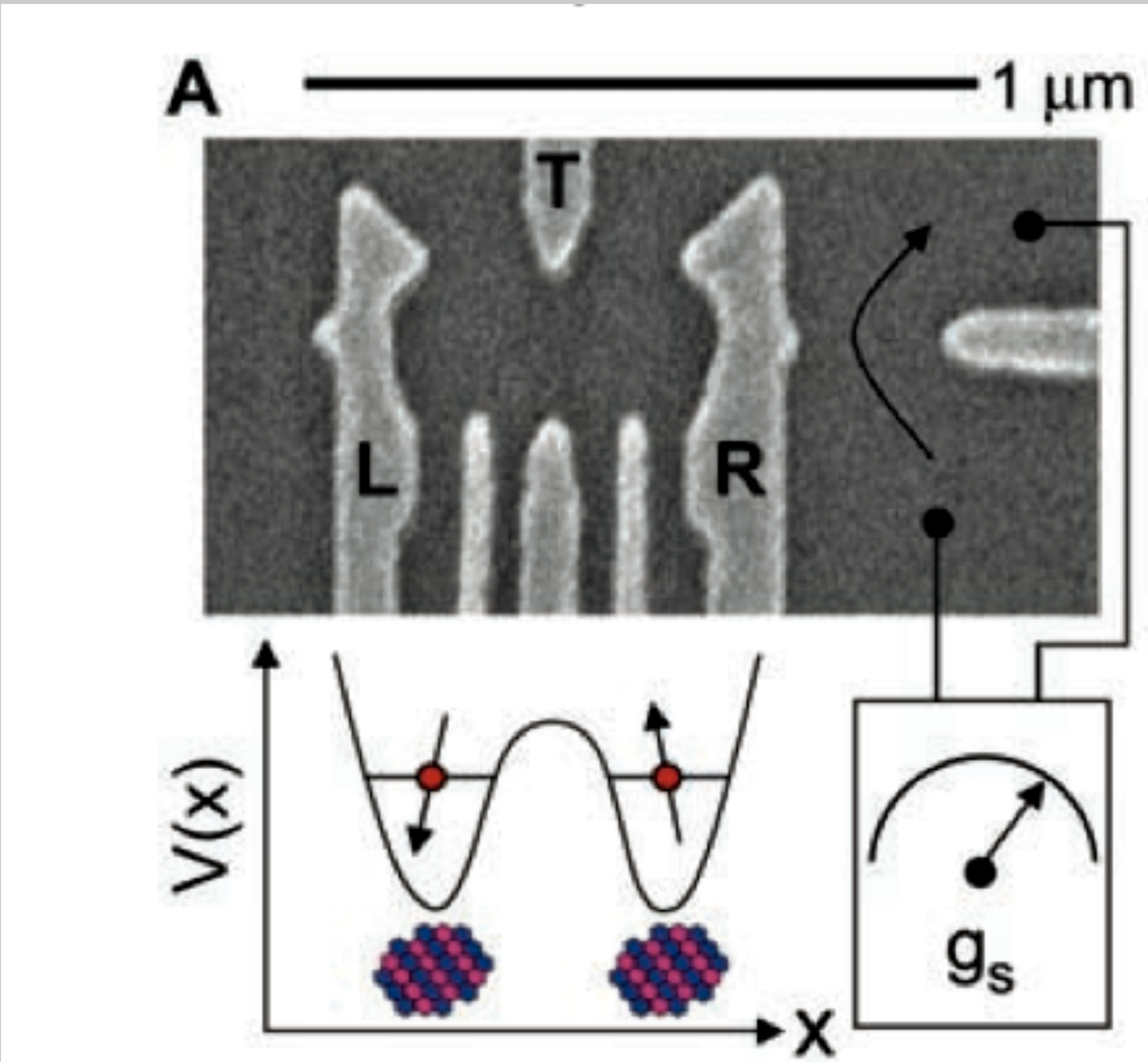

J.R. Petta et al., Science **309**, 2180 (2005)

Coherent Manipulation of Coupled Electron Spins in Semiconductor Quantum Dots

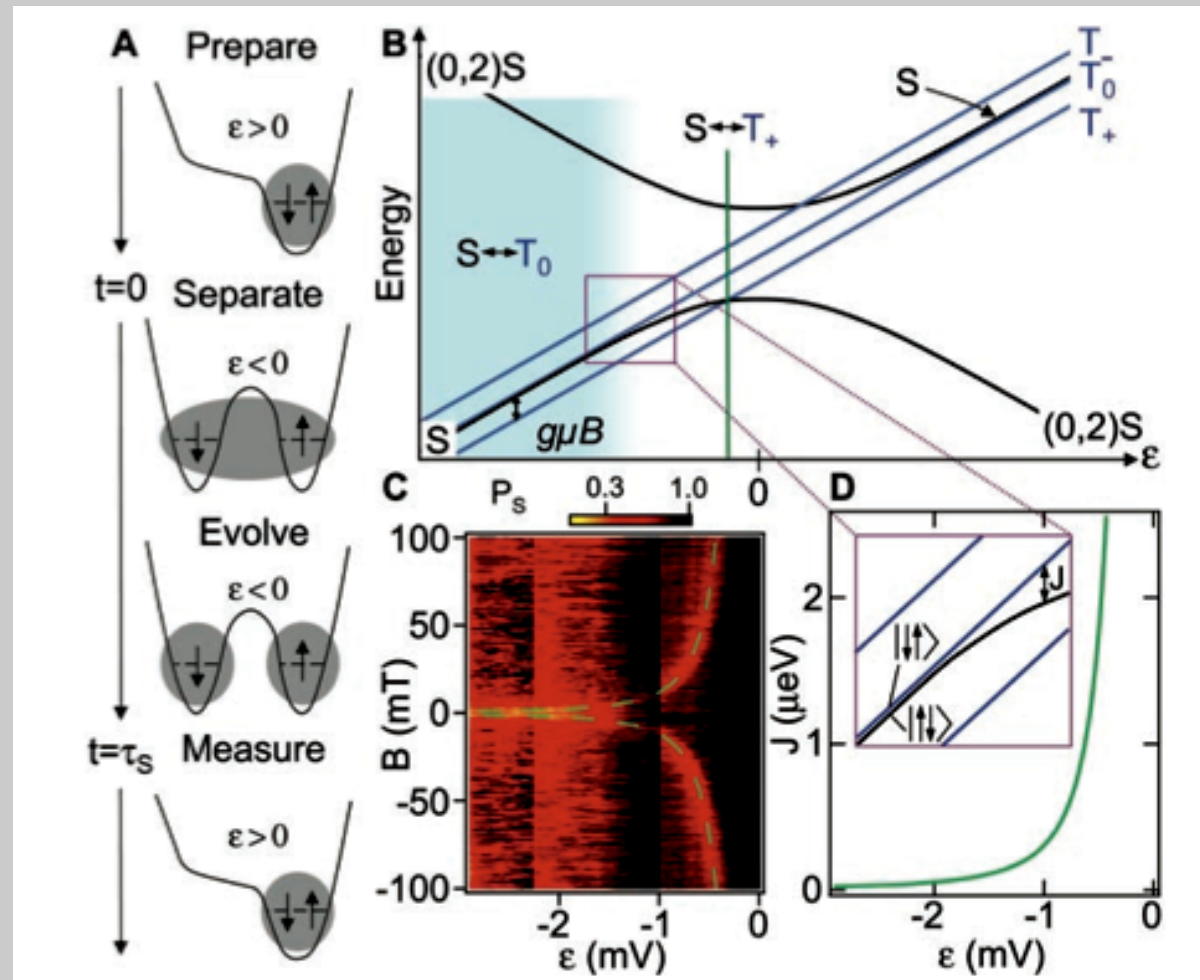

Local control of spin states & interactions between spin states.

Superexchange induced flopping

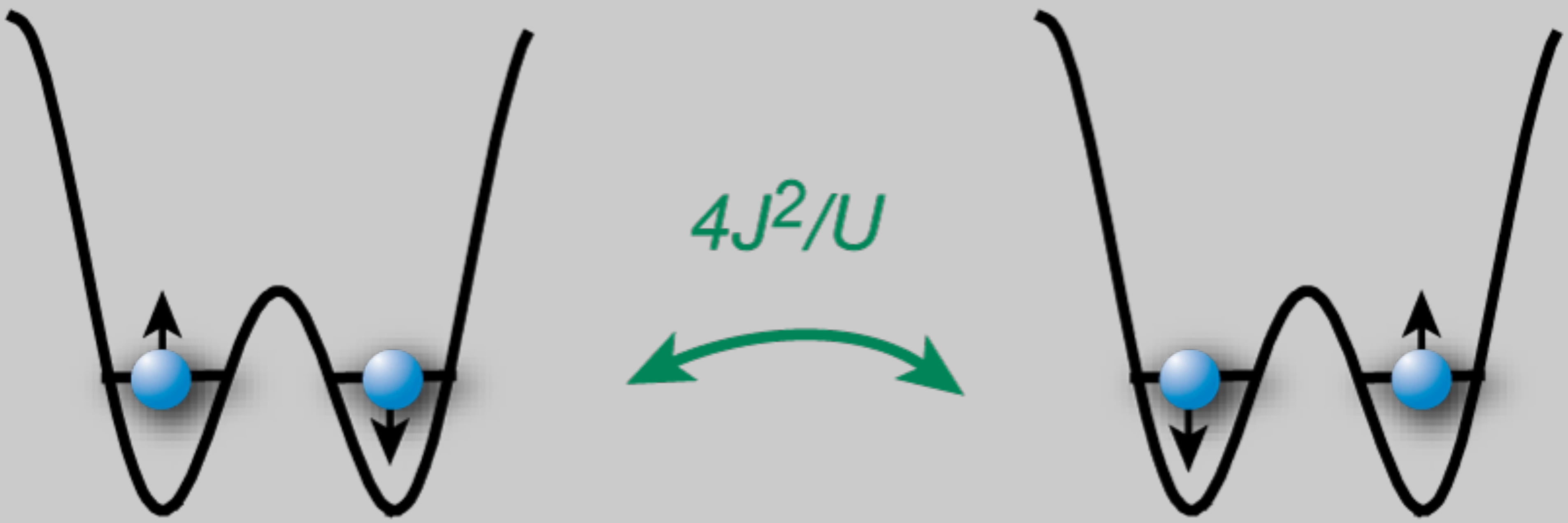

$$H_{eff} = -J_{ex}\vec{S}_i \cdot \vec{S}_j$$
$$= -\frac{J_{ex}}{2}\left(\hat{S}_i^+\hat{S}_j^- + \hat{S}_i^-\hat{S}_j^+\right) - J_{ex}\hat{S}_i^z\hat{S}_j^z$$

Mapping the Spins

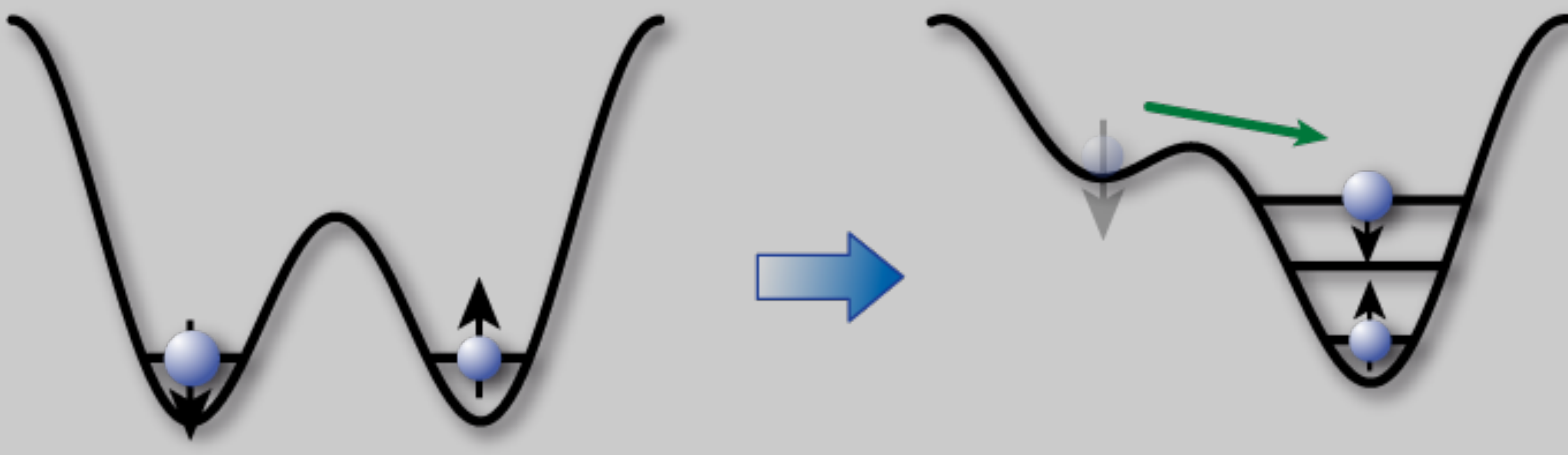

$|\downarrow\rangle$

$|\uparrow\rangle$

Mapping the Spins

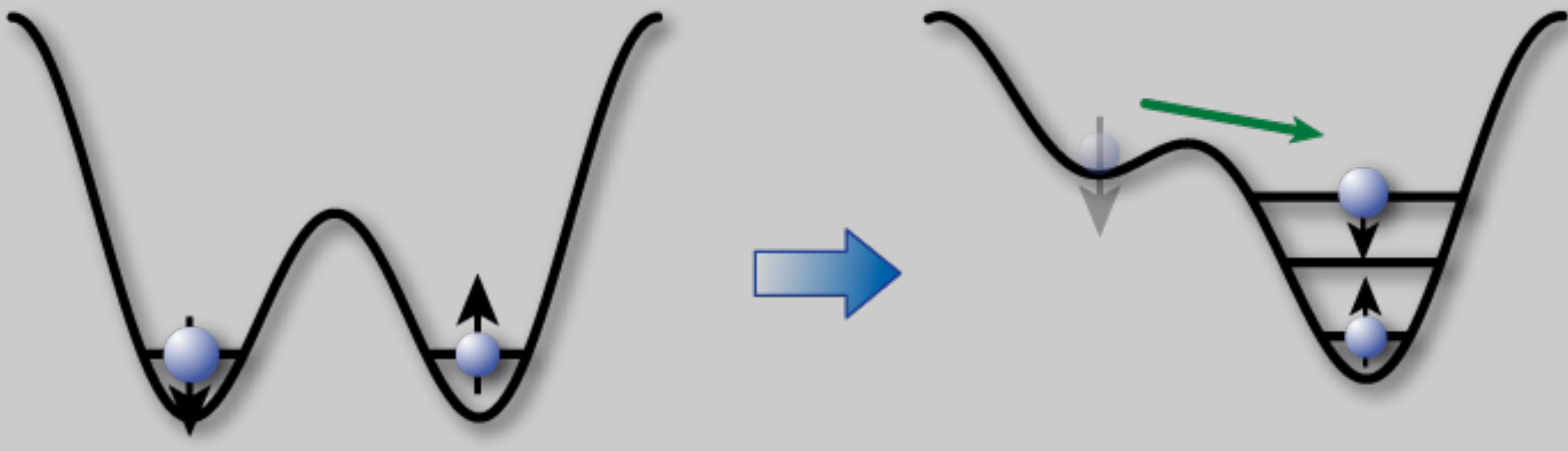

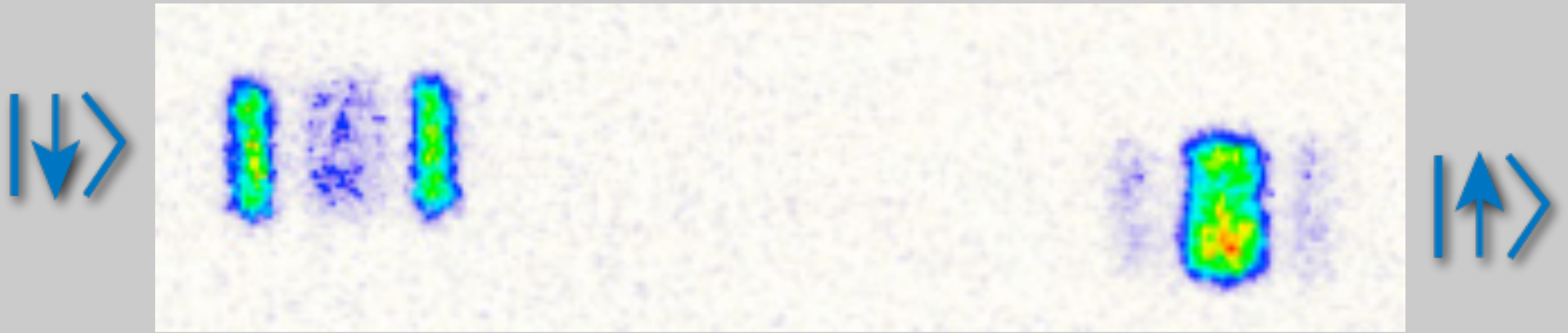

Initial AF order verified in the experiment!

Superexchange induced flopping

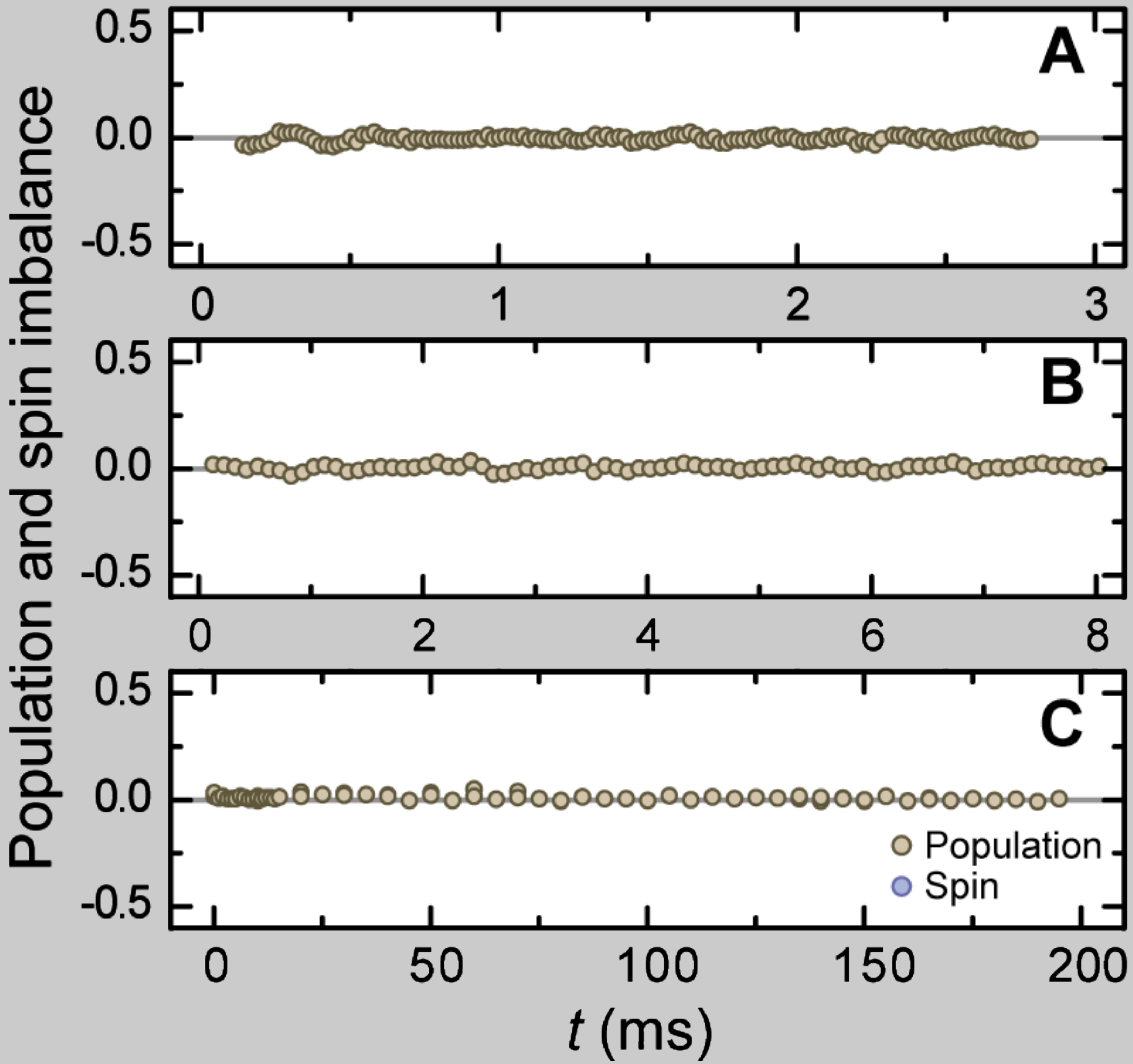

$J/U=1.25$
$V_{short}=6\ E_r$

$J/U=0.26$
$V_{short}=11\ E_r$

$J/U=0.05$
$V_{short}=17\ E_r$

Superexchange induced flopping

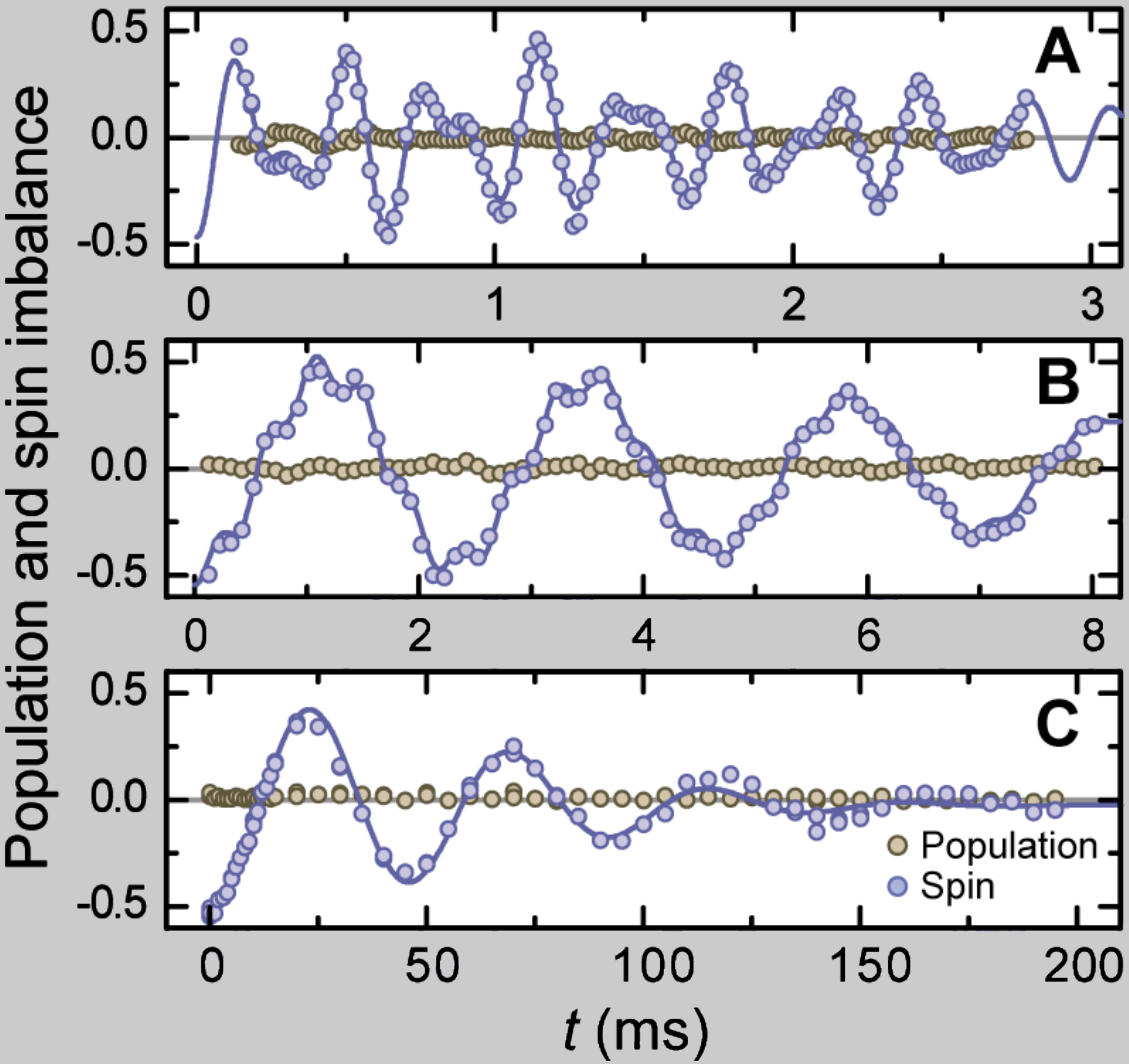

J/U=1.25
V_{short}=6 E_r

J/U=0.26
V_{short}=11 E_r

J/U=0.05
V_{short}=17 E_r

Quantum Dynamic of Mobile Single Spin Impurity

T. Fukuhara, M. Endres, M. Cheneau P. Schauss, Ch. Gross, I. Bloch, S. Kuhr,
U. Schollwöck, A. Kantian, Th. Giamarchi

Sherson et al. Nature 467, 68 (2010),
see also Bakr et al. Nature (2009) & Bakr et al. Science (2010)

Spin impurity dynamics

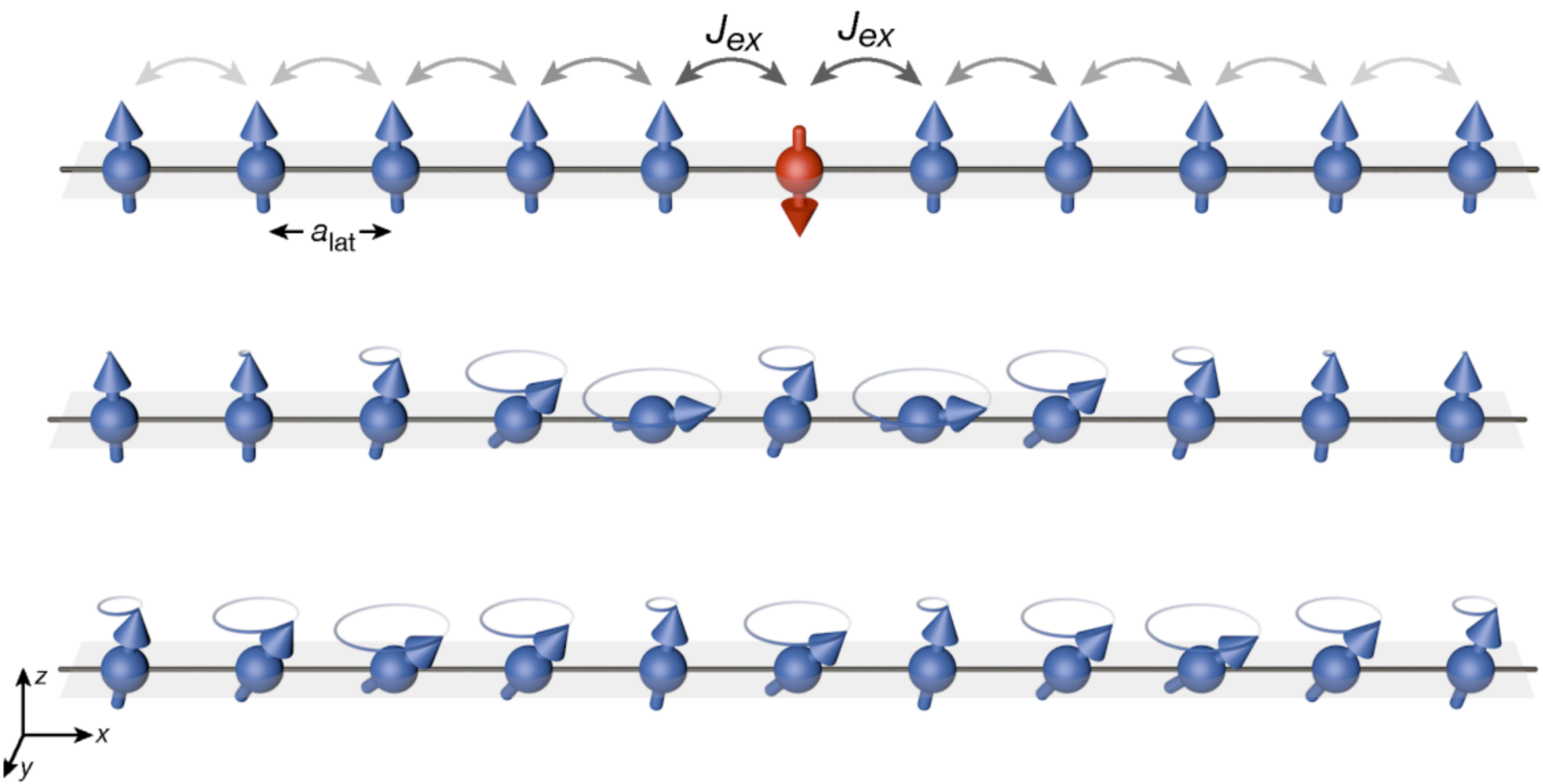

$$-J_{ex}\sum_{\langle i,j\rangle}\mathbf{S}_i\cdot\mathbf{S}_j$$

Ferromagnetic Heisenberg Interaction

Spin impurity dynamics

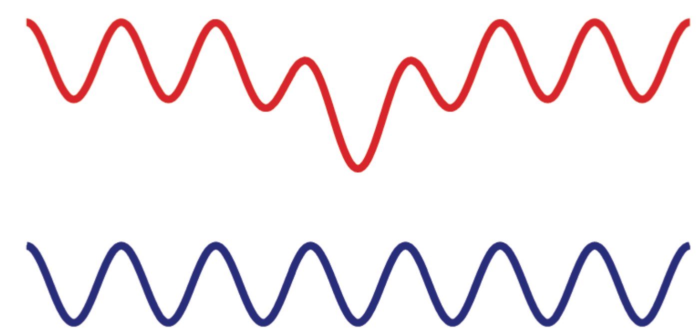

$|2\rangle = |F=2, m_F=-2\rangle$

$|1\rangle = |F=1, m_F=-1\rangle$

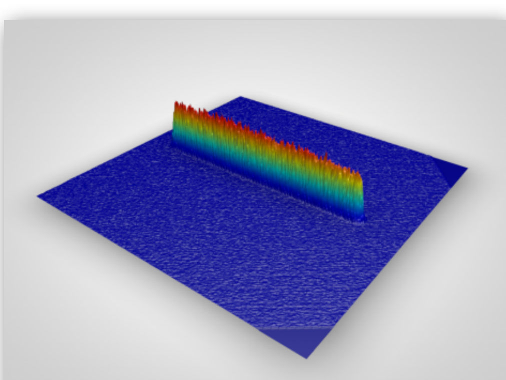

Line-shaped light field created with DMD SLM

Spin impurity dynamics

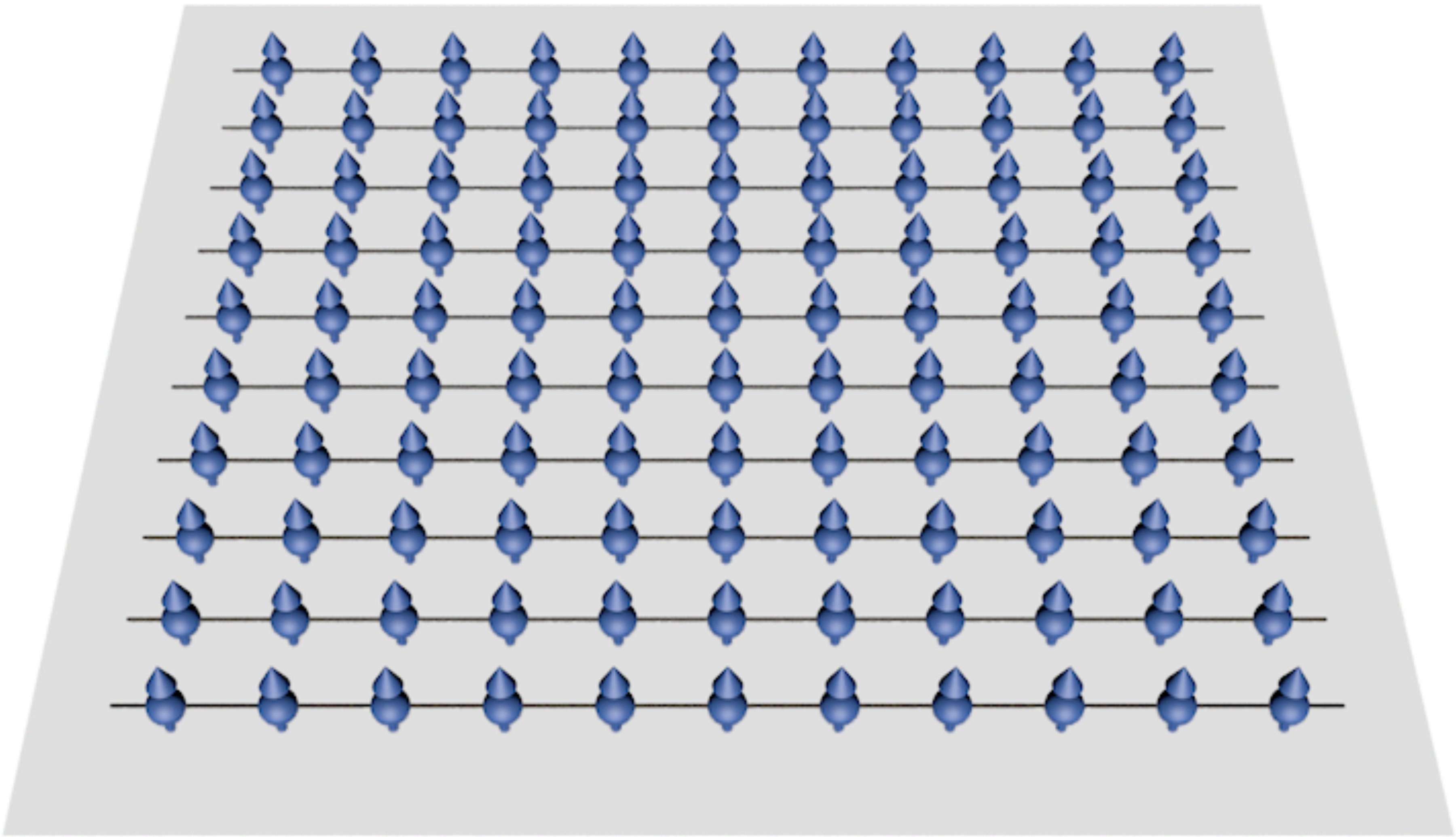

$|2\rangle = |F=2, m_F=-2\rangle$

$|1\rangle = |F=1, m_F=-1\rangle$

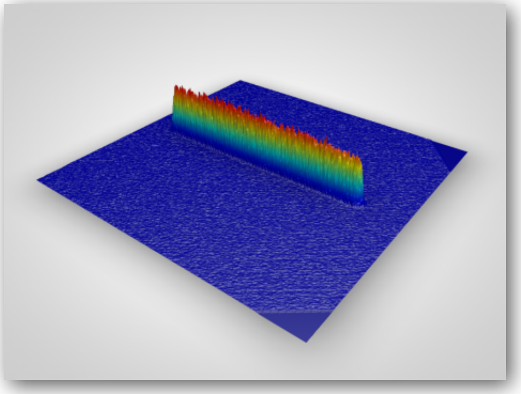

Line-shaped light field created with DMD SLM

Spin impurity dynamics

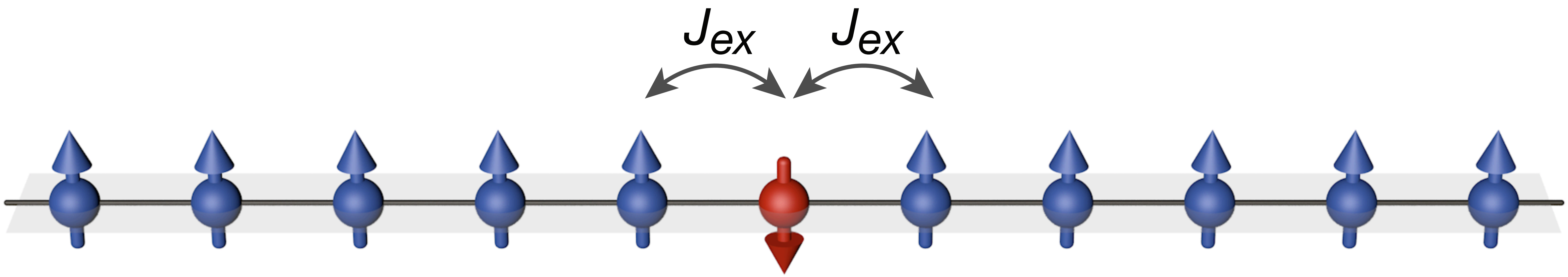

Heisenberg Hamiltonian

$$H = -J_{ex}\sum \mathbf{S}_i \cdot \mathbf{S}_j = -J_{ex}\sum\left(S_i^x S_j^x + S_i^y S_j^y + S_i^z S_j^z\right)$$

$$= -\frac{J_{ex}}{2}\sum\left(S_i^+ S_j^- + S_i^- S_j^+\right) - J_{ex}\sum S_i^z S_j^z$$

$$J_{\text{ex}} = 4\frac{J^2}{U}$$

$$H = -J\sum\left(\hat{a}_i^\dagger \hat{a}_j + \hat{a}_i \hat{a}_j^\dagger\right)$$ single particle tunneling

Spin impurity dynamics

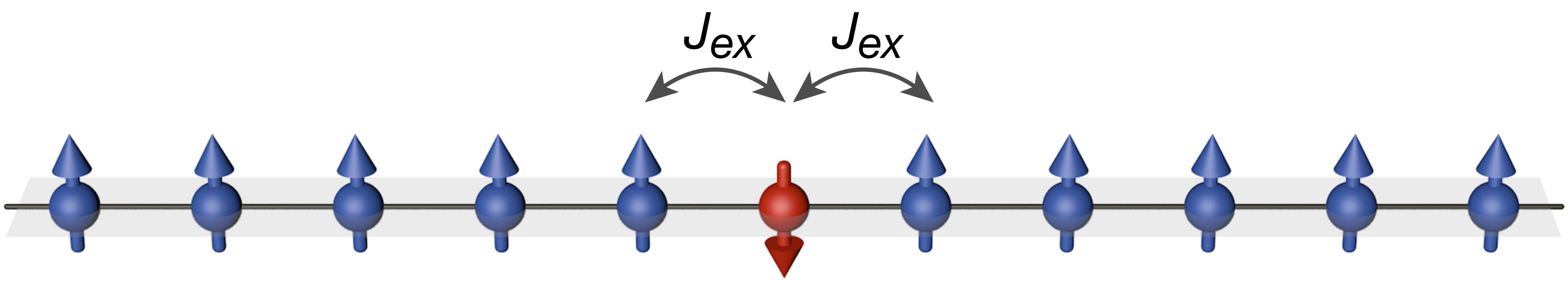

Heisenberg Hamiltonian

$$H = -J_{ex}\sum \mathbf{S}_i \cdot \mathbf{S}_j = -J_{ex}\sum \left(S_i^x S_j^x + S_i^y S_j^y + S_i^z S_j^z\right)$$

$$= -\frac{J_{ex}}{2}\sum \left(S_i^+ S_j^- + S_i^- S_j^+\right) \cancel{- J_{ex}\sum S_i^z S_j^z}$$

$$J_{\mathrm{ex}} = 4\frac{J^2}{U}$$

$$H = -J\sum \left(\hat{a}_i^\dagger \hat{a}_j + \hat{a}_i \hat{a}_j^\dagger\right)$$ single particle tunneling

Detection and "Post-selection"

Our detection is not spin-resolved.

Positive image

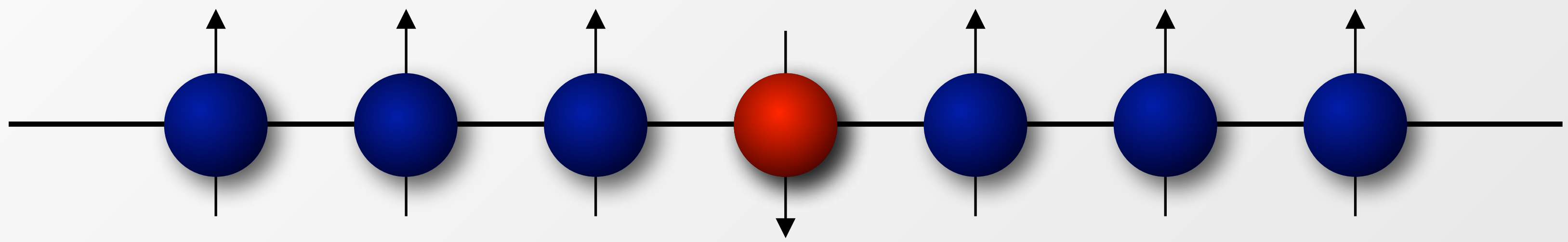

Negative image

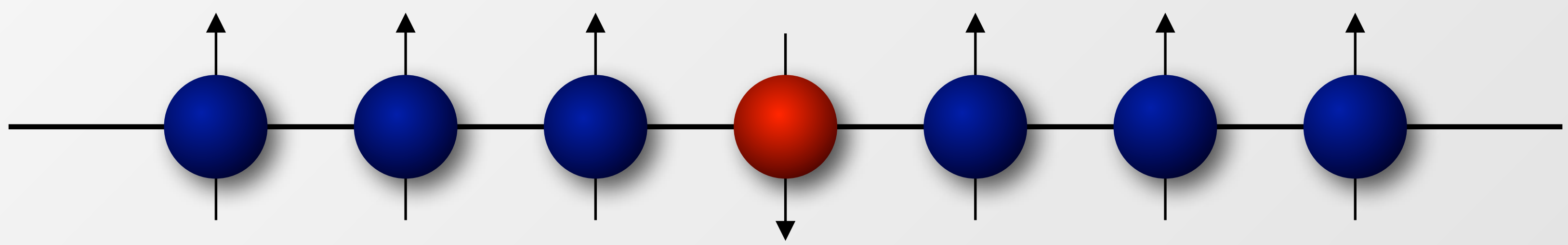

Detection and "Post-selection"

Our detection is not spin-resolved.

Positive image Remove the other spin component (bath spin) before detection

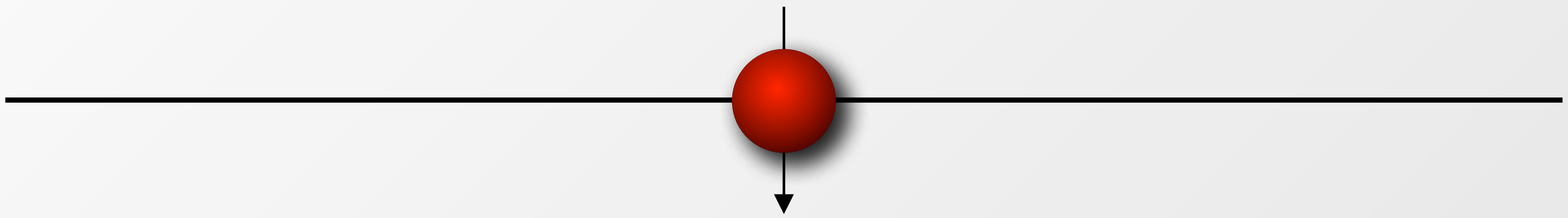

Negative image

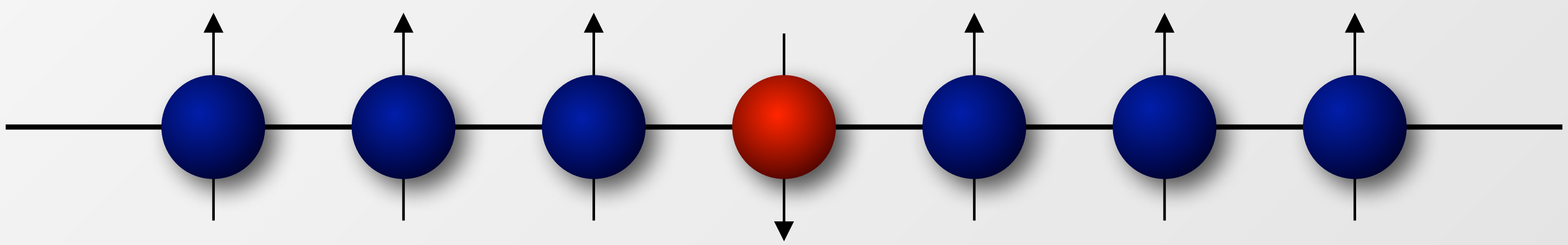

Detection and "Post-selection"

Our detection is not spin-resolved.

Positive image Remove the other spin component (bath spin) before detection

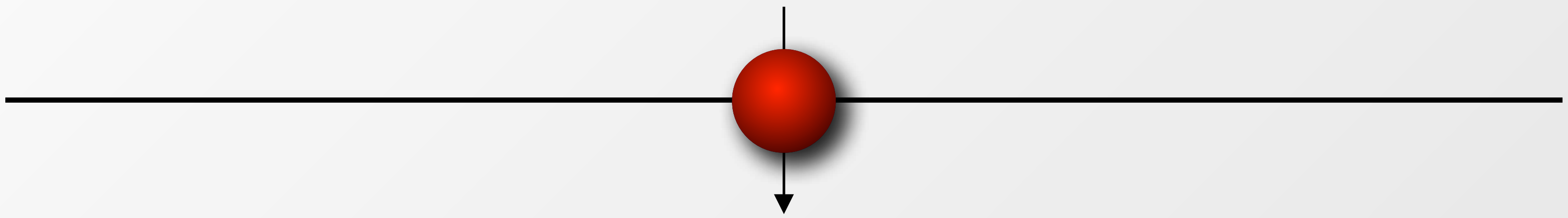

Negative image Measure spin impurities as empty sites by pushing out the impurities

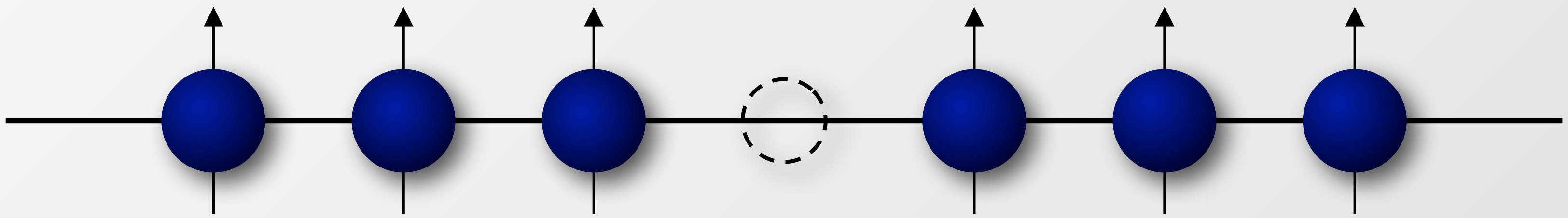

Detection and "Post-selection"

Our detection is not spin-resolved.

Positive image Remove the other spin component (bath spin) before detection

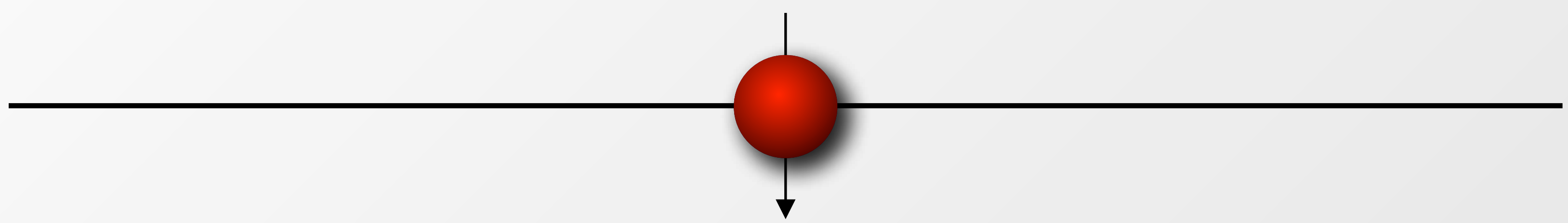

Negative image Measure spin impurities as empty sites by pushing out the impurities

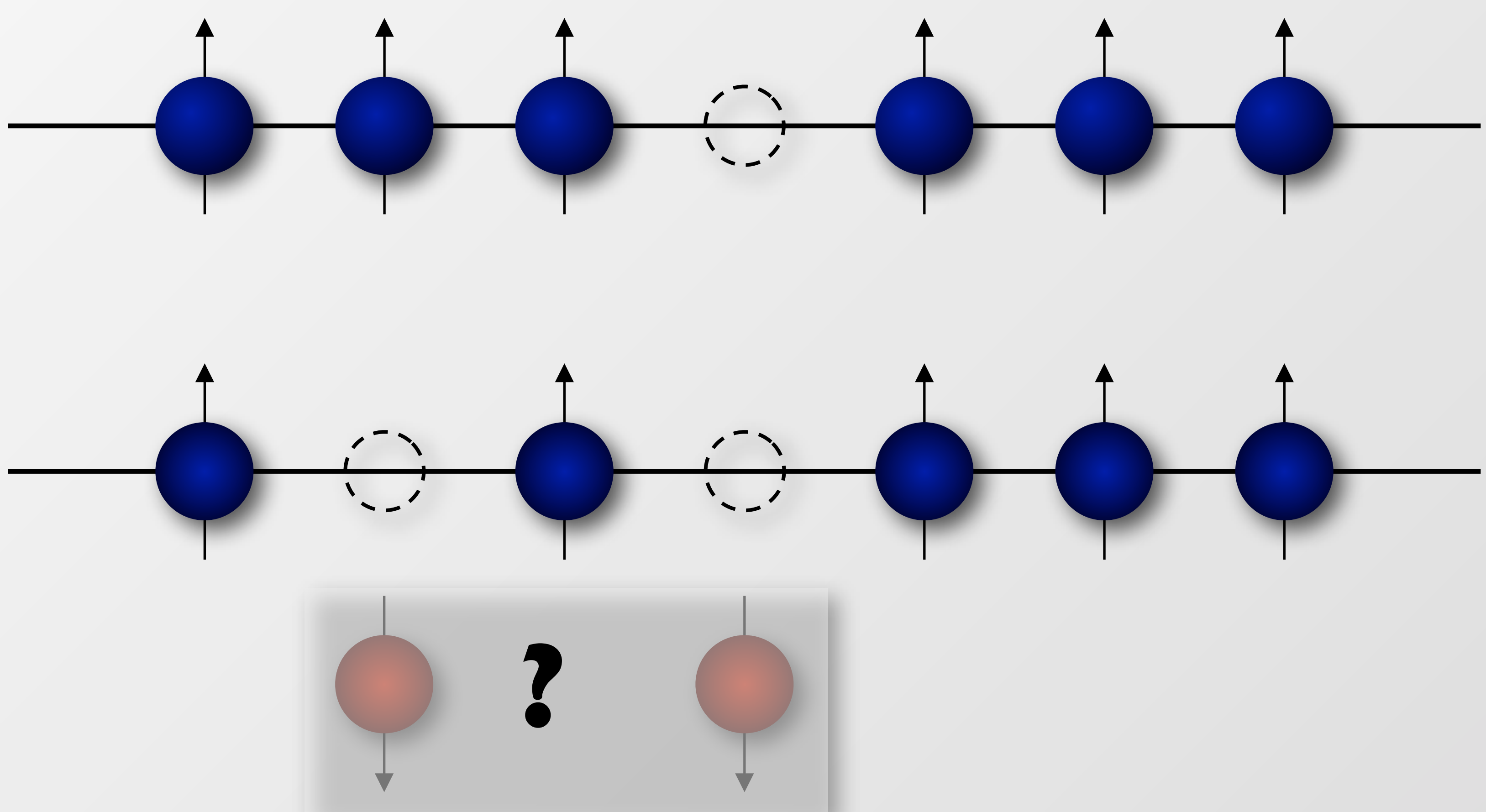

Detection and "Post-selection"

Our detection is not spin-resolved.

Positive image Remove the other spin component (bath spin) before detection

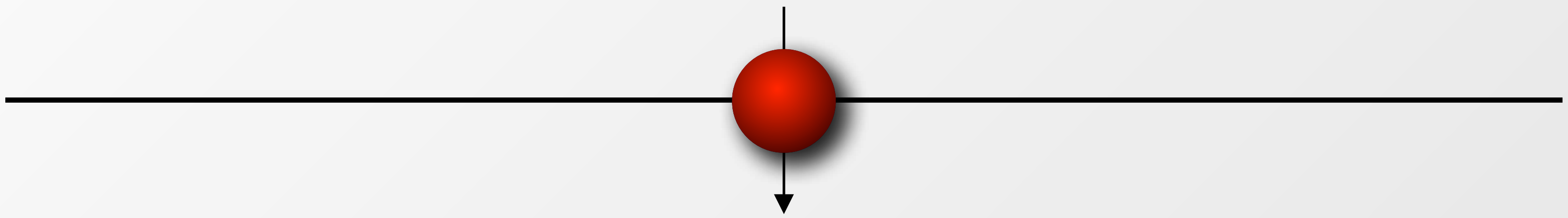

Negative image Measure spin impurities as empty sites by pushing out the impurities

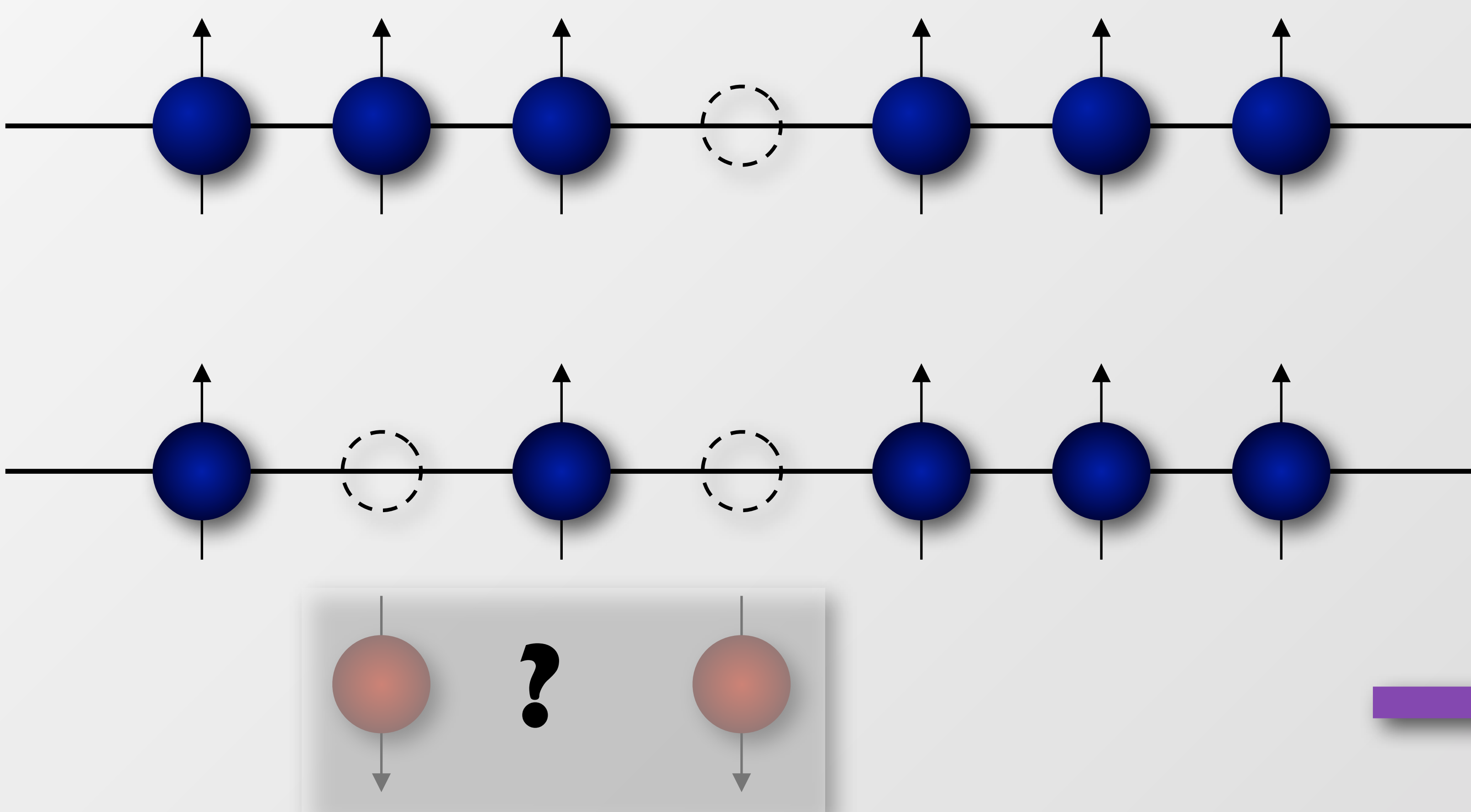

If we only use samples with one empty site …

- the position of the impurity can be determined
- system has no extra excitation

" zero temperature"

Coherent quantum dynamics of single spin at zero temperature

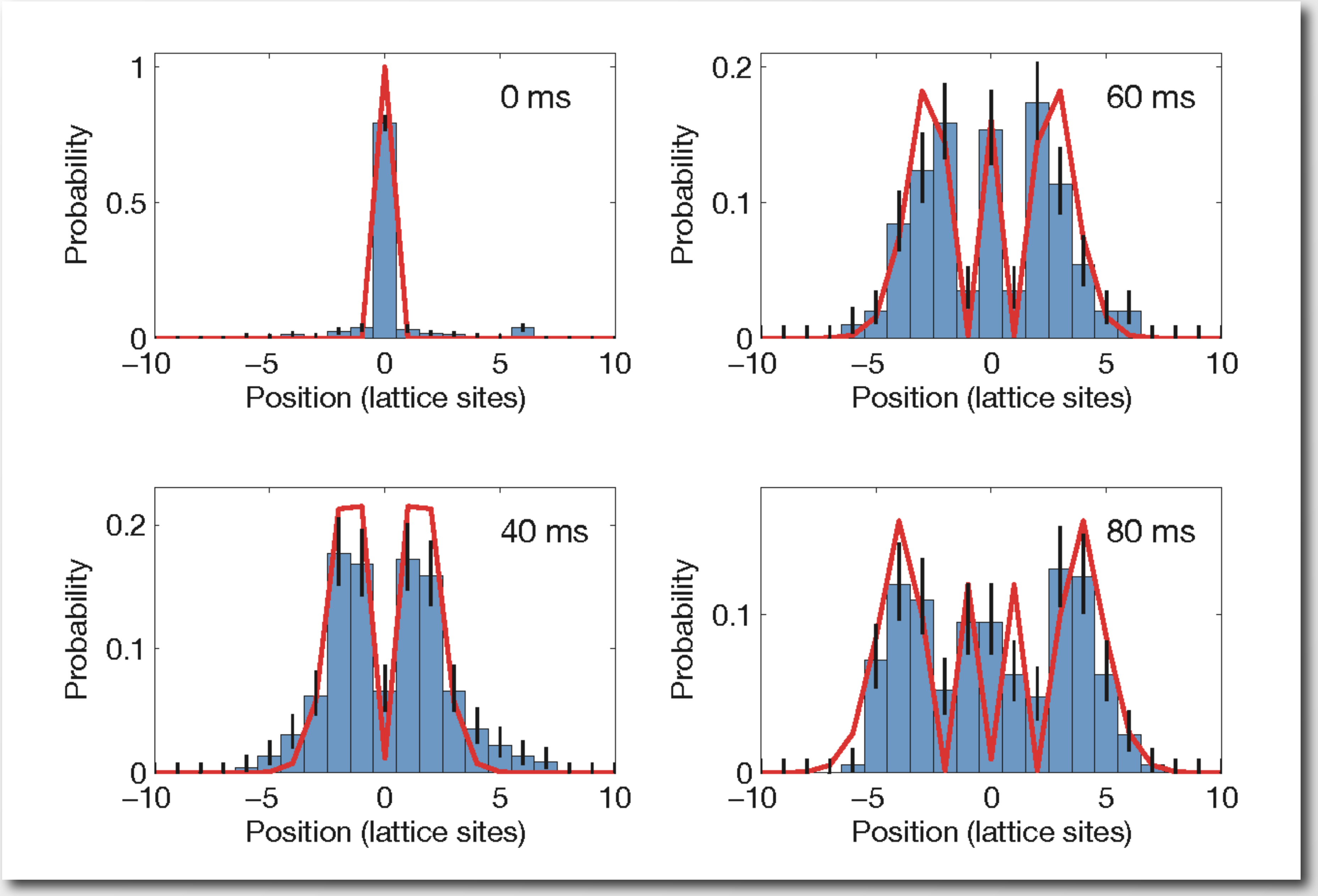

V = 10 Er
U/J = 19

$$H = -\frac{J_{ex}}{2}\sum_{\langle i,j\rangle}\left(S_i^+S_j^- + S_i^-S_j^+\right)$$

$$P_j(t) = \left[\mathscr{J}_j\left(\frac{J_{\text{ex}}t}{\hbar}\right)\right]^2$$

Bessel function of the first kind

Effect from hole excitations

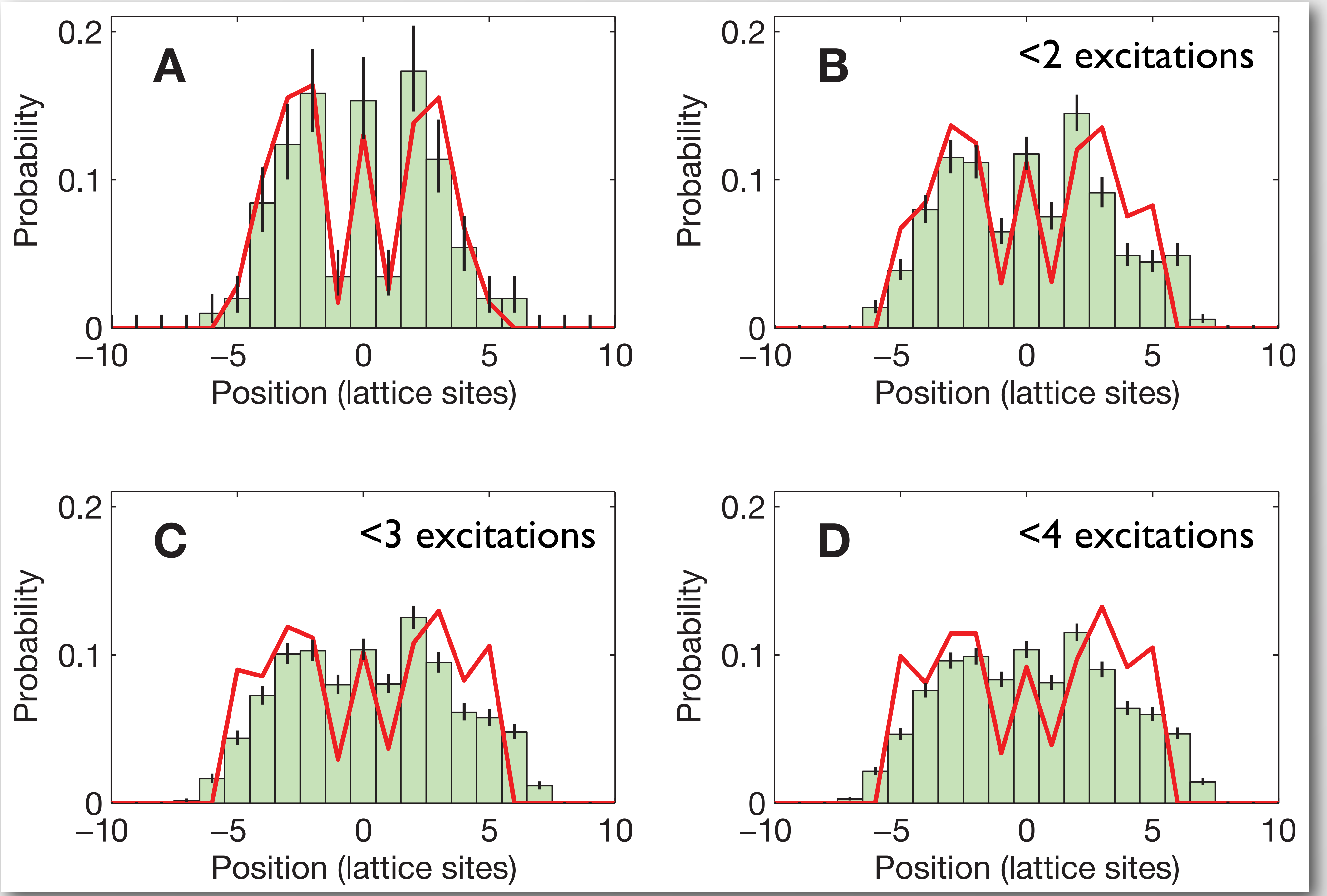

V = 10 Er

U/J = 19

- Only visibility goes down
- Spreading speed almost independent of holes

Temperature Effects

V_{lat}=10 E_r

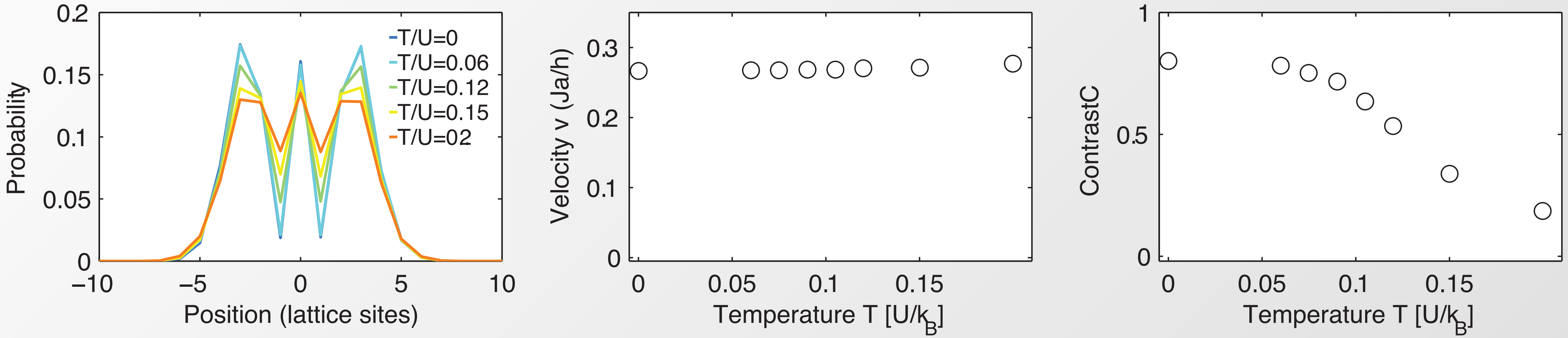

V_{lat}=5 E_r

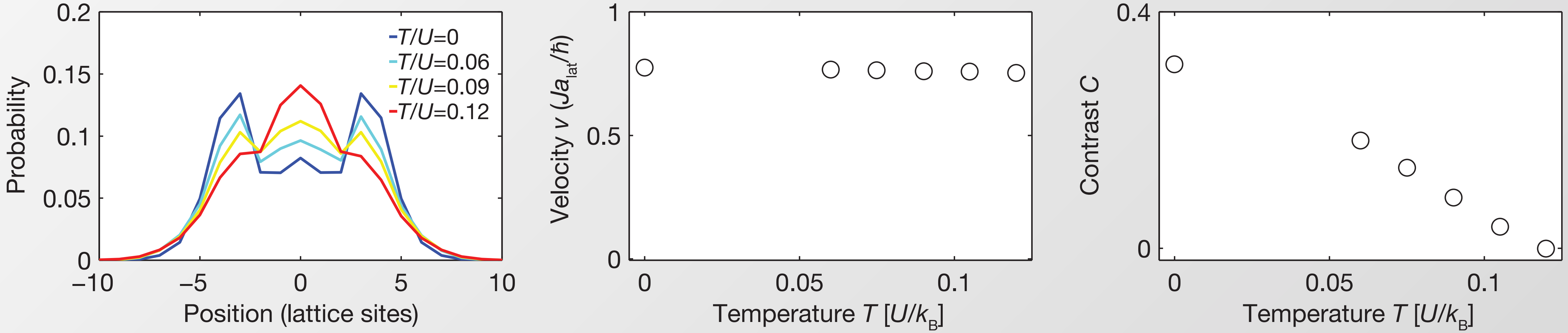

Propagation speed almost constant, Coherence affected!

Propagation velocty

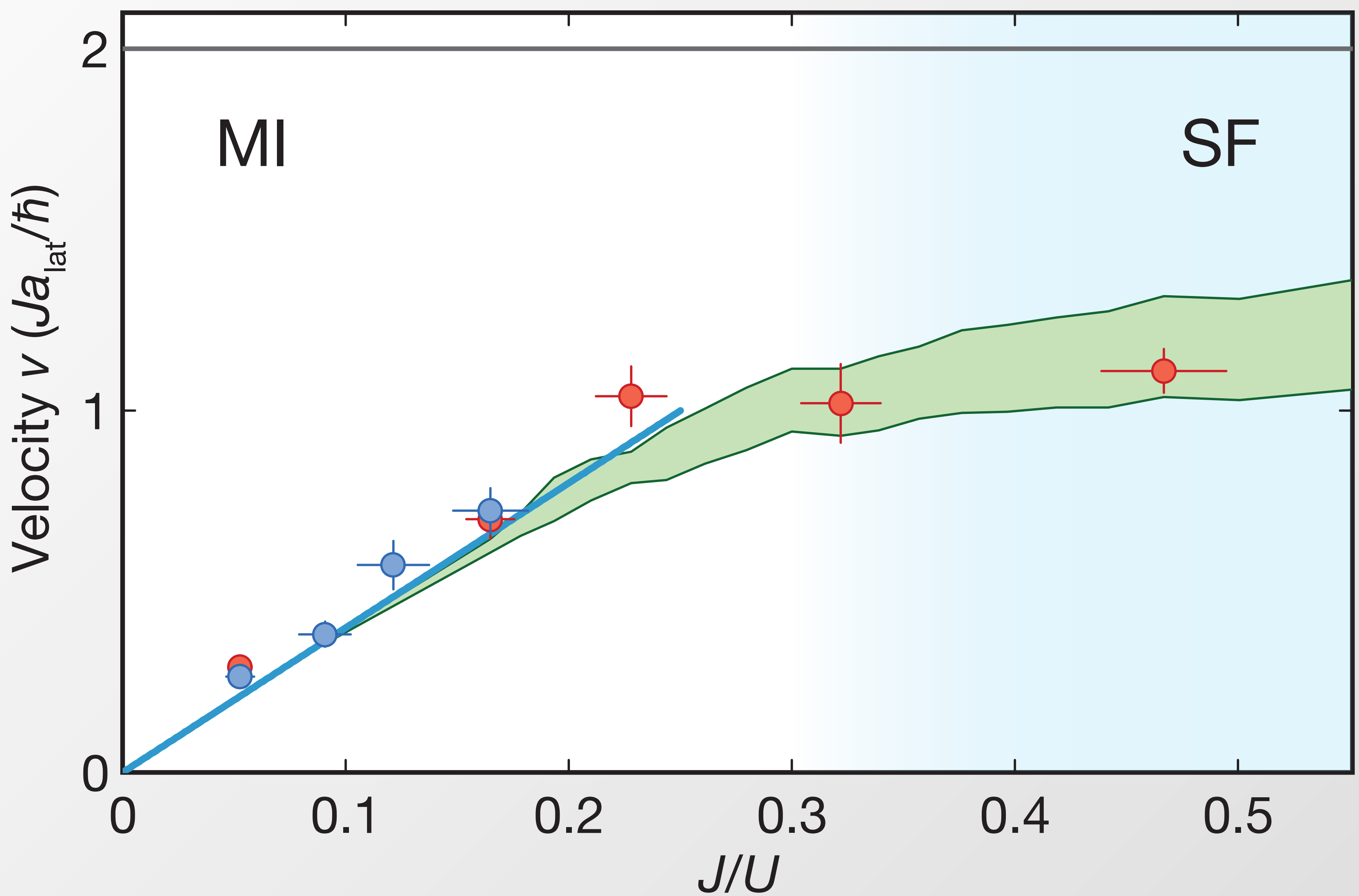

Reference value:

$$v = \frac{2Ja_{lat}}{\hbar}$$ Free particle tunneling

Outlook

Quantum Dynamics of Interacting Atoms/Spins

- Effect of Temperature/Holes on Dynamics
- Dynamics of Magnon bound states
- Domain Walls
- Higher Dimensions (1D, 2D, 3D)
- Entropy Transport
- Probe for Quantum Critical Transport
- Direct measurement of Green's function

$$G(x_i, x_j, t) \propto \langle \Uparrow | \hat{S}^{\dagger}(x_j, t) \hat{S}^{-}(x_i, 0) | \Uparrow \rangle$$

Direct Observation of Magnon Bound States

T. Fukuhara, P. Schauss, S. Hild, J.Zeiher, M. Cheneau, M. Endres, I. Bloch, Ch. Gross

T. Fukuhara et al., Nature **502**, 76 (2013)
for photons: O. Firstenberg et al., Nature **502**, 71 (2013)

Magnon Bound States

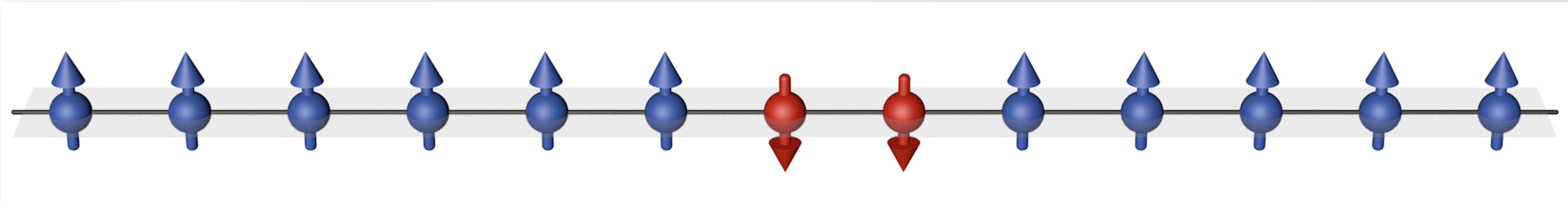

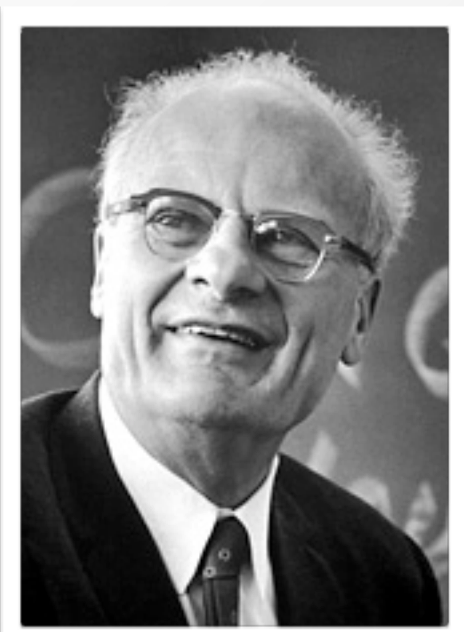

Hans Bethe
(1906-2005)

There can be bound states in a Heisenberg spin chain!
Development of Bethe Ansatz.

$$H = -J_{ex}\sum_i \left(\hat{S}_i^x\hat{S}_{i+1}^x + \hat{S}_i^y\hat{S}_{i+1}^y\right) - \Delta\sum_i \hat{S}_i^z\hat{S}_{i+1}^z$$

H. Bethe, Z. Phys. (1931)
M. Wortis, Phys Rev. (1963)
M. Takahashi & M. Suzuki Prog. Th. Phys. (1972)
M. Karbach, G. Müller (1997)
see also: **repulsively bound pairs & interacting atoms**
K. Winkler et al. Nature (2006); S. Fölling et al. Nature (2007); Y Lahini et al. PRA (2012)

Magnon Bound States

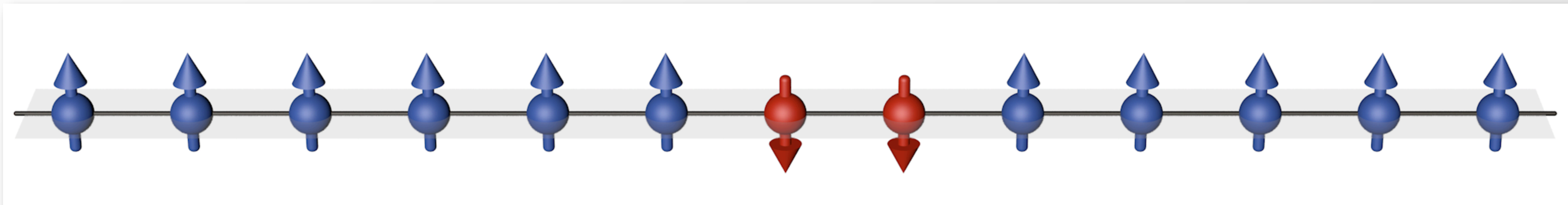

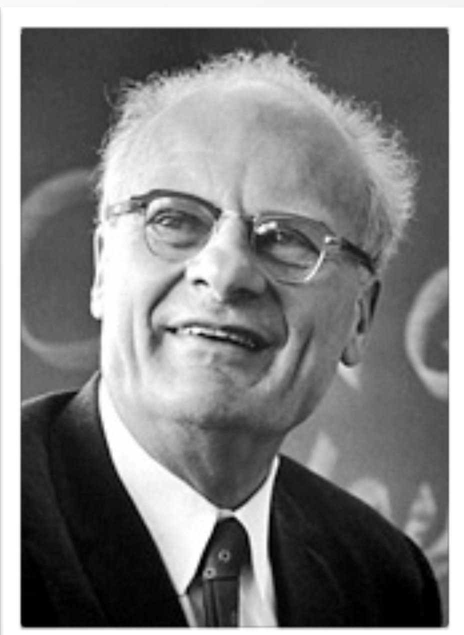

Hans Bethe
(1906-2005)

There can be bound states in a Heisenberg spin chain!
Development of Bethe Ansatz.

$$H = -J_{ex} \sum_i \left(\hat{S}_i^x \hat{S}_{i+1}^x + \hat{S}_i^y \hat{S}_{i+1}^y \right) - \Delta \sum_i \hat{S}_i^z \hat{S}_{i+1}^z$$

General
l-string bound states

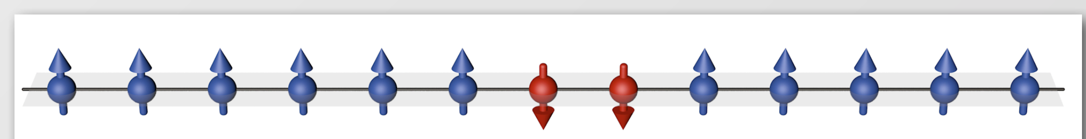

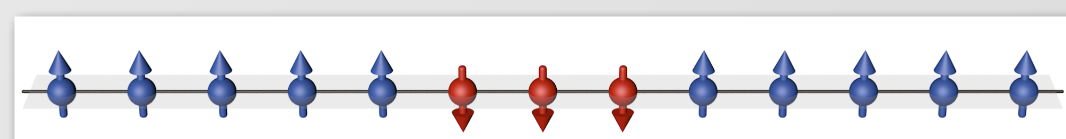

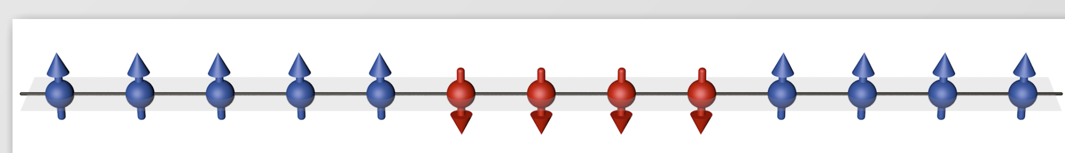

H. Bethe, Z. Phys. (1931)
M. Wortis, Phys Rev. (1963)
M. Takahashi & M. Suzuki Prog. Th. Phys. (1972)
M. Karbach, G. Müller (1997)
see also: **repulsively bound pairs & interacting atoms**
K. Winkler et al. Nature (2006); S. Fölling et al. Nature (2007); Y Lahini et al. PRA (2012)

Magnon Bound States

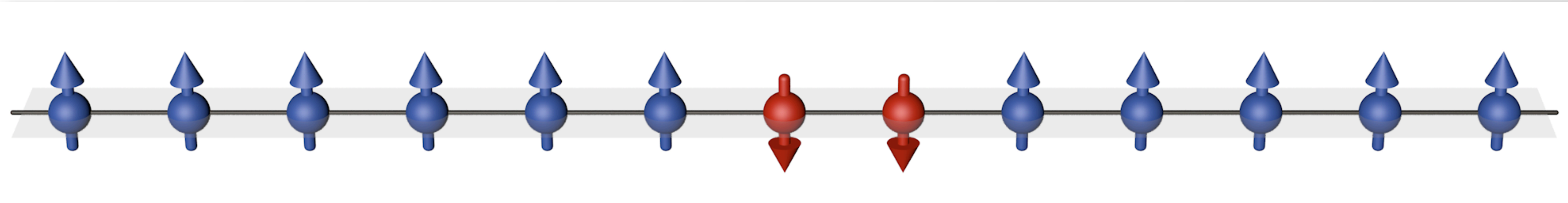

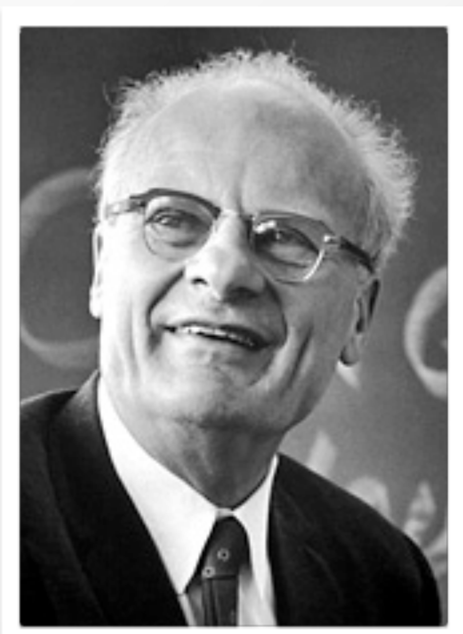

Hans Bethe
(1906-2005)

There can be bound states in a Heisenberg spin chain!
Development of Bethe Ansatz.

$$H = -J_{ex} \sum_i \left(\hat{S}_i^x \hat{S}_{i+1}^x + \hat{S}_i^y \hat{S}_{i+1}^y \right) - \Delta \sum_i \hat{S}_i^z \hat{S}_{i+1}^z$$

$$\boxed{H = -\frac{J_{ex}}{2} \sum_i \left(\hat{S}_i^+ \hat{S}_{i+1}^- + \hat{S}_i^- \hat{S}_{i+1}^+ \right) - \Delta \sum_i \hat{S}_i^z \hat{S}_{i+1}^z}$$

H. Bethe, Z. Phys. (1931)
M. Wortis, Phys Rev. (1963)
M. Takahashi & M. Suzuki Prog. Th. Phys. (1972)
M. Karbach, G. Müller (1997)
see also: **repulsively bound pairs & interacting atoms**
K. Winkler et al. Nature (2006); S. Fölling et al. Nature (2007); Y Lahini et al. PRA (2012)

Bound l-string

Eigenenergies:

$$E(k) = -J_{ex}\frac{sin(\nu)}{sin(l\nu)}\left\{\cos(l\nu) - (-1)^l \cos k\right\}$$

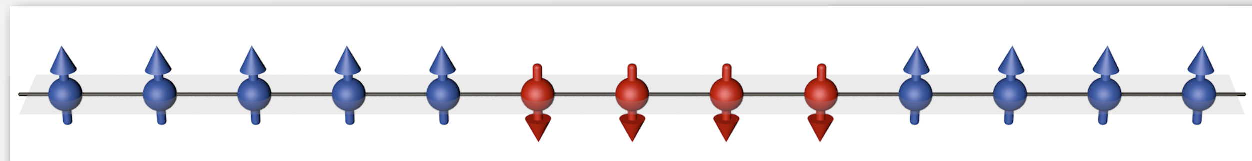

$$\Delta = \cos(\nu)$$

l-string

Maximum propagation velocity:

$$v_{max,l} = \frac{\sin(\nu)}{\sin(l\nu)} \qquad v_{max,2} = \frac{J}{2\Delta}$$

Excitation spectrum:

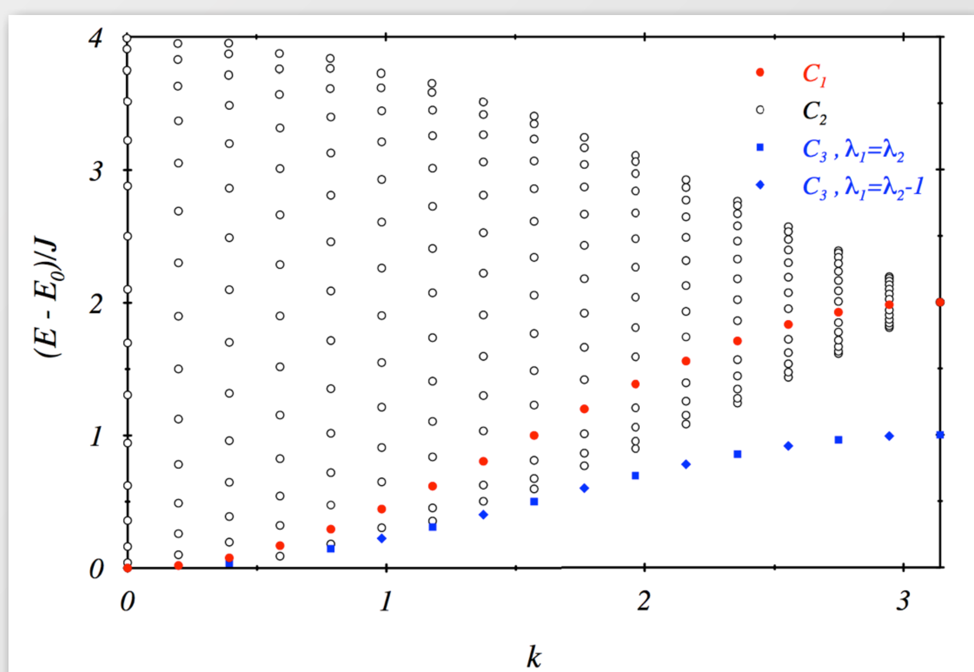

M. Karbach & G. Müller (1997)

Bound magnon

A Challenge for CM Physics

Very difficult to observe in spectroscopic data in real materials!

theory **with** bound states

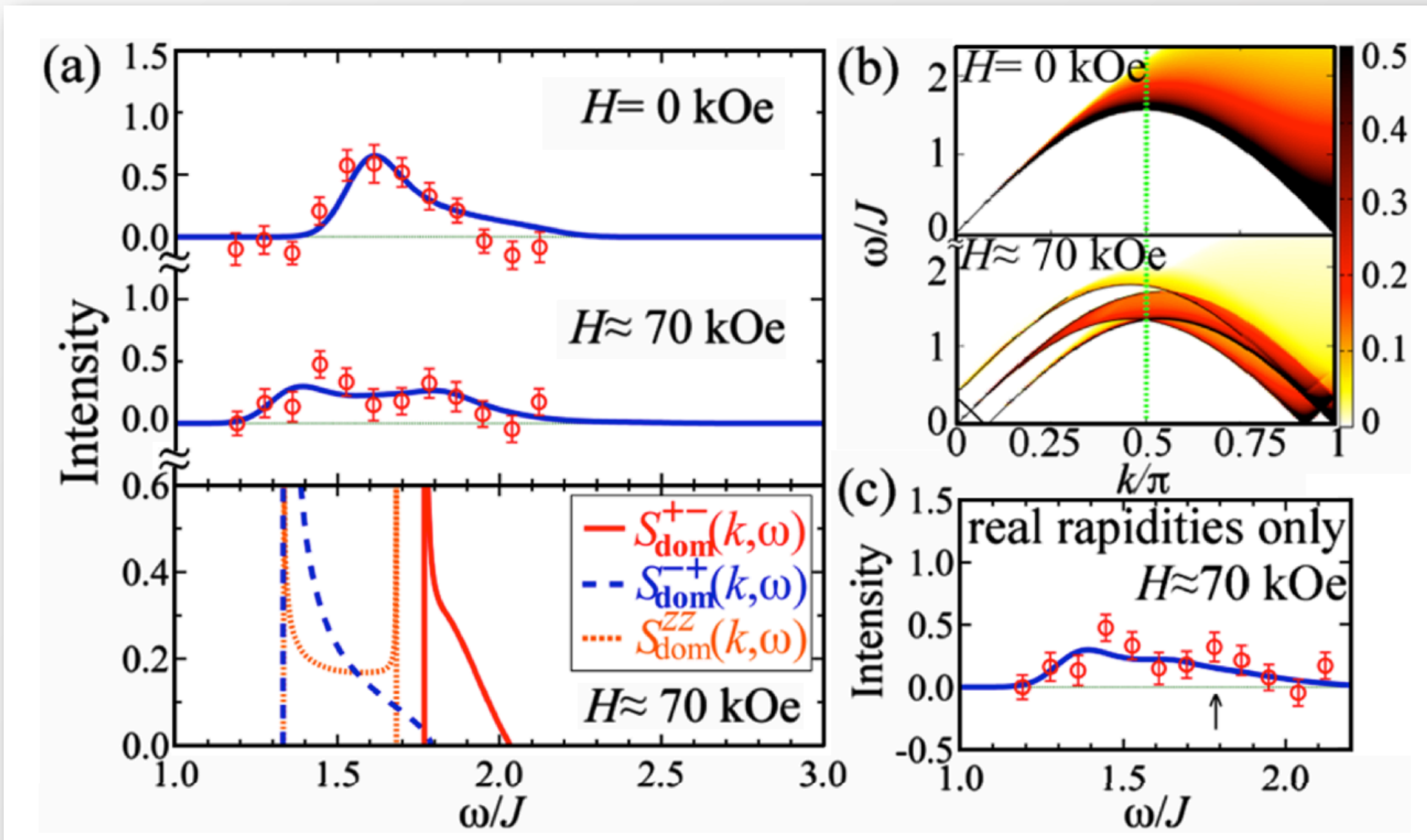

theory **without** bound states

M. Kohno, Phys. Rev. Lett. **102**, 037203 (2009)

Initial State Decomposition

Ansatz

$$|\Psi\rangle = \sum_{1\leq i<j\leq N} a(i,j)|i,j\rangle \qquad |i,j\rangle = \hat{S}_i^- \hat{S}_j^- |\ldots\uparrow\uparrow\uparrow\uparrow\ldots\rangle$$

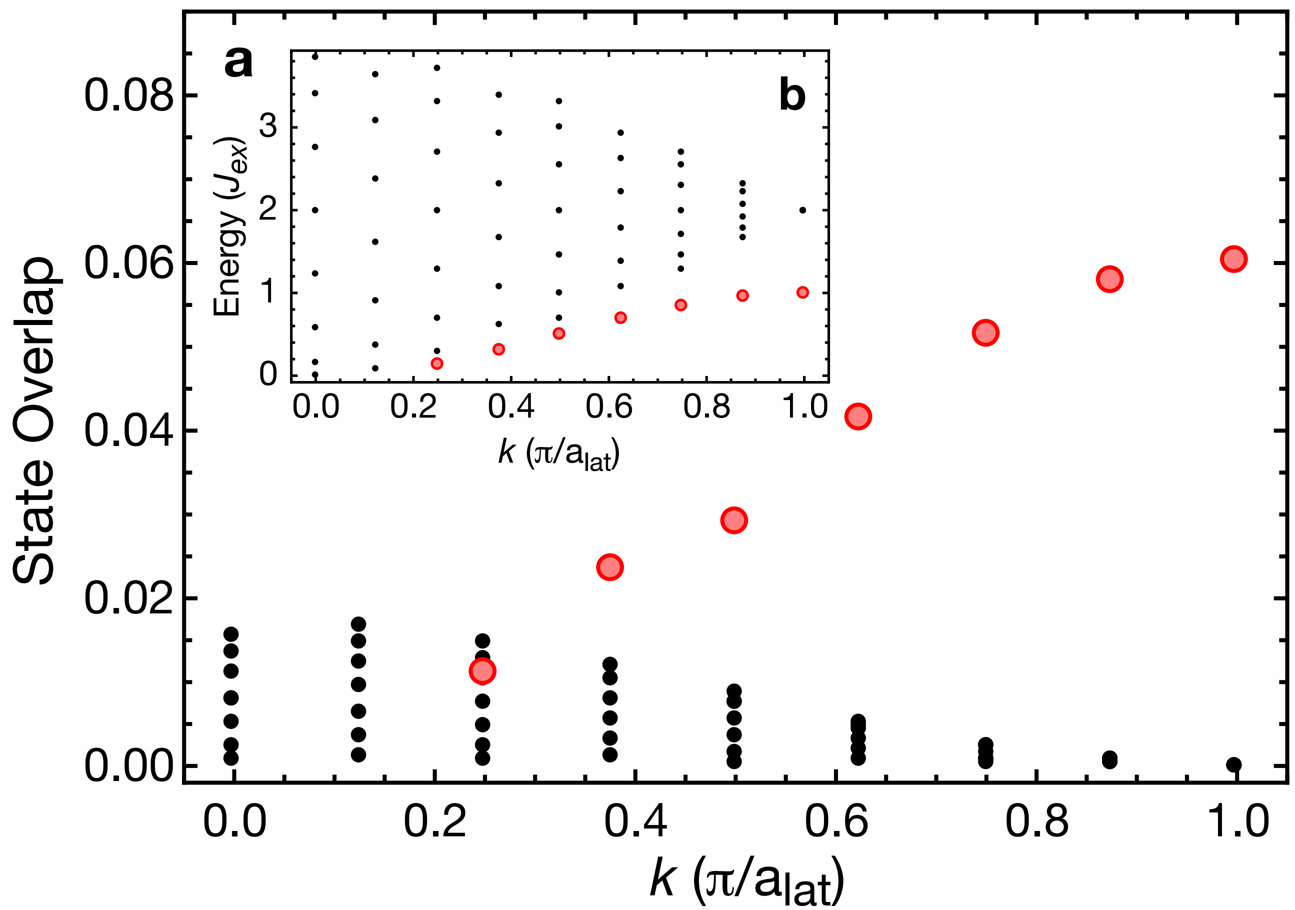

Initial State Overlap with Bound Magnon and Free Magnon States

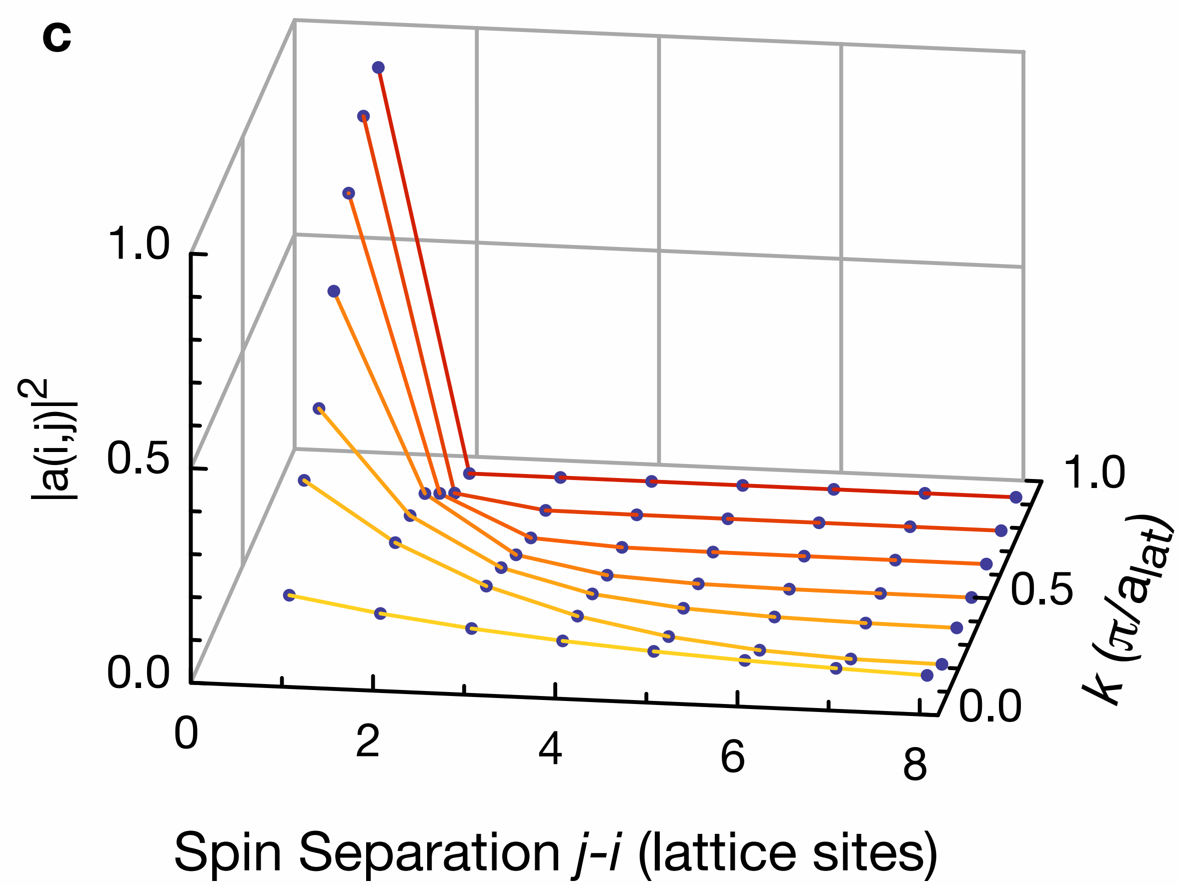

Spin Correlations in Bound Magnon Wavefunction

Dynamical Evolution

Bound Magnon Motion

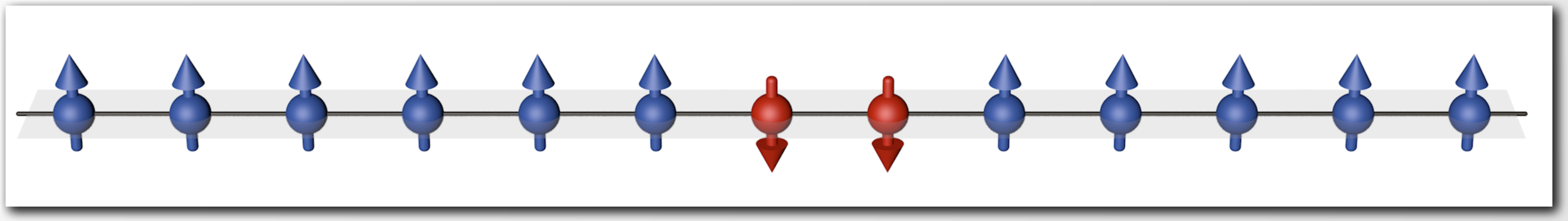

M. Ganahl et al., Phys. Rev. Lett. (2012)

Dynamical Evolution

Bound Magnon Motion

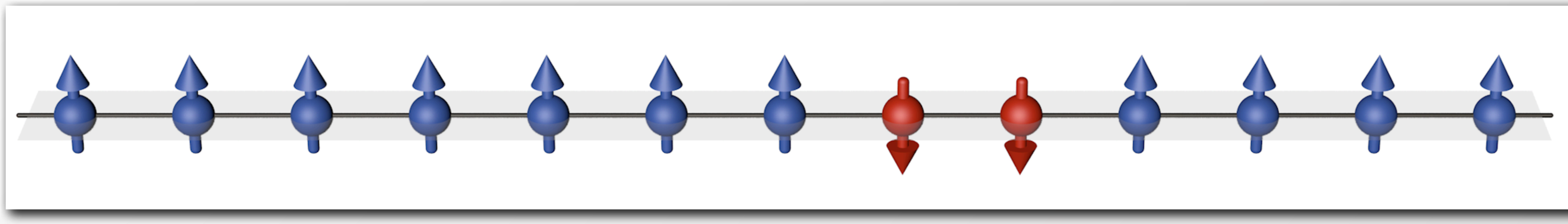

M. Ganahl et al., Phys. Rev. Lett. (2012)

Dynamical Evolution

Bound Magnon Motion

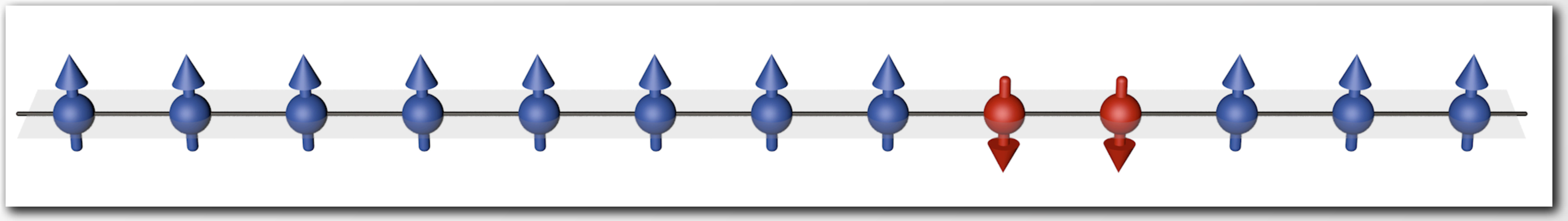

M. Ganahl et al., Phys. Rev. Lett. (2012)

Dynamical Evolution

Bound Magnon Motion

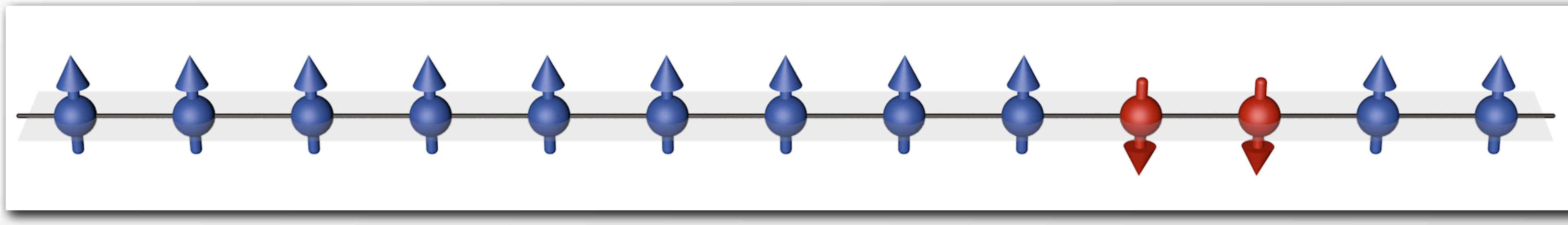

M. Ganahl et al., Phys. Rev. Lett. (2012)

Dynamical Evolution

Bound Magnon Motion

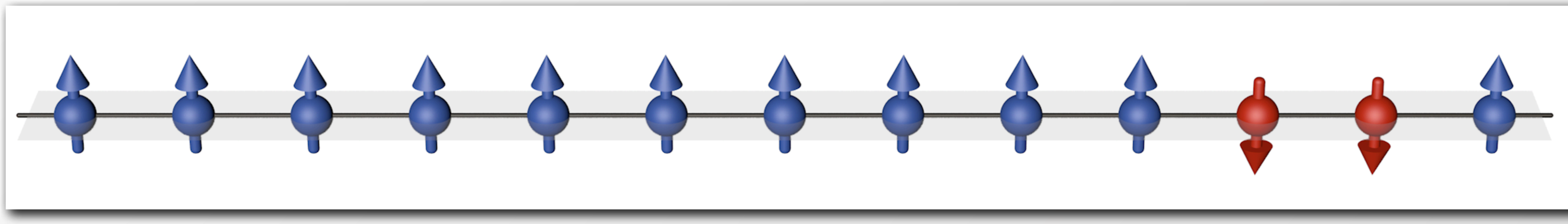

M. Ganahl et al., Phys. Rev. Lett. (2012)

Dynamical Evolution

Bound Magnon Motion

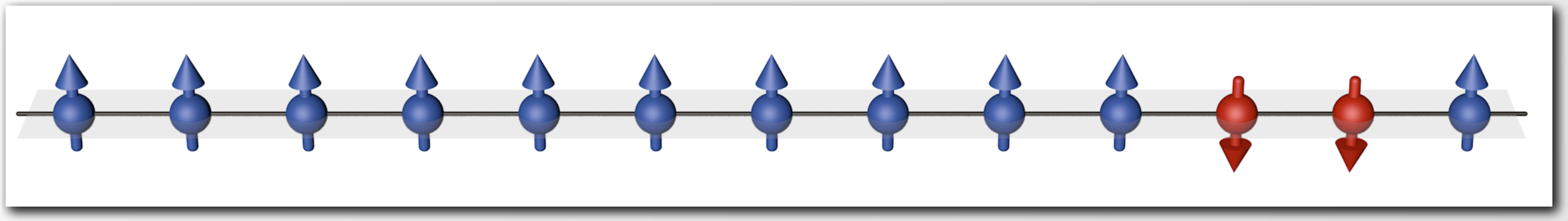

Breakup and Single Spin Motion

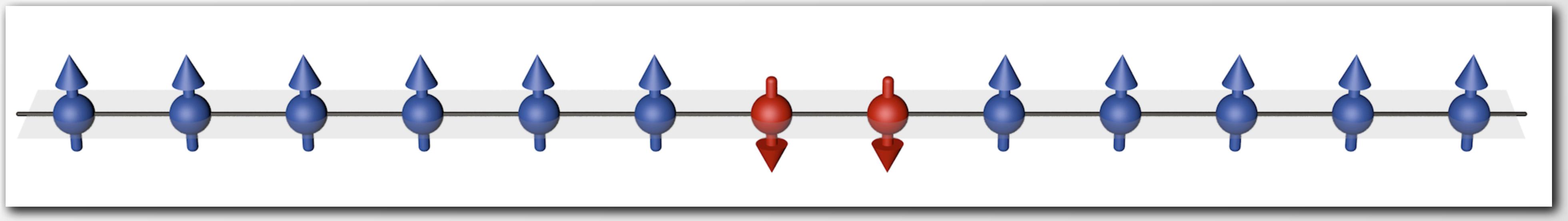

M. Ganahl et al., Phys. Rev. Lett. (2012)

Dynamical Evolution

Bound Magnon Motion

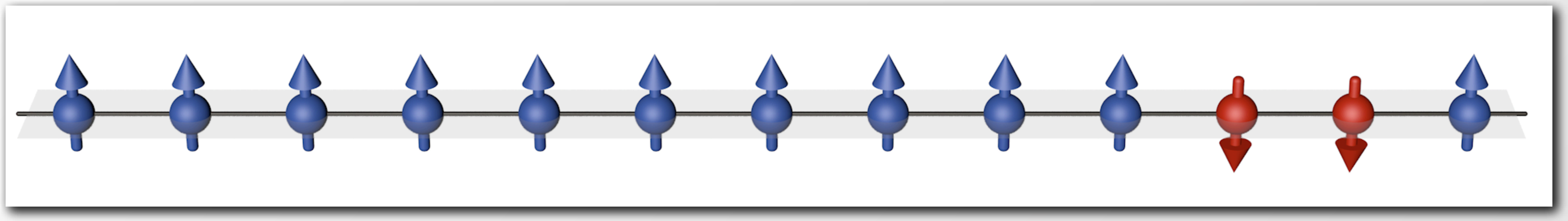

Breakup and Single Spin Motion

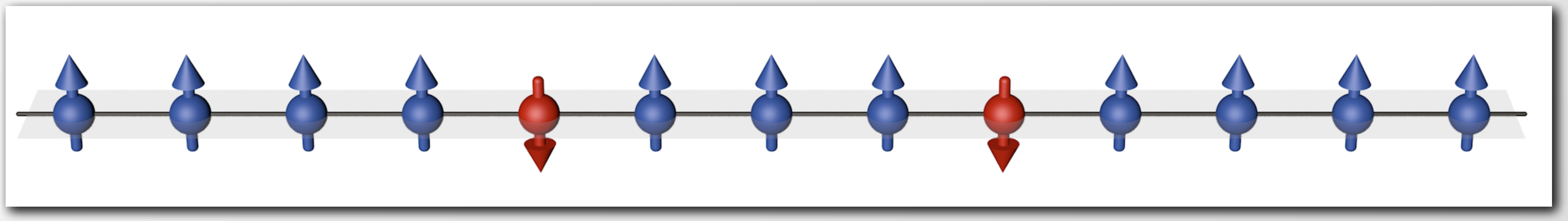

M. Ganahl et al., Phys. Rev. Lett. (2012)

Dynamical Evolution

Bound Magnon Motion

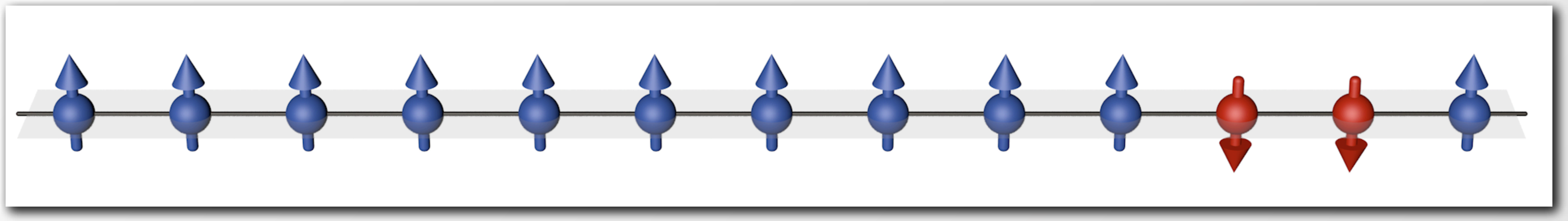

Breakup and Single Spin Motion

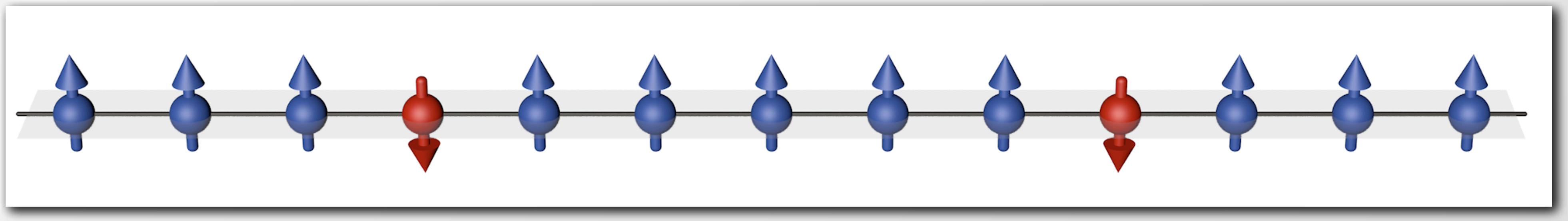

M. Ganahl et al., Phys. Rev. Lett. (2012)

Dynamical Evolution

Bound Magnon Motion

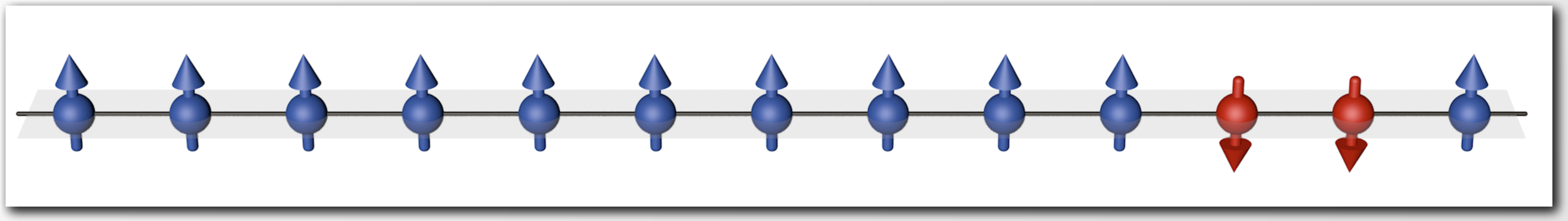

Breakup and Single Spin Motion

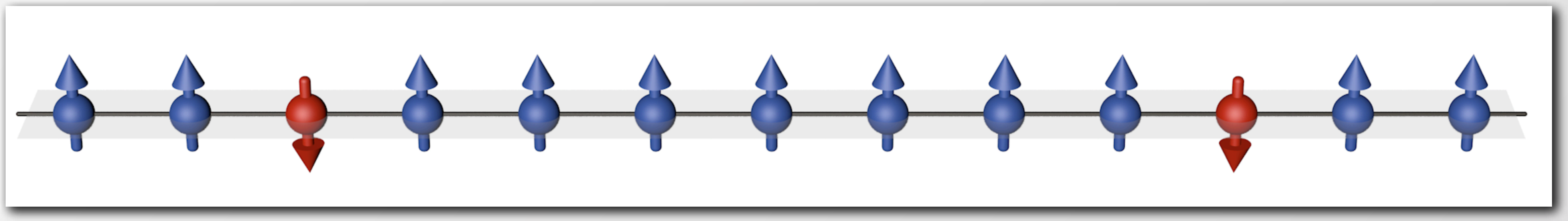

M. Ganahl et al., Phys. Rev. Lett. (2012)

Dynamical Evolution

Bound Magnon Motion

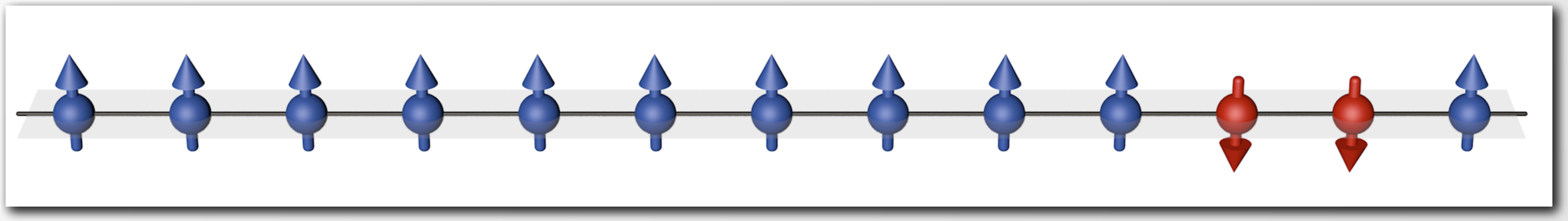

Breakup and Single Spin Motion

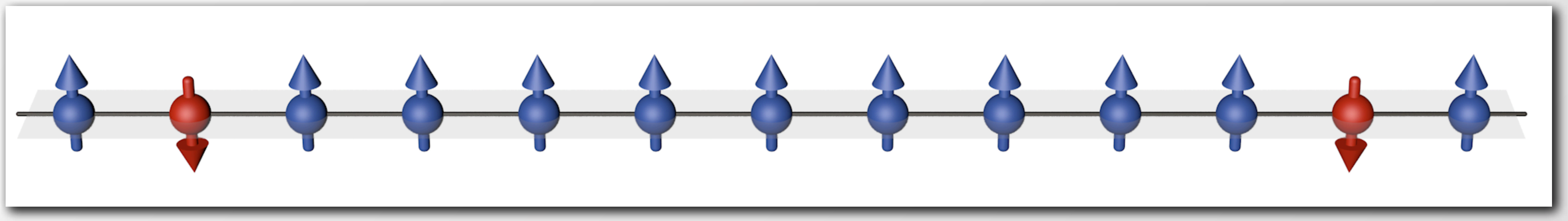

M. Ganahl et al., Phys. Rev. Lett. (2012)

Two-spin excitation in FM ↓↓↓↓↓↓↓↓↑↑↓↓↓↓↓↓↓↓

S_z

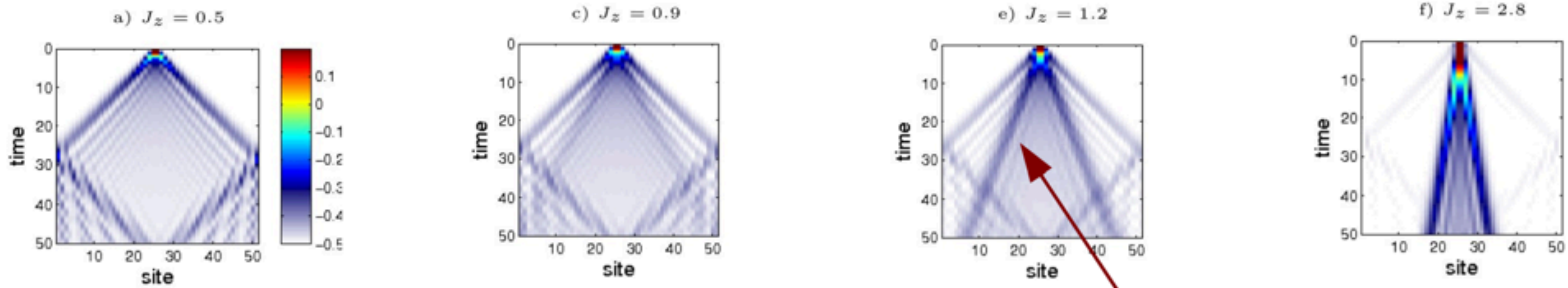

$J_z = 0.5$ $J_z = 0.9$ $J_z = 1.2$ $J_z = 2.8$

- Two distinct propagation branches beyond $J_z = 0.7$
- New lower branch is *bound state*
- It dominates at large J_z, with decreasing velocity
- Low entanglement entropy (see below)

P(↑↑)

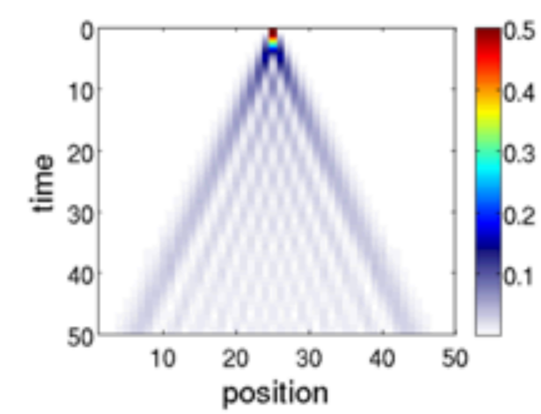

From: H.G. Evertz

M. Ganahl et al., Phys. Rev. Lett. (2012)

Dynamical Evolution

Initial State:

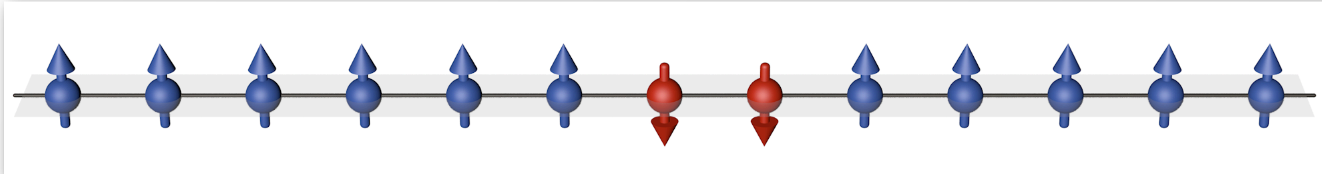

Pair distribution evolution $P(x_1, x_2)$

$\Delta = 0$

Non-Interacting

x_1

x_2

see also: two interacting atoms

Y. Lahini et al., PRA 86, 011603 (2012)

Dynamical Evolution

Initial State:

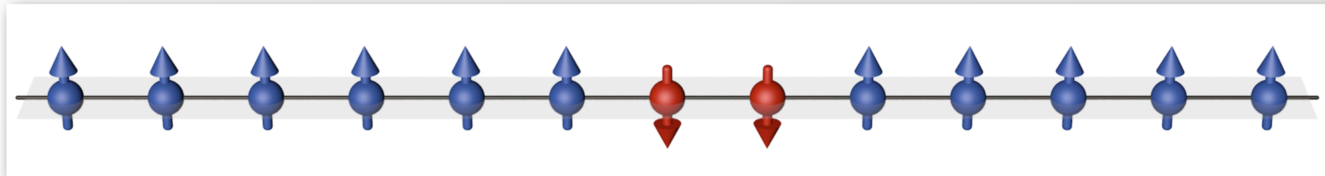

Pair distribution evolution

$P(x_1, x_2)$

x_1

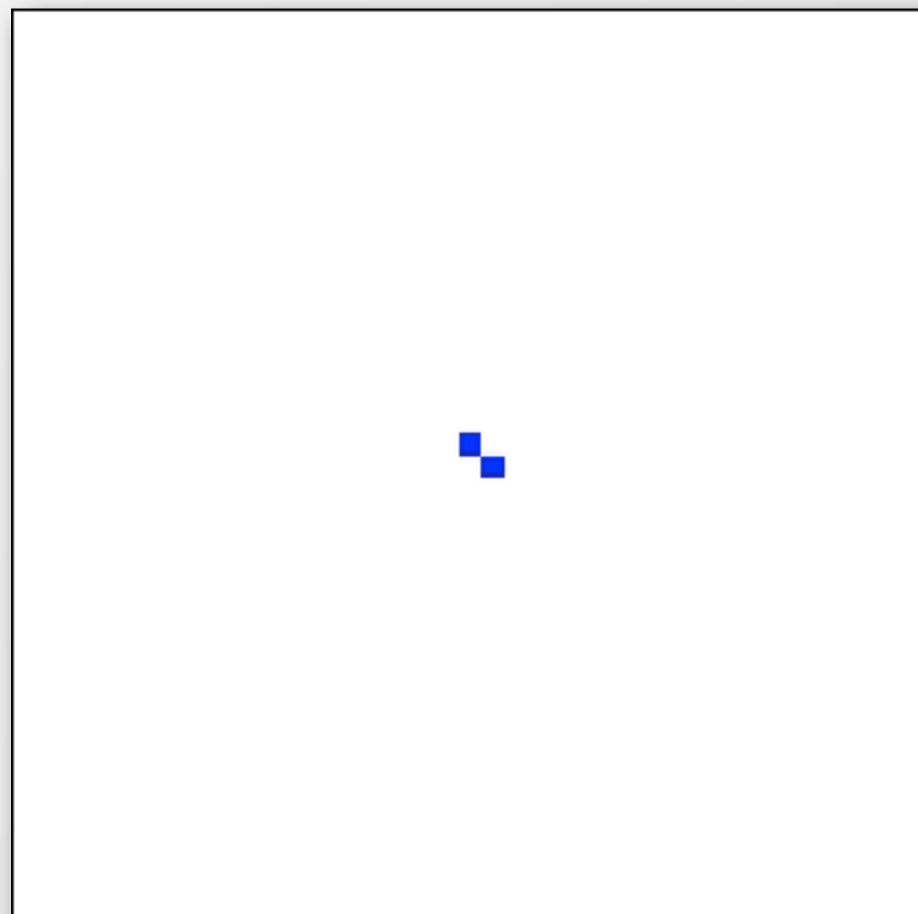

x_2

$\Delta = 0$

Non-Interacting

see also: two interacting atoms

Y. Lahini et al., PRA 86, 011603 (2012)

Dynamical Evolution

Initial State:

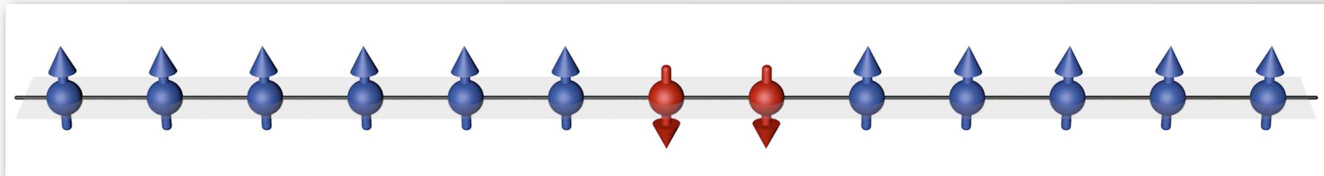

Pair distribution evolution

$$P(x_1, x_2)$$

$\Delta = 1$

Interacting

Isotropic Heisenberg

x_1

x_2

Dynamical Evolution

Initial State:

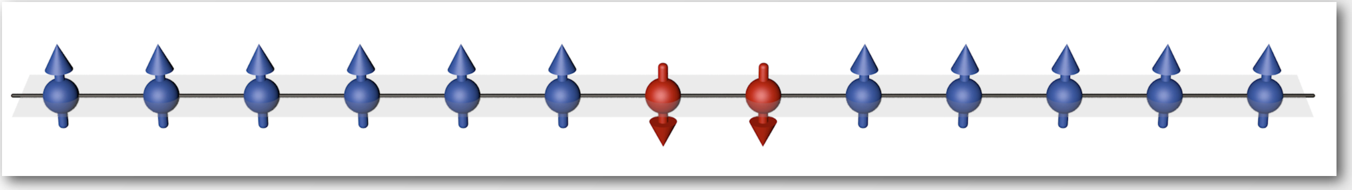

Pair distribution evolution

$P(x_1, x_2)$

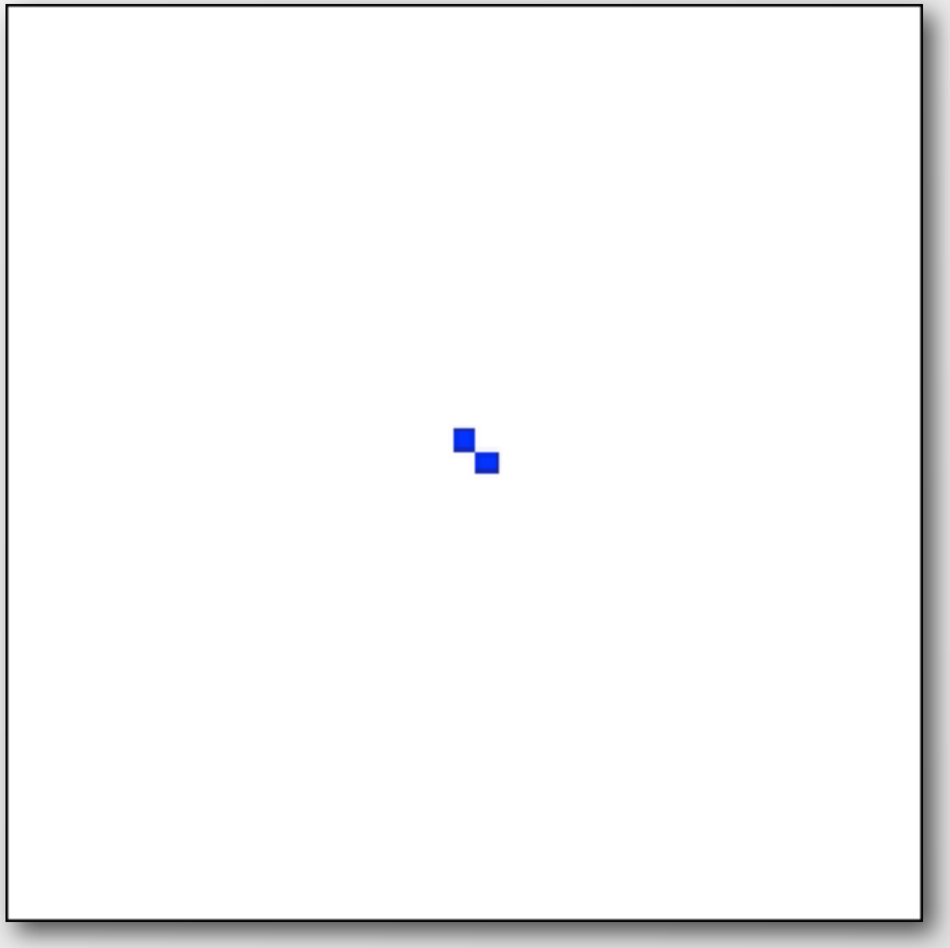

x_1

x_2

$\Delta = 1$

Interacting

Isotropic Heisenberg

Dynamical Evolution

Initial State:

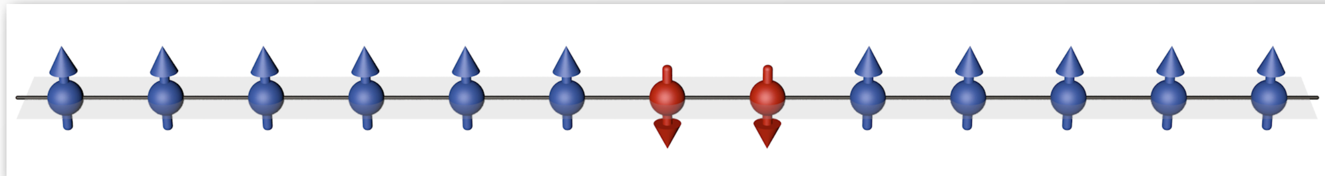

Pair distribution evolution

$P(x_1, x_2)$

$\Delta = 1.6$

Interacting Heisenberg

x_1

x_2

Dynamical Evolution

Initial State: 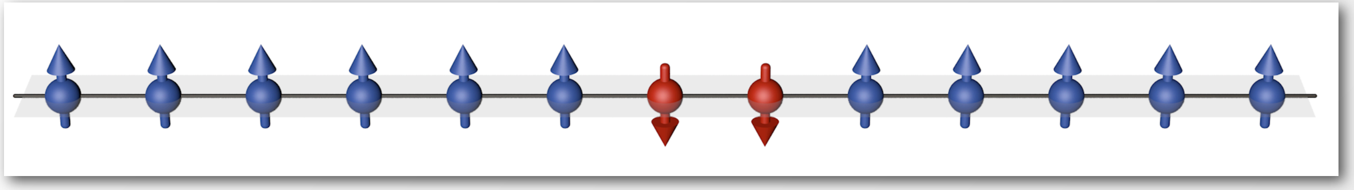

Pair distribution evolution

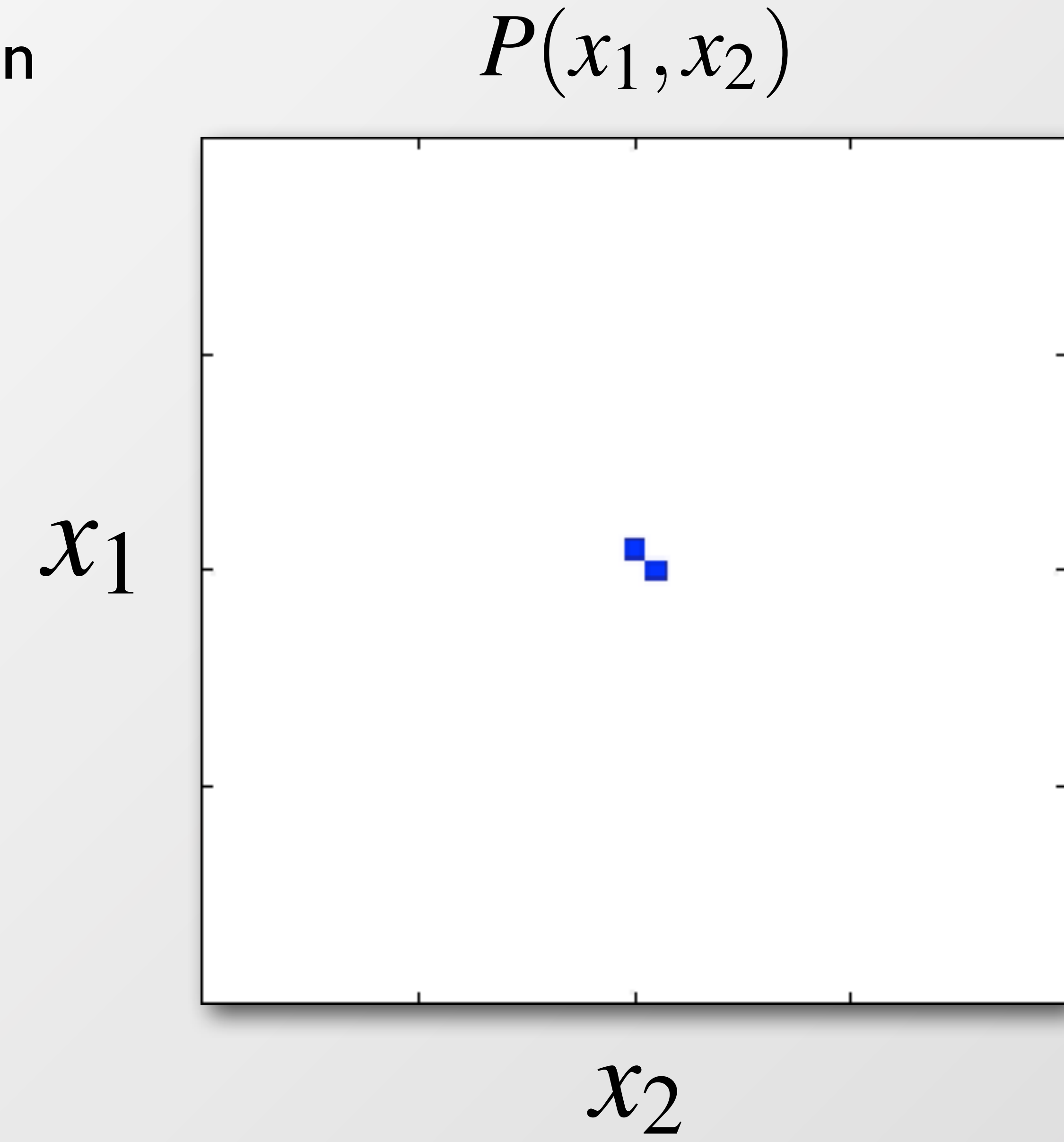

$\Delta = 1.6$
Interacting
Heisenberg

Experimental Results

$$C(x_1, x_2) = P(x_1, x_2) - P(x_1)P(x_2)$$

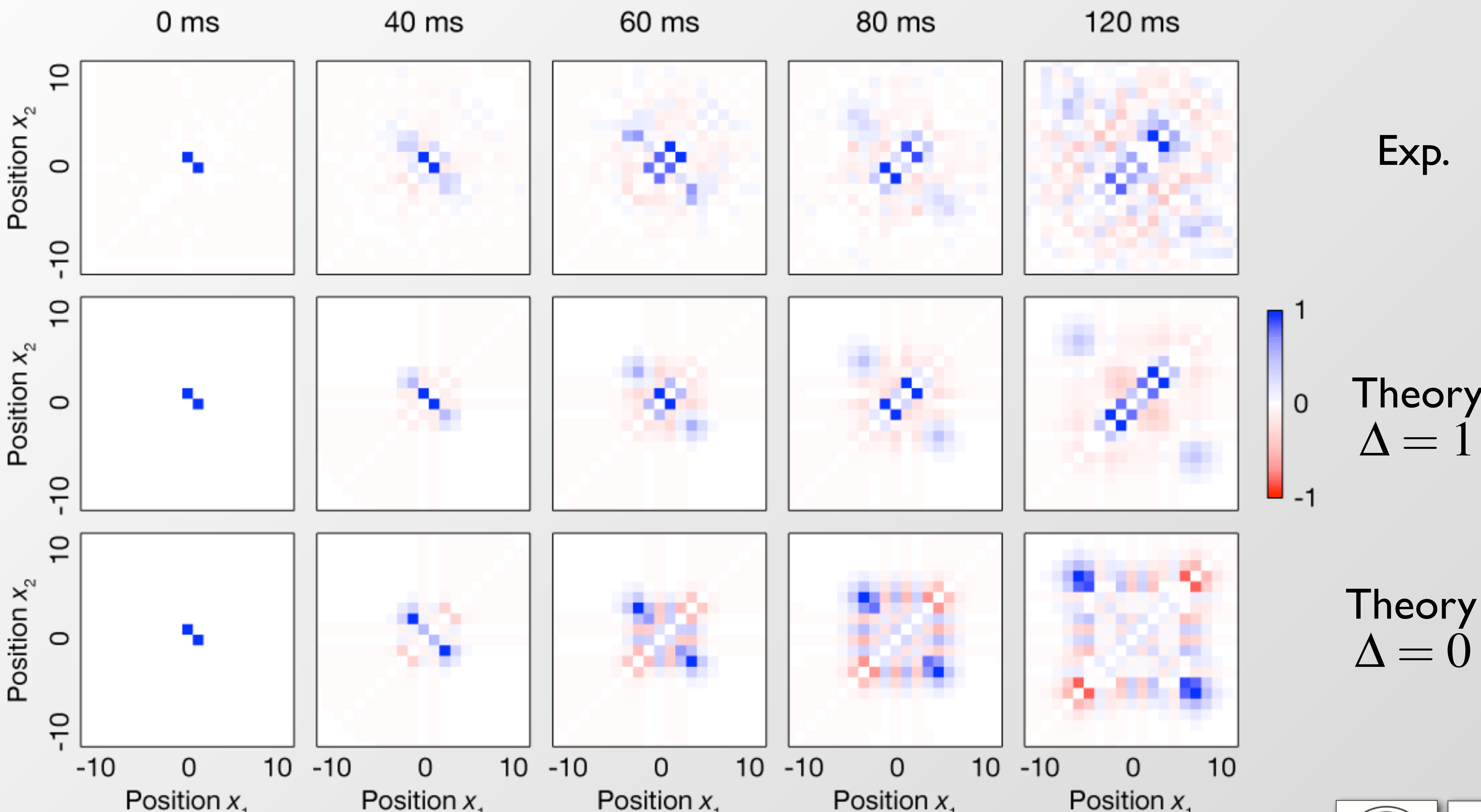

Propagation Velocity

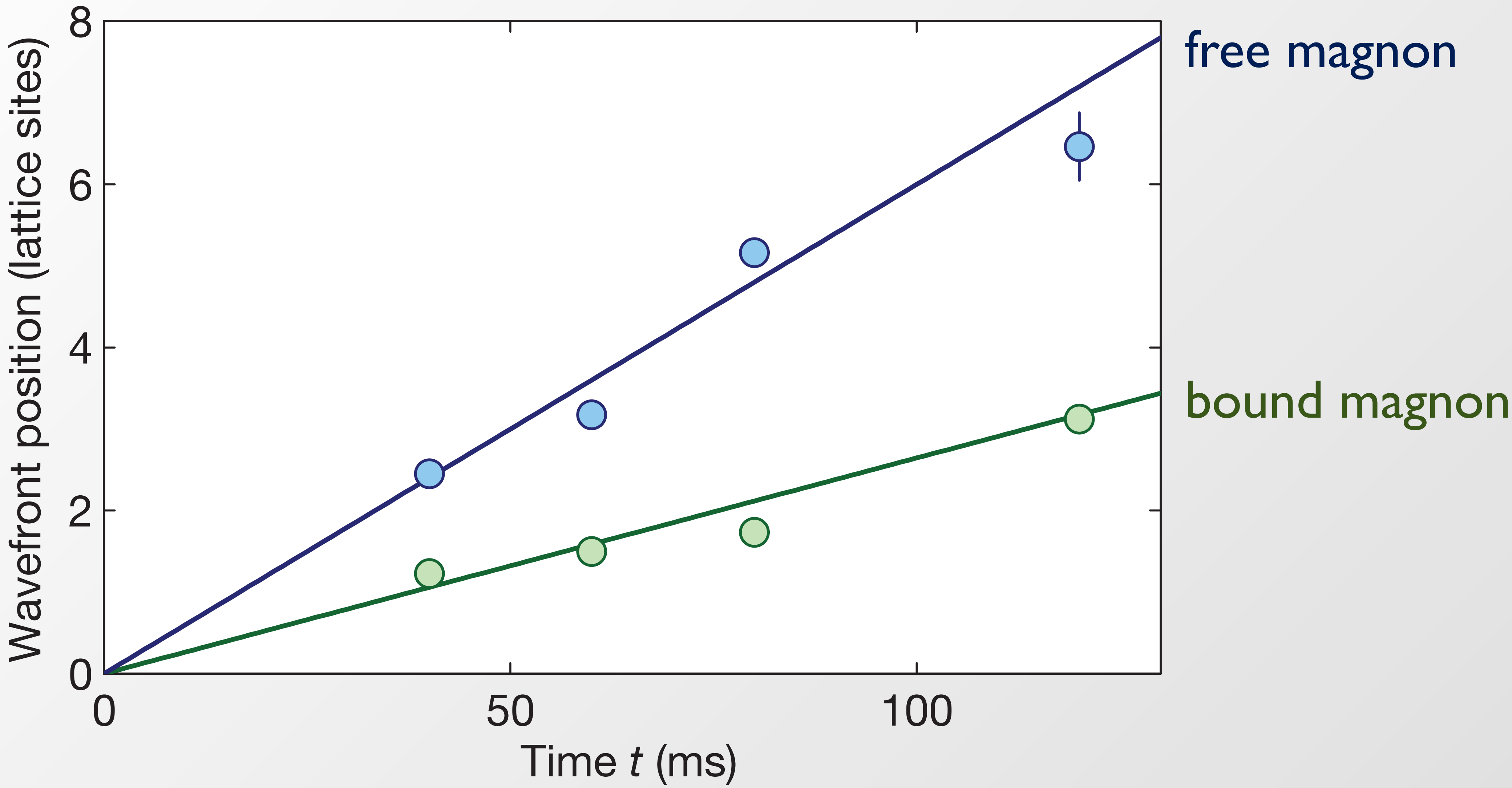

$$v_f = \frac{J_{ex} a}{\hbar}$$

$$v_b = \frac{J_{ex} a}{2\hbar\Delta}$$

$$\Rightarrow \quad \boxed{\frac{v_f}{v_b} = 2\Delta}$$

Propagation Velocity

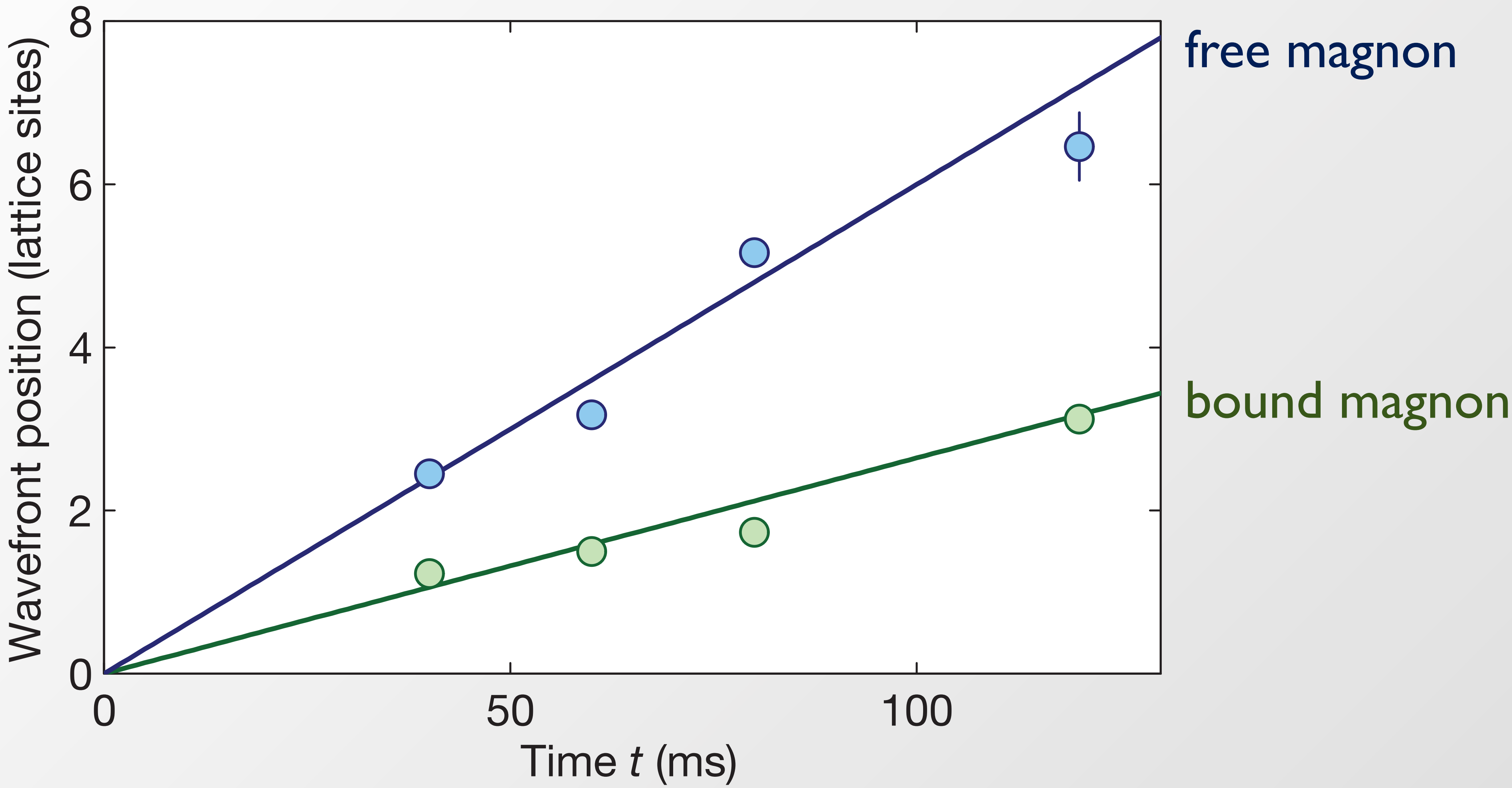

$$v_f = \frac{J_{ex}a}{\hbar}$$

$$v_b = \frac{J_{ex}a}{2\hbar\Delta}$$

$$\boxed{\frac{v_f}{v_b} = 2\Delta}$$

We find: $\frac{v_f}{v_b} = 2.3(3)$

Outlook

Quantum Dynamics of Interacting Atoms/Spins

- Effect of Temperature/Holes on Dynamics
- Dynamics of l-string bound states
- Domain Walls
- Higher Dimensions (1D, 2D, 3D)
- Entropy Transport
- Probe for Quantum Critical Transport
- Direct measurement of Green's function

$$G(x_i, x_j, t) \propto \langle \Uparrow | \hat{S}^{\dagger}(x_j, t) \hat{S}^{-}(x_i, 0) | \Uparrow \rangle$$

M. Knap et al. PRL **111**, 147205 (2013)

Controlling and Detecting Spin Correlations

S. Trotzky et al., Phys. Rev. Lett 105, 265303 (2010)

Splitting a spin pair

- **Spin pairs** in $|F = 1, m_F = \pm 1\rangle \equiv |\uparrow\rangle, |\downarrow\rangle$ (repulsive)
- Barrier raised *slowly* to split

  $\rightarrow$ Crossing a miniature Mott-transition: $n_{\mathrm{Left}} = n_{\mathrm{Right}} = 1$

  *J. Sebby-Strabley et al., PRL **98** (2007)*

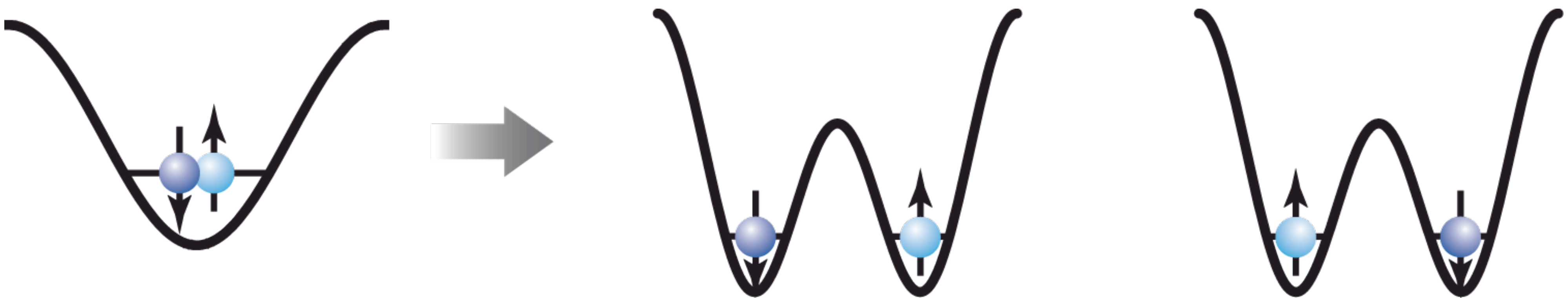

Details on the loading of the Spin-pairs:
*S.T., P. Cheinet et al., Science **319** (2008)*

Splitting a spin pair

- **Spin pairs** in $|F=1, m_F=\pm 1\rangle \equiv |\uparrow\rangle, |\downarrow\rangle$
- Barrier raised *slowly* to split

*J. Sebby-Strabley et al., PRL **98** (2007)*

→ Crossing a miniature Mott-transition: $n_{\text{Left}} = n_{\text{Right}} = 1$

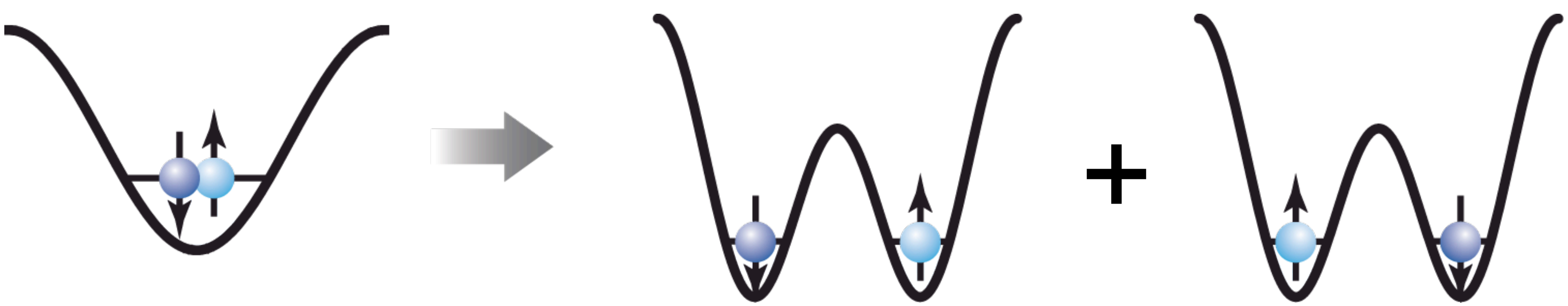

- **Bosons**: Symmetric wavefunction → Triplet $|t_0\rangle$

(Fermions: Antisymmetric wavefunction → Singlet $|s\rangle$)

Details on the loading of the Spin-pairs:
*S.T., P. Cheinet et al., Science **319** (2008)*

Driving Triplet-Singlet oscillations

- **Magnetic field gradient** lifts degeneracy:

$$\Delta_B \propto a \cdot \partial_x B_x$$

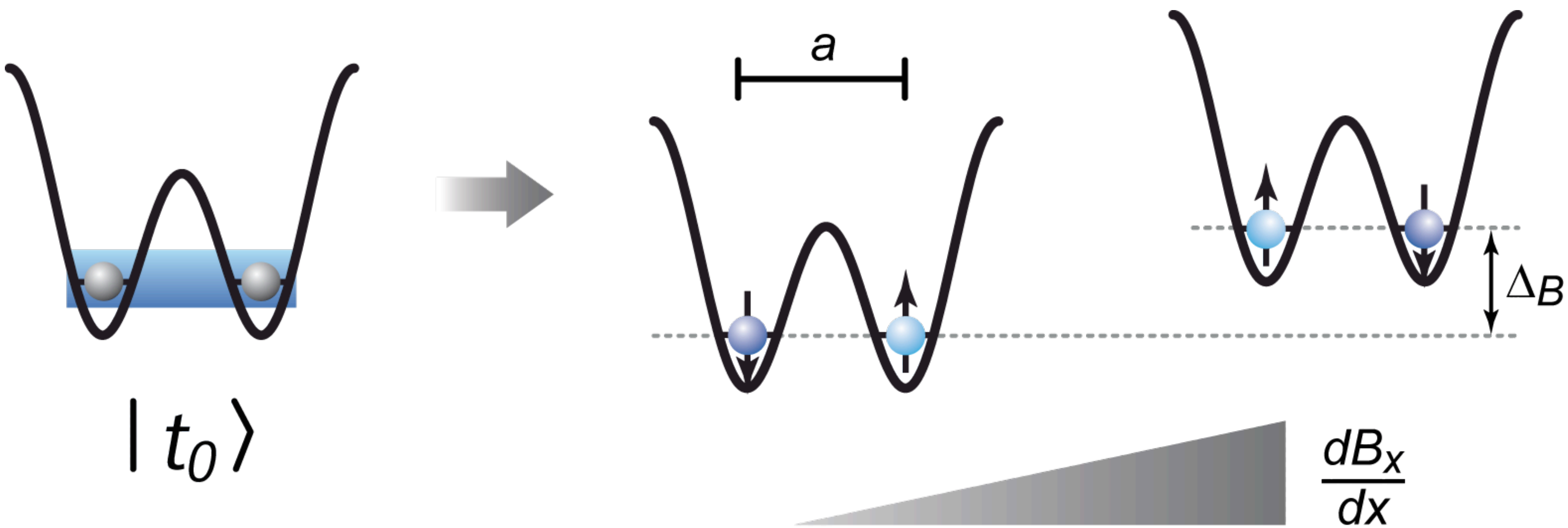

Driving Triplet-Singlet oscillations

- **Magnetic field gradient** lifts degeneracy:

$$\Delta_B \propto a \cdot \partial_x B_x$$

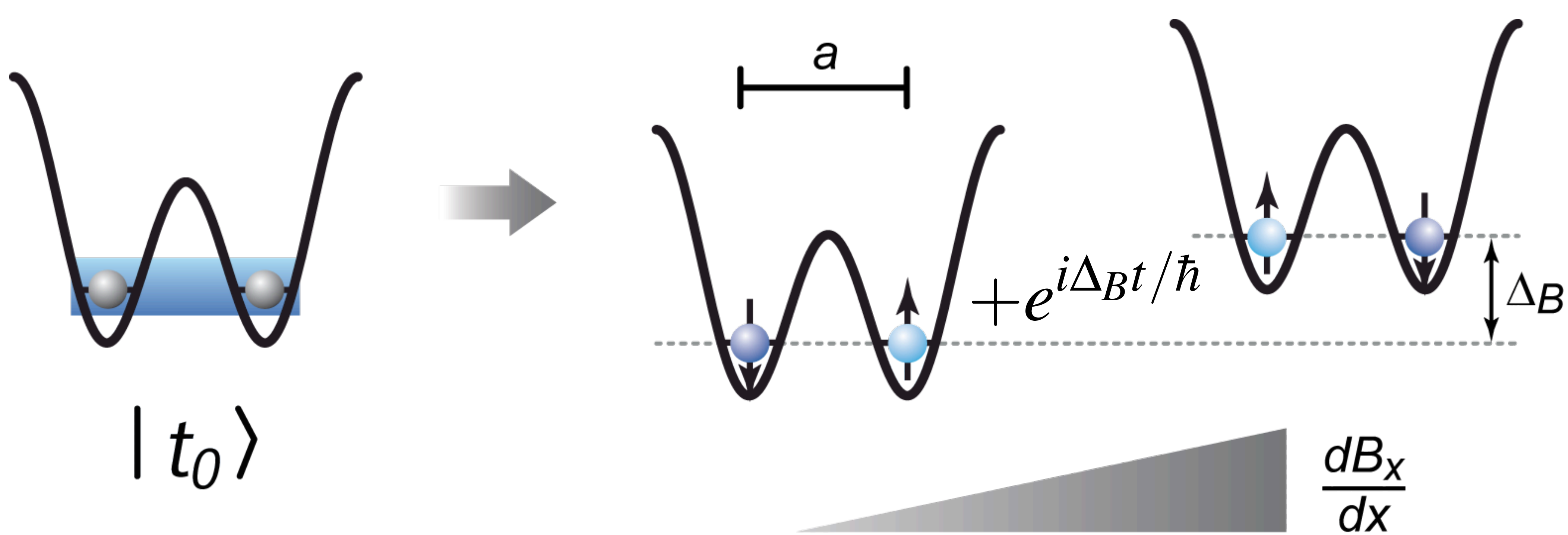

- **Triplet-Singlet oscillations** with frequency $\Delta_B/\hbar$

$$|t_0\rangle \leftrightarrow |s\rangle$$

How to detect triplets and singlets

- Barrier lowered slowly to **merge** double-wells

  → **Triplet**: both atoms reach the **ground state**

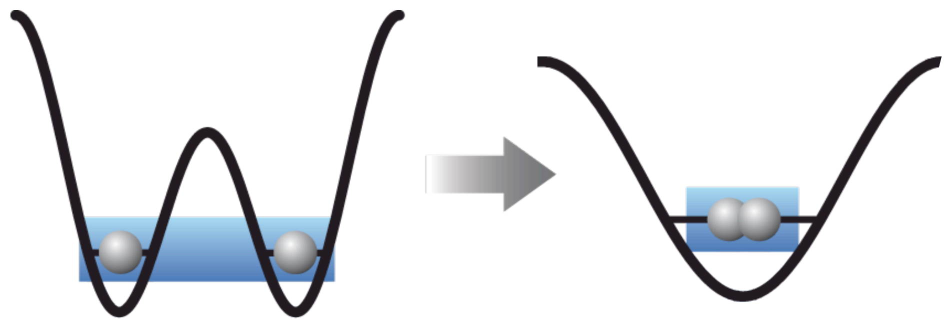

How to detect triplets and singlets

- Barrier lowered slowly to **merge** double-wells

  → **Triplet**: both atoms reach the **ground state**

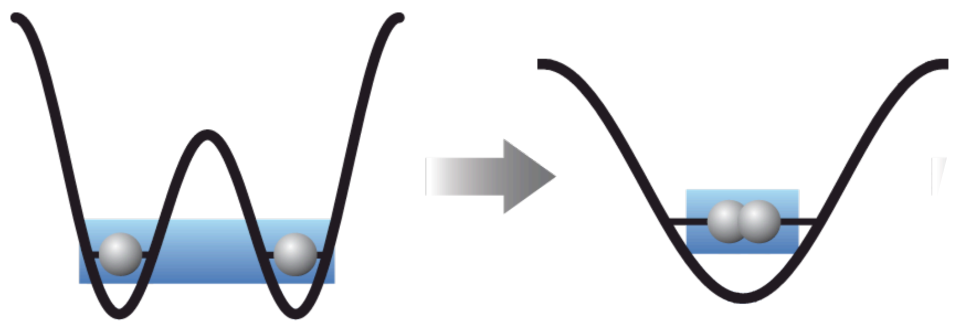

→ **Singlet**: needs anti-symm. spatial wavefunction (Bosons)

One atom transferred to **higher vibrational band**

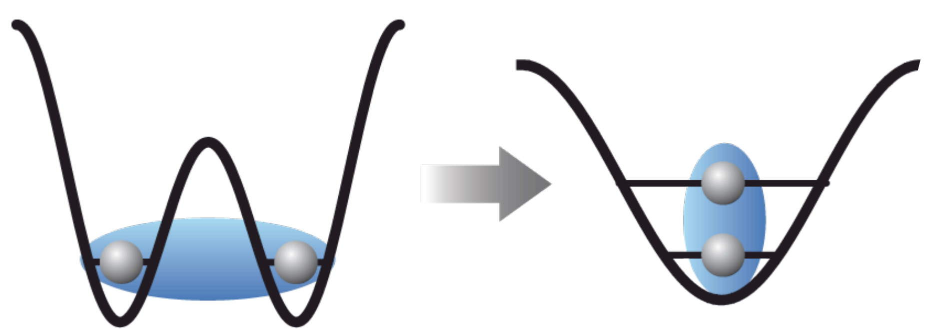

How to detect triplets and singlets

- Barrier lowered slowly to **merge** double-wells

→ **Triplet**: both atoms reach the **ground state**

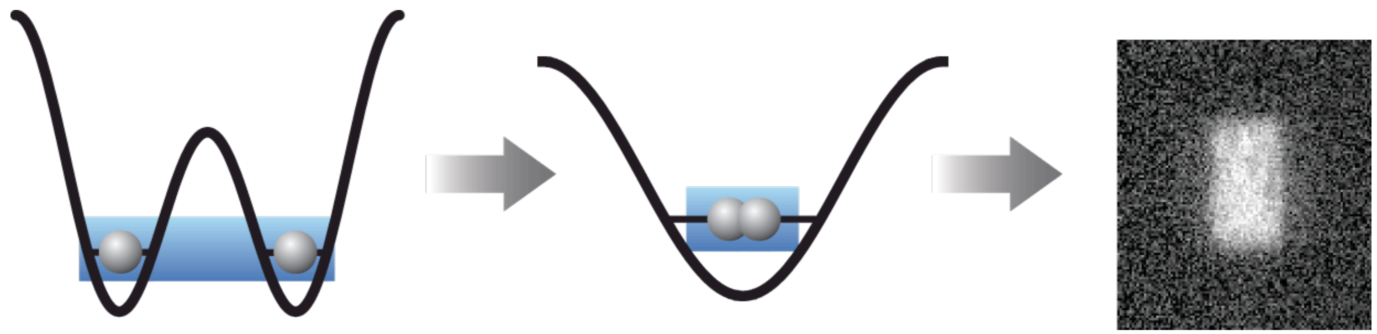

→ **Singlet**: needs anti-symm. spatial wavefunction (Bosons)

One atom transferred to **higher vibrational band**

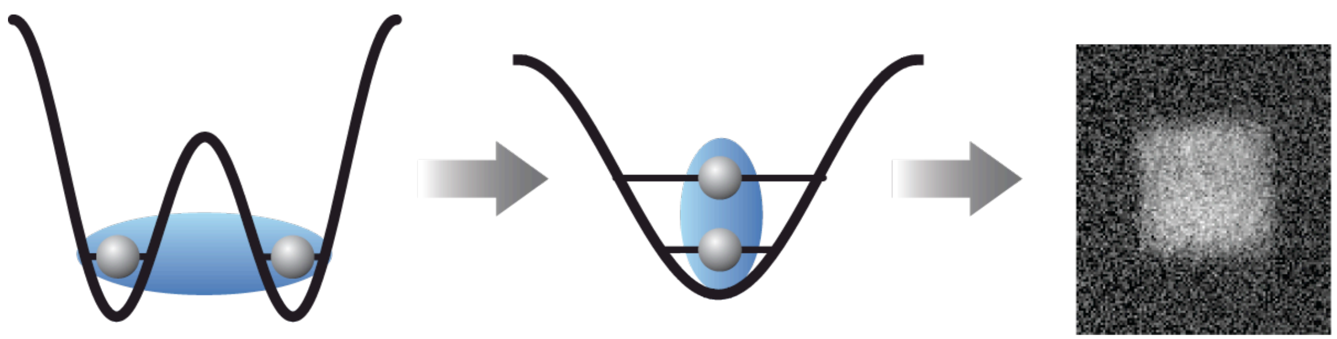

Band-mapping reveals **singlet-contribution in higher Brillouin-Zone**

A sensitive probe of next-neighbor spin-correlations in Mott-insulator type many-body systems

	band excitations		STO amplitude	
	bosons	fermions	bosons	fermions
$\lvert t\rangle$	0%	50%	50%	50%
$\lvert s\rangle$	50%	0%	50%	50%
$\lvert\downarrow,\uparrow\rangle$	25%	25%	0%	0%
$\lvert\uparrow,\downarrow\rangle$	25%	25%	0%	0%
$\lvert\uparrow,\uparrow\rangle$	0%	50%	0%	0%
$\lvert\downarrow,\downarrow\rangle$	0%	50%	0%	0%

→ Capable of probing spin-order in strongly correlated phases at low temperatures

Band-mapping reveals **singlet-contribution in higher Brillouin-Zone**

Singlet-Triplet oscillations

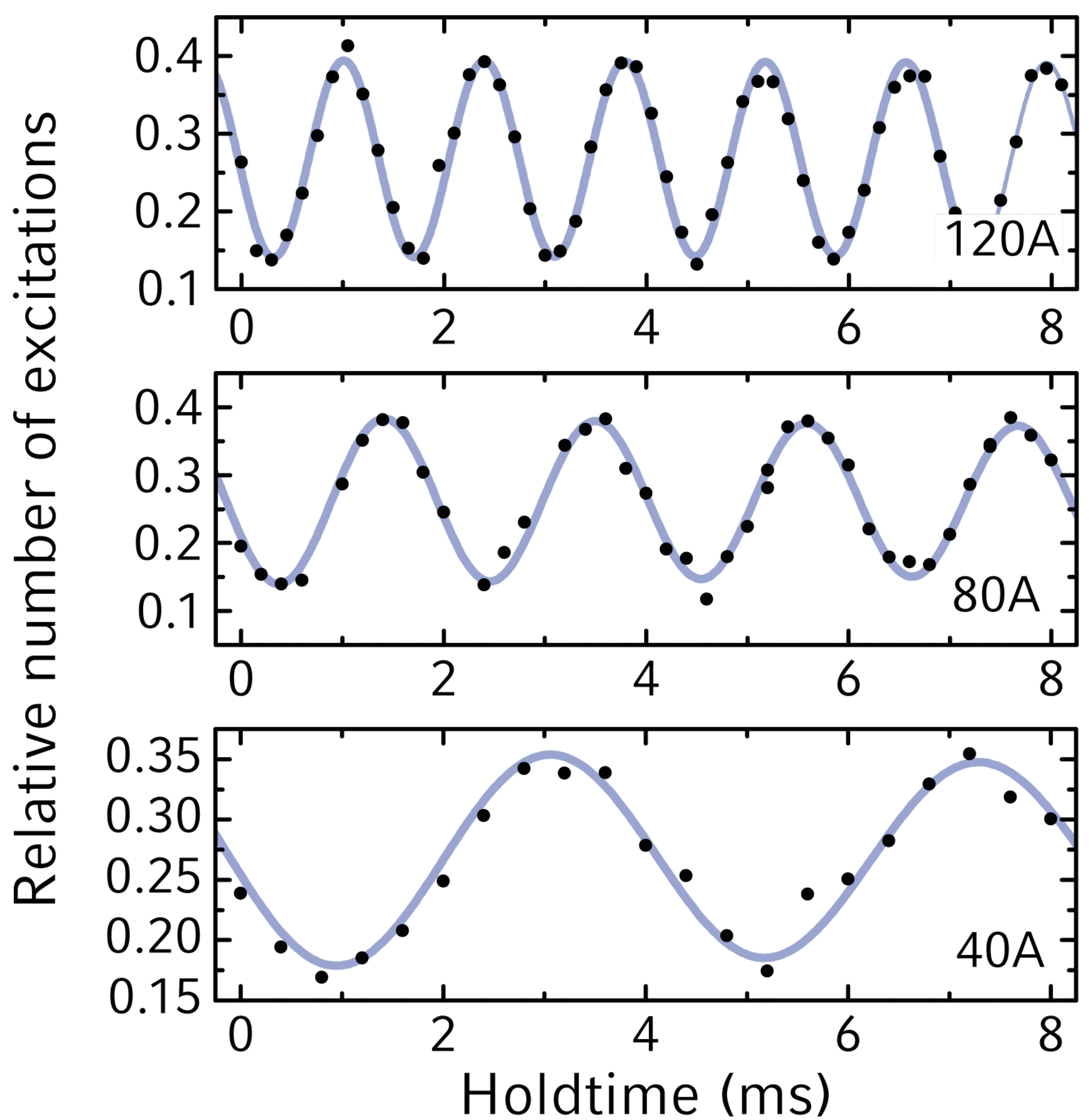

- **Load** system and create **spin pairs**
- Split pairs into **triplets**
- Induce **STO** via gradient
- **Merging** and **band-mapping** for detection

→ **Traces of STO** versus holdtime with gradient

- Vary gradient coil current

Singlet-Triplet oscillations

- **Linear increase** in Frequency with gradient strength
- Frequency = **2x single particle shift** (independently meas.)
  → confirms **2-particle nature** of oscillations

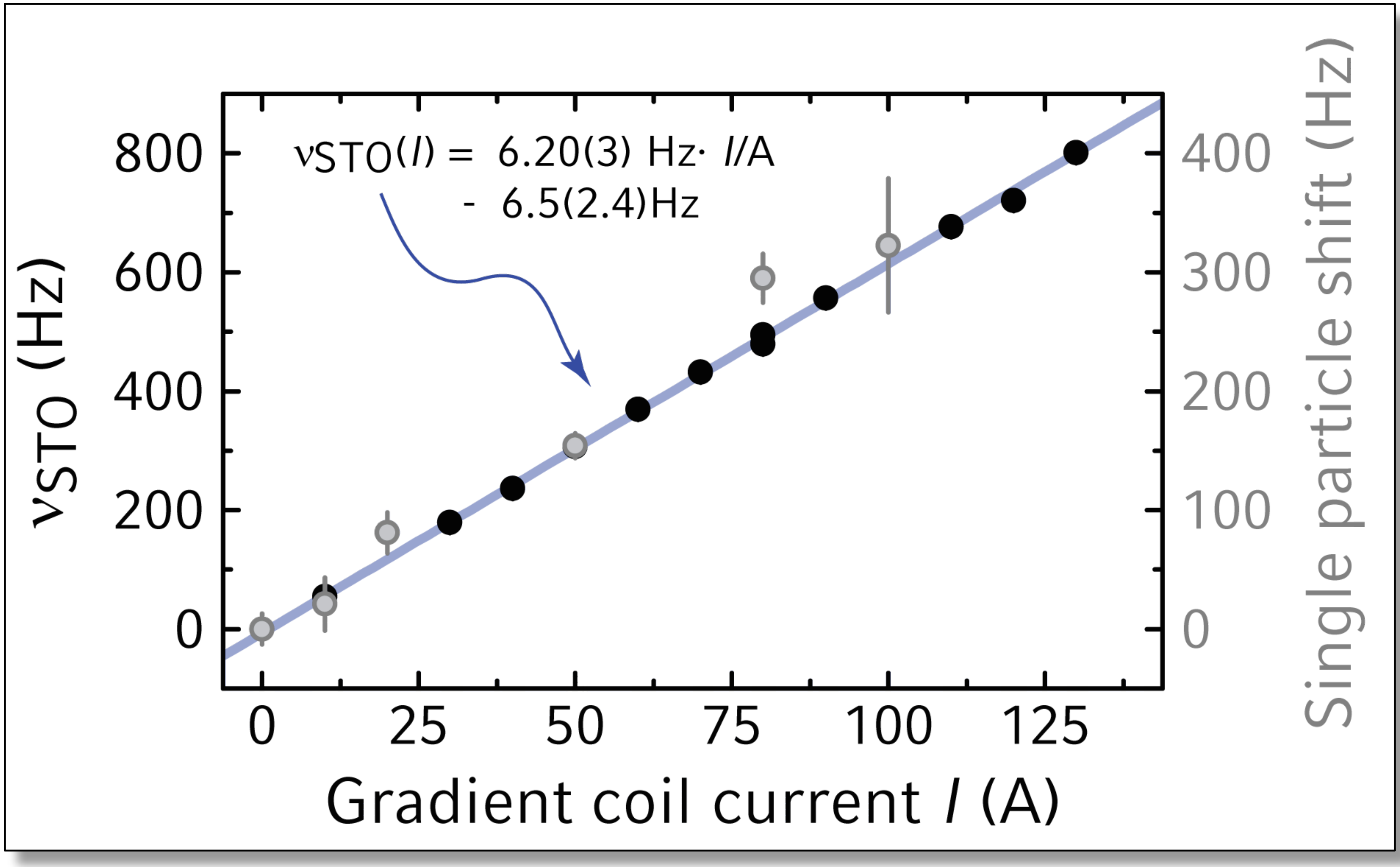

An Optical Lattice of Plaquettes

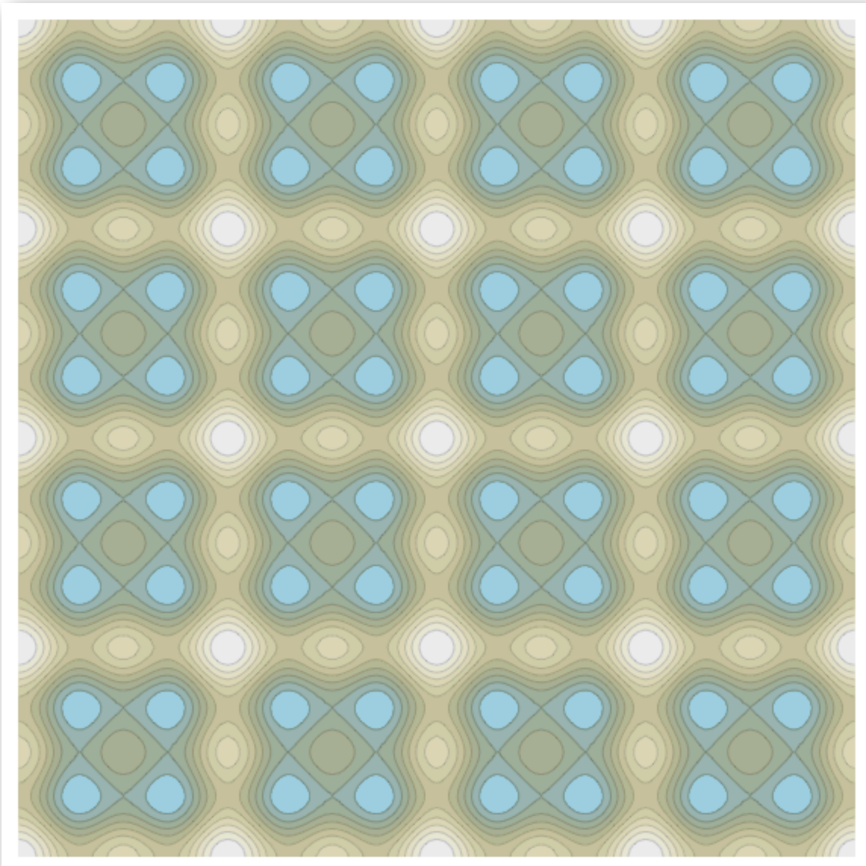

Array of plaquettes
using two superlattices

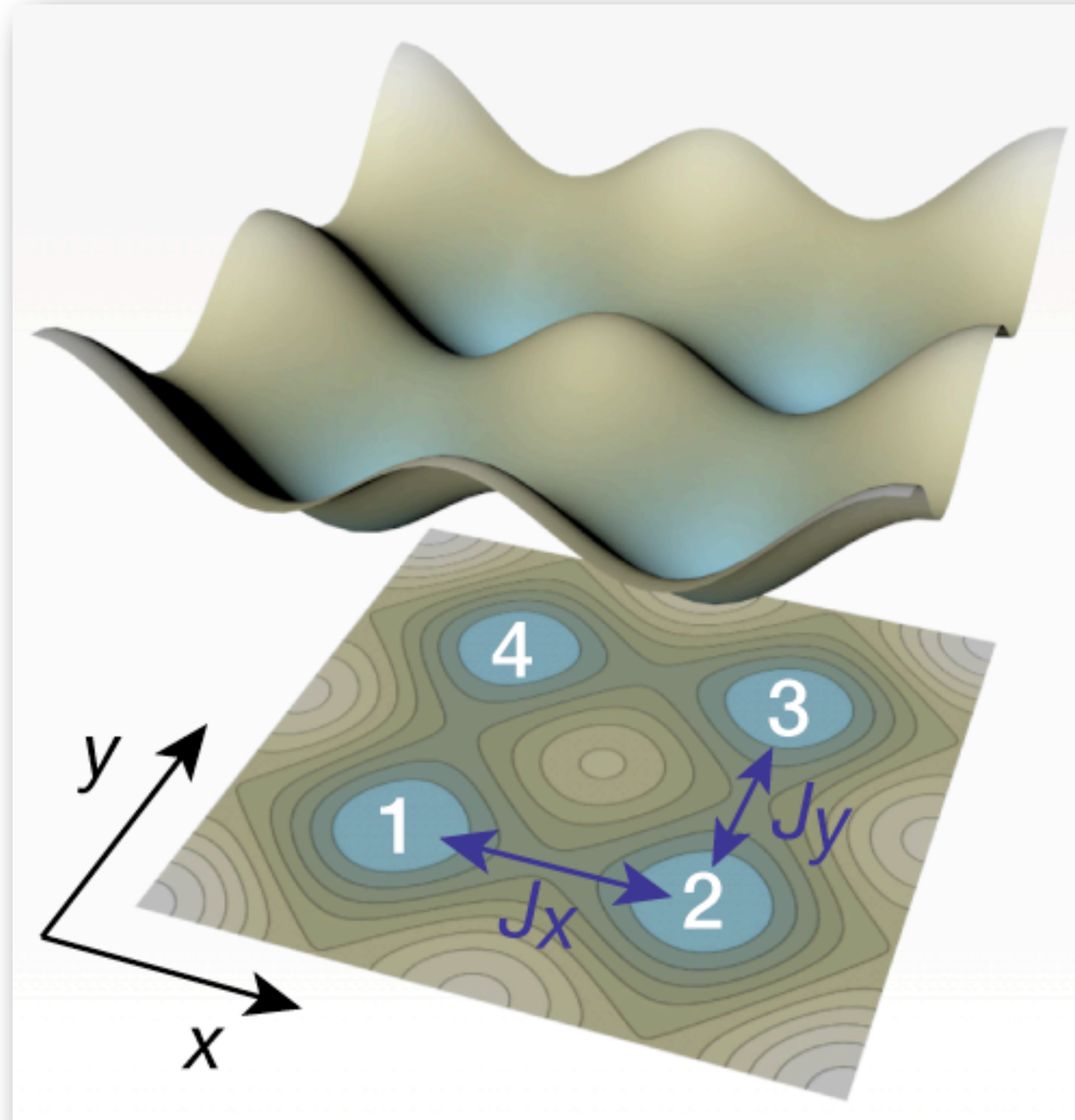

Single plaquette

Quantum states for a plaquette at half filling

At half-filling, t≪U:

$$\hat{H} = -J_X\left(\mathbf{S}_A\cdot\mathbf{S}_B+\mathbf{S}_C\cdot\mathbf{S}_D\right)-J_Y\left(\mathbf{S}_A\cdot\mathbf{S}_D+\mathbf{S}_B\cdot\mathbf{S}_C\right)$$

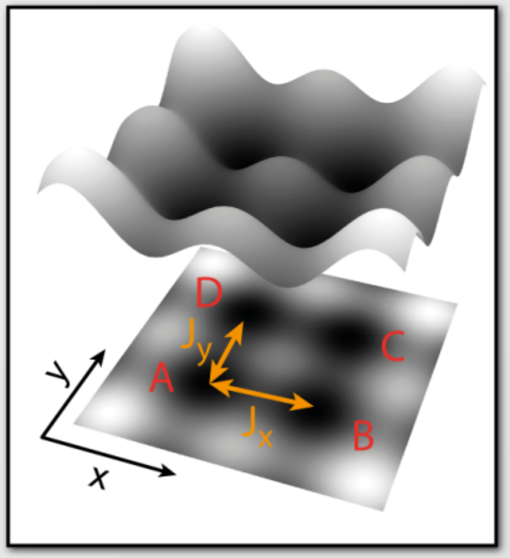

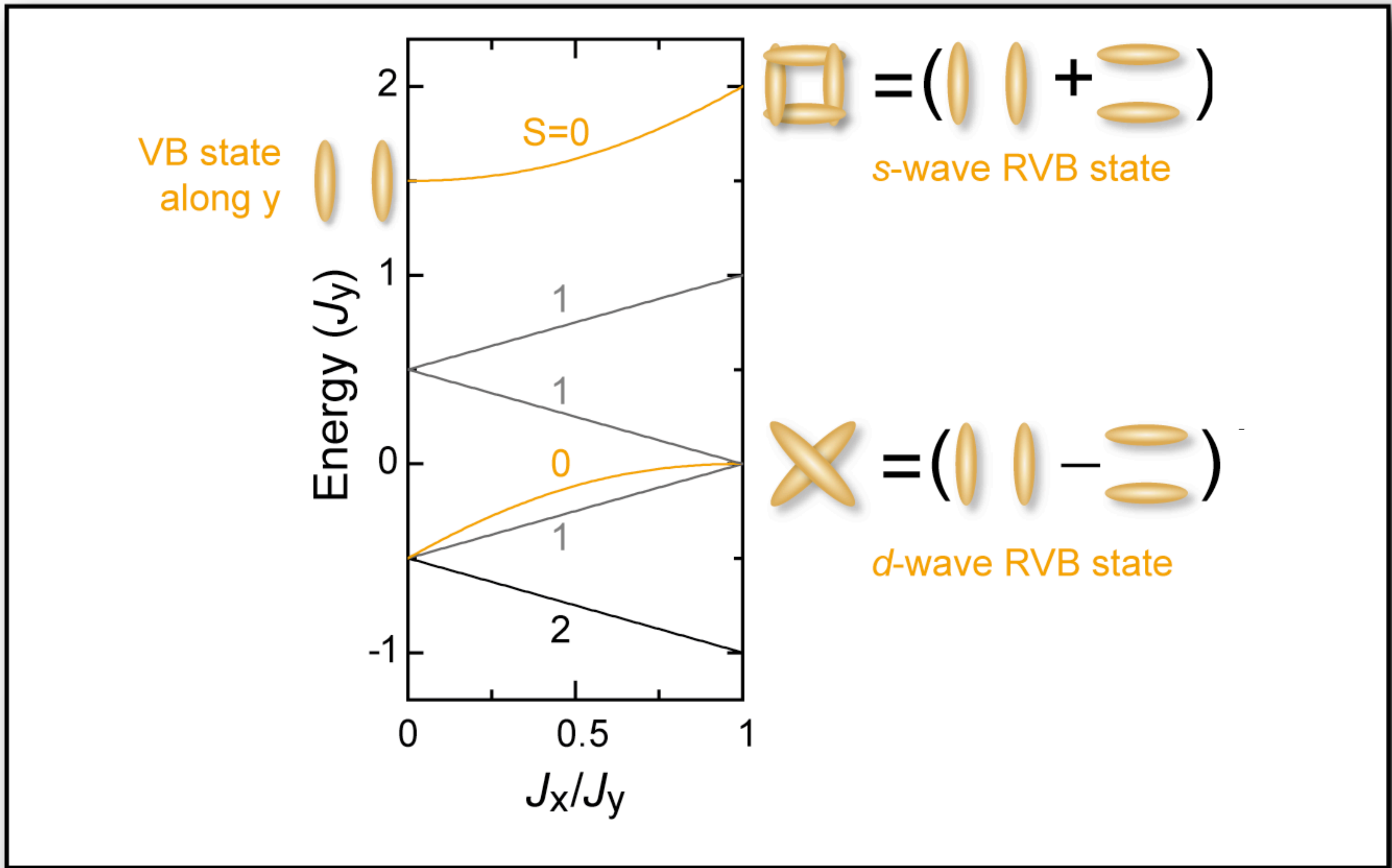

S. Nascimbene et al., Phys. Rev. Lett. **108**, 205301 (2012)

B. Paredes and I. Bloch,
Phys. Rev. A **77**, 023603 (2008)

with Rydbergs:
A. Nielsen and K. Mølmer
Phys. Rev. A **82**, 052326 (2010)

Resonating Bonds

$$\hat{H} = -J_X\left(\mathbf{S}_1\cdot\mathbf{S}_2+\mathbf{S}_3\cdot\mathbf{S}_4\right) - J_Y\left(\mathbf{S}_1\cdot\mathbf{S}_4+\mathbf{S}_2\cdot\mathbf{S}_3\right)$$

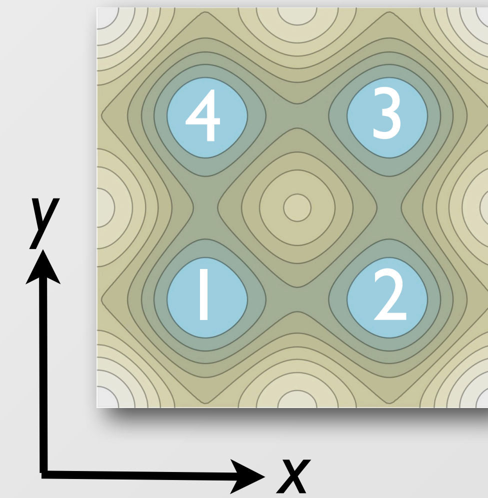

$$\boxed{\hat{X}_{ij} = 2\mathbf{S}_i\cdot\mathbf{S}_j + 1/2}$$

$$\hat{H} = -J_x\hat{X}_x - J_y\hat{X}_y$$

$$\hat{X}_x = (\hat{X}_{12}+\hat{X}_{34})/2$$

$$\hat{X}_y = (\hat{X}_{23}+\hat{X}_{14})/2$$

in S=0 subspace
and $J_x = J_y = J$

$$\boxed{\hat{H} = -J\hat{X}_{xy}}$$

$$\hat{X}_{xy} = (\hat{X}_{13}+\hat{X}_{24})/2$$

Exchange along diagonals!

Valence Bond Resonance

$\{|\,\|\,\rangle, |\,=\,\rangle\}$ Basis States (but non-orthogonal!) $\langle\,=\,|\,\|\,\rangle = 1/2$

$$\hat{X}_{xy}|\,=\,\rangle = |\,\|\,\rangle$$

$$\hat{X}_{xy}|\,\|\,\rangle = |\,=\,\rangle$$

Valence bond resonance!

Eigenstates

$$\boxed{\begin{aligned} |\phi^+\rangle &= \frac{1}{\sqrt{3}}\left(|\,=\,\rangle + |\,\|\,\rangle\right) \\ |\phi^-\rangle &= \frac{1}{\sqrt{2}}\left(|\,=\,\rangle - |\,\|\,\rangle\right) \end{aligned}}$$

s-wave RVB state

d-wave RVB state

Valence-bond oscillations

- We prepare valence bond states along *y*.
- At t=0, we suddenly set J_x=J_y=120(10) Hz

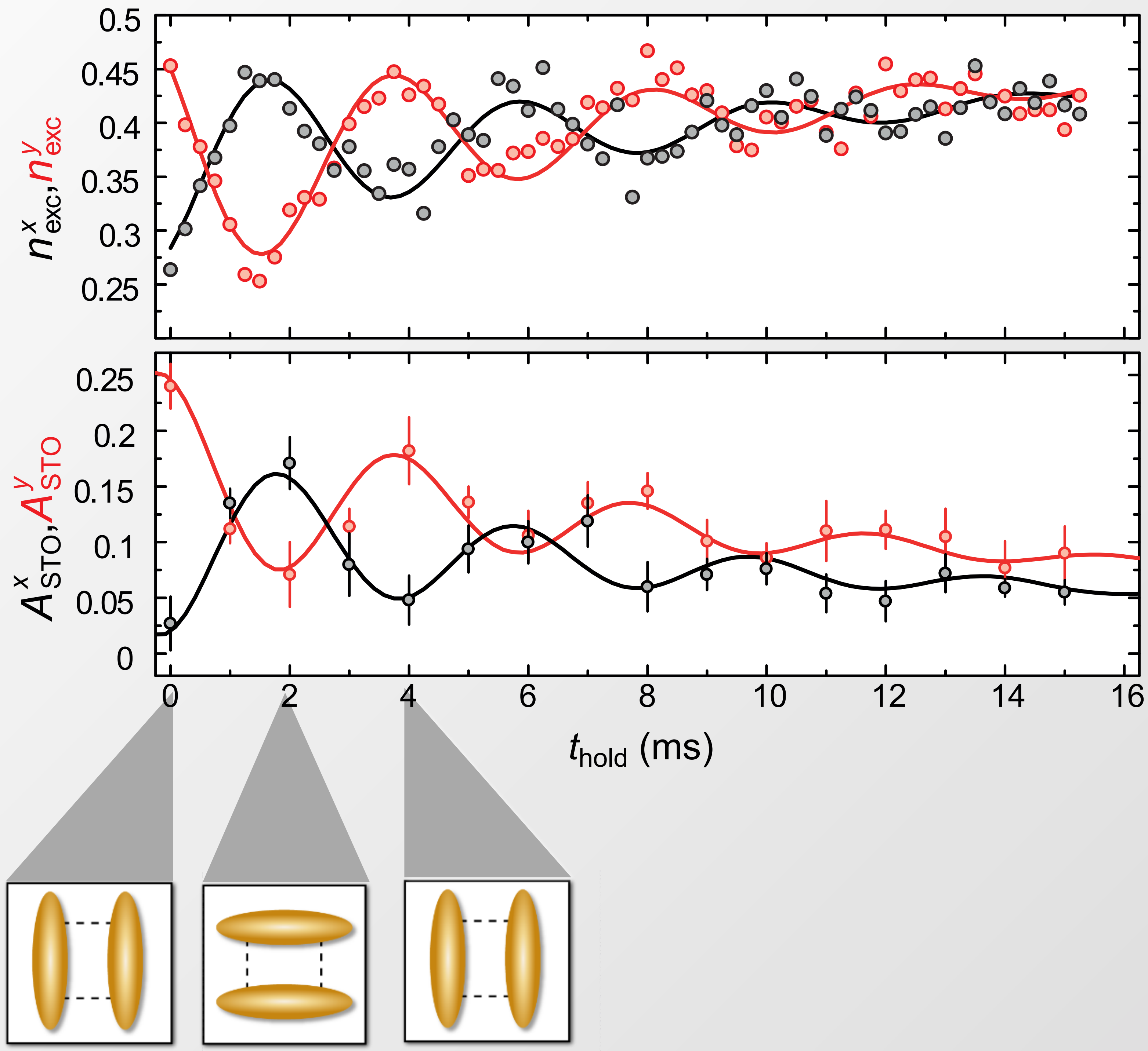

Oscillations observed with almost maximum contrast!

Outlook

- ✓ Generation of **Minimum Instances of Topologically Ordered Quantum States**
- ✓ **Direct Time-Resolved Observation of Resonating Bonds**
- ✓ Use of s- and d-wave RVB states as (minimally) **topologically protected qubits**

 $= |0\rangle$  $= |1\rangle$

- ✓ Generation of **larger RVB states** by connecting Valence Bond Solids on Lattice

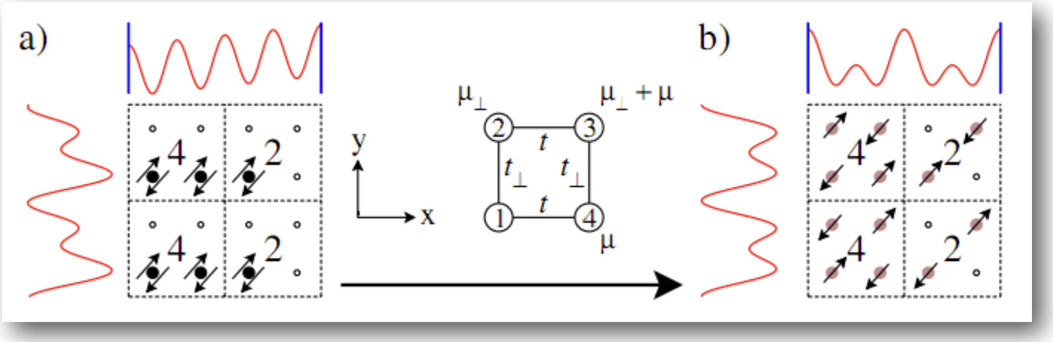

S. Trebst et al. PRL **96**, 250402 (2006), A.-M. Rey et al. EPL 87, 60001 (2009)

Quantum Magnetism in Tilted Lattices

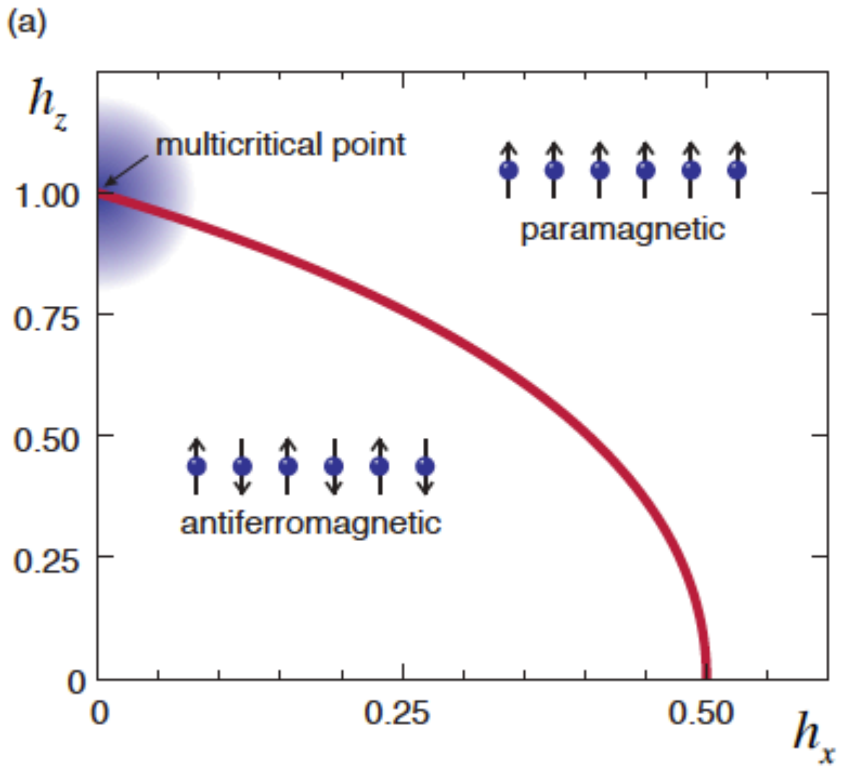

(b)

magnetic fields:

$$H = J\sum_i \overbrace{S_z^i S_z^{i+1} - (1}^{\text{realizes constraint}} \overbrace{\underbrace{-\tilde{\Delta})\, S_z^i}_{h_z \text{ longitudinal}} - \underbrace{2^{3/2}\tilde{t}\, S_x^i}_{h_x \text{ transverse}}}^{\text{drives quantum phase transition}}$$

Mapping onto Quantum Ising Model

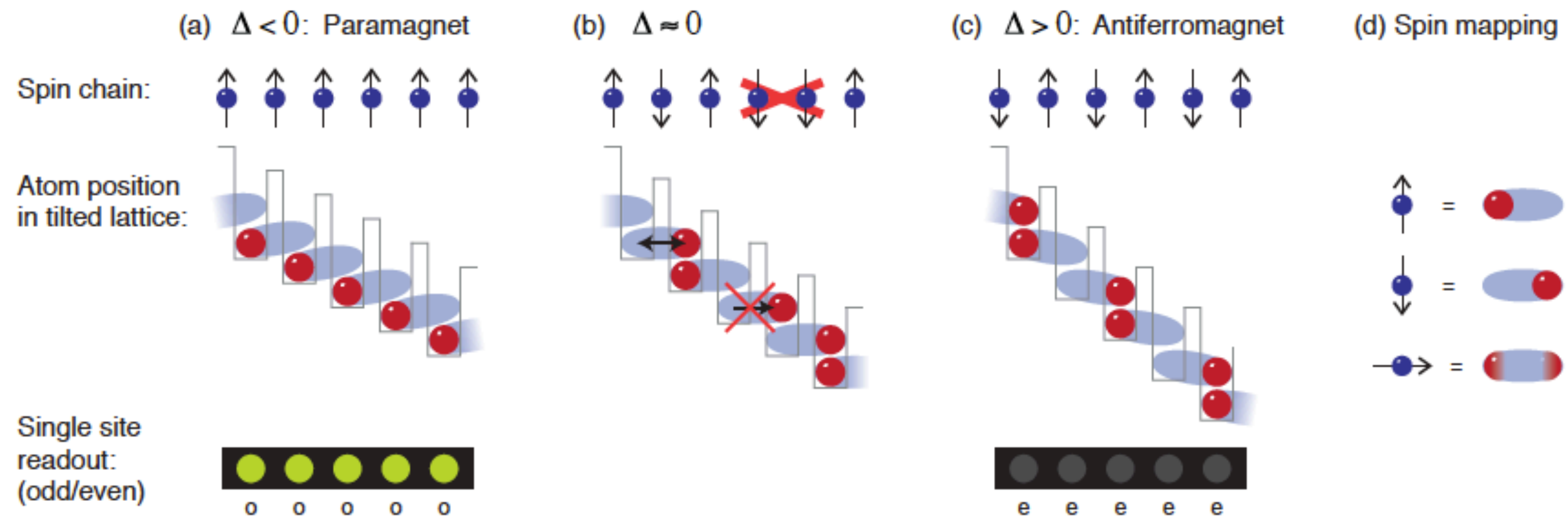

Pseudospin in density sector of MI

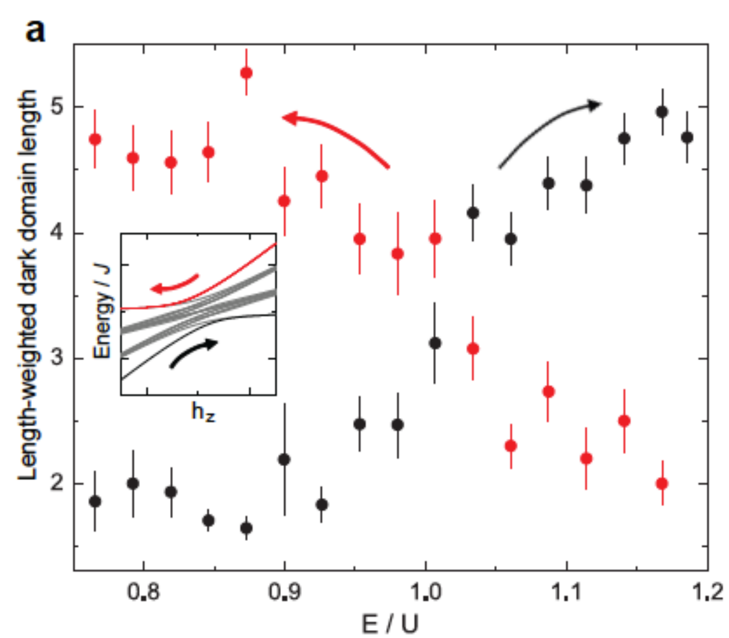

Domain size approx 5 sites

J. Simon et al. Nature (2011)

S. Sachdev et al., PRB (2002) & S. Pielawa et al. PRB (2011)

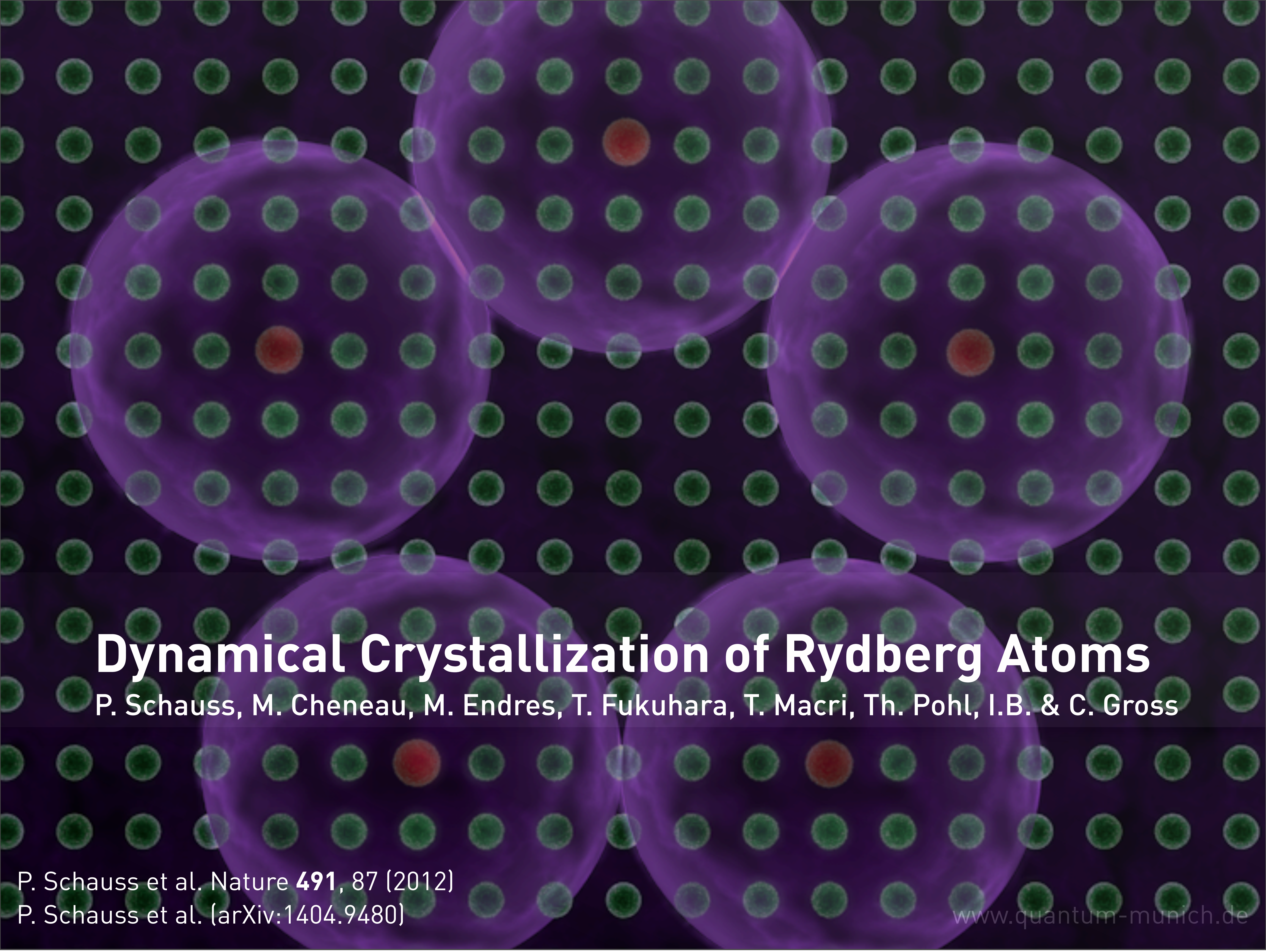

Dynamical Crystallization of Rydberg Atoms

P. Schauss, M. Cheneau, M. Endres, T. Fukuhara, T. Macri, Th. Pohl, I.B. & C. Gross

P. Schauss et al. Nature **491**, 87 (2012)
P. Schauss et al. (arXiv:1404.9480)

Rydberg atoms

- hydrogen-like wave function
  - quantum defect

$$E_{nlj} = -\frac{\mathrm{Ry}}{[n - \delta_{lj}(n)]^2}$$

- Strong switchable interactions

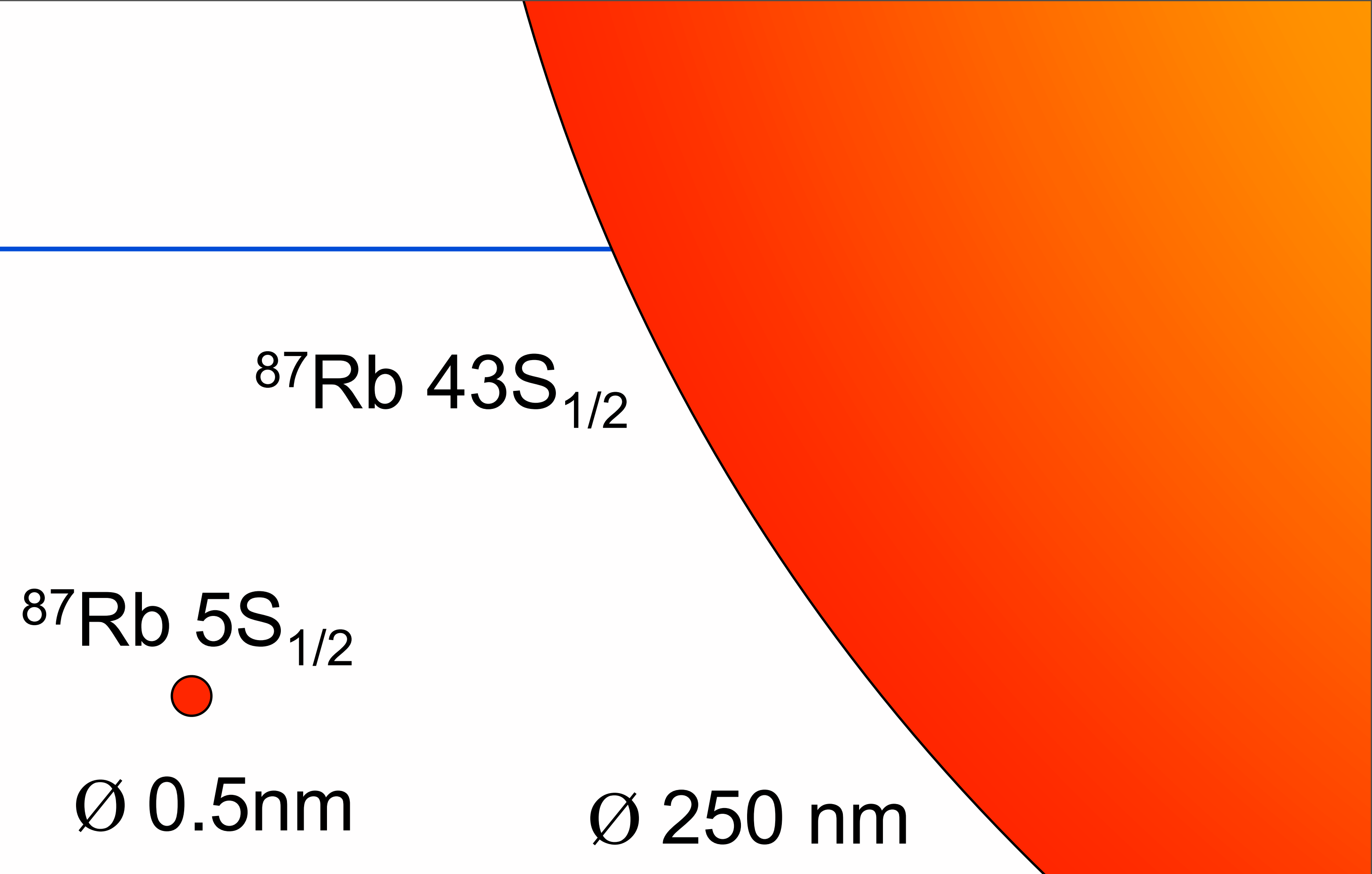

Property	Scaling	^{87}Rb 43S
Radius	$(n^*)^2$	$2400\ a_0 = 127$nm
Lifetime (dominated by black body radiation for large n)	$(n^*)^2$	45 μs @ 20°C
van der Waals coefficient	$(n^*)^{11}$	$C_6 = -1.7 \times 10^{19}$ a.u.
Blockade radius (Ω=2π 200 kHz)	$(n^*)^2$	$\sim 5\ \mu$m

Saffman, Walker, & Mølmer Rev. Mod. Phys. (2010)

see work in: Paris, Madison, Palaiseau, Stuttgart, Heidelberg, Durham, Michigan....

Rydberg blockade

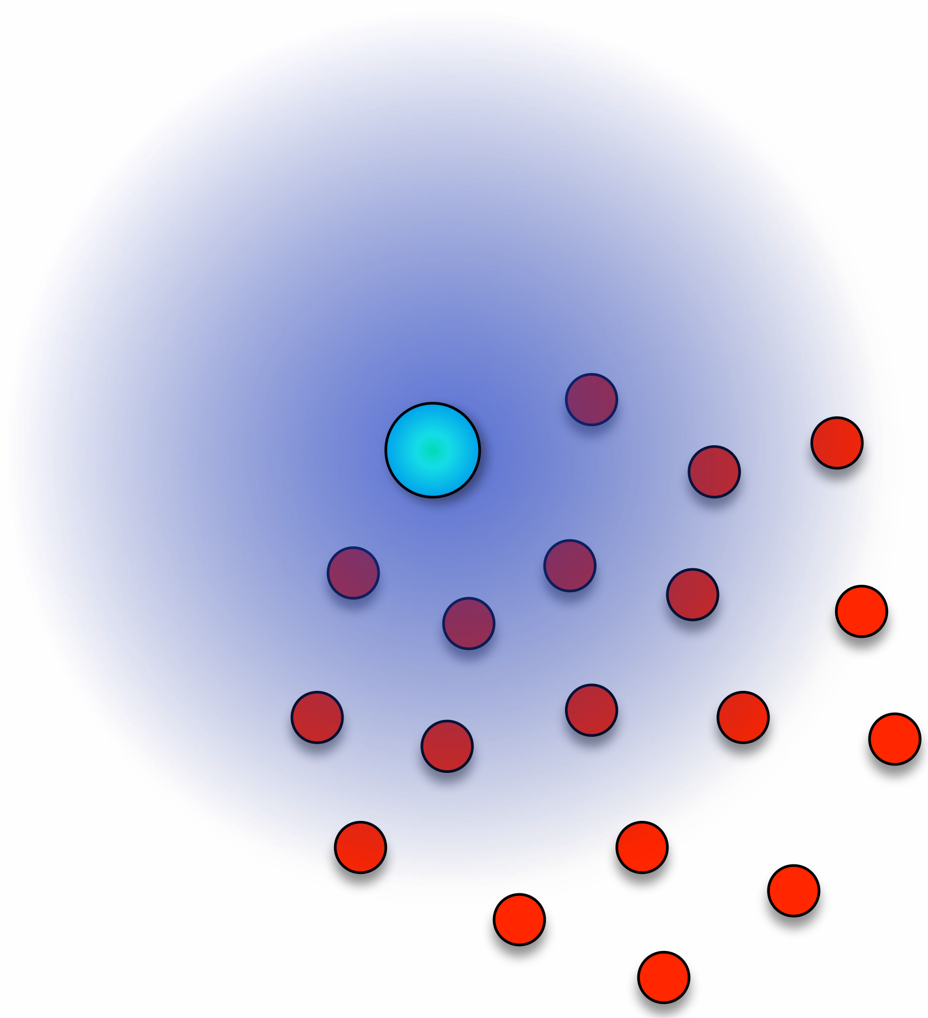

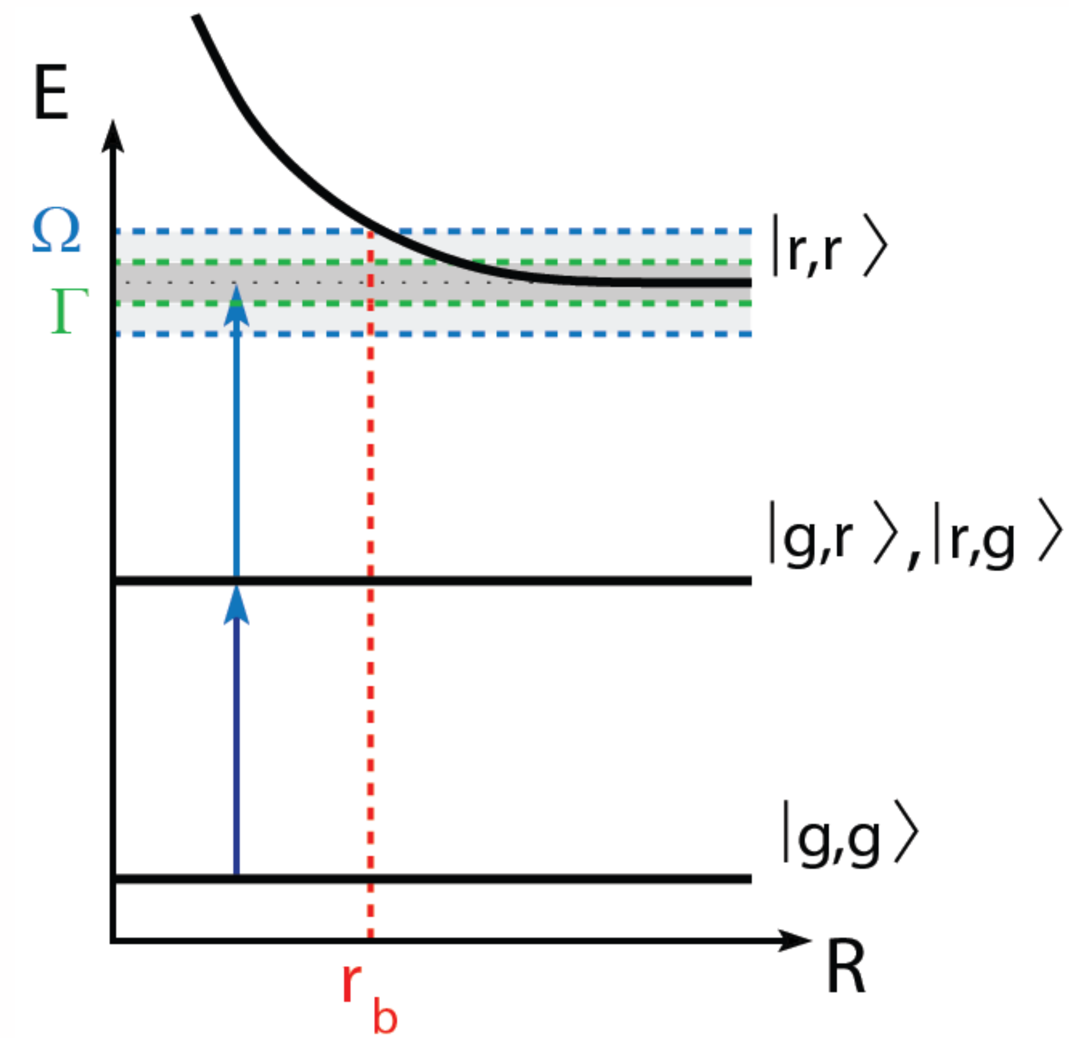

Blockade condition

$$\mathcal{V}_{\mathrm{vdW}} = \frac{C_6}{r^6} > \hbar \max(\Gamma, \Omega)$$

$$r_{\mathrm{b}} \equiv \sqrt[6]{\frac{C_6}{\hbar\Omega}}$$

<u>Each superatom:</u>

$$\frac{1}{\sqrt{N}} \left(|r,0,0,0,\ldots\rangle + |0,r,0,0,\ldots\rangle + |0,0,0,\ldots,r\rangle \right)$$

M. Lukin et al. PRL **87**, 037901 (2001)

Rydberg blockade

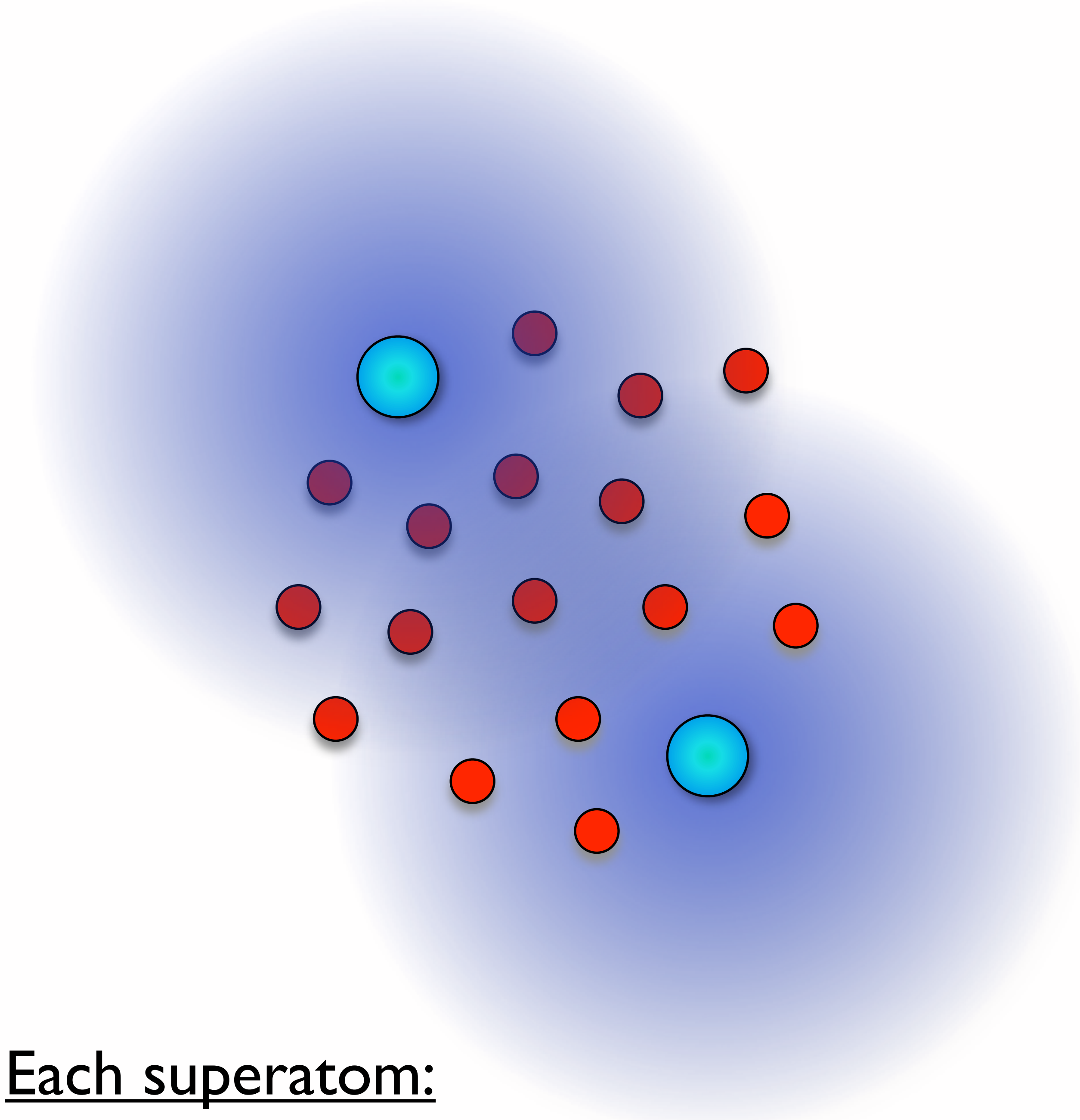

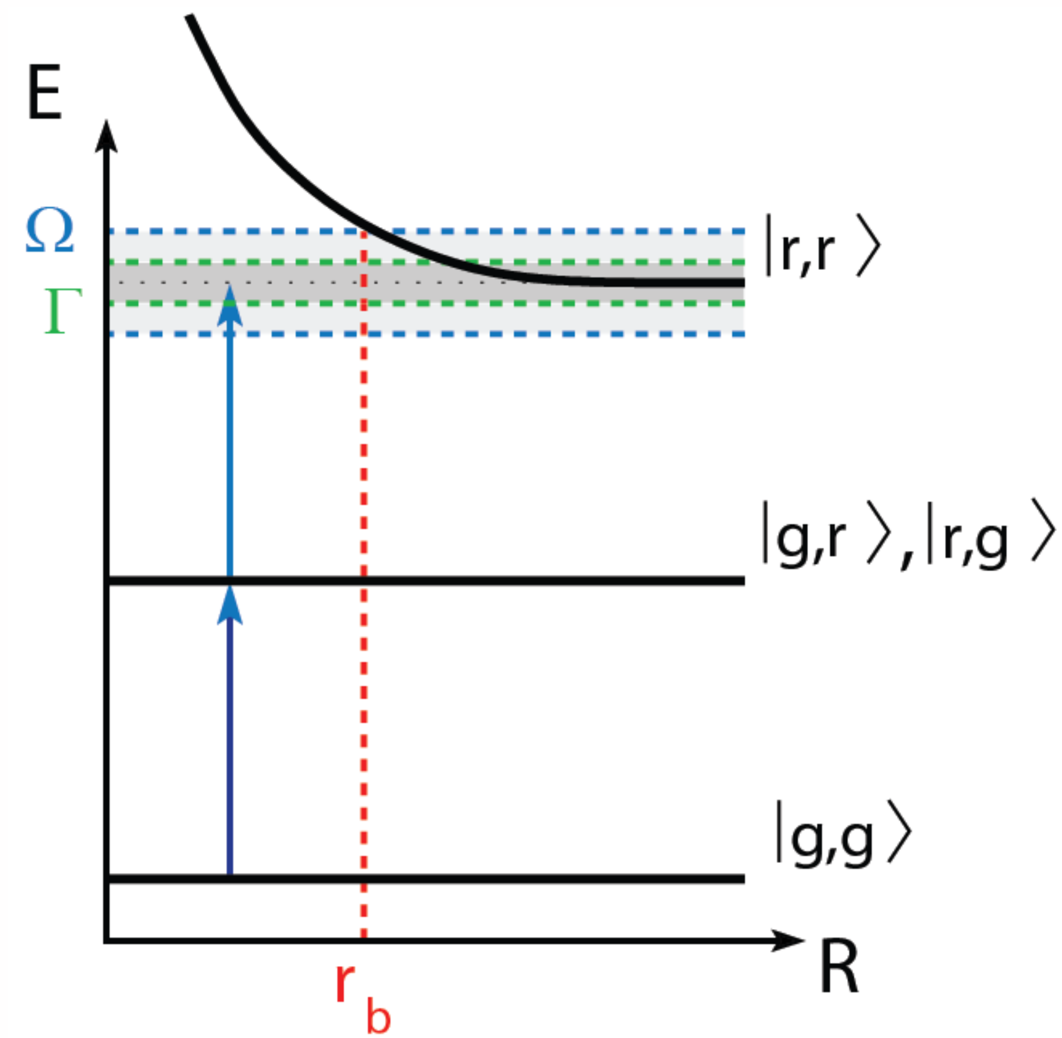

Blockade condition

$$\mathcal{V}_{\mathrm{vdW}} = \frac{C_6}{r^6} > \hbar \max(\Gamma, \Omega)$$

$$r_{\mathrm{b}} \equiv \sqrt[6]{\frac{C_6}{\hbar\Omega}}$$

<u>Each superatom:</u>

$$\frac{1}{\sqrt{N}} \left(|r,0,0,0,\ldots\rangle + |0,r,0,0,\ldots\rangle + |0,0,0,\ldots,r\rangle \right)$$

M. Lukin et al. PRL **87**, 037901 (2001)

Rydberg blockade

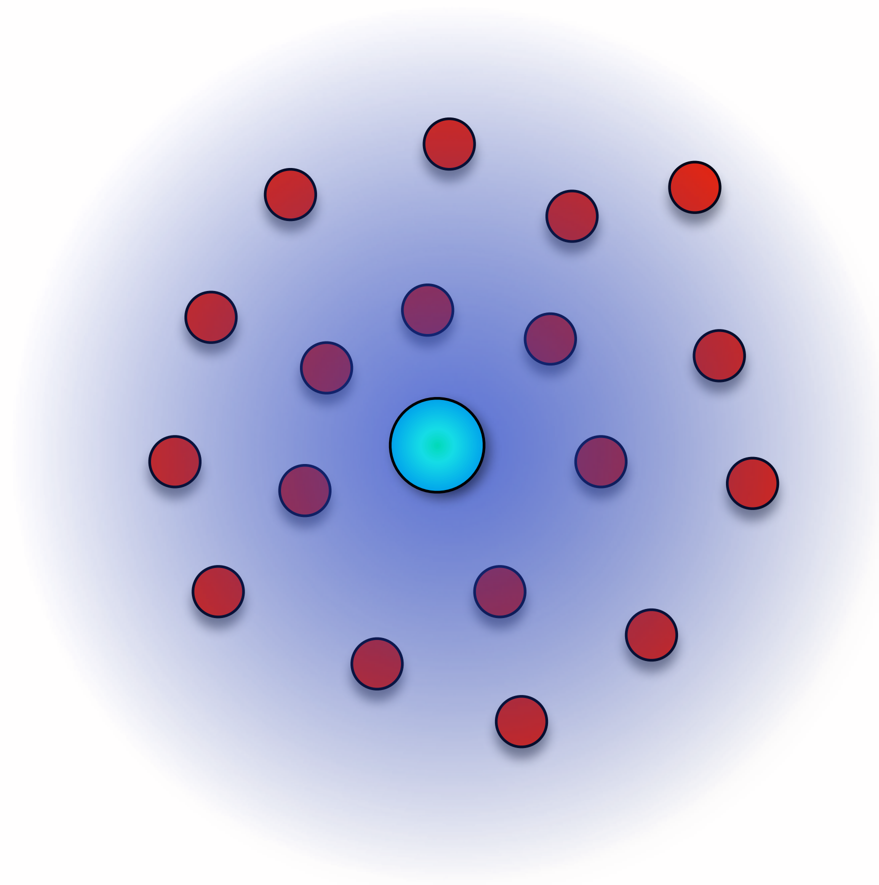

Blockade radius
larger than cloud size!

$\sqrt{N}\Omega_1$ Rabi Oscillations speed up!

<u>Each superatom:</u>

$$\frac{1}{\sqrt{N}}\left(|r,0,0,0,\ldots\rangle + |0,r,0,0,\ldots\rangle + |0,0,0,\ldots,r\rangle\right)$$

M. Lukin et al. PRL **87**, 037901 (2001)

see work by A. Browaeys & Ph. Grangier, M. Saffman, A. Kuzmich, T. Pfau...

Rydberg blockade

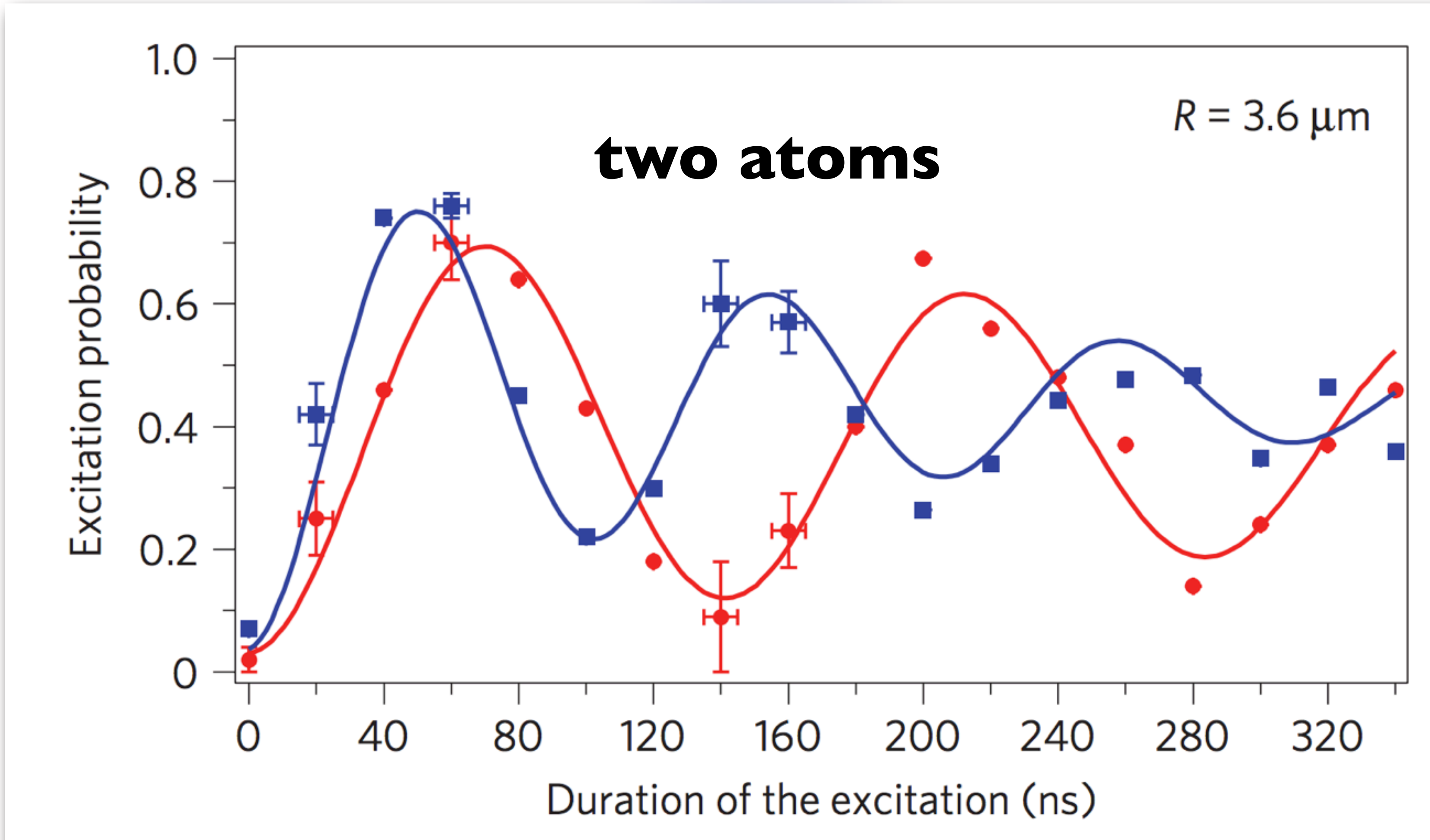

ade radius

er than cloud size!

$\sqrt{N}\Omega_1$ Rabi Oscillations speed up!

<u>Each superatom:</u>

$$\frac{1}{\sqrt{N}}\left(|r,0,0,0,\ldots\rangle + |0,r,0,0,\ldots\rangle + |0,0,0,\ldots,r\rangle\right)$$

M. Lukin et al. PRL **87**, 037901 (2001)

see work by A. Browaeys & Ph. Grangier, M. Saffman, A. Kuzmich, T. Pfau...

Ultimate Size Control in 2D

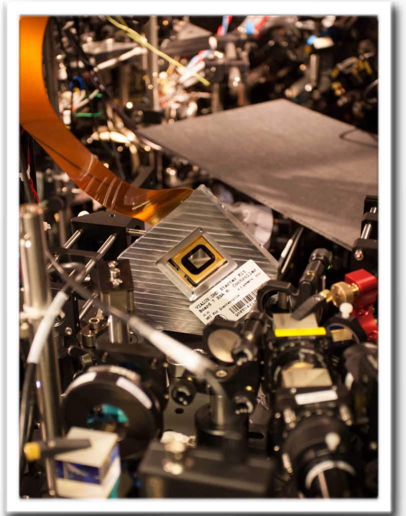

Digital Mirror Device (Size Control)

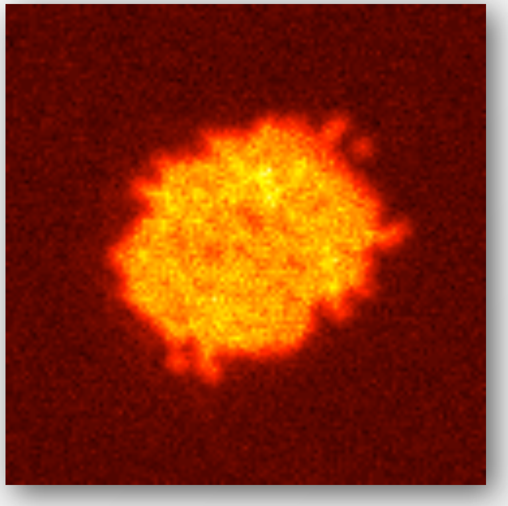

Initial MI

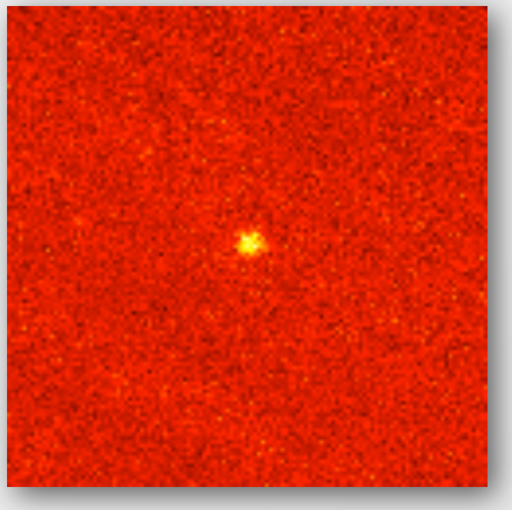

Single Atom

Ultimate Size Control in 2D

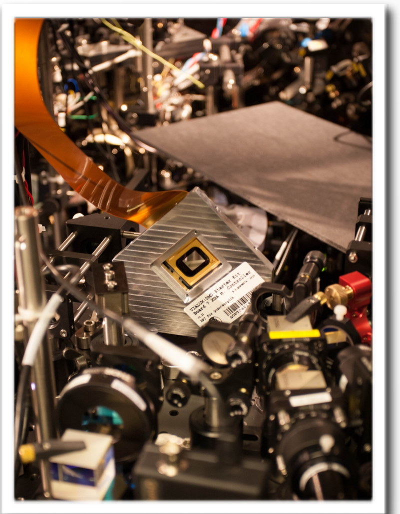

Digital Mirror Device (Size Control)

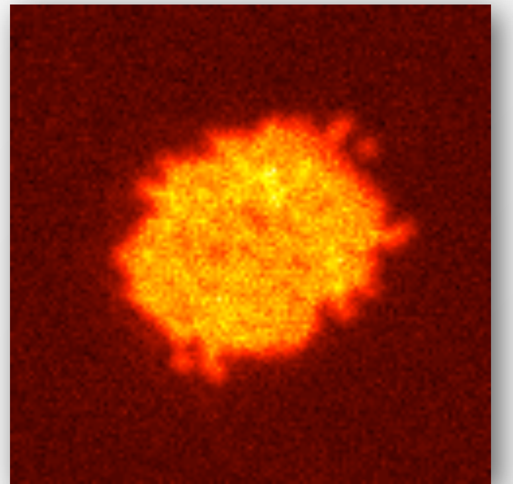

Initial MI

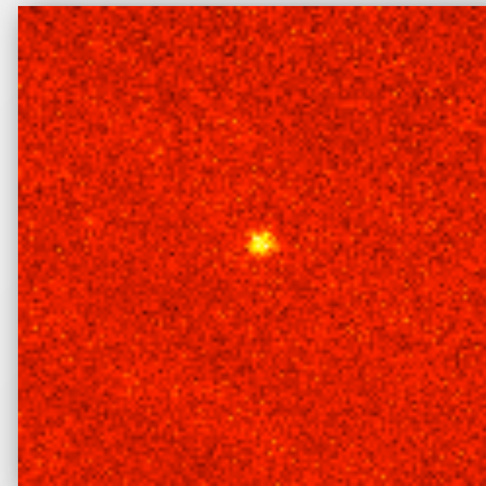

Single Atom

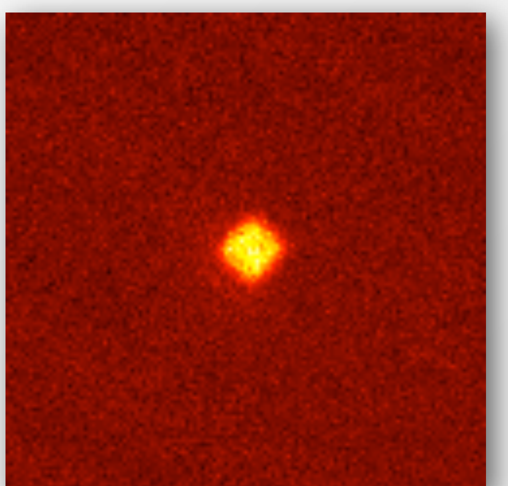

3x3

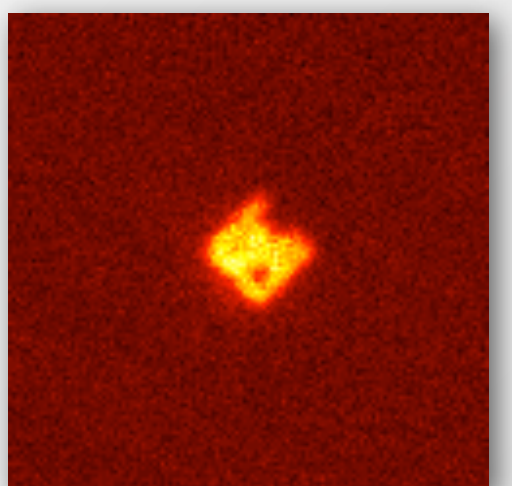

5x5

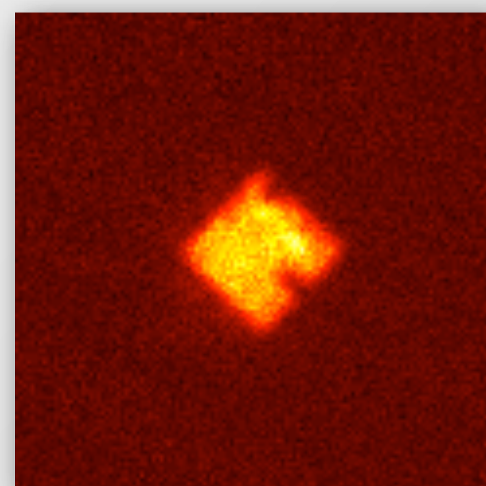

7x7

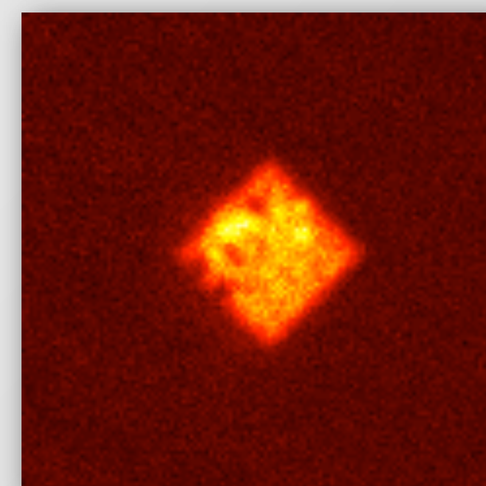

8x8

atoms

Collective Many-Body Rabi Oscillations

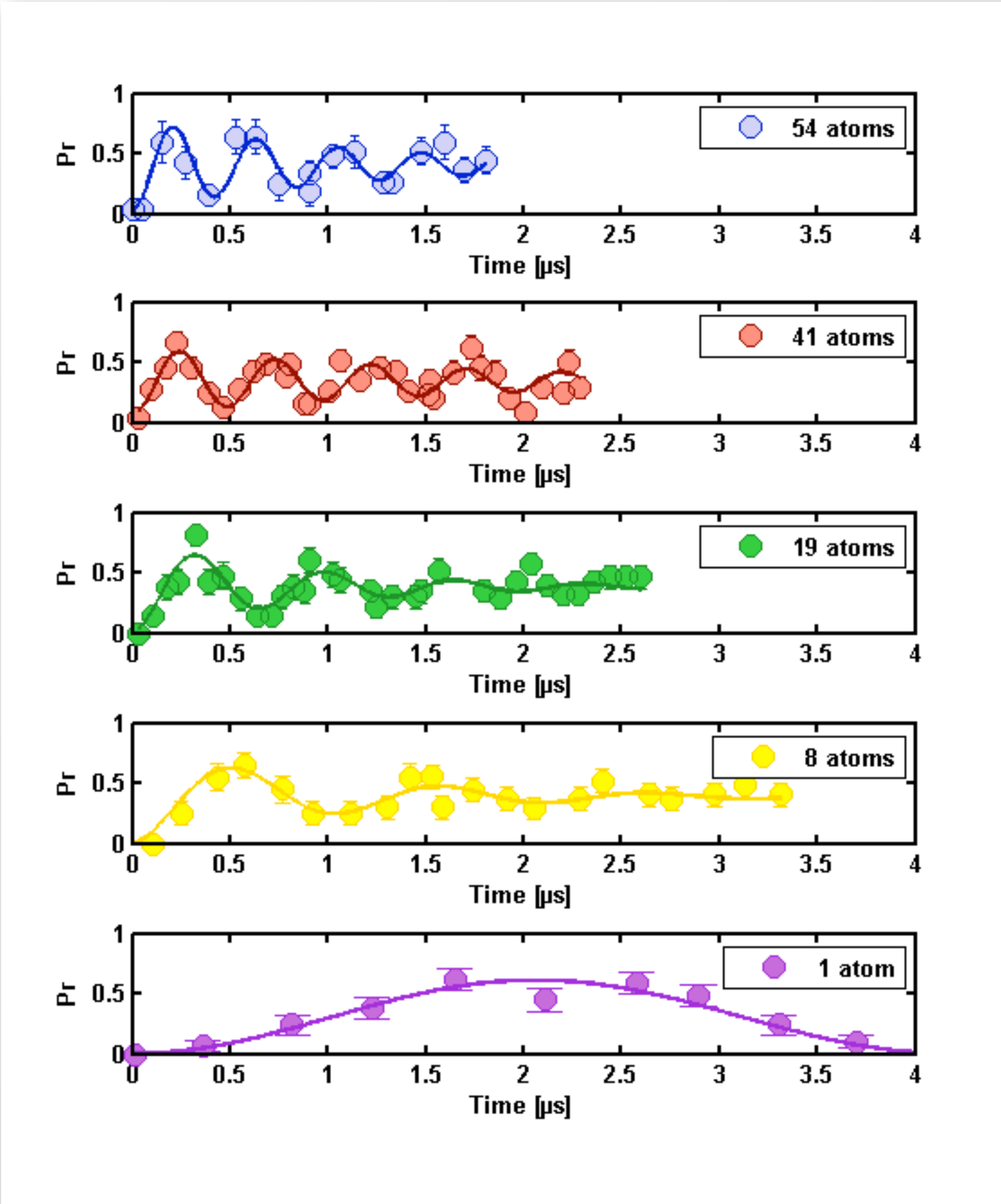

Preliminary Raw Data

Collective Many-Body Rabi Oscillations

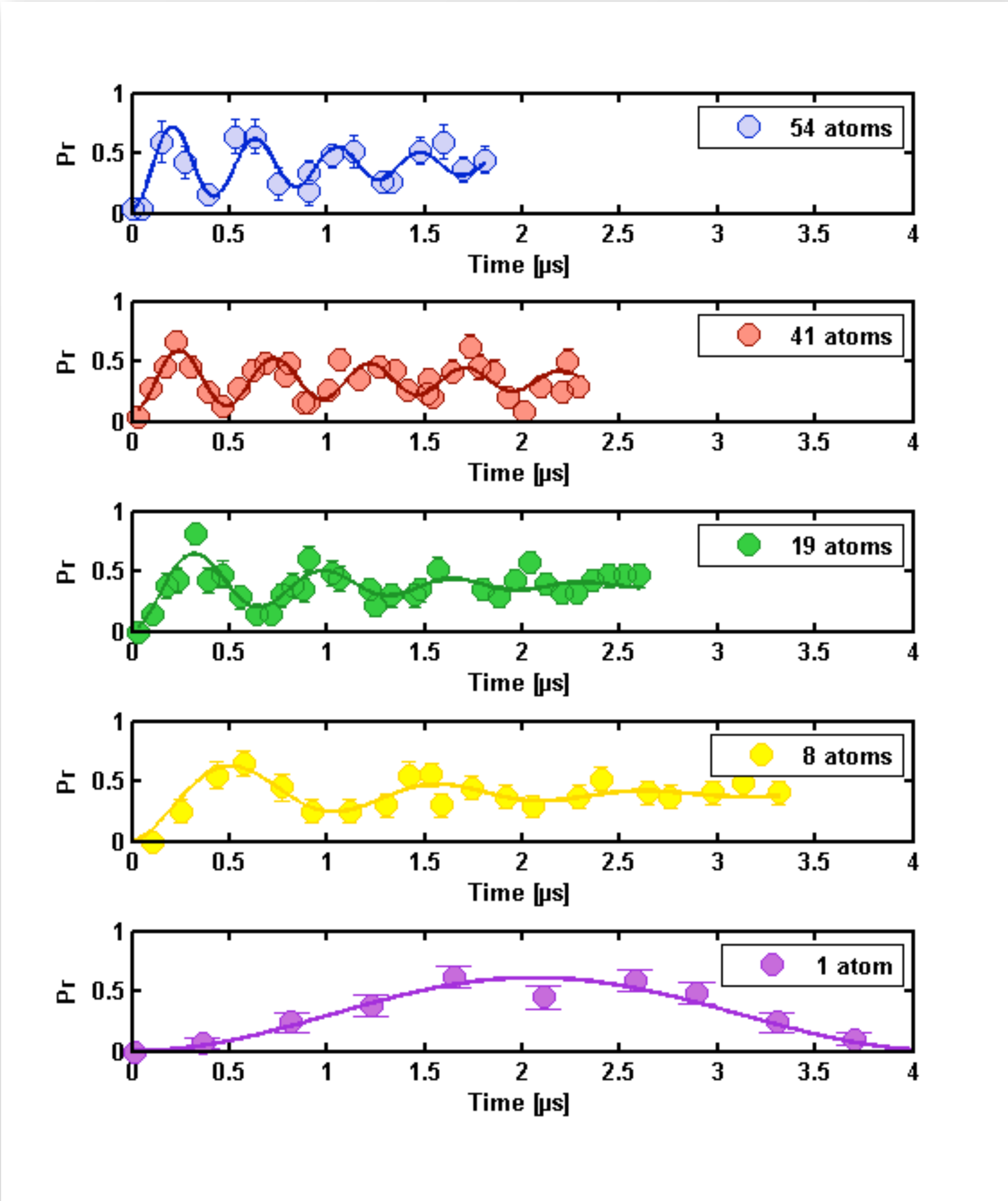

Preliminary Raw Data

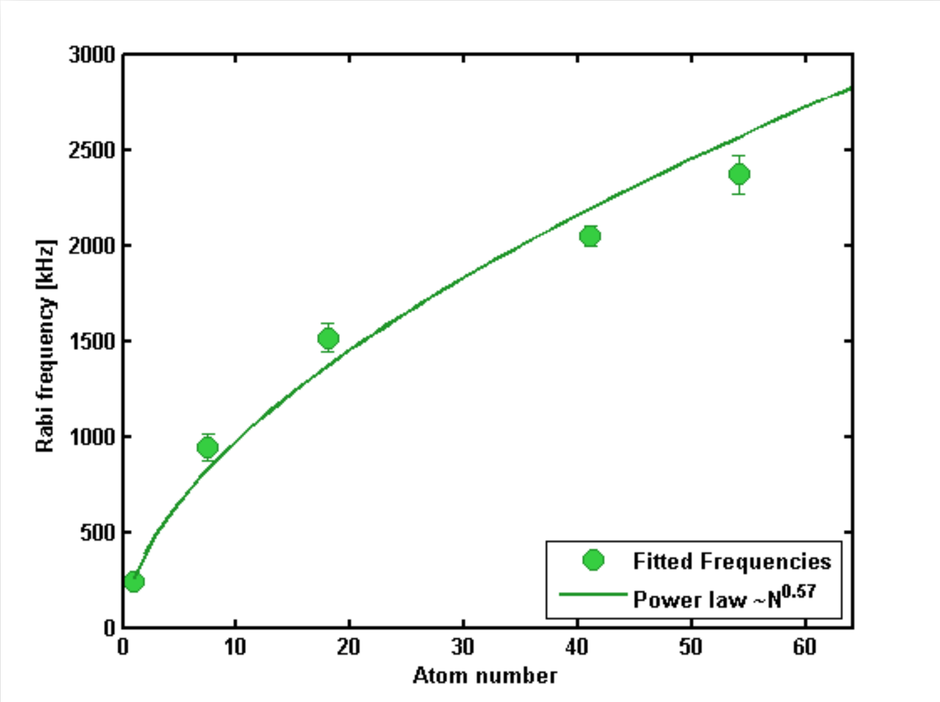

Single atom non-linearity controls dynamics of >50 atoms!

The frozen Rydberg gas - long range QM

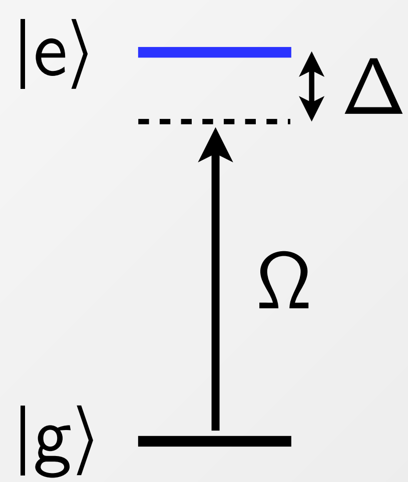

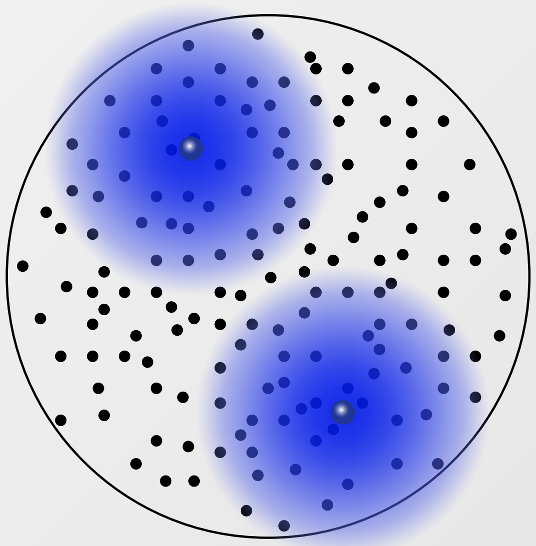

no mechanical motion on the timescale of the internal dynamics

$$H = \frac{\hbar\Omega}{2}\sum_i \left(\sigma_{eg}^{(i)} + \sigma_{ge}^{(i)}\right) + \sum_{i\neq j}\frac{V_{ij}}{2}\sigma_{ee}^{(i)}\sigma_{ee}^{(j)} - \Delta\sum_i \sigma_{ee}^{(i)}$$

coherent coupling

interaction between Rydberg atoms

$$V_{ij} = C_\alpha |r_i - r_j|^{-\alpha}$$

"chemical potential"

This work: α=6, repulsive

Excitation and detection of the Rydberg atoms

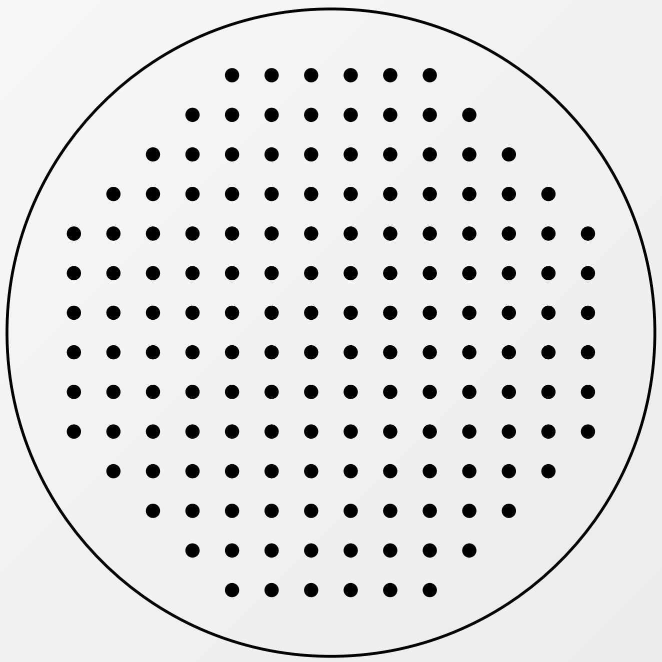

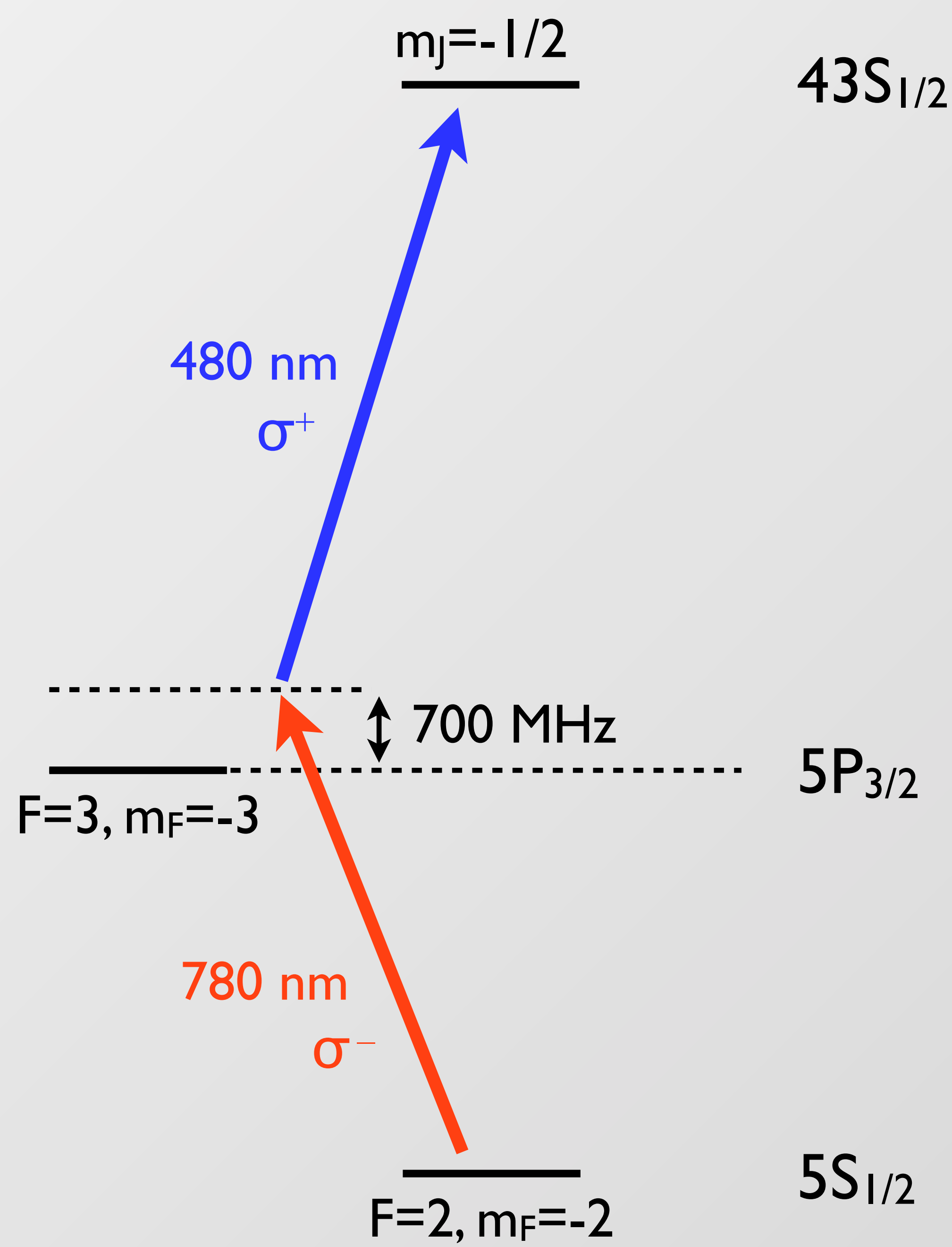

- two-photon Rabi frequency: $\Omega/2\pi$ = 170(20) kHz
- resonant excitation: $\Delta = 0$
- blockade radius: R_b = 4.9(1) μm

Excitation and detection of the Rydberg atoms

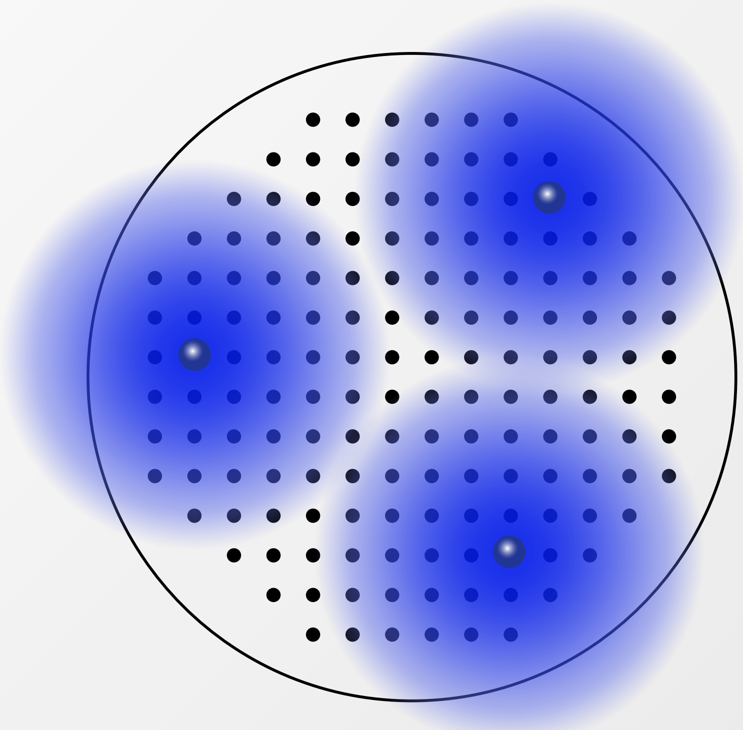

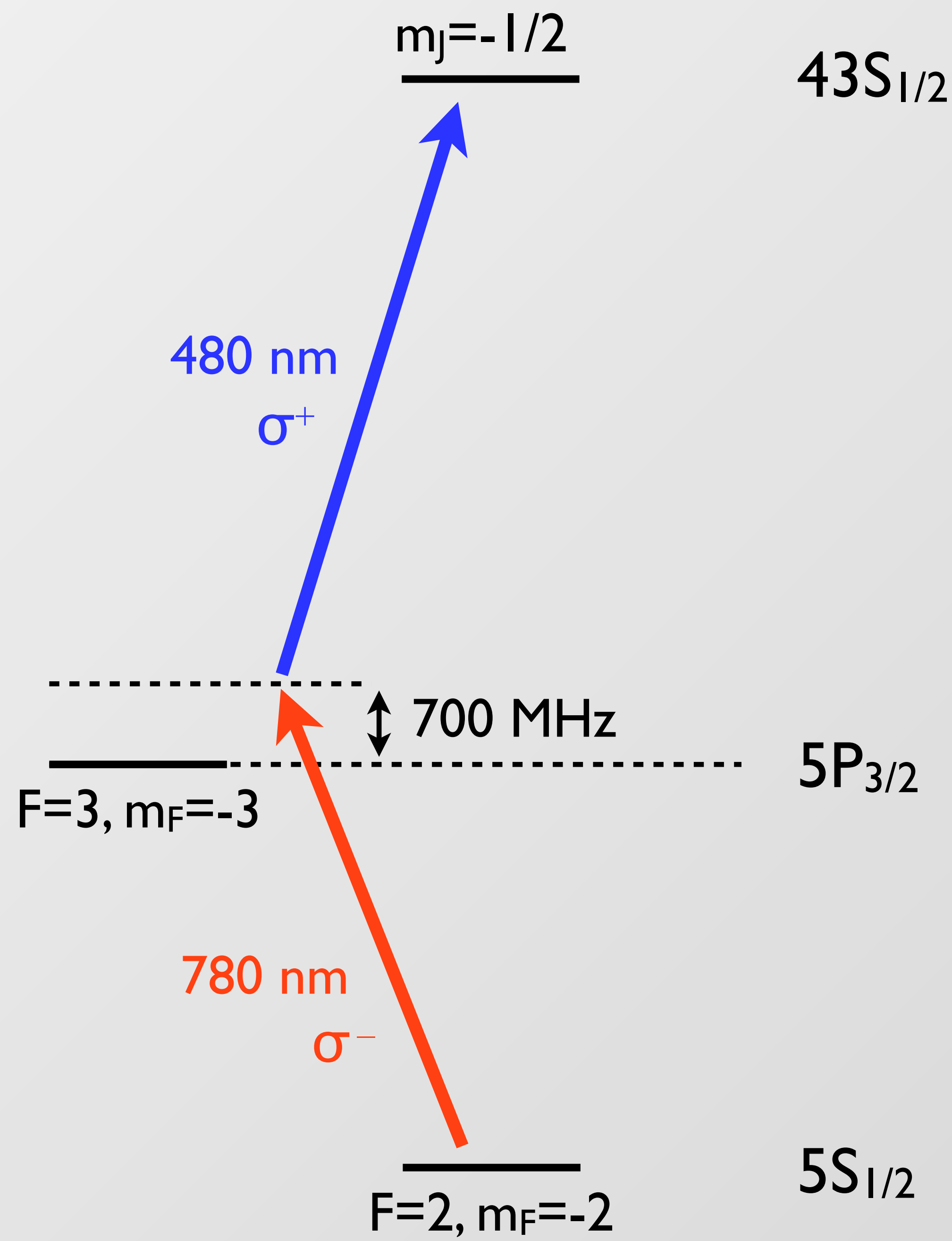

- two-photon Rabi frequency:
  $\Omega/2\pi$ = 170(20) kHz
- resonant excitation:
  $\Delta = 0$
- blockade radius:
  R_b = 4.9(1) μm

Excitation and detection of the Rydberg atoms

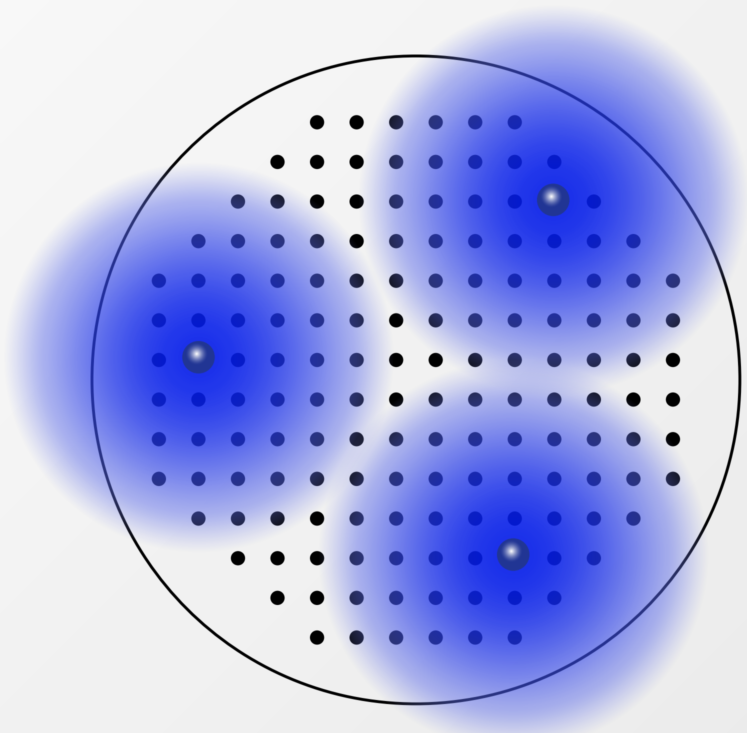

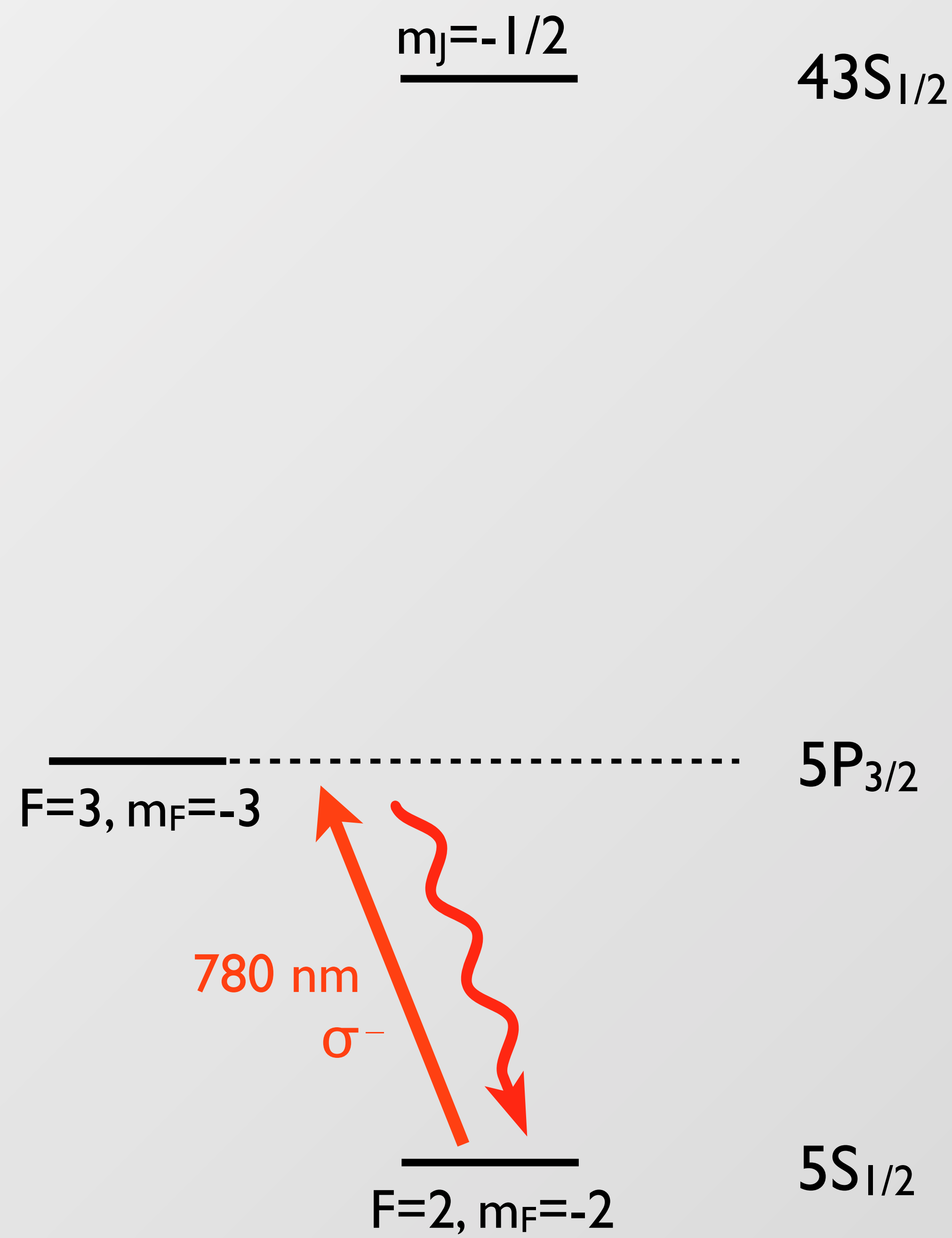

- removal pulse duration: 10 μs
- survival probability: 0.1 %

Excitation and detection of the Rydberg atoms

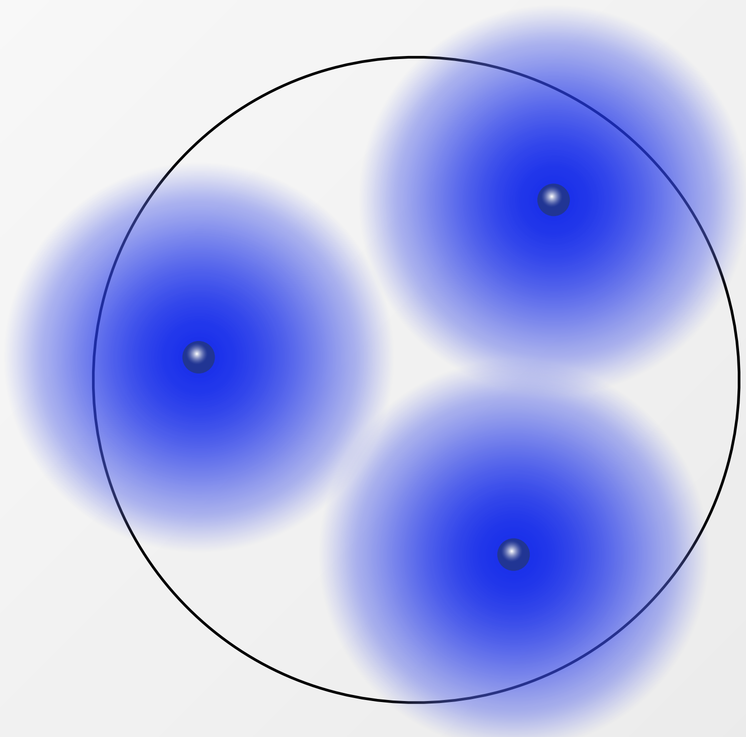

- removal pulse duration: 10 μs
- survival probability: 0.1 %

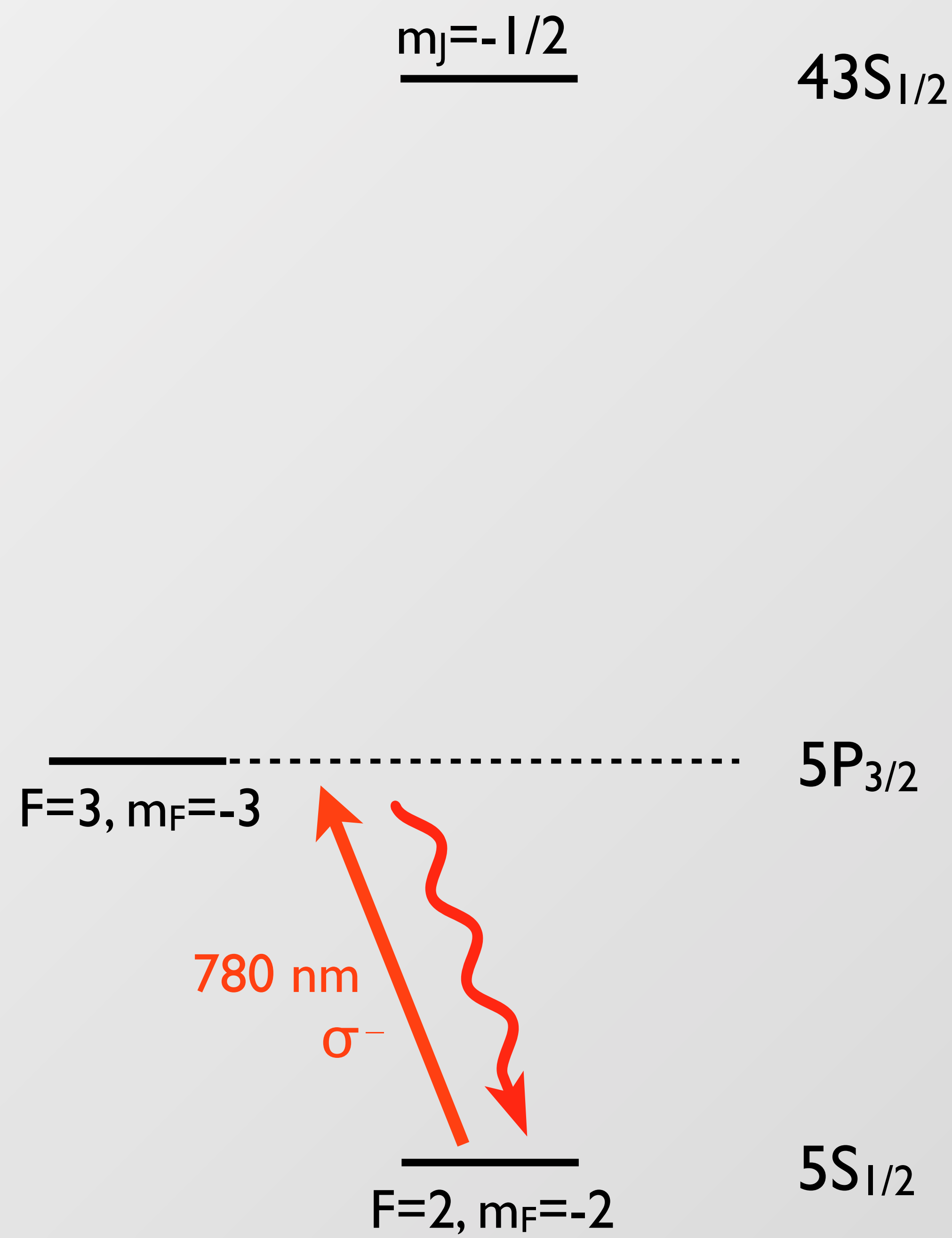

Excitation and detection of the Rydberg atoms

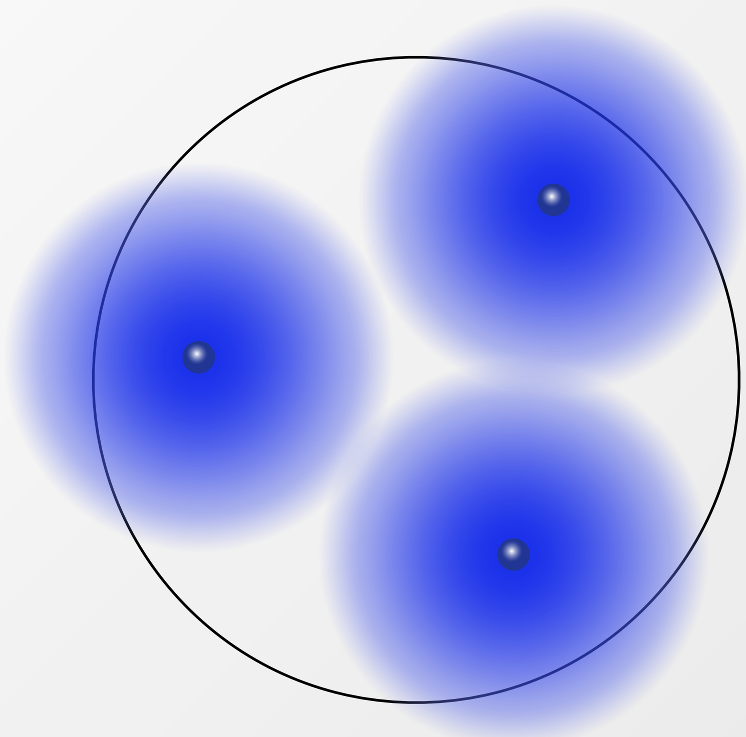

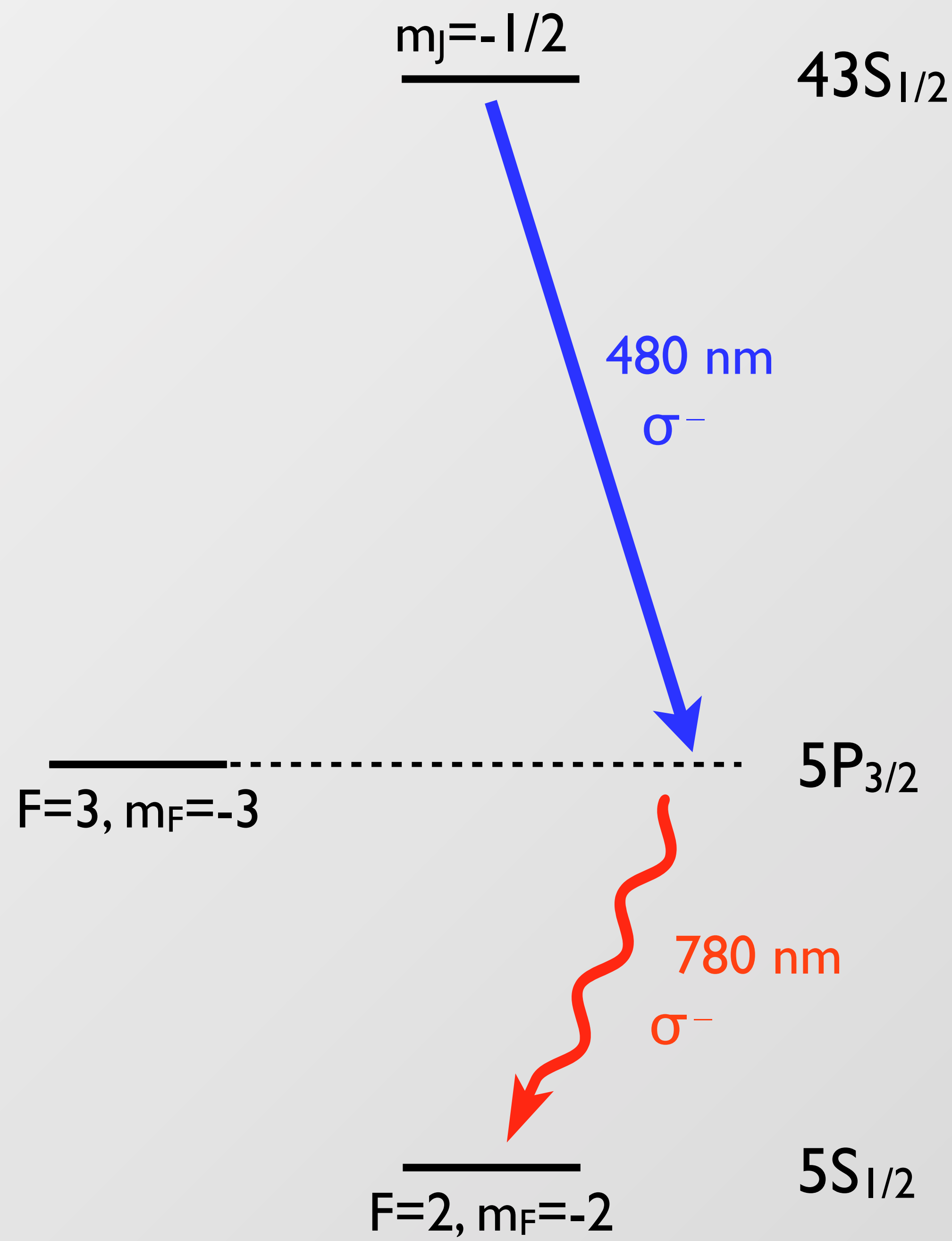

- deexcitation pulse duration: 2 μs
- detection efficiency: 75(10) %
- overall resolution: ~ 500 nm

Excitation and detection of the Rydberg atoms

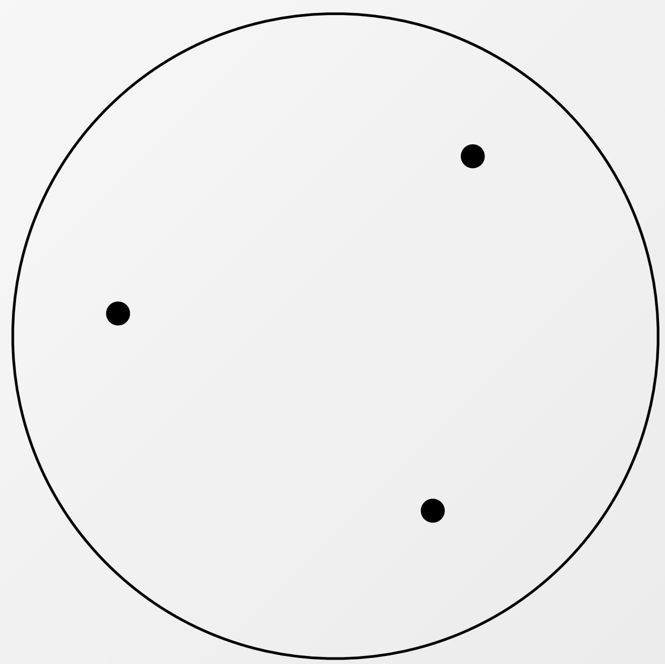

- deexcitation pulse duration: 2 μs
- detection efficiency: 75(10) %
- overall resolution: ~ 500 nm

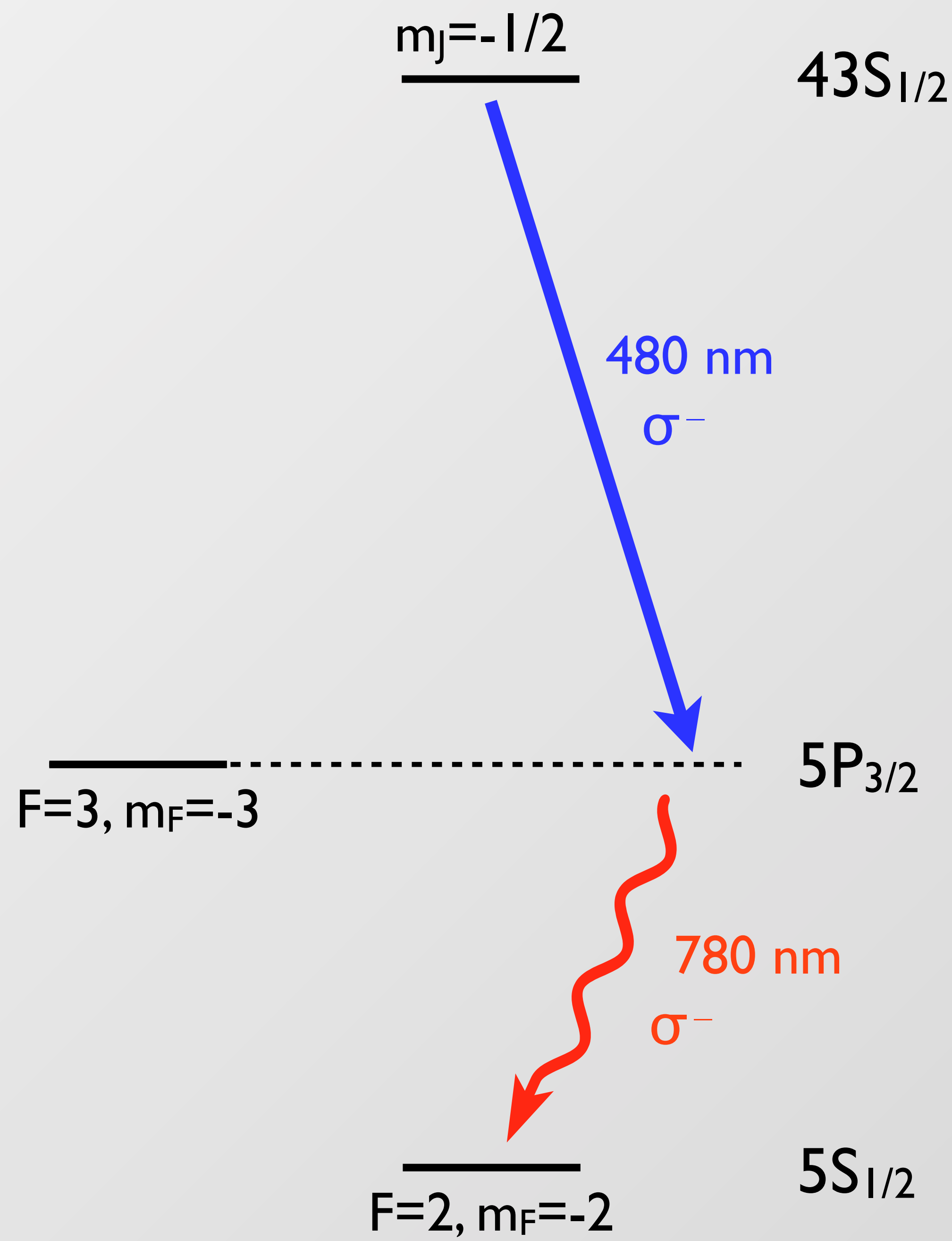

Energy spectrum of the Rydberg gas

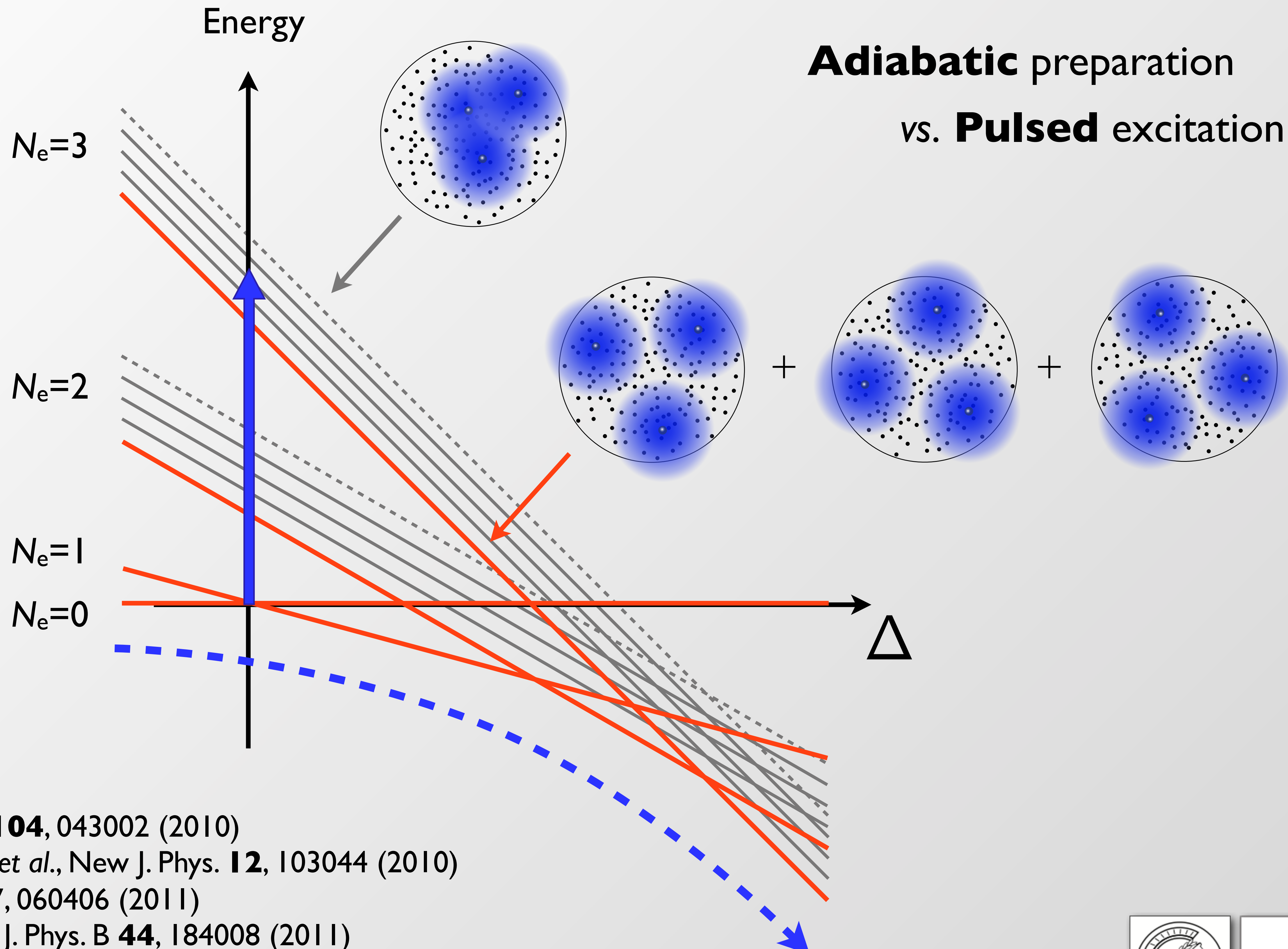

Adiabatic preparation

vs. **Pulsed** excitation

Pohl *et al.*, PRL **104**, 043002 (2010)
Schachenmayer *et al.*, New J. Phys. **12**, 103044 (2010)
Ji *et al.*, PRL **107**, 060406 (2011)
van Bijnen *et al.*, J. Phys. B **44**, 184008 (2011)
Gärttner et al., arXiv:1203.2884v2 (2012)

Pulsed Excitation

Superposition of different many-body Rydberg states!

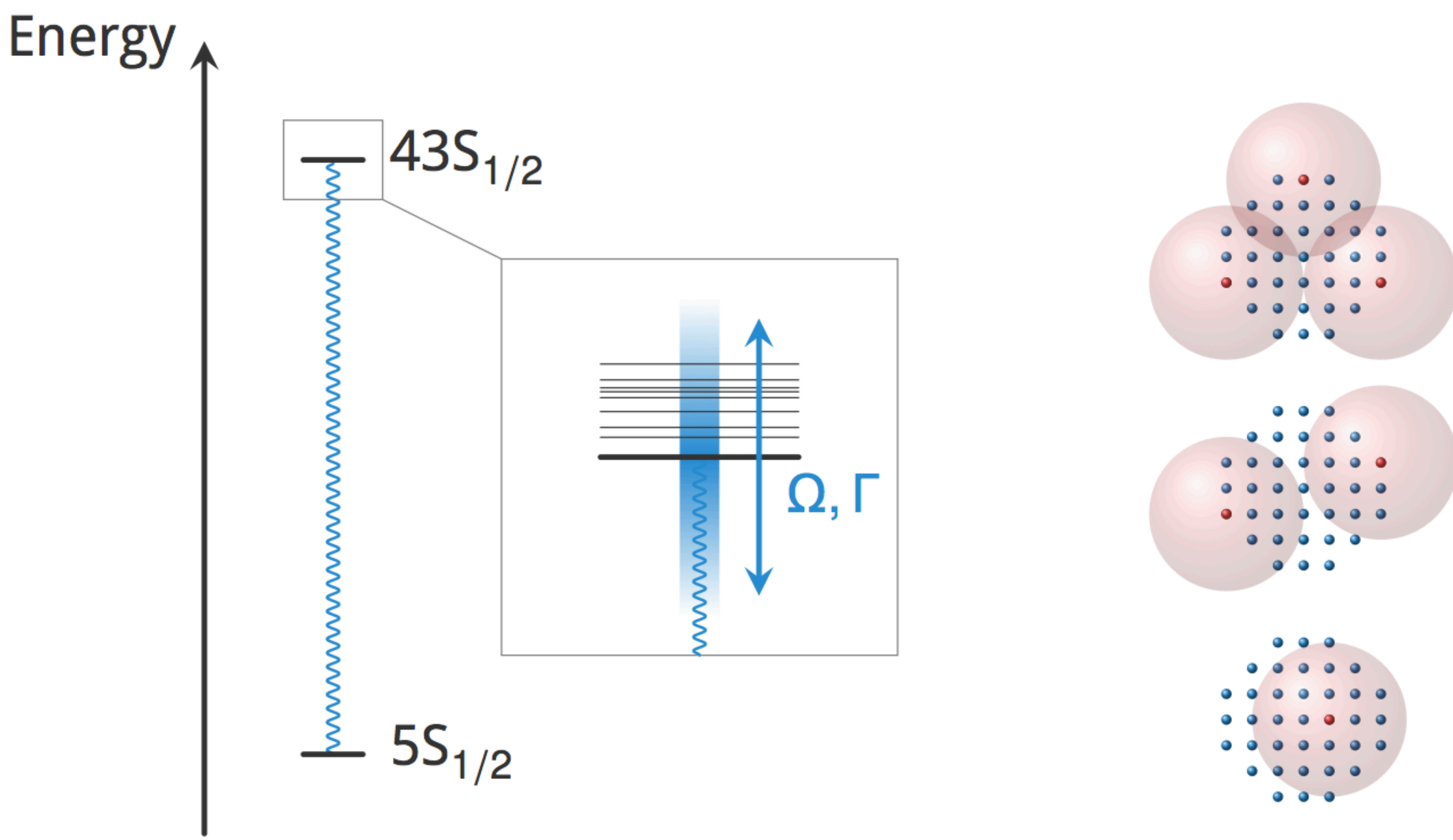

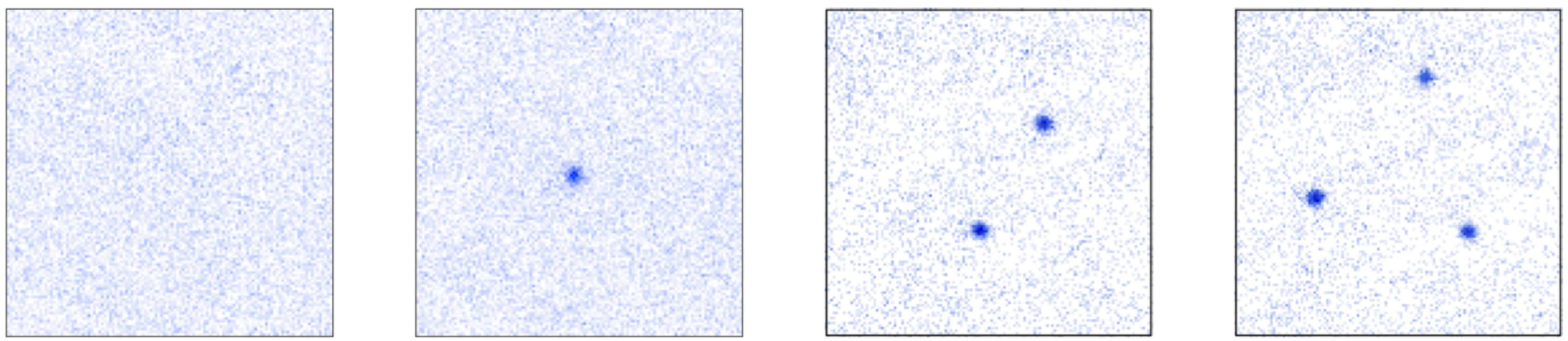

Observation of Spatially Ordered Structures

Post selection according to atom number!

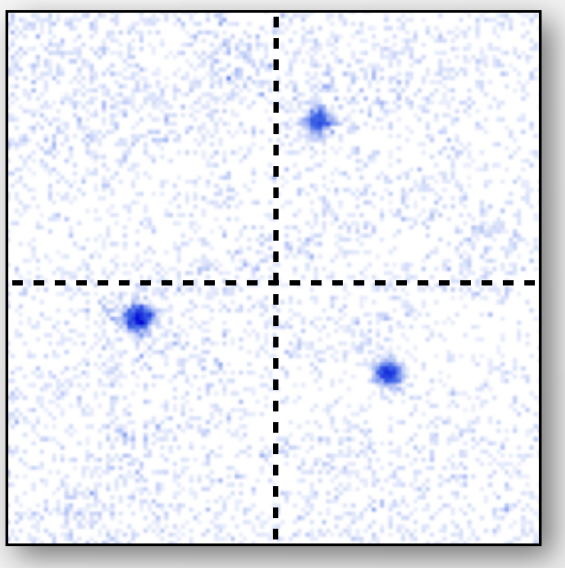

Observation of Spatially Ordered Structures

Post selection according to atom number!

centre onto
the barycenter

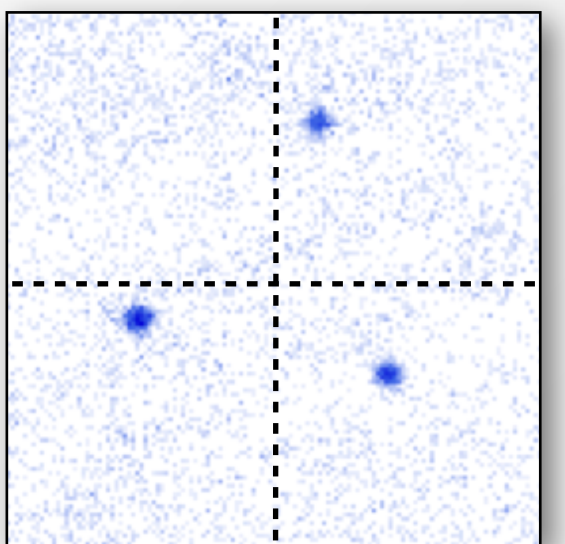

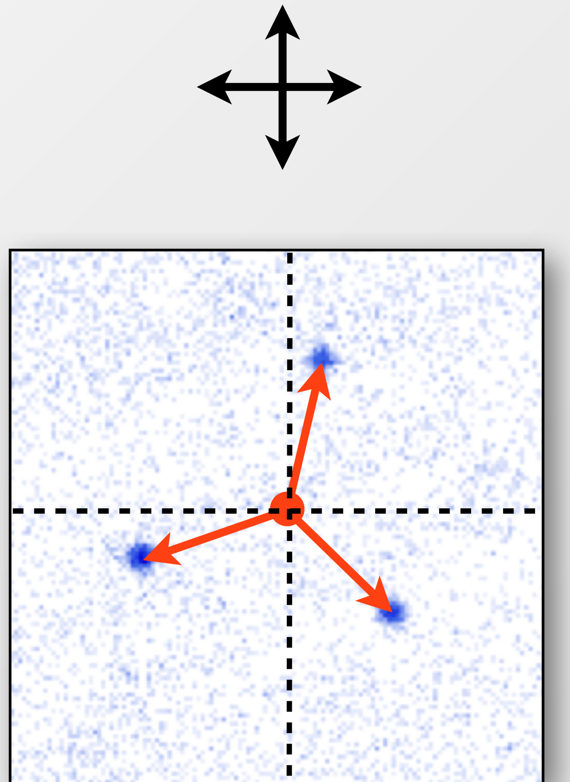

Observation of Spatially Ordered Structures

Post selection according to atom number!

centre onto
the barycenter

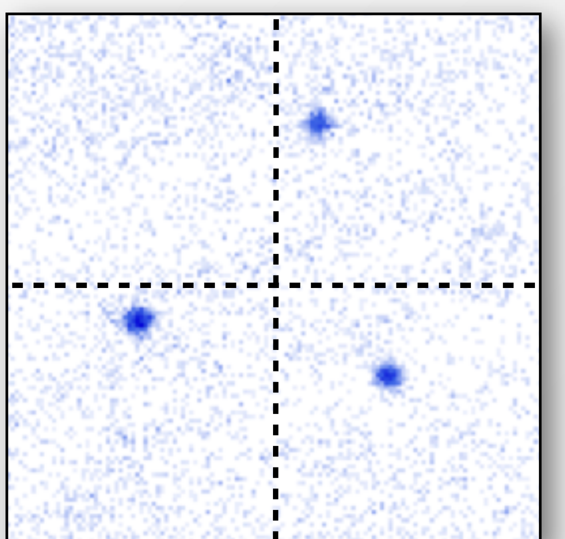

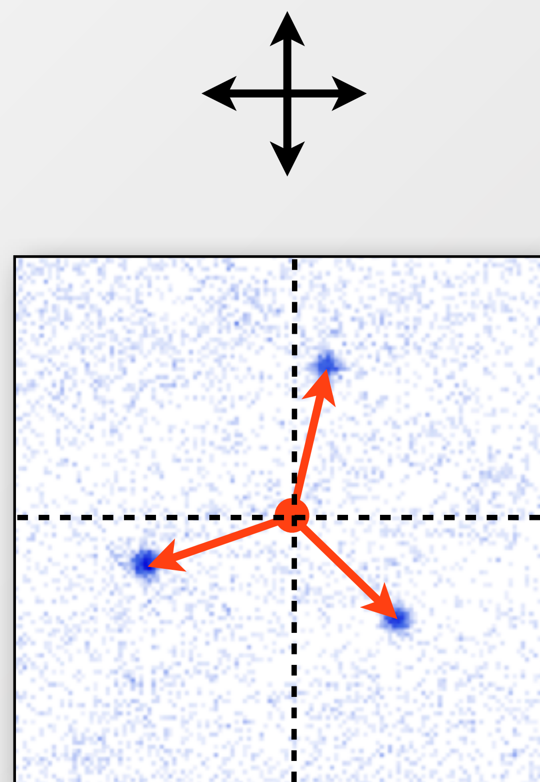

N_e=2

N_e=3

N_e=4

N_e=5

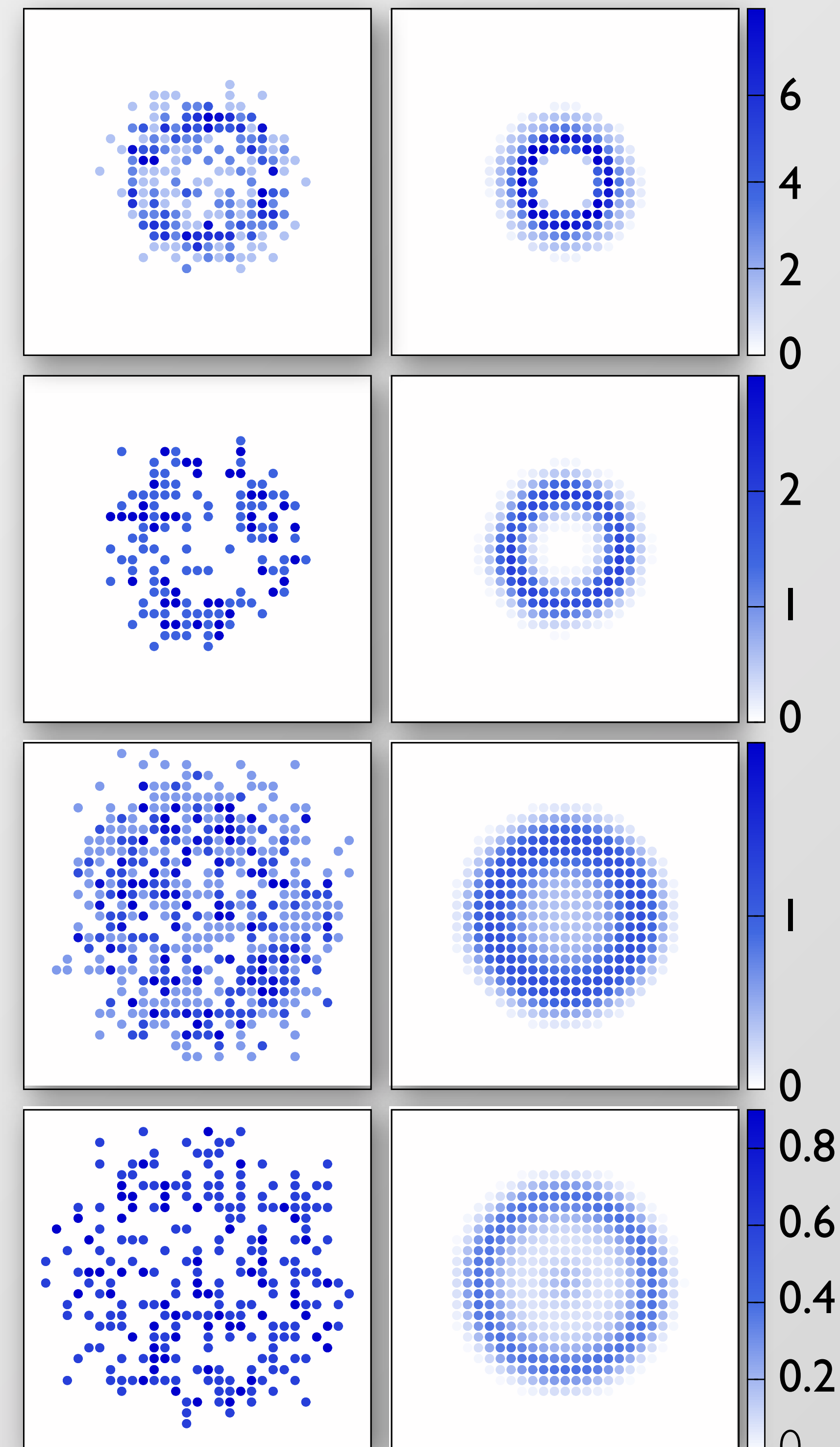

Event probability (10^{-3})

Numerical simulations:

- exact dynamics (truncated Hilbert space)
- average over initial states from the grand canonical ensemble

Observation of Spatially Ordered Structures

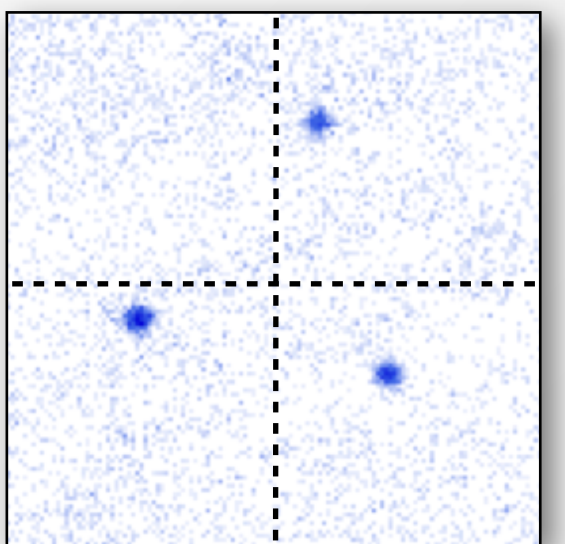

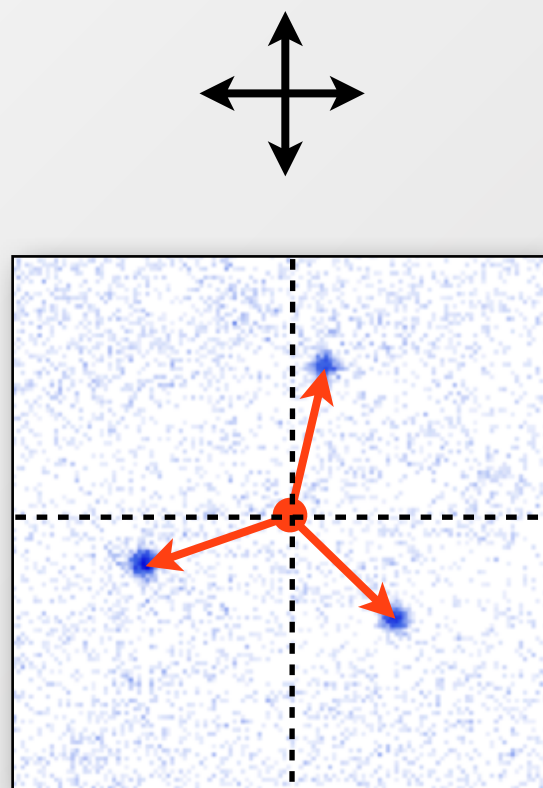

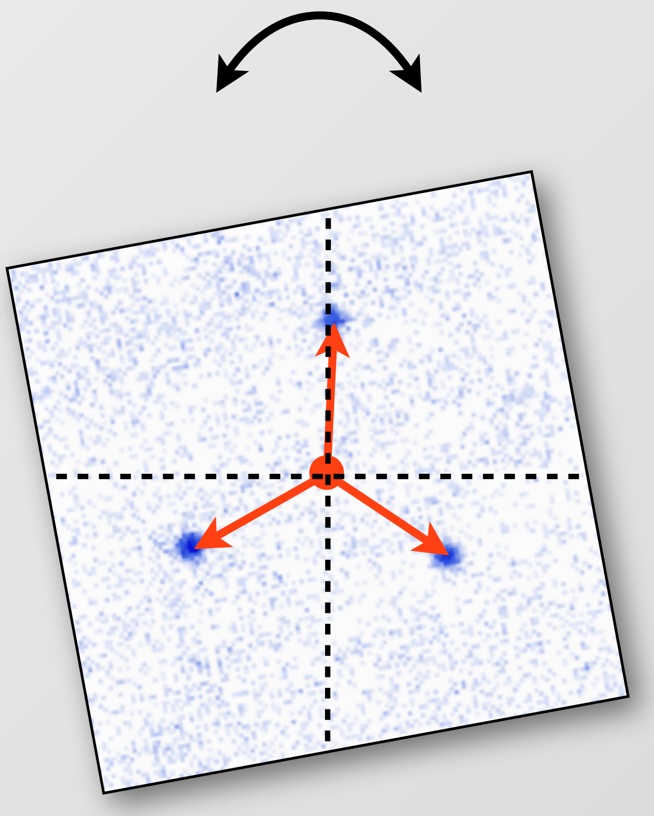

Observation of Spatially Ordered Structures

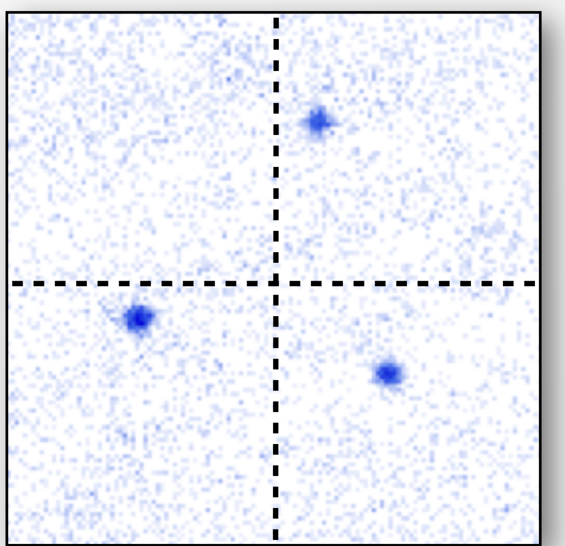

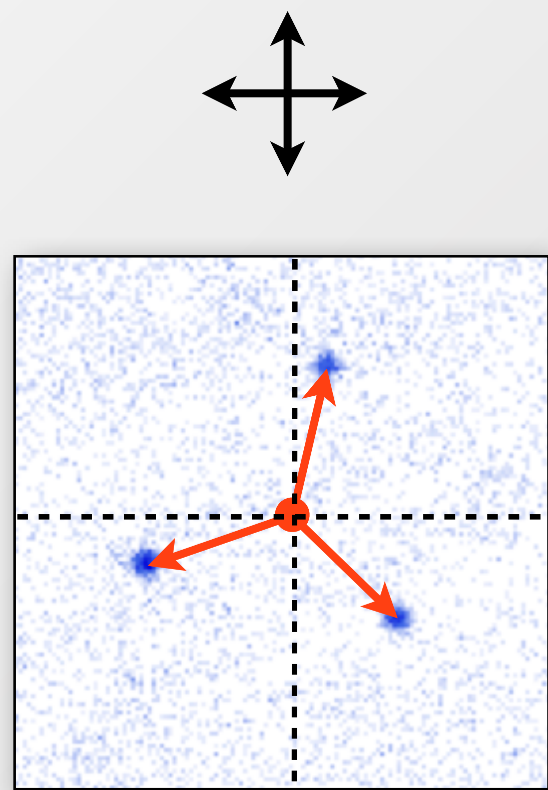

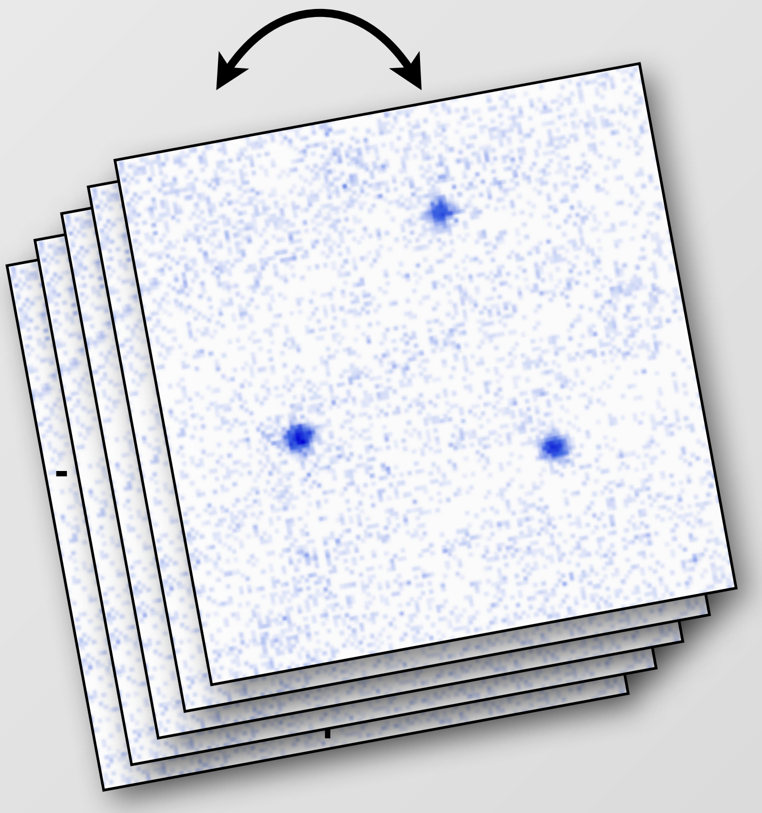

Observation of Spatially Ordered Structures

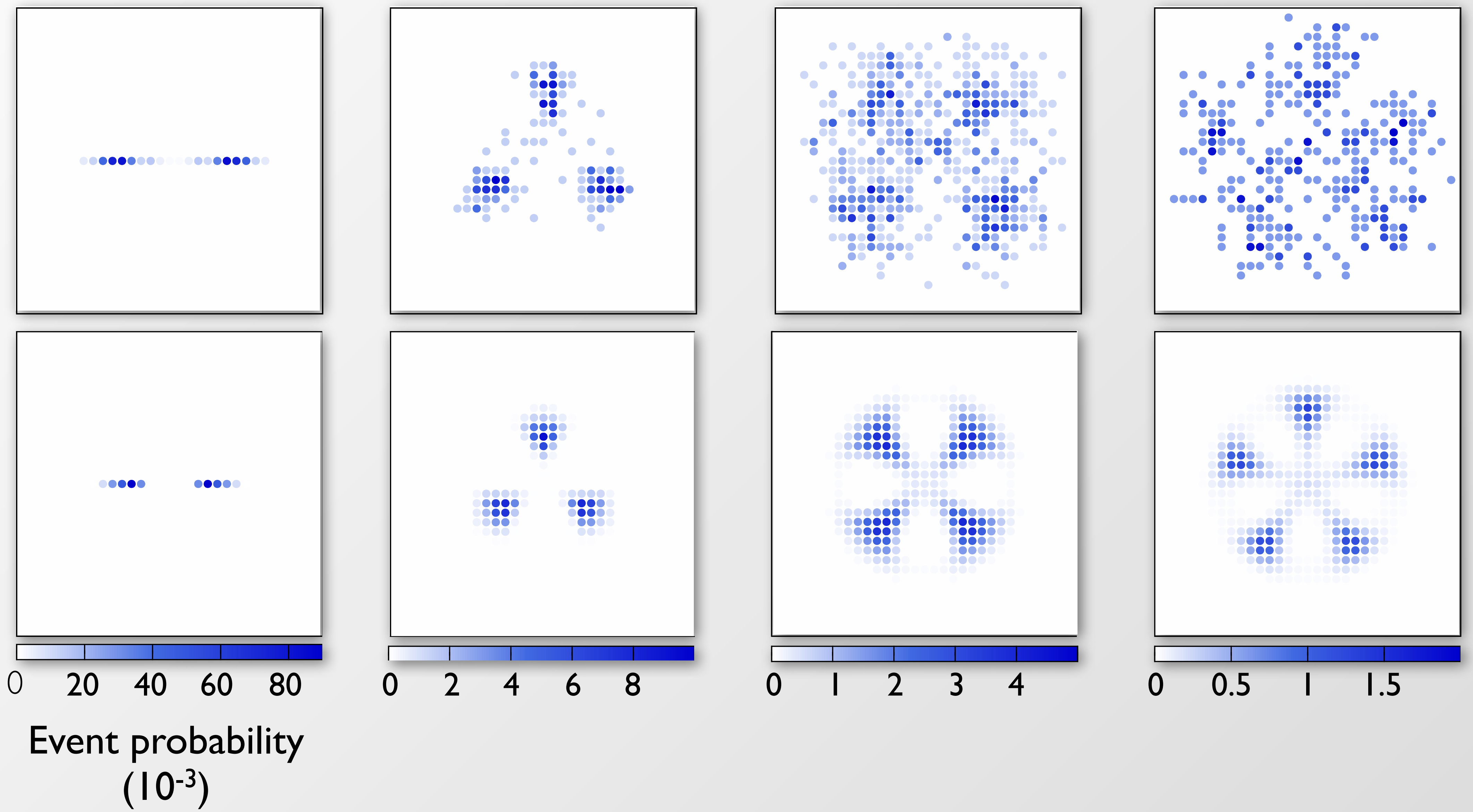

Correlation functions

Pair correlation function:

$$g^{(2)}(r) = \frac{\sum_{i \neq j} \delta_{r,r_{ij}} \langle \sigma_{ee}^{(i)} \sigma_{ee}^{(j)} \rangle}{\sum_{i \neq j} \delta_{r,r_{ij}} \langle \sigma_{ee}^{(i)} \rangle \langle \sigma_{ee}^{(j)} \rangle}$$

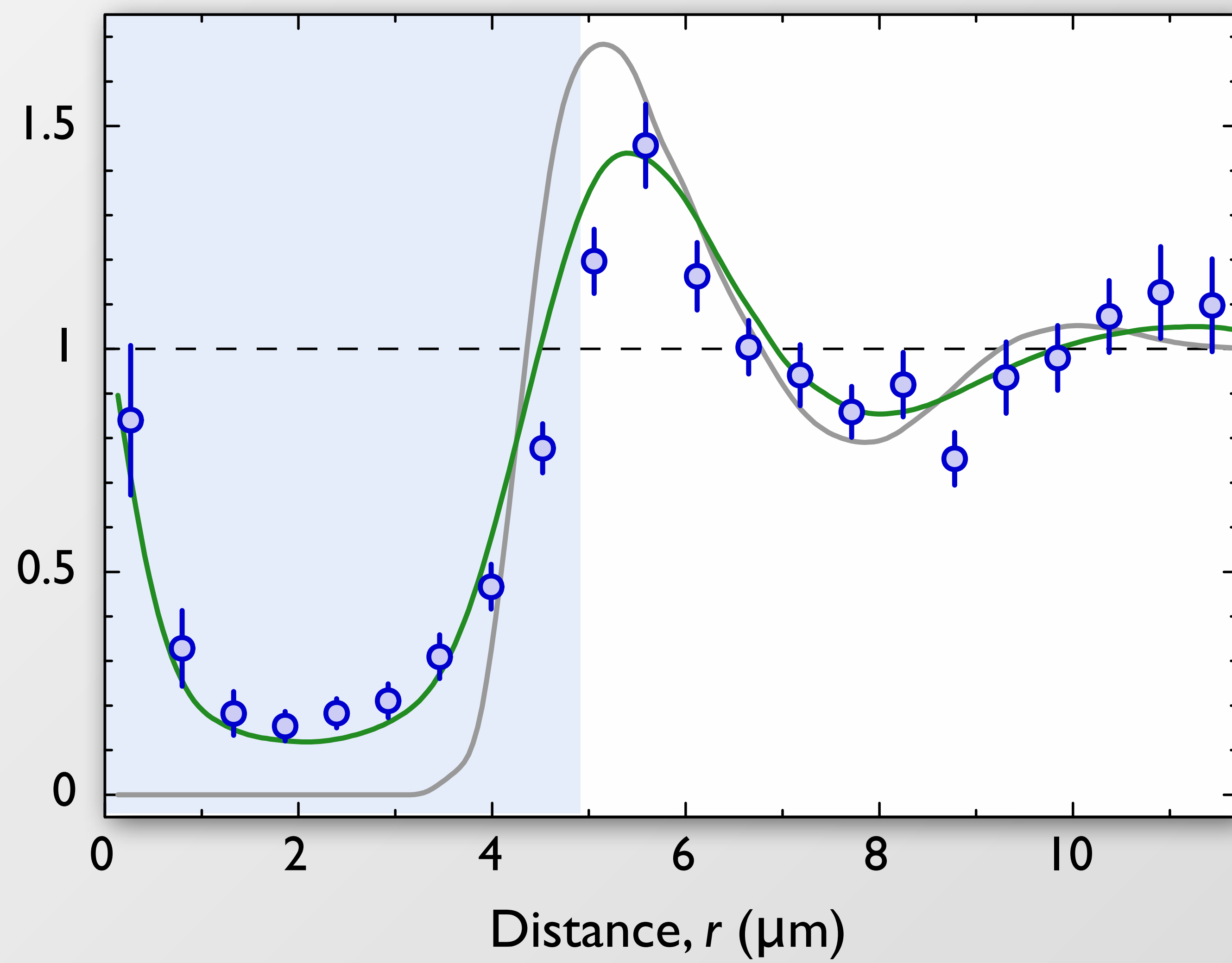

Deviations due to:

- hopping during the fluorescence imaging – *probability ~ 1 %*
- imperfect removal of the ground state atoms – *0.2 atoms per image*
- residual motion of the Rydberg atoms before imaging – *± 0.5 μm*

Blockade radius measurement, see also: Schwarzkopf et al. PRL (2011)

Dynamical Crystallization

$$H = \frac{\hbar\Omega}{2}\sum_i\left(\sigma_{eg}^{(i)} + \sigma_{ge}^{(i)}\right) + \sum_{i\neq j}\frac{V_{ij}}{2}\sigma_{ee}^{(i)}\sigma_{ee}^{(j)} - \Delta\sum_i\sigma_{ee}^{(i)}$$

Frozen Gas Phase Diagram

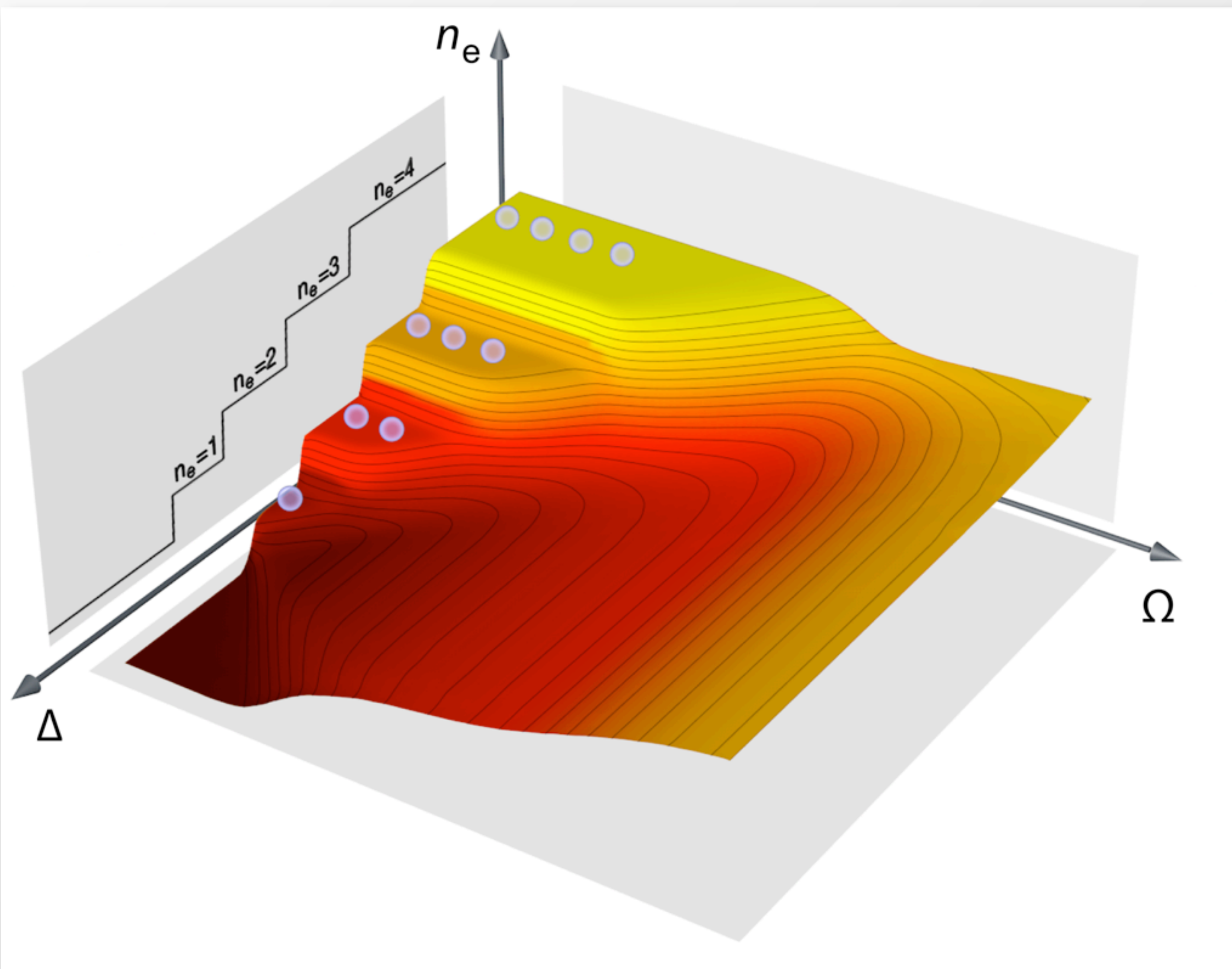

PRL 104, 043002 (2010) PHYSICAL REVIEW LETTERS week ending 29 JANUARY 2010

Dynamical Crystallization in the Dipole Blockade of Ultracold Atoms

T. Pohl,[1,2] E. Demler,[2,3] and M. D. Lukin[2,3]
[1]*Max Planck Institute for the Physics of Complex Systems, 01187 Dresden, Germany*
[2]*ITAMP-Harvard-Smithsonian Center for Astrophysics, Cambridge Massachusetts 02138, USA*
[3]*Physics Department, Harvard University, Cambridge Massachusetts 02138, USA*
(Received 26 July 2009; revised manuscript received 23 October 2009; published 27 January 2010)

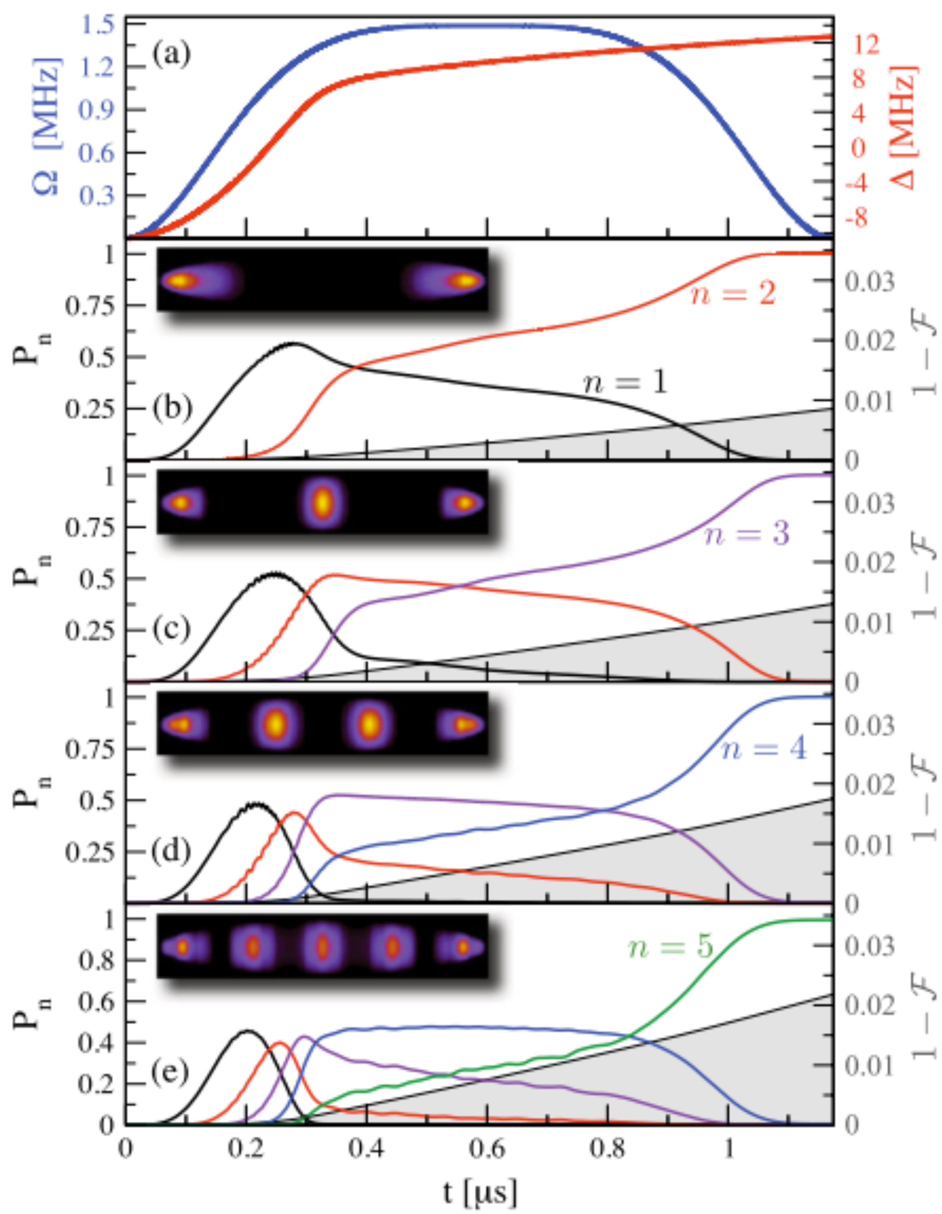

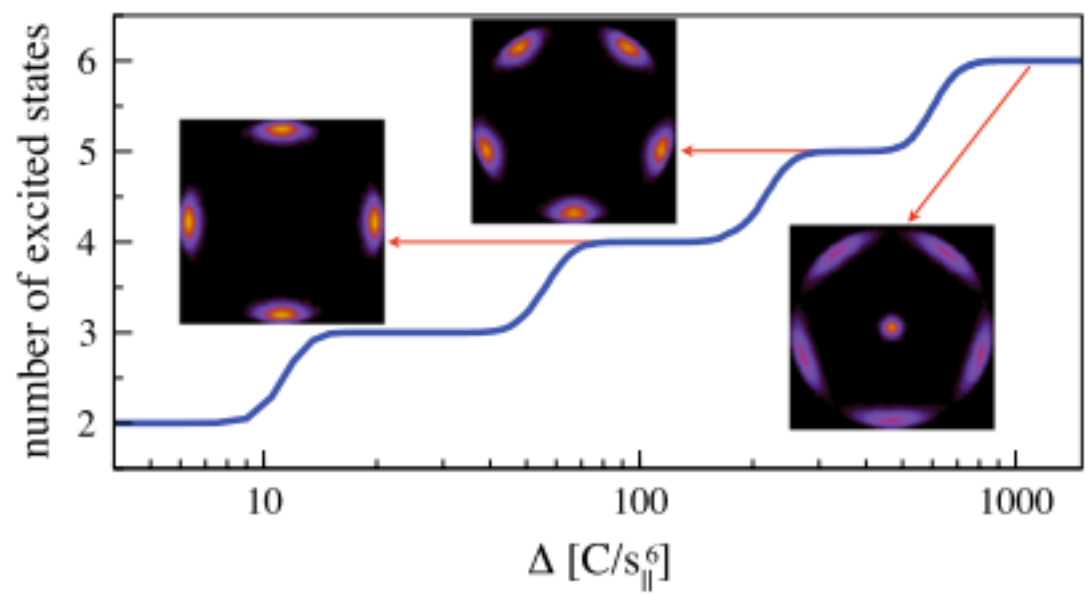

Coherent Control of Many-Body System through Adiabatic Sweeps

Theory see:
T. Pohl et al. PRL 2010; G. Pupillo et al. PRL 2010,
R.M.W van Bijnen et al. J. Phys. B: At. Mol. Opt. Phys. (2011)
see also: H. Weimer et al., PRL 2008

Energy spectrum of the Rydberg gas

Adiabatic preparation

vs. **Pulsed** excitation

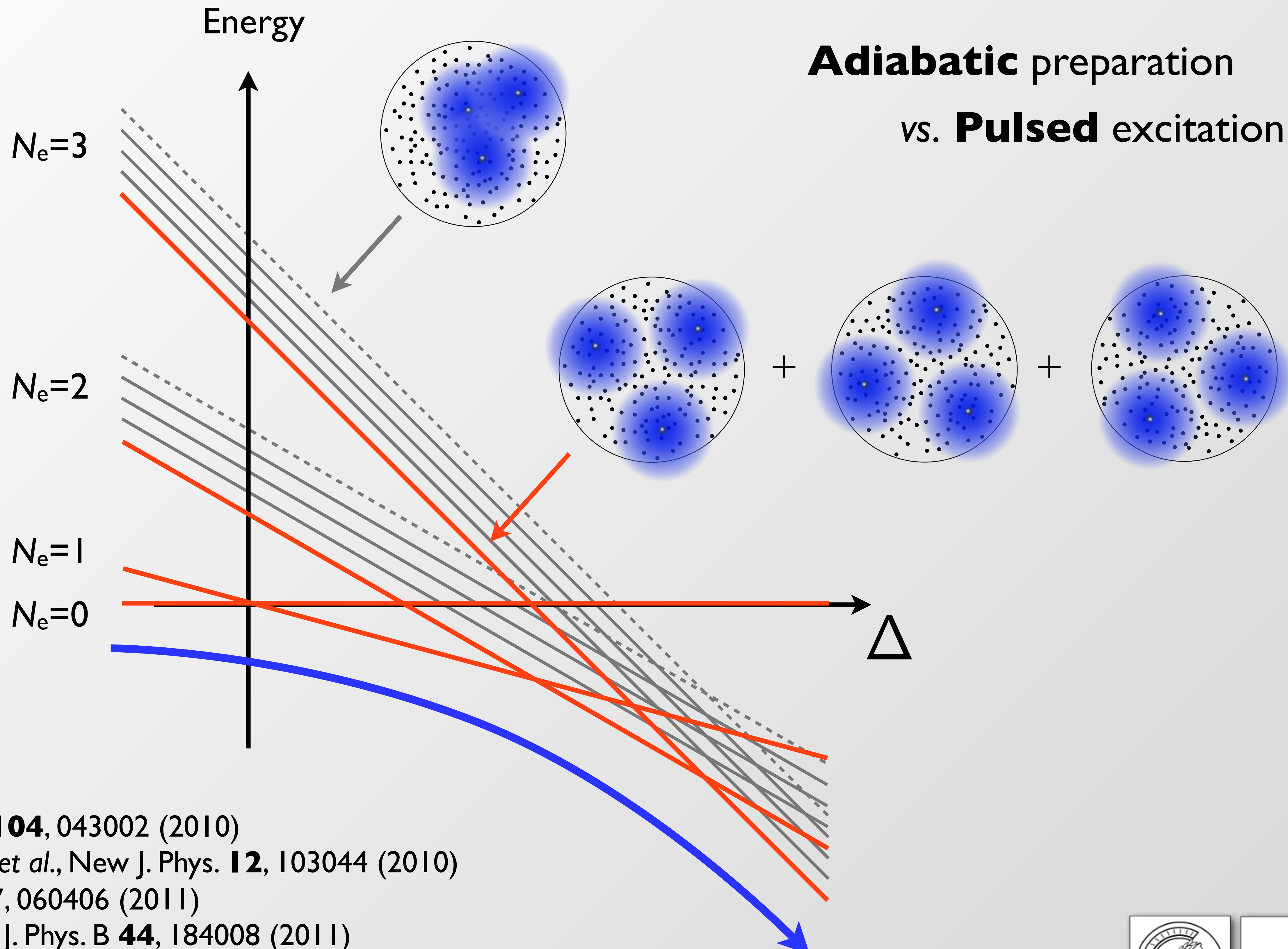

Pohl *et al.*, PRL **104**, 043002 (2010)
Schachenmayer *et al.*, New J. Phys. **12**, 103044 (2010)
Ji *et al.*, PRL **107**, 060406 (2011)
van Bijnen *et al.*, J. Phys. B **44**, 184008 (2011)
Gärttner et al., arXiv:1203.2884v2 (2012)

1D Rydberg Chains: Preparing Different Lengths

DMD: Keep 3xN lattice sites

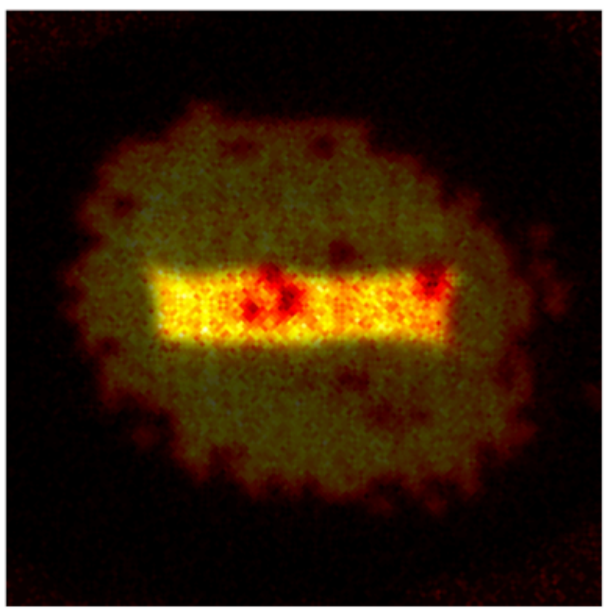

Constant sweep, different length

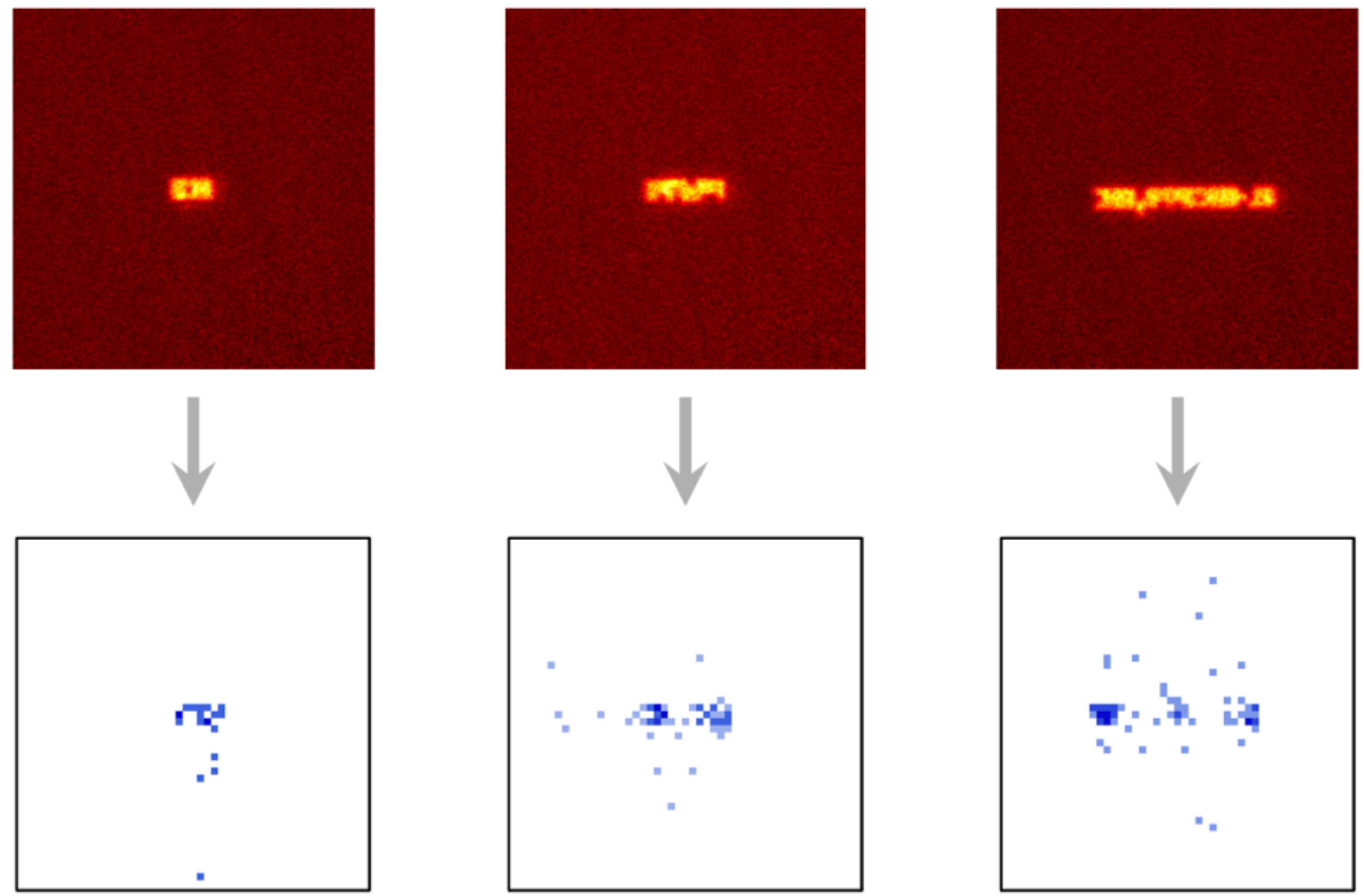

Rydberg Crystals - Compressibility

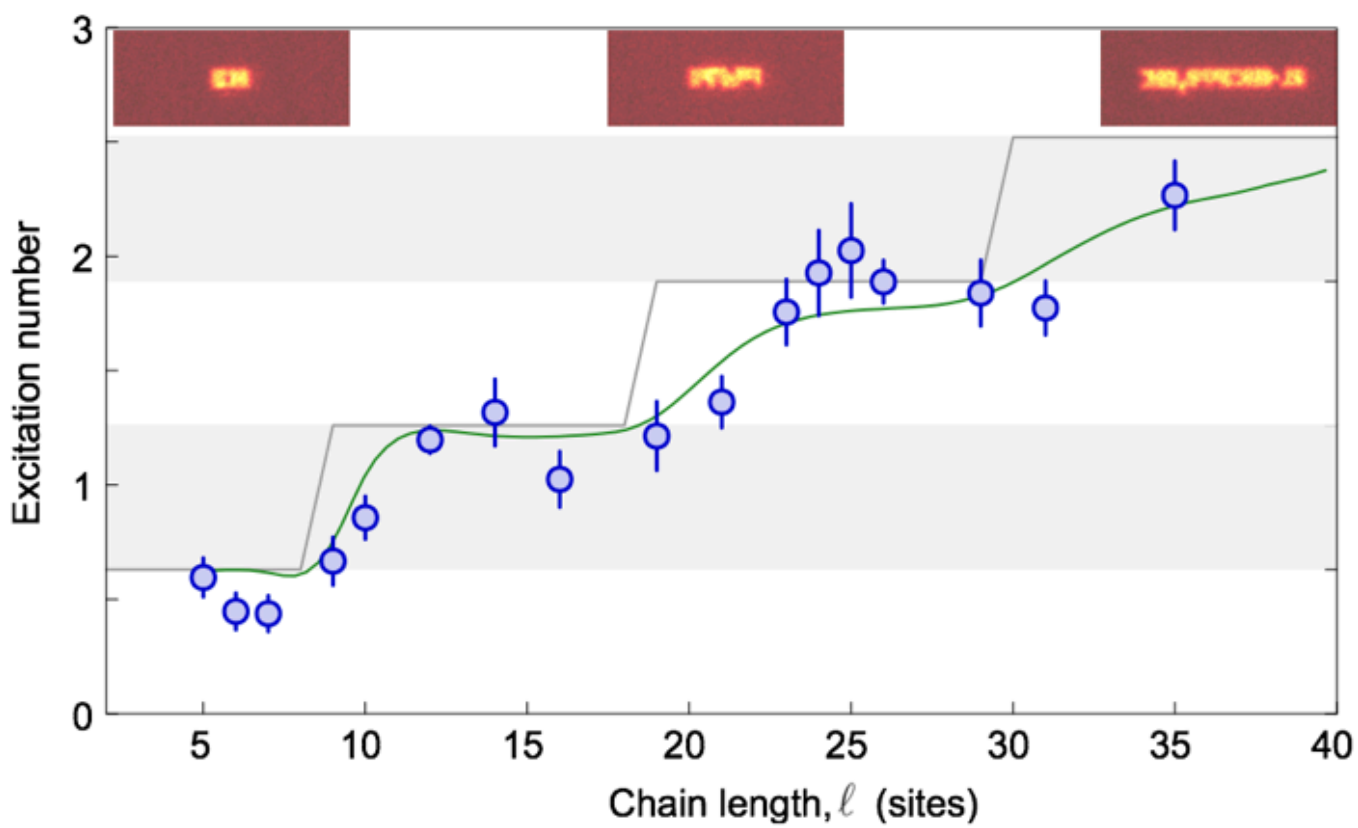

Measure excitation number vs length

- Longer system
  = Try to squeeze in more excitations

Rydberg Crystals - Compressibility

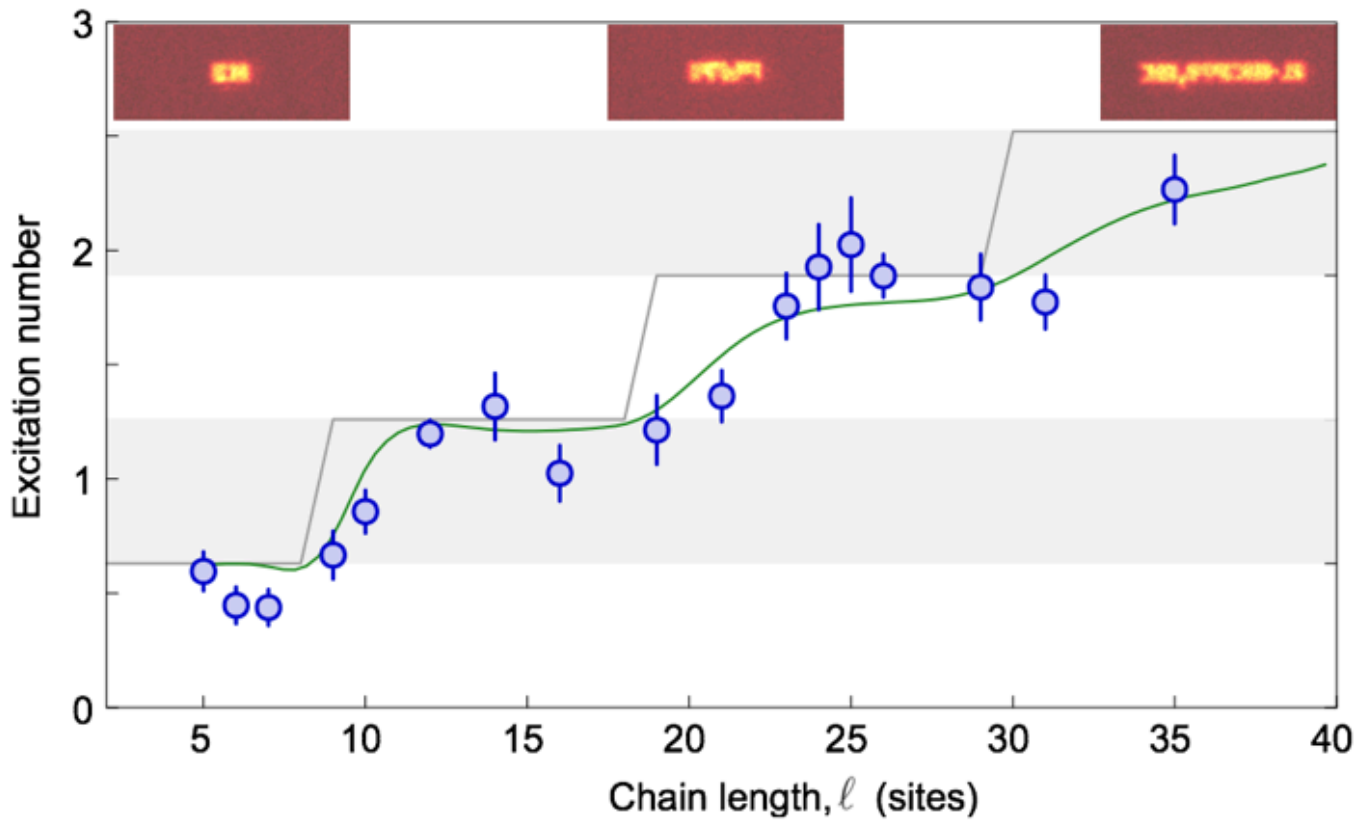

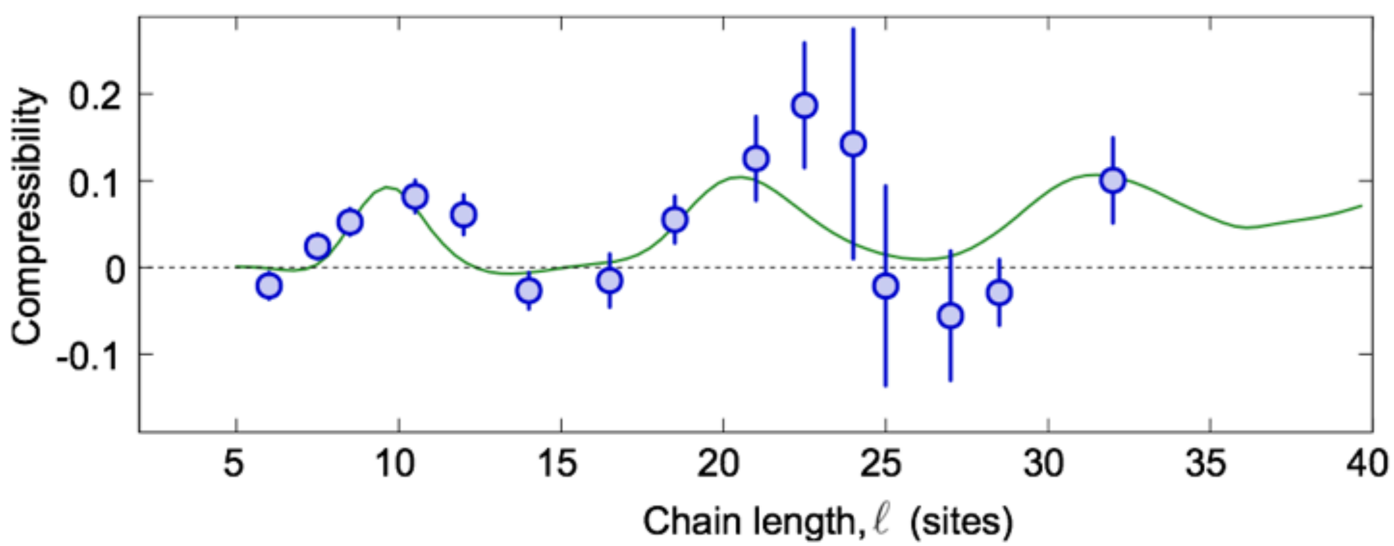

Measure excitation number vs length

- Longer system = Try to squeeze in more excitations

- Compressibility

$$\kappa = \frac{\partial n_e}{\partial \Delta} = \frac{\partial n_e}{\partial \ell} \frac{\partial \ell}{\partial \Delta}$$

Ultimate Size Control in 2D

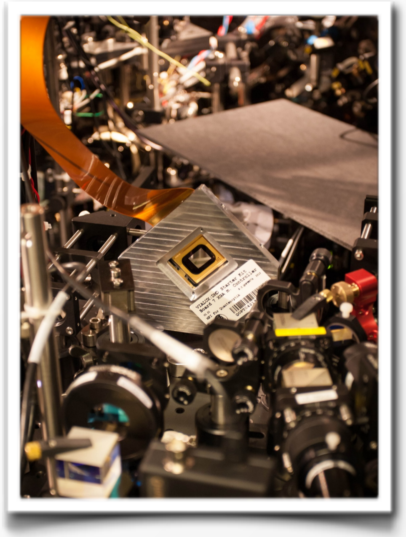

Digital Mirror Device (Size Control)

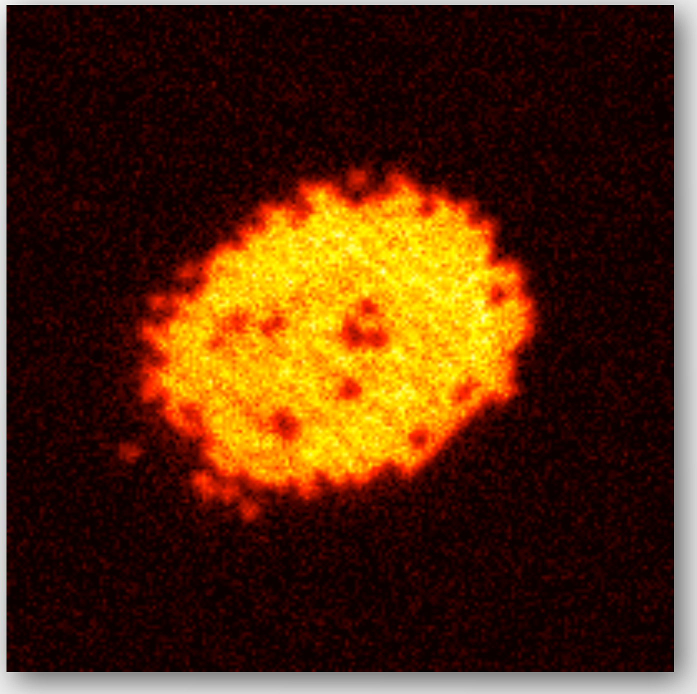

Fluctuating Size and non-perfect shape

Ultimate Size Control in 2D

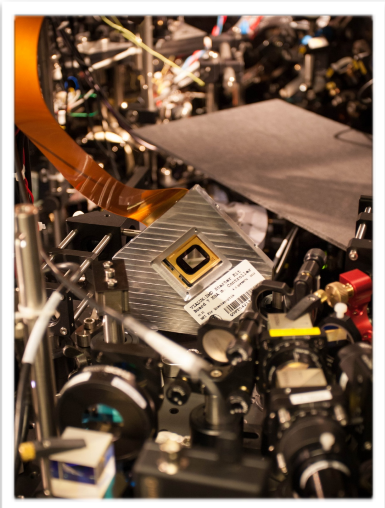

Digital Mirror Device (Size Control)

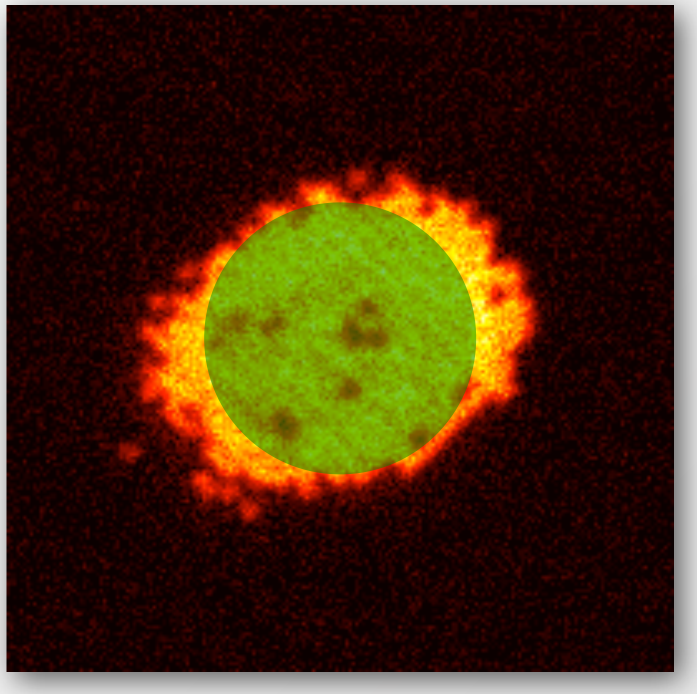

Fluctuating Size and non-perfect shape

Ultimate Size Control in 2D

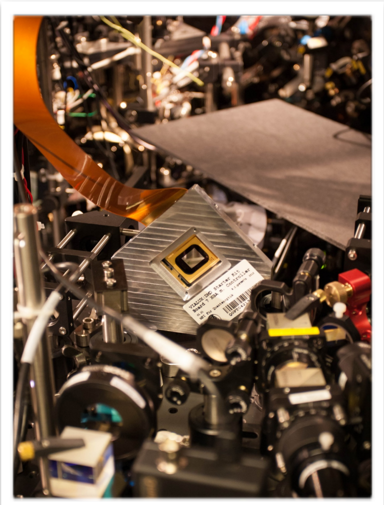

Digital Mirror Device (Size Control)

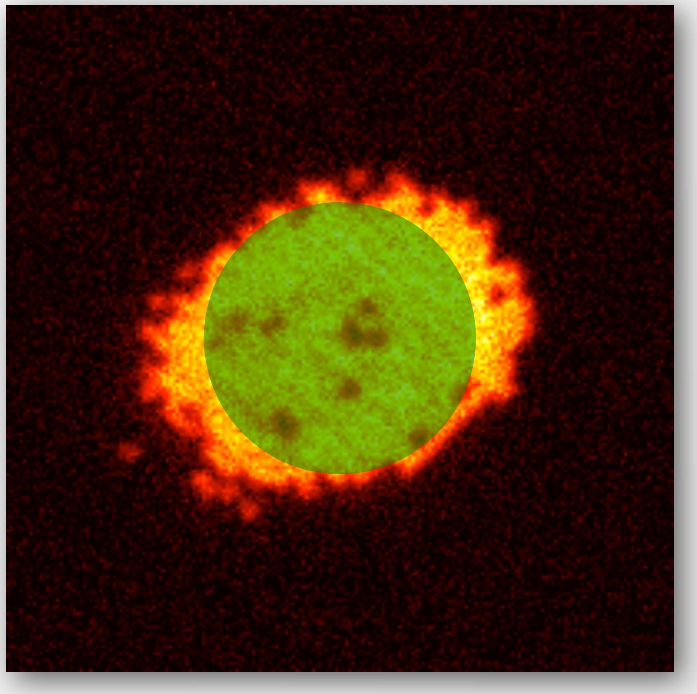

Fluctuating Size and non-perfect shape

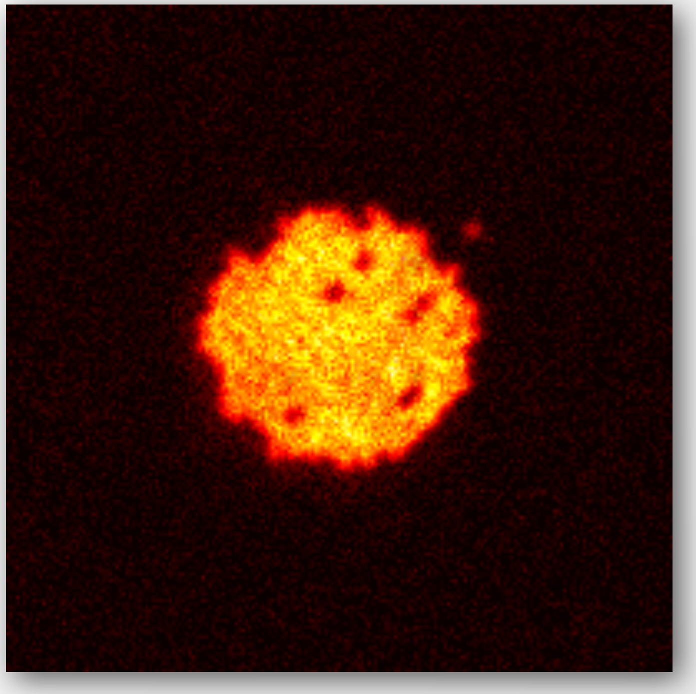

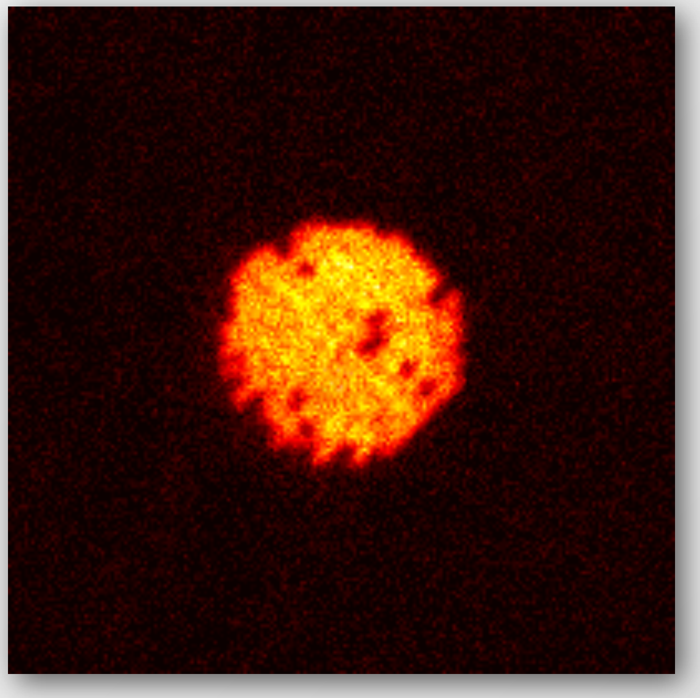

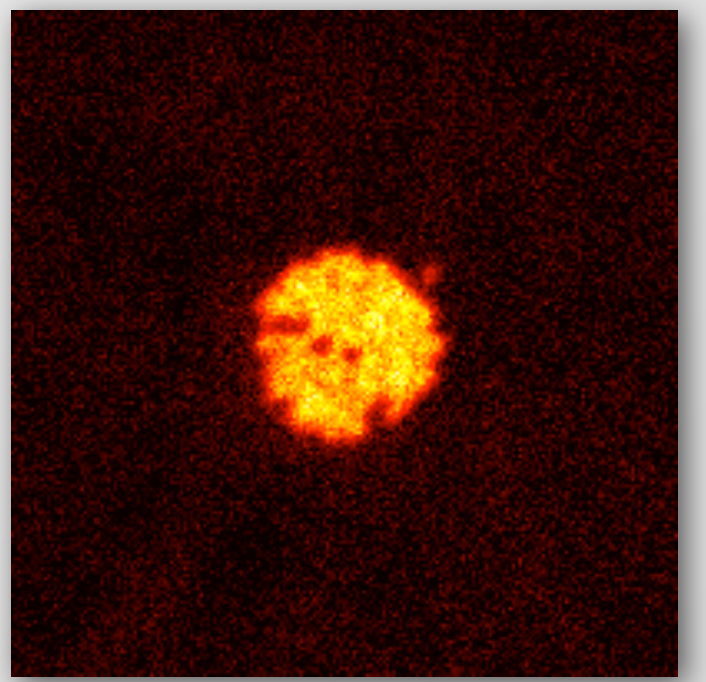

Size & atom number perfectly controlled

Ultimate Size Control in 2D

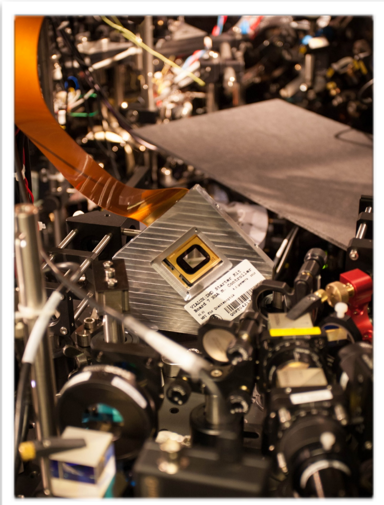

Digital Mirror Device (Size Control)

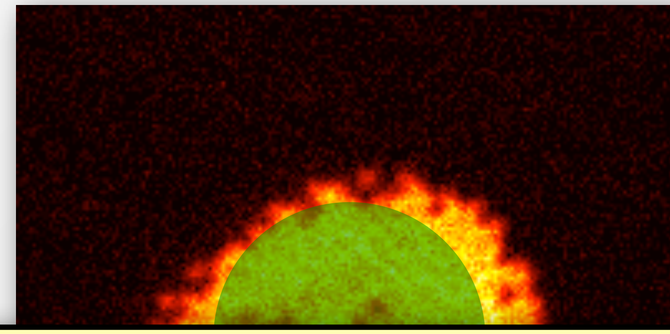

Fluctuating Size and

•Sub Shot Noise Atom Number Preparation

•Geometric & atom number control
(crucial e.g. for quantum criticality)

•Hard wall potentials realized
(crucial for edge states)

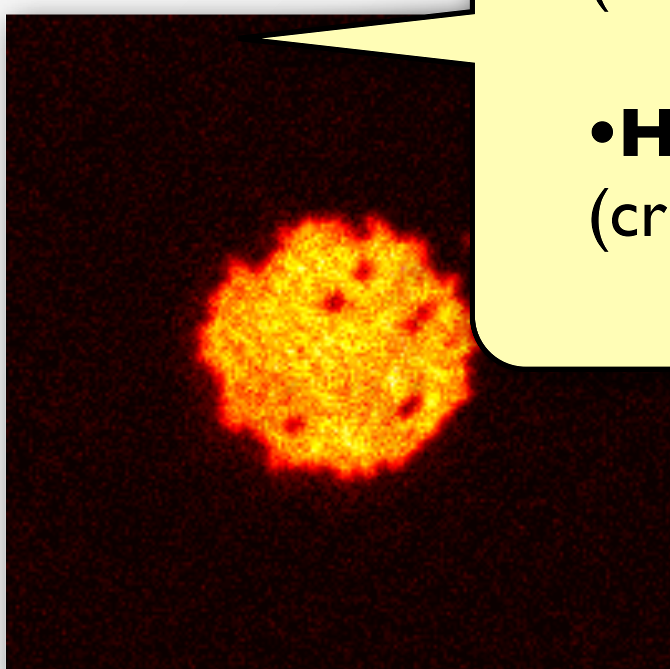

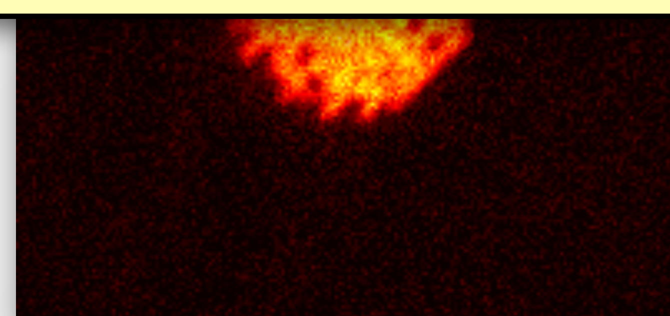

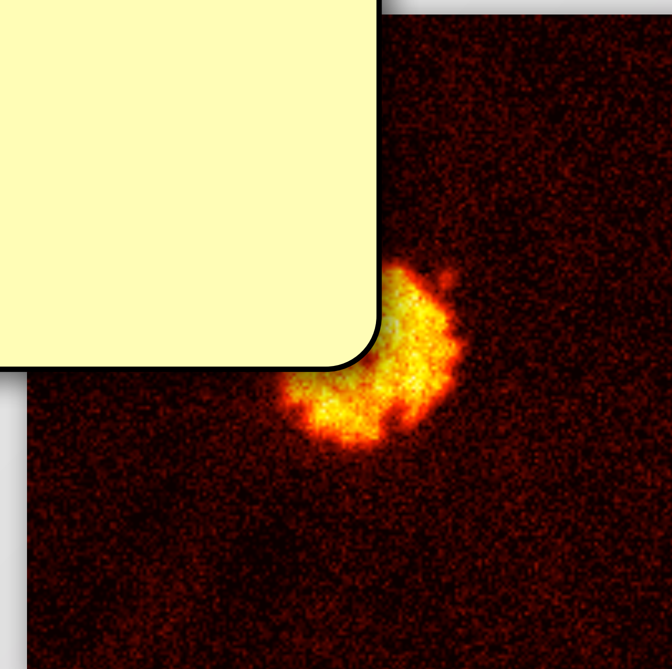

Size & atom number perfectly controlled

Adiabatic Sweeps in 2D

Pulsed vs sweeped excitation - localization of excitations to border of system!

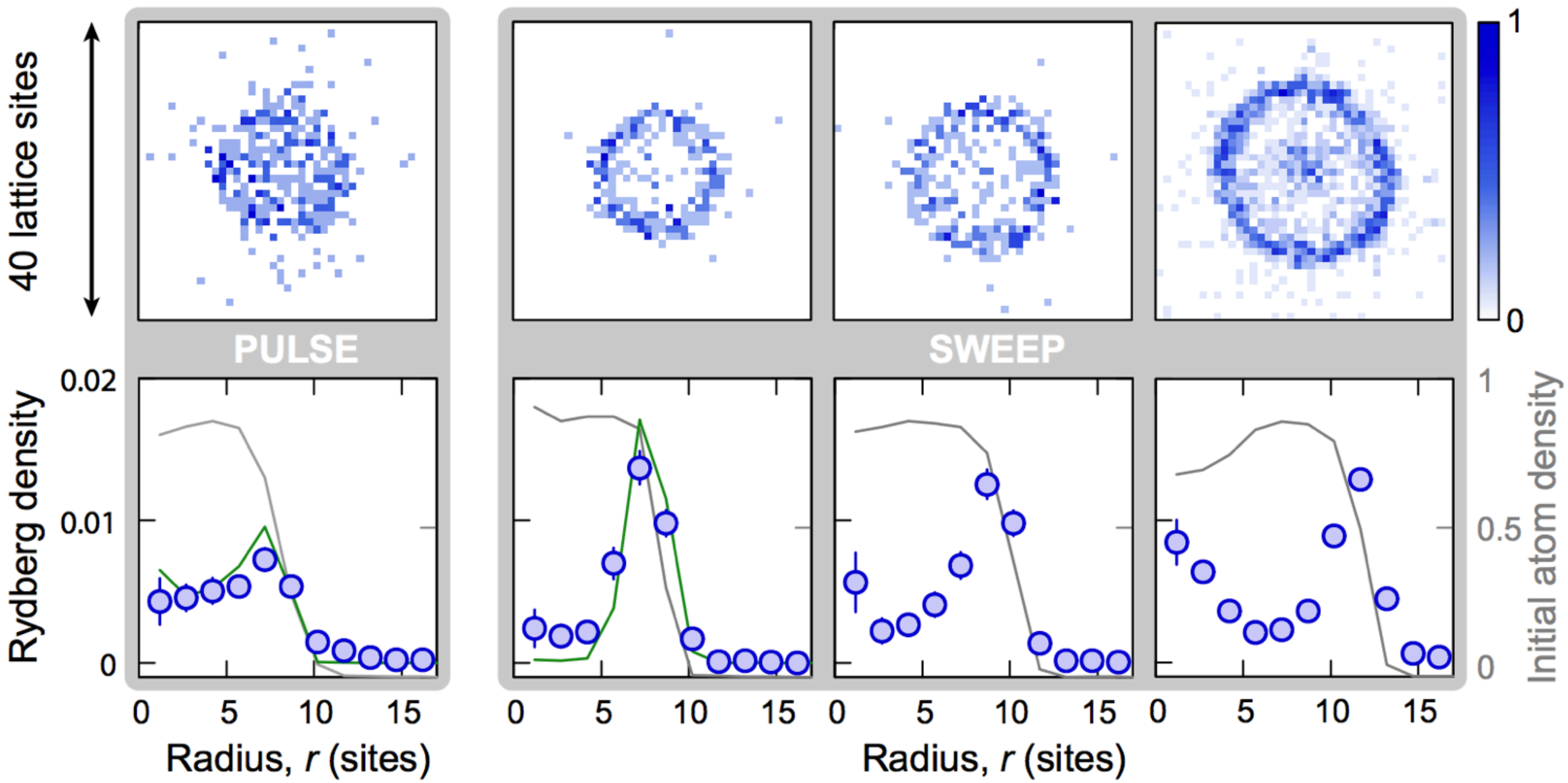

Adiabatic Sweeps in 2D

Pulsed vs sweeped excitation - localization of excitations to border of system!

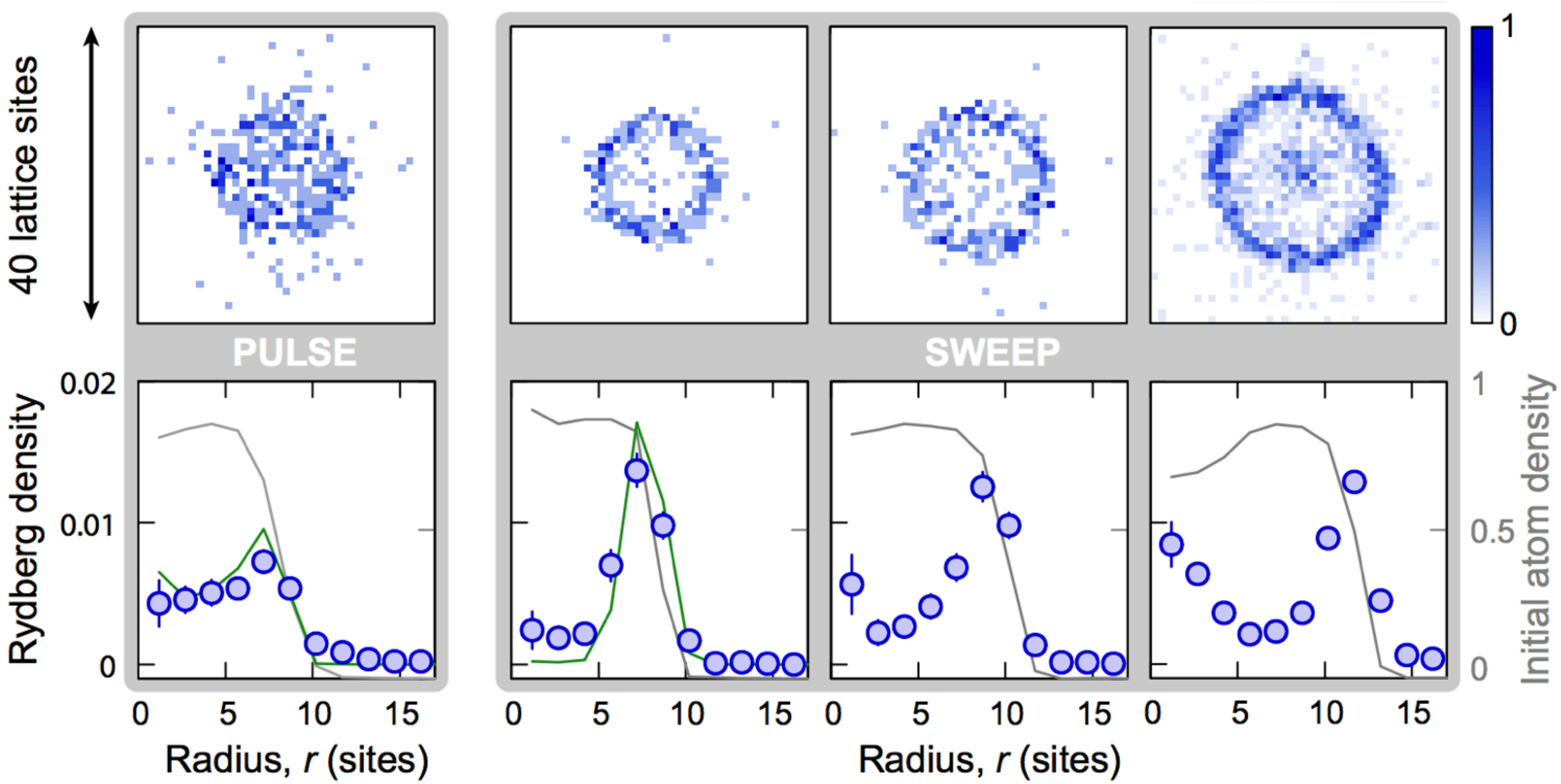

Single-Shot Rydberg Crystal Configurations

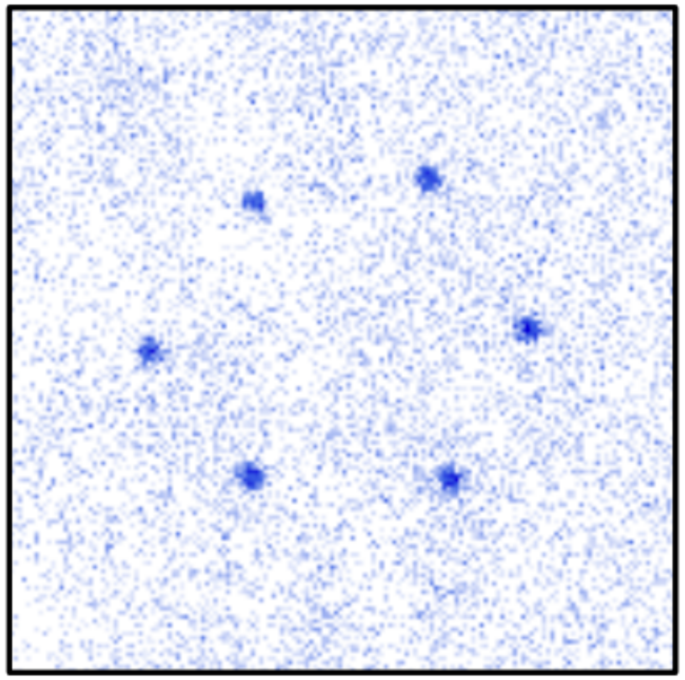

6

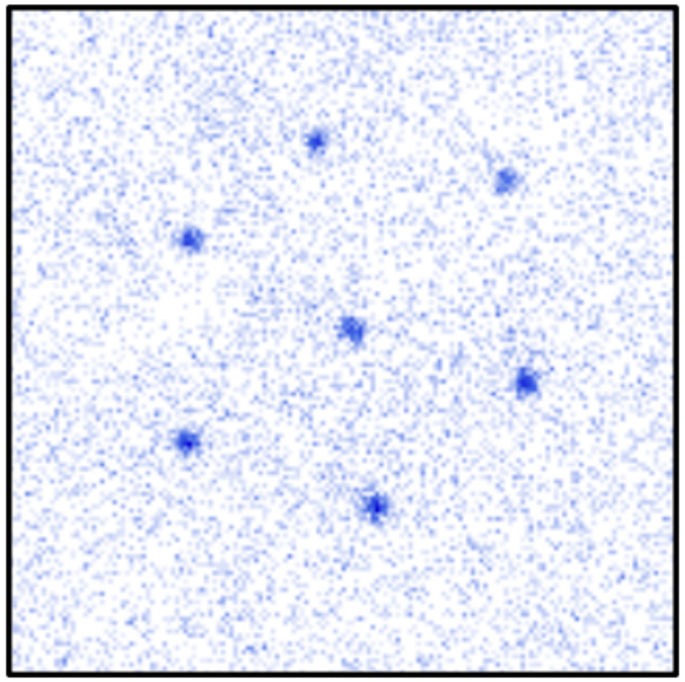

7

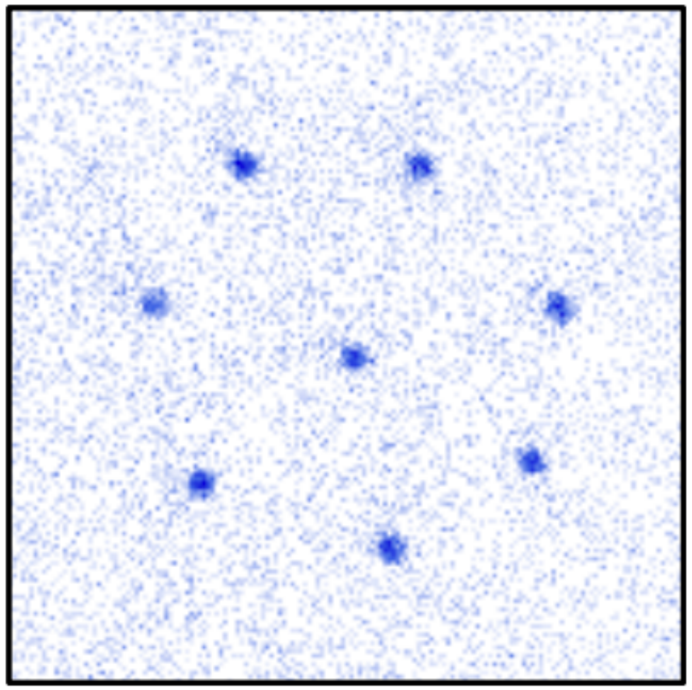

8

Rydberg Crystal configurations

Configurational Change

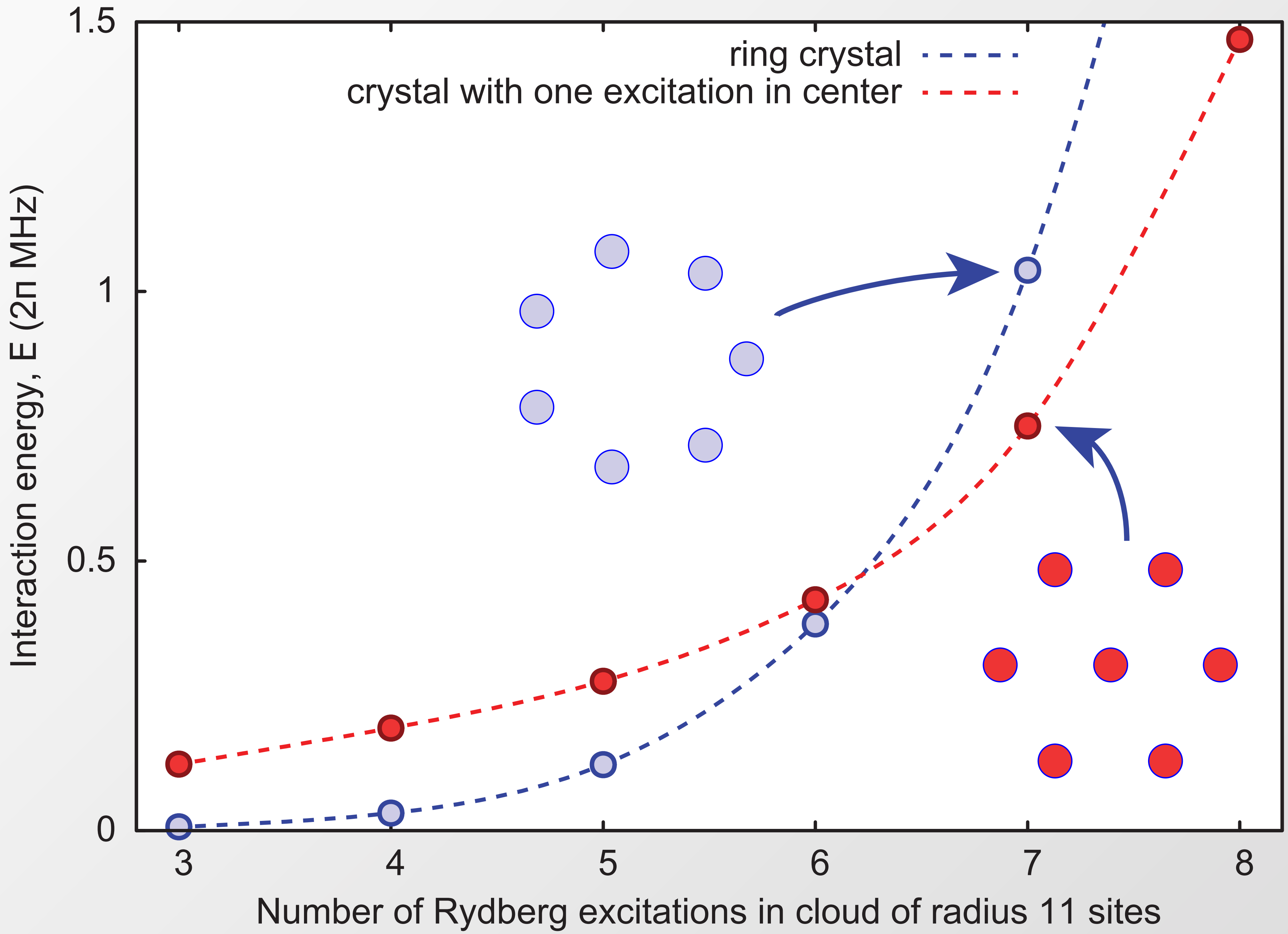

Outlook

Smaller Blockade/Larger Cloud

- ✓ Larger Rydberg Crystals
- ✓ Larger Rydberg Atoms cp. to Lattice Spacing
- ✓ Adiabatic Sweeps to Deterministically Prepare Crystal Structures
- ✓ Show Coherence of Crystalline Superpositions! a Quantum Crystal?

T. Pohl et al, (2010), van Bijnen et al. (2011), Gärtner et al. (2012),...

Larger Blockade/Smaller Cloud

- ✓ Collectively enhanced Rabi oscillations
- ✓ Large Entangled states (e.g. EIT schemes)

M. Lukin et al. (2001), D. Moller et al. (2008), M. Müller et al. (2009), H. Weimer et al. (2009)...

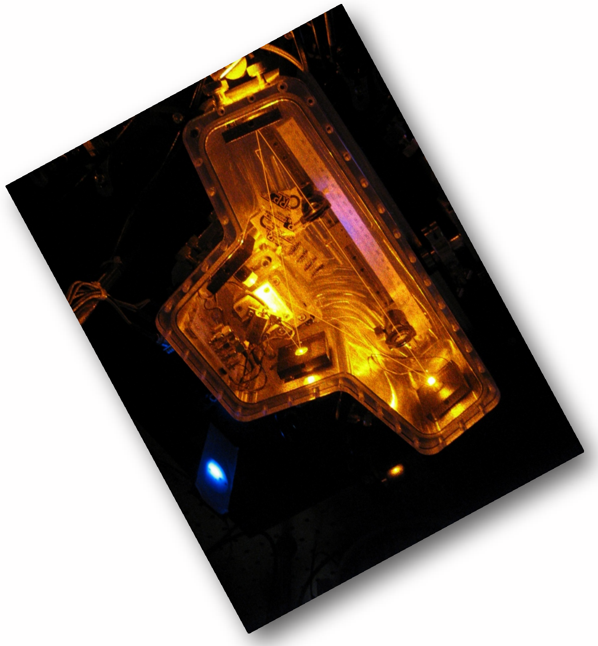

Dressed Rydberg Atom Regime

- ✓ Admix controlled long range interactions

G. Pupillo et al, (2010), Henkel et al. (2010), Schachenmeyer et al. (2010), Honer et al. (2010), Cinti et al. (2010), Johnson & Rolston (2010)...